

ISSN 2686-7575 (Online)

ТОНКИЕ ХИМИЧЕСКИЕ ТЕХНОЛОГИИ

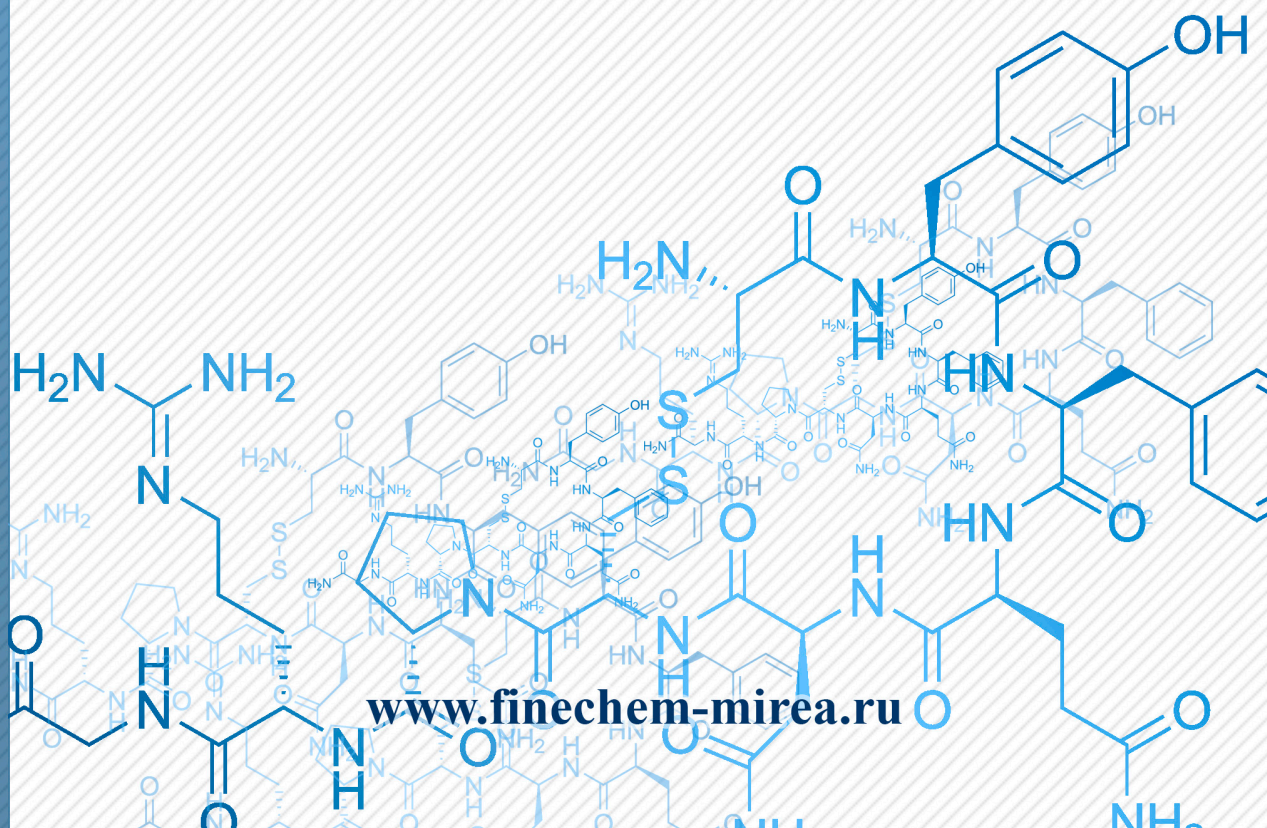
Fine Chemical Technologies

- | Theoretical Bases of Chemical Technology
- | Chemistry and Technology of Organic Substances
- | Chemistry and Technology of Medicinal Compounds and Biologically Active Substances
- | Biochemistry and Biotechnology
- | Synthesis and Processing of Polymers and Polymeric Composites
- | Chemistry and Technology of Inorganic Materials
- | Analytical Methods in Chemistry and Chemical Technology
- | Mathematical Methods and Information Systems in Chemical Technology

17(4)

2022

www.finechem-mirea.ru





ISSN 2686-7575 (Online)

ТОНКИЕ ХИМИЧЕСКИЕ ТЕХНОЛОГИИ

Fine Chemical Technologies

- | Theoretical Bases of Chemical Technology
- | Chemistry and Technology of Organic Substances
- | Chemistry and Technology of Medicinal Compounds and Biologically Active Substances
- | Biochemistry and Biotechnology
- | Synthesis and Processing of Polymers and Polymeric Composites
- | Chemistry and Technology of Inorganic Materials
- | Analytical Methods in Chemistry and Chemical Technology
- | Mathematical Methods and Information Systems in Chemical Technology

Tonkie Khimicheskie Tekhnologii =
Fine Chemical Technologies
Vol. 17, No. 4, 2022

Тонкие химические технологии =
Fine Chemical Technologies
Том 17, № 4, 2022

<https://doi.org/10.32362/2410-6593-2022-17-4>
www.finechem-mirea.ru

**Tonkie Khimicheskie Tekhnologii =
Fine Chemical Technologies
2022, vol. 17, no. 4**

The peer-reviewed scientific and technical journal *Fine Chemical Technologies* highlights the modern achievements of fundamental and applied research in the field of fine chemical technologies, including theoretical bases of chemical technology, chemistry and technology of medicinal compounds and biologically active substances, organic substances and inorganic materials, biochemistry and biotechnology, synthesis and processing of polymers and polymeric composites, analytical and mathematical methods and information systems in chemistry and chemical technology.

Founder and Publisher

Federal State Budget

Educational Institution of Higher Education

“MIREA – Russian Technological University”

78, Vernadskogo pr., Moscow, 119454, Russian Federation.

Publication frequency: bimonthly.

The journal was founded in 2006. The name was *Vestnik MITHT* until 2015 (ISSN 1819-1487).

The journal is included into the List of peer-reviewed science press of the State Commission for Academic Degrees and Titles of the Russian Federation.

The journal is indexed:

SCOPUS, DOAJ, Chemical Abstracts, Science Index, RSCI, Ulrich's International Periodicals Directory

Editor-in-Chief:

Andrey V. Timoshenko – Dr. Sci. (Eng.), Cand. Sci. (Chem.), Professor, MIREA – Russian Technological University, Moscow, Russian Federation. Scopus Author ID 56576076700, ResearcherID Y-8709-2018, <https://orcid.org/0000-0002-6511-7440>, timoshenko@mirea.ru

Deputy Editor-in-Chief:

Valery V. Fomichev – Dr. Sci. (Chem.), Professor, MIREA – Russian Technological University, Moscow, Russian Federation. Scopus Author ID 57196028937, <http://orcid.org/0000-0003-4840-0655>, fomichev@mirea.ru

Executive Editor:

Sergey A. Durakov – Cand. Sci. (Chem.), Associate Professor, MIREA – Russian Technological University, Moscow, Russian Federation, Scopus Author ID 57194217518, ResearcherID AAS-6578-2020, <http://orcid.org/0000-0003-4842-3283>, durakov@mirea.ru

Editorial staff:

Managing Editor Cand. Sci. (Eng.) Galina D. Seredina
Science editors Dr. Sci. (Chem.), Prof. Tatyana M. Buslaeva
Dr. Sci. (Chem.), Prof. Anatolii A. Ischenko
Dr. Sci. (Eng.), Prof. Valery F. Kornushko
Dr. Sci. (Eng.), Prof. Anatolii V. Markov
Dr. Sci. (Chem.), Prof. Yuri P. Miroshnikov
Dr. Sci. (Chem.), Prof. Vladimir A. Tverskoy
Desktop publishing Larisa G. Semernya

86, Vernadskogo pr., Moscow, 119571, Russian Federation.

Phone: +7(495) 246-05-55 (#2-88)

E-mail: seredina@mirea.ru

The registration number ПИ № ФС 77-74580 was issued in December 14, 2018 by the Federal Service for Supervision of Communications, Information Technology, and Mass Media of Russia.

The subscription index of *Pressa Rossii*: **36924**

**Тонкие химические технологии =
Fine Chemical Technologies
2022, том 17, № 4**

Научно-технический рецензируемый журнал «Тонкие химические технологии» освещает современные достижения фундаментальных и прикладных исследований в области тонких химических технологий, включая теоретические основы химической технологии, химию и технологию лекарственных препаратов и биологически активных соединений, органических веществ и неорганических материалов, биохимию и биотехнологию, синтез и переработку полимеров и композитов на их основе, аналитические и математические методы и информационные системы в химии и химической технологии.

Учредитель и издатель

федеральное государственное бюджетное

образовательное учреждение высшего образования

«МИРЭА – Российский технологический университет»

119454, РФ, Москва, пр-кт Вернадского, д. 78.

Периодичность: один раз в два месяца.

Журнал основан в 2006 году. До 2015 года издавался под названием «Вестник МИТХТ» (ISSN 1819-1487).

Журнал входит в Перечень ведущих рецензируемых научных журналов ВАК РФ.

Индексируется:

SCOPUS, DOAJ, Chemical Abstracts,

РИНЦ (Science Index), RSCI,

Ulrich's International Periodicals Directory

Главный редактор:

Тимошенко Андрей Всеволодович – д.т.н., к.х.н., профессор, МИРЭА – Российский технологический университет, Москва, Российская Федерация. Scopus Author ID 56576076700, ResearcherID Y-8709-2018, <https://orcid.org/0000-0002-6511-7440>, timoshenko@mirea.ru

Заместитель главного редактора:

Фомичёв Валерий Вячеславович – д.х.н., профессор, МИРЭА – Российский технологический университет, Москва, Российская Федерация. Scopus Author ID 57196028937, <http://orcid.org/0000-0003-4840-0655>, fomichev@mirea.ru

Выпускающий редактор:

Дураков Сергей Алексеевич – к.х.н., доцент, МИРЭА – Российский технологический университет, Москва, Российская Федерация, Scopus Author ID 57194217518, ResearcherID AAS-6578-2020, <http://orcid.org/0000-0003-4842-3283>, durakov@mirea.ru

Редакция:

Зав. редакцией к.т.н. Г.Д. Середина
Научные редакторы д.х.н., проф. Т.М. Буслаева
д.х.н., проф. А.А. Ищенко
д.т.н., проф. В.Ф. Корнюшко
д.т.н., проф. А.В. Марков
д.х.н., проф. Ю.П. Мирошников
д.х.н., проф. В.А. Тверской
Компьютерная верстка Л.Г. Семерня

119571, Москва, пр. Вернадского, 86, оф. Л-119.

Тел.: +7(495) 246-05-55 (#2-88)

E-mail: seredina@mirea.ru

Регистрационный номер и дата принятия решения о регистрации СМИ: ПИ № ФС 77-74580 от 14.12.2018 г. СМИ зарегистрировано Федеральной службой по надзору в сфере связи, информационных технологий и массовых коммуникаций (Роскомнадзор).

Индекс по Объединенному каталогу «Пресса России»: **36924**

Editorial Board

Andrey V. Blokhin – Dr. Sci. (Chem.), Professor, Belarusian State University, Minsk, Belarus. Scopus Author ID 7101971167, ResearcherID AAF-8122-2019 <https://orcid.org/0000-0003-4778-5872> blokhin@bsu.by.

Sergey P. Verevkin – Dr. Sci. (Eng.), Professor, University of Rostock, Rostock, Germany. Scopus Author ID 7006607848, ResearcherID G-3243-2011, <https://orcid.org/0000-0002-0957-5594>, sergey.verevkin@uni-rostock.de.

Konstantin Yu. Zhizhin – Corresponding Member of the Russian Academy of Sciences (RAS), Dr. Sci. (Chem.), Professor, N.S. Kurnakov Institute of General and Inorganic Chemistry of the RAS, Moscow, Russian Federation. Scopus Author ID 6701495620, ResearcherID C-5681-2013, <http://orcid.org/0000-0002-4475-124X>, kyuzhizhin@igic.ras.ru.

Igor V. Ivanov – Dr. Sci. (Chem.), Professor, MIREA – Russian Technological University, Moscow, Russian Federation. Scopus Author ID 34770109800, ResearcherID I-5606-2016, <http://orcid.org/0000-0003-0543-2067>, ivanov_i@mirea.ru.

Carlos A. Cardona – PhD (Eng.), Professor, National University of Columbia, Manizales, Colombia. Scopus Author ID 7004278560, <http://orcid.org/0000-0002-0237-2313>, ccardonaal@unal.edu.co.

Oskar I. Koifman – Academician at the RAS, Dr. Sci. (Chem.), Professor, President of the Ivanovo State University of Chemistry and Technology, Ivanovo, Russian Federation. Scopus Author ID 6602070468, ResearcherID R-1020-2016, <http://orcid.org/0000-0002-1764-0819>, president@isuct.ru.

Elvira T. Krut'ko – Dr. Sci. (Eng.), Professor, Belarusian State Technological University, Minsk, Belarus. Scopus Author ID 6602297257, ela_krutko@mail.ru.

Anatolii I. Miroshnikov – Academician at the RAS, Dr. Sci. (Chem.), Professor, M.M. Shemyakin and Yu.A. Ovchinnikov Institute of Bioorganic Chemistry of the RAS, Member of the Presidium of the RAS, Chairman of the Presidium of the RAS Pushchino Research Center, Moscow, Russian Federation. Scopus Author ID 7006592304, ResearcherID G-5017-2017, aiv@ibch.ru.

Aziz M. Muzafarov – Academician at the RAS, Dr. Sci. (Chem.), Professor, A.N. Nesmeyanov Institute of Organoelement Compounds of the RAS, Moscow, Russian Federation. Scopus Author ID 7004472780, ResearcherID G-1644-2011, <https://orcid.org/0000-0002-3050-3253>, aziz@ineos.ac.ru.

Редакционная коллегия

Блохин Андрей Викторович – д.х.н., профессор Белорусского государственного университета, Минск, Беларусь. Scopus Author ID 7101971167, ResearcherID AAF-8122-2019 <https://orcid.org/0000-0003-4778-5872> blokhin@bsu.by.

Верёвкин Сергей Петрович – д.т.н., профессор Университета г. Росток, Росток, Германия. Scopus Author ID 7006607848, ResearcherID G-3243-2011, <https://orcid.org/0000-0002-0957-5594>, sergey.verevkin@uni-rostock.de.

Жижин Константин Юрьевич – член-корр. Российской академии наук (РАН), д.х.н., профессор, Институт общей и неорганической химии им. Н.С. Курнакова РАН, Москва, Российская Федерация. Scopus Author ID 6701495620, ResearcherID C-5681-2013, <http://orcid.org/0000-0002-4475-124X>, kyuzhizhin@igic.ras.ru.

Иванов Игорь Владимирович – д.х.н., профессор, МИРЭА – Российский технологический университет, Москва, Российская Федерация. Scopus Author ID 34770109800, ResearcherID I-5606-2016, <http://orcid.org/0000-0003-0543-2067>, ivanov_i@mirea.ru.

Кардона Карлос Ариэль – PhD, профессор Национального университета Колумбии, Манизалес, Колумбия. Scopus Author ID 7004278560, <http://orcid.org/0000-0002-0237-2313>, ccardonaal@unal.edu.co.

Койфман Оскар Иосифович – академик РАН, д.х.н., профессор, президент Ивановского государственного химико-технологического университета, Иваново, Российская Федерация. Scopus Author ID 6602070468, ResearcherID R-1020-2016, <http://orcid.org/0000-0002-1764-0819>, president@isuct.ru.

Крутько Эльвира Тихоновна – д.т.н., профессор Белорусского государственного технологического университета, Минск, Беларусь. Scopus Author ID 6602297257, ela_krutko@mail.ru.

Мирошников Анатолий Иванович – академик РАН, д.х.н., профессор, Институт биоорганической химии им. академиков М.М. Шемякина и Ю.А. Овчинникова РАН, член Президиума РАН, председатель Президиума Пушкинского научного центра РАН, Москва, Российская Федерация. Scopus Author ID 7006592304, ResearcherID G-5017-2017, aiv@ibch.ru.

Музафаров Азиз Мансурович – академик РАН, д.х.н., профессор, Институт элементоорганических соединений им. А.Н. Несмеянова РАН, Москва, Российская Федерация. Scopus Author ID 7004472780, ResearcherID G-1644-2011, <https://orcid.org/0000-0002-3050-3253>, aziz@ineos.ac.ru.

Ivan A. Novakov – Academician at the RAS, Dr. Sci. (Chem.), Professor, President of the Volgograd State Technical University, Volgograd, Russian Federation. Scopus Author ID 7003436556, ResearcherID I-4668-2015, <http://orcid.org/0000-0002-0980-6591>, president@vstu.ru.

Alexander N. Ozerin – Corresponding Member of the RAS, Dr. Sci. (Chem.), Professor, Enikolopov Institute of Synthetic Polymeric Materials of the RAS, Moscow, Russian Federation. Scopus Author ID 7006188944, ResearcherID J-1866-2018, <https://orcid.org/0000-0001-7505-6090>, ozerin@ispm.ru.

Tapani A. Pakkanen – PhD, Professor, Department of Chemistry, University of Eastern Finland, Joensuu, Finland. Scopus Author ID 7102310323, tapani.pakkanen@uef.fi.

Armando J.L. Pombeiro – Academician at the Academy of Sciences of Lisbon, PhD, Professor, President of the Center for Structural Chemistry of the Higher Technical Institute of the University of Lisbon, Lisbon, Portugal. Scopus Author ID 7006067269, ResearcherID I-5945-2012, <https://orcid.org/0000-0001-8323-888X>, pombeiro@ist.utl.pt.

Dmitrii V. Pyshnyi – Corresponding Member of the RAS, Dr. Sci. (Chem.), Professor, Institute of Chemical Biology and Fundamental Medicine, Siberian Branch of the RAS, Novosibirsk, Russian Federation. Scopus Author ID 7006677629, ResearcherID F-4729-2013, <https://orcid.org/0000-0002-2587-3719>, pyshnyi@niboch.nsc.ru.

Alexander S. Sigov – Academician at the RAS, Dr. Sci. (Phys. and Math.), Professor, President of MIREA – Russian Technological University, Moscow, Russian Federation. Scopus Author ID 35557510600, ResearcherID L-4103-2017, sigov@mirea.ru.

Alexander M. Toikka – Dr. Sci. (Chem.), Professor, Institute of Chemistry, Saint Petersburg State University, St. Petersburg, Russian Federation. Scopus Author ID 6603464176, ResearcherID A-5698-2010, <http://orcid.org/0000-0002-1863-5528>, a.toikka@spbu.ru.

Andrzej W. Trochimczuk – Dr. Sci. (Chem.), Professor, Faculty of Chemistry, Wrocław University of Science and Technology, Wrocław, Poland. Scopus Author ID 7003604847, andrzej.trochimczuk@pwr.edu.pl.

Aslan Yu. Tsivadze – Academician at the RAS, Dr. Sci. (Chem.), Professor, A.N. Frumkin Institute of Physical Chemistry and Electrochemistry of the RAS, Moscow, Russian Federation. Scopus Author ID 7004245066, ResearcherID G-7422-2014, tsiv@phych.ac.ru.

Новаков Иван Александрович – академик РАН, д.х.н., профессор, президент Волгоградского государственного технического университета, Волгоград, Российская Федерация. Scopus Author ID 7003436556, ResearcherID I-4668-2015, <http://orcid.org/0000-0002-0980-6591>, president@vstu.ru.

Озерин Александр Никифорович – член-корр. РАН, д.х.н., профессор, Институт синтетических полимерных материалов им. Н.С. Ениколопова РАН, Москва, Российская Федерация. Scopus Author ID 7006188944, ResearcherID J-1866-2018, <https://orcid.org/0000-0001-7505-6090>, ozerin@ispm.ru.

Пакканен Тапани – PhD, профессор, Департамент химии, Университет Восточной Финляндии, Йоенсуу, Финляндия. Scopus Author ID 7102310323, tapani.pakkanen@uef.fi.

Помбейро Армандо – академик Академии наук Лиссабона, PhD, профессор, президент Центра структурной химии Высшего технического института университета Лиссабона, Португалия. Scopus Author ID 7006067269, ResearcherID I-5945-2012, <https://orcid.org/0000-0001-8323-888X>, pombeiro@ist.utl.pt.

Пышный Дмитрий Владимирович – член-корр. РАН, д.х.н., профессор, Институт химической биологии и фундаментальной медицины Сибирского отделения РАН, Новосибирск, Российская Федерация. Scopus Author ID 7006677629, ResearcherID F-4729-2013, <https://orcid.org/0000-0002-2587-3719>, pyshnyi@niboch.nsc.ru.

Сигов Александр Сергеевич – академик РАН, д.ф.-м.н., профессор, президент МИРЭА – Российского технологического университета, Москва, Российская Федерация. Scopus Author ID 35557510600, ResearcherID L-4103-2017, sigov@mirea.ru.

Тойкка Александр Матвеевич – д.х.н., профессор, Институт химии, Санкт-Петербургский государственный университет, Санкт-Петербург, Российская Федерация. Scopus Author ID 6603464176, ResearcherID A-5698-2010, <http://orcid.org/0000-0002-1863-5528>, a.toikka@spbu.ru.

Трохимчук Анджей – д.х.н., профессор, Химический факультет Вроцлавского политехнического университета, Вроцлав, Польша. Scopus Author ID 7003604847, andrzej.trochimczuk@pwr.edu.pl.

Цивадзе Аслан Юсупович – академик РАН, д.х.н., профессор, Институт физической химии и электрохимии им. А.Н. Фрумкина РАН, Москва, Российская Федерация. Scopus Author ID 7004245066, ResearcherID G-7422-2014, tsiv@phych.ac.ru.

CONTENTS

СОДЕРЖАНИЕ

**Chemistry and Technology
of Organic Substances**

Durakov S.A., Kolobov A.A., Flid V.R.
Features of heterogeneous catalytic
transformations of strained carbocyclic
compounds of the norbornene series

275

*Zotov Yu.L., Zapravdina D.M., Shishkin E.V.,
Popov Yu.V.*
Synthesis of stabilizers based on glycerides
of monocarboxylic acids for industrial
chloroparaffins

298

**Chemistry and Technology
of Medicinal Compounds
and Biologically Active Substances**

*Grebenkina L.E., Prutkov A.N., Matveev A.V.,
Chudinov M.V.*
Synthesis of 5-oxymethyl-1,2,4-triazole-
3-carboxamides

311

**Химия и технология
органических веществ**

Дураков С.А., Колобов А.А., Флид В.Р.
Особенности гетерогенно-каталитических
превращений напряженных карбоциклических
соединений норборненового ряда

*Зотов Ю.Л., Заправдина Д.М., Шишкин Е.В.,
Попов Ю.В.*
Синтез стабилизаторов на основе глицеридов
монокарбоновых кислот для промышленных
хлорпарафинов

**Химия и технология лекарственных
препаратов и биологически
активных соединений**

*Гребенкина Л.Е., Прутков А.Н., Матвеев А.В.,
Чудинов М.В.*
Синтез 5-оксиметил-1,2,4-триазол-
3-карбоксамидов

*Eshtukova-Shcheglova E.A., Perevoshchikova K.A.,
Eshtukov-Shcheglov A.V., Cheshkov D.A.,
Maslov M.A.*

Amination of epoxides as a convenient
approach for lipophilic polyamines synthesis

323

*Ештукова-Щеглова Е.А., Перевощикова К.А.,
Ештуков-Щеглов А.В., Чешков Д.А.,
Маслов М.А.*

Аминирование эпоксидов как удобный
способ синтеза липофильных полиаминов

Ha A.C., Nguyen T., Nguyen P.A., Nguyen V.M.
Antibacterial activity of green fabricated
silver-doped titanates

335

Ha A.C., Nguyen T., Nguyen P.A., Nguyen V.M.
Antibacterial activity of green fabricated
silver-doped titanates

Synthesis and Processing of Polymers and Polymeric Composites

Синтез и переработка полимеров и композитов на их основе

Nikolaev A.A., Kondratov A.P.
Method for hidden marking of transparent
polypropylene film

346

Николаев А.А., Кондратов А.П.
Скрытая маркировка прозрачной пленки
полипропилена

Chemistry and Technology of Inorganic Materials

Химия и технология неорганических материалов

Medennikov O.A., Shabelskaya N.P.
Technology for processing phosphogypsum
into a fluorescent dye
based on calcium sulfide

357

Меденников О.А., Шабельская Н.П.
Технология переработки фосфогипса
в люминесцентный краситель
на основе сульфида кальция

ISSN 2686-7575 (Online)

<https://doi.org/10.32362/2410-6593-2022-17-4-275-297>



UDC 547.315+544.478

REVIEW ARTICLE

Features of heterogeneous catalytic transformations of strained carbocyclic compounds of the norbornene series

Sergey A. Durakov[✉], Alexey A. Kolobov, Vitaly R. Flid

MIREA – Russian Technological University (M.V. Lomonosov Institute of Fine Chemical Technologies), Moscow, 119571 Russia

[✉] Corresponding author, e-mail: s.a.durakov@mail.ru

Abstract

Objectives. Catalytic processes involving norbornene (NBN) and norbornadiene (NBD) offer exceptional opportunities for the synthesis of a wide range of hard-to-reach polycyclic hydrocarbons. The problems of selectivity and manufacturability of these reactions are fundamentally important for their practical implementation. The aim of this review is to summarize the latest advances in the field of designing heterogeneous catalysts for the preparation and transformation of promising NBN- and NBD-derivatives with the maintenance of a strained carbocyclic framework in isomerization and dimerization reactions of these compounds.

Results. Various strategies for the selection of catalysts and prospects for the development of heterogeneous catalysis for syntheses based on NBN and NBD derivatives were considered. The possibility of selective cyclic dimerization and isomerization of NBN and NBD was shown. The factors that affect the direction of the reactions and make it possible to maintain the strained norbornane structure were discussed.

Conclusions. An analysis of the current state of this problem showed that at present, the technological parameters of the conversion of NBD and NBN derivatives with the participation of heterogeneous catalysts are significantly inferior to homogeneous systems. In order to improve the productivity of these processes and design catalyst regeneration, further investigations are required. However, some progress in these areas has already been made. In a number of processes, it is possible not only to maintain the strained carbocyclic framework, but also to

establish ways to control regio- and stereo-selectivity. In some cases, the use of heterogeneous catalysts allows the process to be direct into a completely new path, which has no analogues for homogeneous systems.

Keywords: norbornene, norbornadiene, heterogeneous catalysis, dimerization, isomerization, transition metals, zeolites, strained carbocyclic compounds

For citation: Durakov S.A., Kolobov A.A., Flid V.R. Features of heterogeneous catalytic transformations of strained carbocyclic compounds of the norbornene series. *Tonk. Khim. Tekhnol. = Fine Chem. Technol.* 2022;17(4):275–297 (Russ., Eng.). <https://doi.org/10.32362/2410-6593-2022-17-4-275-297>

ОБЗОРНАЯ СТАТЬЯ

Особенности гетерогенно-каталитических превращений напряженных карбоциклических соединений норборненового ряда

С.А. Дураков[✉], А.А. Колобов, В.Р. Флид

МИРЭА – Российский технологический университет (Институт тонких химических технологий им. М.В. Ломоносова), Москва, 119571 Россия

[✉]Автор для переписки, e-mail: s.a.durakov@mail.ru

Аннотация

Цели. Каталитические процессы с участием норборнена (НБН) и норборнадиена (НБД) открывают исключительные возможности для синтеза широкого круга труднодоступных полициклических углеводов. Проблемы избирательности и технологичности этих реакций принципиально важны для их практической реализации. Целью обзора является обобщение последних достижений в области создания гетерогенных катализаторов для получения и превращений перспективных НБН- и НБД-производных с сохранением напряженного карбоциклического каркаса в реакциях их изомеризации и димеризации.

Результаты. Рассмотрены различные стратегии подбора катализаторов и перспективы развития гетерогенного катализа для синтезов на основе НБН и НБД производных. Показана возможность селективного проведения циклической димеризации и изомеризации НБН и НБД. Обсуждены факторы, влияющие на направление реакций и позволяющие сохранять напряженную норборнановую структуру.

Выводы. Анализ современного состояния данной проблемы показывает, что в настоящее время технологические показатели процессов превращения НБД и НБН-производных с участием гетерогенных катализаторов существенно уступают гомогенным системам. Их оптимизация, увеличение производительности и регенерация катализатора требует дальнейшего изучения и совершенствования. Тем не менее, на данном этапе достигнуты определенные успехи. В ряде процессов удается не только сохранить напряженный карбоциклический каркас, но и установить пути управления регио- и стерео-селективностью. В некоторых случаях применение гетерогенных катализаторов позволяет направить процесс в совершенно новое русло, не имеющее аналогов для гомогенных систем.

Ключевые слова: норборнен, норборнадиен, гетерогенный катализ, димеризация, изомеризация, переходные металлы, цеолиты, напряженные карбоциклические соединения

Для цитирования: Дураков С.А., Колобов А.А., Флид В.Р. Особенности гетерогенно-каталитических превращений напряженных карбоциклических соединений норборненового ряда. *Тонкие химические технологии.* 2022;17(4):275–297. <https://doi.org/10.32362/2410-6593-2022-17-4-275-297>

INTRODUCTION

Norbornadiene (NBD), norbornene (NBN), and their derivatives hold an important place in organic and petrochemical synthesis [1]. Over a 70-year history, these compounds have found application in the perfume industry [2–5], medicine [6–9], agriculture [10–12], in the production of polymeric materials with unique properties [13–22], microelectronics, and photonics [23–27], as solar energy converters [28–34], fuels with different properties [35–47], and so on. The number of publications and patents related to the preparation and use of NBN and NBD derivatives exceeded 35000 in 2022. Due to their unique structure, these compounds are coming to the fore in modern chemistry and chemical technology (Fig. 1).

NBN, NBD, and some of their simplest derivatives have a reliable raw material base, since they are formed from large-scale products of oil or coal processing: dicyclopentadiene (DCPD), 1,3-cyclopentadiene (CPD), acetylene, alkenes, and alkadienes of various structures [46, 48–50]. The production of CPD can be easily combined with the production of other products, in particular, ethylene and isoprene [46, 51, 52]. Currently, not all CPD finds a qualified application, so the search for new promising ways to use it is very relevant. At the same time, the CPD itself can already now be obtained not only during the processing of oil fractions or the technology of indirect liquefaction of coal raw materials, but also by synthesis from natural products (Fig. 2) [53, 54].

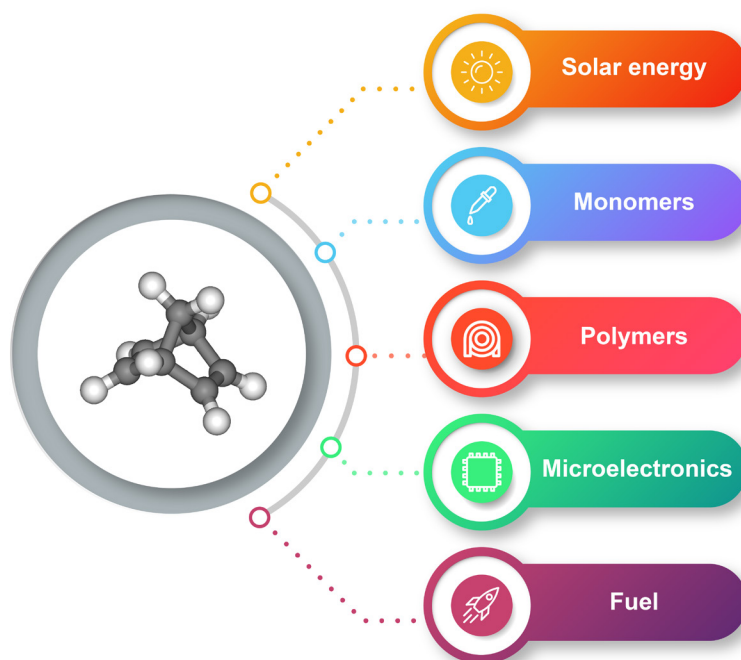


Fig. 1. Application areas of norbornene and norbornadiene derivatives.

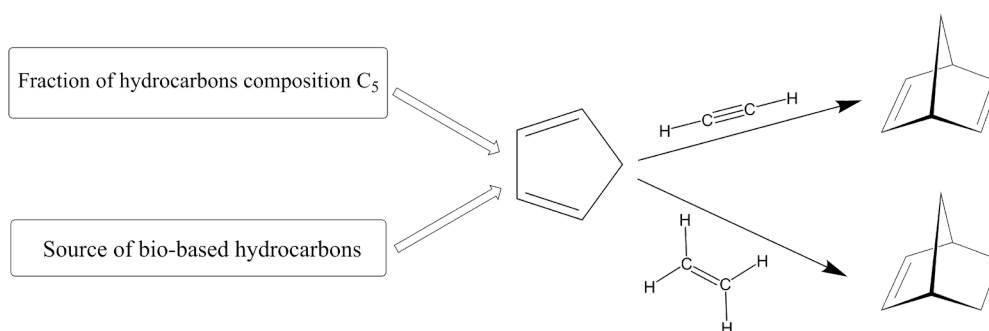


Fig. 2. Scheme of obtaining NBD and NBN.

Despite the extremely rich synthetic possibilities, the use of NBN and NBD derivatives as universal substrates is currently quite limited. The structural features of the norbornane carbocyclic skeleton suggest that such compounds have all types of isomerism: skeletal, regio-, stereo-, and enantio-isomerism. In real syntheses, this leads to the formation of mixtures of isomers. Difficulties in the separation of isomeric products with similar properties, their analysis, including the establishment of the structure of isomers, as well as modern problems of the rational use of reagents, largely limit the large-scale use of NBN and NBD. On the other hand, cycloaddition reactions (Fig. 3) involving NBD have unlimited possibilities for studying and implementing various directions and levels of isomerism. These circumstances can be very productive for developing new methods and approaches that solve the problems of manufacturability and selectivity of various levels in such processes.

At present, the vast majority of works on the synthesis of carbocyclic compounds based on NBN and NBD are associated with the use

of homogeneous metal complex catalysis. The application of its methods and approaches through the targeted selection of the metal, ligand environment and reaction conditions made it possible to determine the strategic directions for improving these processes.

Great progress has been made in the last 15–20 years, when systematic studies of the kinetics and mechanisms of reactions involving NBN and NBD began [55–59], and quantum chemistry methods began to be applied to such objects and processes [60–65]. The synergy of these intensively developing areas allows targeted developing and optimizing reaction conditions in order to obtain individual products and materials with special properties based on them. Further development of a strategy associated with a close combination of theoretical and experimental approaches will not only reduce labor intensity and optimize experimental studies, but will also allow a better understanding of the mechanisms of the investigating processes to create highly efficient catalysts.

In the same period, studies began on the development of heterogeneous catalytic systems,

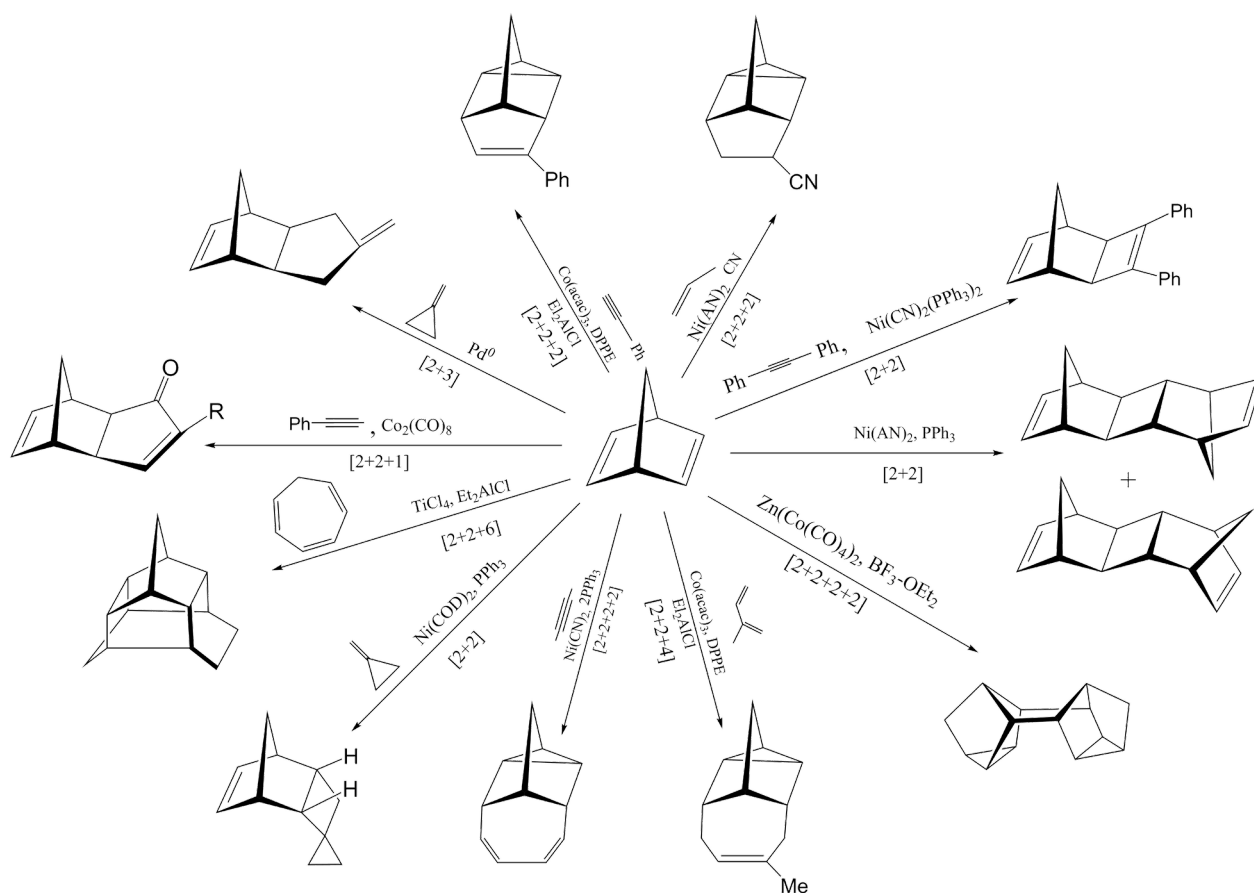


Fig. 3. Some catalytic codimerization reactions involving NBD.

which have undoubted technological advantages over homogeneous ones. The possibility of simple separation of the catalyst from the reaction products and the use of flow type reactors in the case of heterogeneous catalysis significantly increases the economic efficiency of such processes [66–68]. However, it should be emphasized here that the main and fundamental problem in the use of heterogeneous systems is the maintenance of the strained norbornane structure in the products. Heterogeneous catalysts exhibit activity under more severe conditions than homogeneous ones, which can lead to the destruction of the strained framework of NBN and NBD derivatives. In addition, the inhomogeneity of the surface and composition of the active centers of catalysts of this type leads to a significant decrease in their activity and selectivity compared to homogeneous systems [69].

Considering that the number of works in the field of catalytic chemistry of NBN- and NBD-derivatives is extremely large and synthetic aspects have been shown in a significant number of fundamental reviews and monographs [1, 29, 44, 70–76], in this work, emphasis is placed on the application and development of heterogeneous catalysis predominantly to the starting reagents. Consideration of the processes for obtaining polymeric materials based on NBN and NBD, as well as the catalytic transformations of quadricyclane (QC) and its derivatives obtained as a result of photochemical isomerization or decomposition of NBD, is beyond the scope of this work. If necessary, this and additional information can be obtained from [1, 20, 77, 78]. This review mainly considers the current state of heterogeneous catalytic transformations involving NBN, NBD and their derivatives, aimed at obtaining important monomers and intermediates that maintain the original norbornane structure and, if possible, an active double bond in the norbornene ring.

ISOMERIZATION OF NORBORNADIENE

Reversible valence isomerization of NBD to energy-rich QC is a promising solar energy storage reaction. It is known that during one hour the Sun gives more energy to the Earth's surface than people consume in a whole year, while most of it is simply inefficiently dissipated on the surface. In this regard, the ability to draw on this huge potential is an important stage in the development of the energy sector, and the creation of efficient technologies in this area is critically

needed. In the NBD→QC system, solar energy is accumulated and converted into a stored form at the molecular level, since as a result of the NBD→QC photoreaction, a metastable structure is formed containing highly stressed fragments: two cyclopropane and cyclobutane rings. In the future, the accumulated energy can be quickly released in the form of heat (110 kJ/mol) by the reverse catalytic reaction QC→NBD. Additional advantages of systems based on this reaction are that they bypass the problems associated with the batch type of energy production by solar panels, and the low molecular weight of NBD provides high efficiency and energy storage capacity (Fig. 4)

Despite the fact that several fundamental reviews have been devoted to the NBD↔QC system [28–31, 79], it is constantly being improved in terms of optimizing the conditions for both the direct photoreaction and the reverse catalytic process.

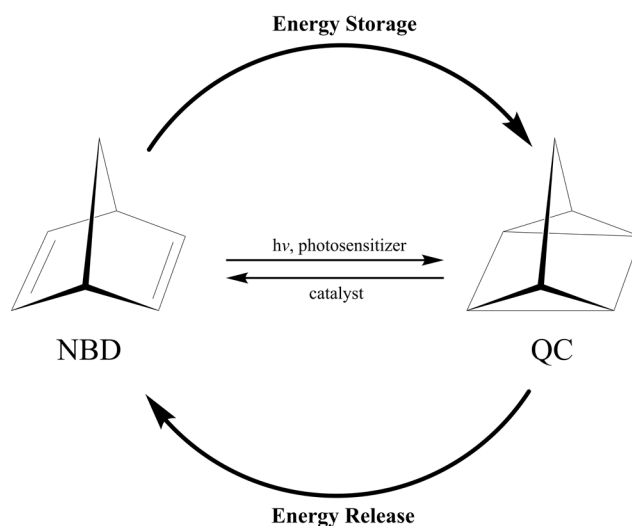


Fig. 4. Scheme of isomerization in the NBD↔QC system.

Direct isomerization of NBD→QC

NBD isomerization to QC occurs upon irradiation, but NBD molecules cannot directly absorb solar energy. This isomerization is facilitated by sensitizers or photocatalysts. In this regard, to implement this process, scientists used Michler's ketones, benzophenone, as well as CuCl_2 and Ru compounds in this reaction [78, 80, 81]. Despite the fact that these sensitizers exhibit high activity and selectivity, they have a number of disadvantages, in particular, they are unstable under irradiation and prone to decomposition. Homogeneous sensitizers are soluble in the

solution of the reagent itself, which makes it difficult to recycle and purify the product. From the point of view of practical application, heterogeneous photocatalysts are more advantageous. Initially, it was reported that semiconductors, including ZnO, ZnS, and CdS, can catalyze $\text{NBD} \rightarrow \text{QC}$ isomerization [82] with yields up to 90–100%; however, during their operation, sulfur is washed out into the reaction mass. Subsequently, it was reported that Y zeolites substituted with K^+ , Cs^+ , and Tl^+ ions also sensitize the process due to the heavy atom effect [83]. In this case, the reagent is pre-adsorbed in the micropores of the support. Attempts have been made to use Y zeolites with the exchange of La, Cs, Zn and K for the photoisomerization of NBD in the liquid phase. It was found that LaY exhibits a relatively high activity [84], which is explained by the heavy atom effect and the presence of Brønsted acid sites.

These approaches to the heterogenization of catalysts for the direct reaction were significantly improved in [85–88], where titanium-containing materials were synthesized in the pores of MCM-41¹ silica gel in order to replace homogeneous analogues. Initially, chemical grafting of titanium dioxide led to the formation of fine quantum size TiO_2 crystallites in the pores of MCM-41. Isomorphic substitution leads to inclusion of Ti into the framework, which disrupts the ordered porous structure of MCM-41; however, with an increase in the Ti content, some non-framework Ti particles are formed. It has been found that Ti-containing materials based on MCM-41 silica gel exhibit a significantly higher photocatalytic activity than bulk TiO_2 , and framework Ti particles are more active than surface-dispersed particles. For the photocatalytic reaction, the yield of the $\text{NBD} \rightarrow \text{QC}$ reaction exceeds 90%, but with an increase in the amount of Ti particles in the system in the series: $\text{Ti-MCM-41(30)} > \text{Ti-MCM-41(50)} > \text{TiO}_2\text{-MCM-41} > \text{Ti-MCM-41(70)} > \text{TiO}_2$, a decrease in the yield to 30% is observed, since it is the isolated Ti framework particles that are the most active. Doping of this system with ions of various metals (V, Fe, Ce, Cu, Cr) makes it possible to increase the activity of the catalytic system by an order of

magnitude in the photomeasurement of NBD in QC. At the same time, the efficiency of the systems decreases in the series: $\text{Fe-TiO}_2 > \text{V-TiO}_2 > \text{Cr-TiO}_2 > \text{Ce-TiO}_2 > \text{TiO}_2 > \text{Cu-TiO}_2$. It is assumed that the local structure and type of dopant are critical, since photoreactivity correlates with the amount of oxygen on the lattice surface.

Reverse isomerization of $\text{QC} \rightarrow \text{NBD}$

To realize the main advantage of the $\text{NBD} \leftrightarrow \text{QC}$ system, namely, the release of stored energy on demand, an efficient method for the reverse isomerization of QC to NBD derivatives is required. Thermal initiation is possible for this process, but it is not favorable for energy reasons. From a practical point of view, an induced catalytic back reaction is more desirable. Previously, most approaches used catalysis using unsaturated coordination complexes of transition metals and metal oxides, such as MoO_3 , WO_3 , V_2O_5 , and copper(II) sulfate [29, 89–91]. In these cases, the reverse reaction usually proceeds through the oxidized form of QC, which is why only a few of these types of catalysts meet the most important technological requirements, such as the absence of side reactions, high turnover rates and long-term stability. The most promising results were obtained for square planar Co(II) complexes [92, 93], which became the starting point for creating heterogeneous catalysts based on them. Using approaches to immobilization of homogeneous catalysts, Co(II) compounds were grafted onto various oxide and carbon supports [94–97]. Among them, cobalt phthalocyanine complexes covalently bonded to silica gel showed the highest efficiency in combination with stability to immobilization. The valence isomerization of quadricyclane to norbornadiene in the presence of such a catalyst proceeds at a temperature of 0–60°C both in an indifferent solvent and in a bulk of QC with conversions up to 100% and reaction selectivity up to 99.9%. The number of catalytic cycles varies in the range from 10000 to 40000 depending on the composition of the catalyst. However, in addition to the aspect of purification of the reaction mass from the catalyst, it is also necessary to take into account the activity of the immobilized catalyst, because, depending on the material of the solid support, access to the active centers of the catalyst can be difficult. The technical application of systems of the $\text{NBD} \leftrightarrow \text{QC}$ type requires the development of simple, reliable, inexpensive and efficient methods for each stage of the reversible isomerization of the NBD-QC system along with easy purification. In this regard, in recent years, interest has increased in metal

¹ MCM-41 (Mobil Composition of Matter No. 41) is a mesoporous material with a hierarchical structure with a hexagonal array of unidirectional and non-communicating pores from a family of silicate and aluminosilicate solids, which were first developed by researchers at Mobil Oil Corporation (USA) and can be used as catalysts or catalyst carriers.

oxide nanoparticles, which are an excellent platform for solving this problem due to the high surface-to-volume ratio compared to bulk material [98], the possibility of tuning their surface properties [99], and the simplicity of their synthesis. Systems of the Fe_3O_4 -CoCat type synthesized in this way, which are complexes of cobalt (Co) with salphene and phthalocyanine ligands (Cat) immobilized on iron oxide nanoparticles (Fe_3O_4), turned out to be able to catalyze the reverse reaction of QC isomerization in NBD, showing excellent characteristics with high the initial turnover frequency of the catalyst is up to 3.64 s^{-1} and the turnover number is more than 3305 [100, 101]. However, a solvent dependent catalyst performance was observed, whereby a more polar and coordinating solvent degraded the catalyst performance. A comparison of all currently available heterogeneous catalytic systems for the isomerization reaction of QC derivatives in NBD is presented in Table 1.

Analyzing the achievements in direct and reverse isomerization in the $\text{NBD} \leftrightarrow \text{QC}$ system, we can say that significant progress has been made in both directions in recent years. Efficient ways of photosensitization have been developed using metal complexes or various photosensitizers, while the activity of catalytic systems is maintained over a large number of cycles. Undoubtedly, systems using 2,3-disubstituted NBD derivatives, which can absorb solar energy not in the ultraviolet, but in the visible light range ($\lambda > 400 \text{ nm}$), come to the fore in the issue of solar energy absorption. However, due to the importance of the $\text{NBD} \leftrightarrow \text{QC}$ system in other areas: as molecular switches, optical waveguides, chemosensors, photo-switchable materials and fuels, a number of more technologically advanced heterogeneous catalysts have recently been developed that can achieve 100% selectivity and conversion for the direct as well as the reverse reaction. However, despite the undeniable advantage of using heterogeneous catalysts and the statements of researchers about the absence of negative side processes, there is usually practically no information in publications about the technological parameters of such catalytic systems: the turnover number of catalyst, conversion, selectivity, etc.

DIMERIZATION OF NBN AND NBD

Depending on the number of active bonds and the type of substituents in the molecule, NBN- and NBD-derivatives can participate in

various $[2\pi+2\pi]$, $[2\pi+4\pi]$, and $[4\pi+4\pi]$ type cycloaddition reactions, which leads to the diversity and complexity of the resulting dimers. Figure 5 shows the structures of the main possible dimers of NBN and NBD [72, 74, 102]. However, it should be noted that although the formation of NBD **4**, **5**, and **6** isomers, as well as NBN **26**, **27**, and **28** isomers is purely theoretically possible, these isomers have not yet been obtained in practice, since their formation is energetically less favorable [1].

Dimerization of NBN, NBD and their derivatives is usually widely used in the field of fuel technology [43]. In particular, some NBD dimers have high densities and high volumetric net calorific values, making them good candidates for high density fuels. High-density hydrocarbon fuels are key materials for increasing range and payload for aircraft with limited fuel tank capacity. However, in addition to the wide use of norbornyl polycyclic compounds as various fuels, dimerization products of NBN and NBD derivatives are already being used in biology [103] and in the development of new multifunctional materials [104–106]. Thus, studies of the dimerization of NBD and its derivatives are of great academic and industrial importance, especially for the purpose of highly selective production of individual stereoisomers. In recent decades, research in this area has developed greatly. At the moment, the amount of literature on the dimerization of NBN, NBD, and their derivatives is extremely large, and relative synthetic aspects have already been systematically developed in many reviews and articles, in particular, in the recently published review [44]. Nevertheless, the synthetic possibilities of such processes are insufficiently realized. This is equally related to both the low selectivity of obtaining individual isomers and the difficulties of separating their mixtures and the need to remove the catalyst from the reaction mass. In this regard, in this review, we have focused in detail on the problem of creating heterogeneous catalysts for reactions of this type.

Dimerization of NBD

Cyclodimerization of NBN and NBD derivatives always proceeds in the presence of a catalyst. As in the case of NBD valence isomerization in QC, the first and best studied catalysts are systems based on transition metal complexes [1, 2, 74, 102, 107]. As a rule, these are complex compounds of Ni, Co, Fe, and Rh in the lowest oxidation states. Separate examples of the use of Cr, Ti, Pd and Ir compounds

Table 1. Isomerization catalysts of the NBD \rightleftharpoons QC system

Isomerization NBD \rightarrow QC						
Catalyst	Conversion, %	Selectivity, %	TON*	T, °C**	Reaction time, h	Link
ZnO, ZnS, CdS, Ge	90–100	—	—	30	28–32	[82]
LaY (t) > LaY > CsY > ZnY > KY	35–83	100	—	—	7.0	[84]
Ti-MCM-41(30) > Ti-MCM-41(50) > TiO ₂ -MCM-41 > Ti-MCM-41(70) > TiO ₂	35–91	~100	—	25	12.0	[85]
Fe-TiO ₂ > V-TiO ₂ > Cr-TiO ₂ > Ce-TiO ₂ > TiO ₂ > Cu-TiO ₂	63–83	~100	—	—	4.0	[86, 87]
Isomerization QC \rightarrow NBD						
Catalyst	Conversion, %	Selectivity, %	TON*	T, °C**	Reaction time, h	Link
CuSO ₄	75	—	—	70	24.0	[91]
MoO ₃ , WO ₃ , V ₂ O ₅ , and other oxides	100	~100	—	28	24.0	[89]
CoPc(C ₂ NEt ₂)/SiO ₂ ²	up to 100	99.9	up to 40000	0–60	0.5–1.0	[96]
Fe ₃ O ₄ -CoSalphen ³	100	100	more than 3305	25–110	1.0	[100]
Fe ₃ O ₄ -Cat3	100	100	more than 3305	25	0.5–1.0	[101]

* TON – Turnover number.

** Temperature of the process.

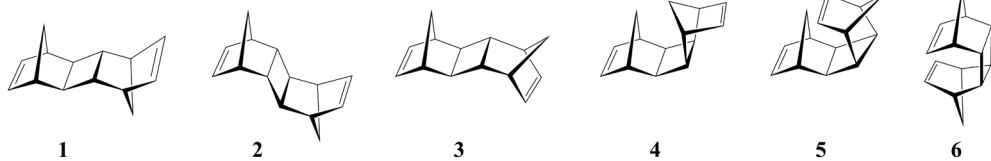
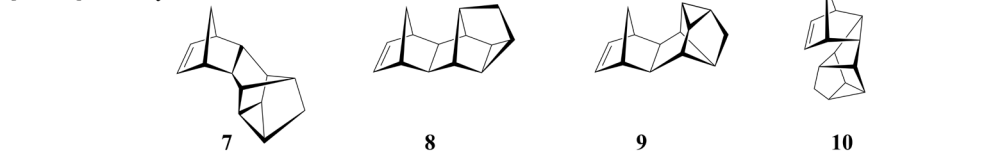
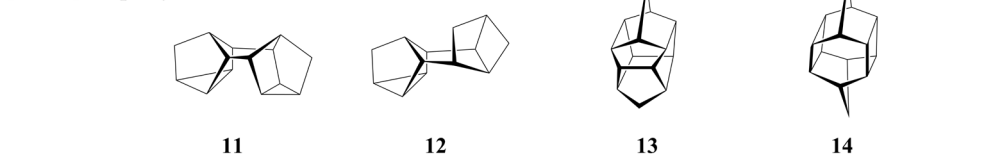
are also known. Depending on the type of metal used and its ligand environment, it is already quite selective to obtain paired mixtures of substances or individual isomers with a high substrate conversion (Table 2).

In order to improve the manufacturability of the process of cyclodimerization of NBN- and

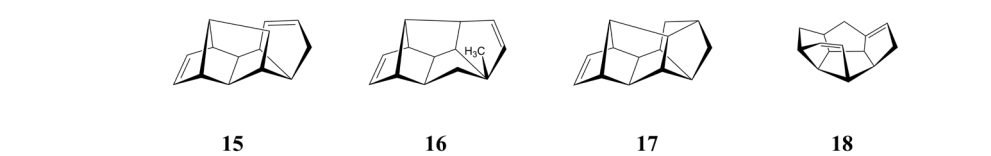
NBD-derivatives, various heterogeneous catalysts have been created and tested in recent years. The first among them were catalysts in the form of rhodium on a carbon support [108, 109]. The result of catalytic dimerization of NBD in the presence of 5% Rh/C catalyst is a mixture containing 57% *endo-endo* **7** and 8%

² Pc – phthalocyanine.³ Salphen – *N,N'*-phenylenebis(salicylideneimine).

NBD Dimers

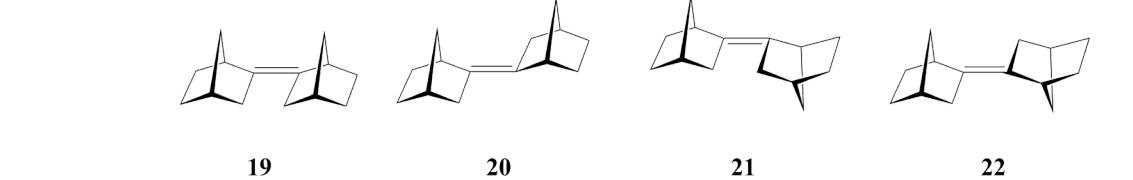
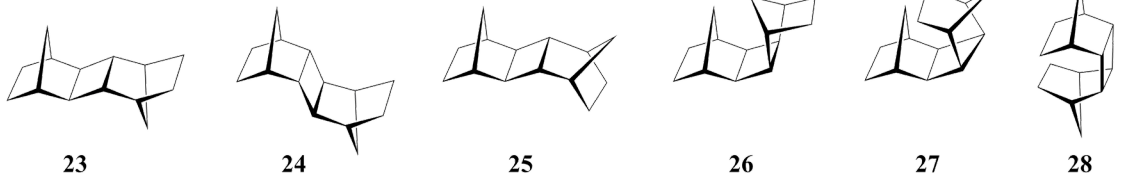
[2 π +2 π] - pentacyclic[2 π +4 π] - hexacyclic[4 π +4 π] - heptacyclic

Isomers



NBN Dimers

Isomers of 2,2'-bisorbornylidene

[2 π +2 π] - pentacyclic

Isomers

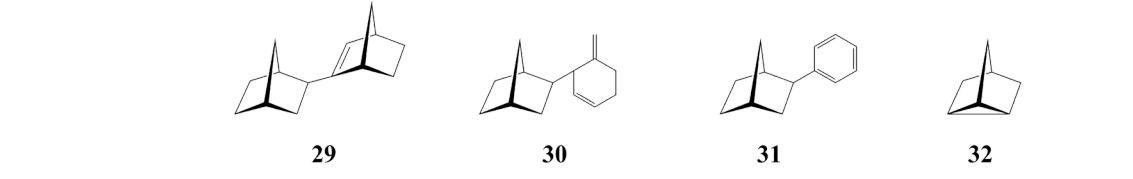
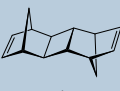
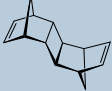
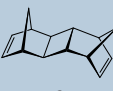
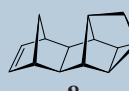

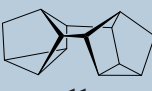


Fig. 5. Structures of NBN and NBD dimers.

exo-endo **9** dimers and 25% trimers as main products. Further development of this direction occurred more than 20 years later, when it was reported on the use of transition metals supported on zeolite as NBD dimerization catalysts [110]. Transition metals were introduced into the zeolite by ion exchange and impregnation using $\text{Ni}(\text{NO}_3)_2$, $[\text{Rh}(\text{NH}_3)_5\text{Cl}]\text{Cl}_2$, RhCl_3 , and PdCl_2 as precursors. The main reaction product in this case is *exo-endo* dimer **9**, together with a small amount of *endo-endo* (**7**) and *exo-trans-exo* (**1**) dimers. Alcohols and ethers are also formed in trace amounts. The effect of the precursor structure, preparation methods, and pretreatment temperature on activity and selectivity was studied. Various types of zeolites were used as carriers for the main component of the catalysts. On a 0.3% $\text{Rh}/\text{Na-TsVM}^4$ catalyst prepared by ion exchange using RhCl_3 as a precursor, the highest selectivity for the formation of NBD dimers (97%) was achieved: 82% of dimer **9** and 15% of dimer **7**. However, the conversion of NBD did not exceed 50% after 3 h reaction at 130°C. In the presence of Rh ions or acid sites, the dimerization of NBD leads to side reactions—the formation of alcohols and esters. Most likely, this is due to the hydration of NBD with water on the acid sites of the zeolite. The temperature of catalyst pretreatment and reaction also affects its selectivity. An important effect can be exerted

by water, which participates in the NBD hydration reaction and changes the adsorption behavior of the zeolite. With an increase in the pretreatment temperature, the yield of dimers increases, while the yield of alcohols and ethers decreases significantly. Changes in the activity of the catalyst during its treatment with hydrogen over a wide temperature range allowed the authors to suggest that the main active species in the dimerization of NBD are centers in which Rh is in the +1 oxidation state. When bulky ligands, such as triphenylphosphine (TPP), which cannot penetrate the zeolite channel, are added to the catalytic system, the reactivity is significantly reduced. Taking into account the strong coordination ability of TPP with rhodium atoms, it was concluded that the dimerization reaction occurred on the surface of the zeolite. In addition, in the presence of TPP, heptacyclic dimer **11** appeared among the reaction products, which is also formed during NBD dimerization using the $[\text{Rh}(\text{NBD})\text{CF}_3\text{COO}]_2\text{-TPP}$ catalytic system [111]. It was suggested that TPP in the Rh–zeolite catalytic system can change the type of cycloaddition from $[2\pi+4\pi]$ to $[4\pi+4\pi]$, as occurs during catalysis by the $[\text{Rh}(\text{NBD})\text{CF}_3\text{COO}]_2$ complex. The Rh-containing zeolite probably catalyzes the process similarly to the homogeneous Rh(I) complex. Thus, at the initial stage, much

Table 2. Achievements of homogeneous catalysis in NBD dimerization

Conditions for obtaining	Dimer					
	 1	 2	 3	 8	 10	 11
Catalyst active site	[Ni]	[Ni]	[Ni]	[Fe]	[Fe], [Co]	[Co–Zn]
Maximum isomer yield, %	95	20	90	60–75	50–75	95
Selectivity, %	98	25	95	75	75	98
TON*	8000	5000	5000	5000	5000	3500

* TON – Turnover number.

⁴ Na-pentasil, analog of pentasil ZSM-5 (see below), synthesized without an organic matrix, ratio $\text{SiO}_2/\text{Al}_2\text{O}_3 = 33.3$.

attention was paid to the development of Rh-containing heterogeneous catalysts, such as Rh/C, Rh/zeolites. Heterogeneous catalysts based on Rh have good selectivity for *endo-endo* (**7**) and *exo-endo* (**9**) dimers (65% and 82%, respectively). However, their activity is much lower than that of homogeneous catalytic systems. It should be noted separately that Rh complexes can catalyze NBD dimerization with the selective formation of *exo-endo* dimer **9**, which is not formed in the presence of other transition metal catalysts.

Further development of this direction led to the creation of heterogeneous catalysts based on nickel. As expected, the catalysts obtained by impregnating polystyrene with Ni salts followed by their high-temperature reduction with heavy paraffins [112] show rather high activity and selectivity with respect to pentacyclic dimers [113, 114].

By applying bis(η^3 -allyl)nickel onto phosphinated polystyrene containing a different number of coordinating centers, a catalyst similar to the homogeneous $\text{Ni}(\text{NBD})_2$ -phosphine system was obtained in terms of specific activity and selectivity of action with respect to individual isomers. Its productivity was 120–150 g/h of dimers per liter of solution. The catalyst itself is regenerated with molecular hydrogen followed by washing with toluene. The time of continuous operation of the catalyst without regeneration reaches 40–50 h. The catalyst showed a rather high productivity, however, it was still lower than that typical for homogeneous systems by a factor of 1.8–2.5.

Further development of the direction of heterogenization of homogeneous metal complexes led to the creation of a catalyst in which Pd(0) was heterogeneously supported on a silica support with the content of polyethylene glycol (PEG) controlled to increase its stability and the possibility of reuse with a limited decrease in the activity and selectivity of dimers. The

structure of the silica support was tuned to achieve proper interaction with PEG and the Pd(0) complex. Chain length and PEG concentration were adjusted to further optimize the state of the Pd(0) complex on silica. The developed heterogeneous Pd(0) complex deposited on PEG2000⁵ controlled dendritic mesoporous silica nanospheres demonstrated excellent performance for the production of high energy density fuels through the selective codimerization of NBD with QC, with an 80% yield in a nitrogen atmosphere at a temperature of 110°C, dimer **8** was obtained [115]. However, even though the authors of this work managed not only to reduce the proportion of inactive Pd(II) catalyst particles and the aggregation of active Pd(0) particles in this reaction due to PEG, the time stability of heterogenized catalysts for dimerization processes continues to be a stumbling block. when creating effective technologies based on them.

Recently, there has been an active interest in the use of various zeolites as catalysts for the dimerization of NBN, NBD, and their derivatives.

The use of zeolites HY⁶, H β ⁷, HZSM-5⁸, Al-MCM-41⁹, KIT-6¹⁰, and Co/HY¹¹ [116–120] in the dimerization of NBD leads not to the formation of traditional products **23–28**, but to the formation of 4 stereoisomers 2,2'-binorbornylidene **19–22** and, in some cases, to isomers **29–31**. The activity of zeolites largely depends on the reaction temperature, and as it increases from 100 to 250°C, the NBD conversion increases from 2% to 42%. Among zeolite catalysts, HY shows the highest yield of NBD dimers. This is probably due to the combination of the high concentration of Brønsted acid sites and the suitable pore structure of the HY zeolite. When HY zeolite is impregnated with cobalt salts, the concentration of Brønsted acid sites decreases, while that of Lewis sites, on the contrary, increases. The conversion of NBD

⁵ PEG 2000 is a high-quality ethylene glycol polymer with a molecular weight close to 2000 a.u.

⁶ HY is a hydrogen-type molecular zeolite catalyst with a Y-type crystal structure, is a faujasite molecular sieve with a pore diameter of 7.4 Å and a three-dimensional pore structure, which is directly calcined by the ammonium exchange of the NaY synthetic molecular sieve. The basic structural units of Y zeolites are sodalite cells, which are arranged in such a way that they form supercells large enough to accommodate spheres with a diameter of 1.2 nm.

⁷ H β is a hydrogen-type molecular zeolite catalyst with the β -crystal structure, which is a microporous crystalline aluminosilicate with a three-dimensional system of pores, the intersecting channels of which are formed by 12-membered rings with a diameter of 0.67 nm.

⁸ H-ZSM-5 is the H-form or proton type of ZSM-5 zeolite (see below).

⁹ Al-MCM-41 belongs to the ExxonMobil M41S family of mesoporous molecular sieves.

¹⁰ KIT-6 is a high quality mesoporous silica molecular sieve available from ACS Material (USA). KIT-6 has a bicontinuous cubic mesostructure with Ia3d symmetry and an interpenetrating cylindrical pore system.

¹¹ Co/HY is a cobalt catalyst supported on a hydrogen-type molecular zeolite catalyst with a Y-type crystal structure.

and the yield of dimers on Co/HY were higher than on the HY catalyst, which was explained by the presence of a high concentration of Lewis acid sites [118].

In [119], the efficiency of mesoporous aluminosilicate Al-KIT-6¹² containing both Lewis and Brønsted acid sites for NBD dimerization was studied. The influence of the nature of acid sites and the structure of pores on the activity of the catalyst and selectivity for dimers is described. The catalyst can be reused, but the yield of NBD dimers turned out to be low (<40%).

By applying the Co–Ni metals by the impregnation method on Al–MCM-41, MCM-48¹³, and γ -alumina, it was possible to carry out the dimerization of NBD with yields up to 85%. The activity of the supported Ni/Al–MCM-41 catalyst turned out to be much higher than that of MCM-48 and γ -Al₂O₃. The catalyst itself can be easily reduced and regenerated by filtration and calcination [121].

The advantages of zeolite catalysts are their low cost, reproducibility and reusability. But their disadvantages are also obvious. Not only the conversion of NBD, but also the selectivity of dimers on such catalysts is much lower than in the case of homogeneous catalysis with transition metals. The highest yield achieved on HY or Co/HY is 40–50%. In addition, the distribution of NBD isomeric dimers is complex, not all of them have been fully identified.

When a Cr/SiO₂ catalyst is used, the indicators are slightly higher: *exo-trans-exo* isomer **1** is formed [122]. The conversion reaches 85% and the selectivity is about 76%. The performance of this zeolite catalyst is also somewhat higher.

Dimerization of NBN

The number of published data on the dimerization of NBN itself is currently much less. This process has been well studied only for porous materials: zeolites and supported SiO₂/Cr catalysts [109, 122–127].

Patent [122] describes a method for obtaining reduced CrO₃ on large-pore silica gel,

¹² Al-KIT-6 is an aluminum-substituted mesoporous material KIT-6.

¹³ MCM-48 (Mobil Composition of Matter No. 48) is a mesoporous material with a hierarchical structure with a three-dimensional cubic pore structure from the family of silicate and aluminosilicate solids, which were first developed by researchers at Mobil Oil Corporation (USA) and can be used as catalysts or catalyst carriers.

which allows NBN dimerization according to the $[2\pi+2\pi]$ type to obtain a saturated *exo-trans-exo* isomer **23**, while a 71% yield of NBN dimers was achieved, among of which the content of dimer **23** is 85%. In the presence of zeolites of the ZSM family (Zeolite Socony Mobil), including MSM-22¹⁴, PSH-3¹⁵, SSZ-25¹⁶, and H β zeolites, compounds **19–22** are the main products [123]. The NBN conversion in the presence of ZSM-5 zeolite reaches 81% at room temperature in a nitrogen atmosphere. The selectivity of the oligomers exceeds 95%, of which 79% are NBN dimers and 21% are trimers. Under similar conditions for zeolite H β , the selectivity for NBN dimers decreases to 70%.

In [125], the influence of the porous structure of zeolites and reaction conditions on the selectivity of NBN dimerization was studied. It has been shown that in chloroalkanes in argon, the NBN conversion reaches 100%, and the dimer selectivity is 90% in the presence of HZSM-12¹⁷ and H β zeolites.

When using ZSM-5¹⁸, the NBN conversion was 5%, which is explained by the lower concentration of “strong” acidic sites and the narrow pore size of the zeolite. The direct channel diameter in HZSM-12 is 0.56–0.67 nm, while for ZSM-5 this value is 0.51–0.56 nm. Therefore, bulky NBN dimers are practically not formed on ZSM-5; only smaller isomerization products are formed on them, in particular, QC, however, the mechanism of its production has not been described.

The possibility of using amorphous mesoporous aluminosilicates ASM-40¹⁹ in this

¹⁴ MCM-22 is a type of MWW zeolite with a pore size of 10-MR and a layered structure with two independent pore channels. One consists of two-dimensional sinusoidal slightly elliptical 10-MR channels, and the other has a supercylindrical 12-MR cage between the layers.

¹⁵ PSH-3 is a zeolite with the chemical formula M₂/nO·Al₂O₃·(20–150)SiO₂, where M is an *n*-valent cation.

¹⁶ SSZ-25 is a zeolite with the chemical formula (from 0.1 to 2.0) (Q₂O·(0.1–2.0)M₂O·W₂O₃·(20–200)YO₂, where M is an alkali metal cation, W is aluminum, gallium, iron, boron and/or mixtures thereof, Y is silicon, germanium and/or mixtures thereof, and Q is the quaternary ammonium ion adamantane.

¹⁷ HZSM-12 is a hydrogen-type molecular zeolite catalyst, which is a silica-rich zeolite with a one-dimensional 12-member system of annular channels and a pore opening of 5.7 × 6.1 Å, which is slightly larger than that of ZSM-5 (see below).

¹⁸ ZSM-5—Zeolite Socony Mobil-5, patented by Mobil in 1975 with the chemical formula Na_nAl_nSi₉₆–nO₁₉₂·16H₂O (0 < *n* < 27).

¹⁹ ASM-40 is a mesoporous aluminosilicate with an atomic ratio of Si/Al = 40.

reaction was also reported [126]. NBN is selectively converted to dimers **19–22**, QC, and part of trimers in 40%, 24%, and 31% yields, respectively. On heterogeneous catalysts such as zeolite and amorphous mesoporous aluminosilicate, dimers **19–22** are the main components of the products. The possibility of reuse, stability and catalytic activity of zeolite catalysts is higher than that of metal complexes. In particular, under the conditions of catalysis with ZSM-12²⁰ and H β zeolites, the yield of NBN dimers exceeds 90% within one hour, which meets the requirements of green chemistry and industrial economy. However, these heterogeneous catalysts are sensitive to water and oxygenated compounds. An urgent task at the moment is to increase their resistance to oxygen.

In [127], the authors performed dimerization of NBN on zeolites with acid sites. The influence of the structure of the acidic properties of zeolites on the catalytic properties and selectivity of dimeric products was studied. The results indicate that, at the first stage, NBN isomerization occurs to give isomeric product **32** (nortricyclene), which then turns into dimers **19–22**.

Among acid zeolites, H β -25²¹ shows the best performance in NBN conversion and dimer selectivity due to the synergistic effect of the appropriate ratio of Brønsted and Lewis acid sites (B/L) and suitable pore size. Under optimal reaction conditions (140°C, 8 h, H β -25), an NBN conversion of 99.5% was achieved, and the dimer selectivity was 72.9%.

It should be noted that it is difficult to selectively synthesize [2+2]-cyclodimers using NBN dimerization. On the other hand, NBN dimerization in the presence of tungsten complexes or H-type zeolites can lead to four stereoisomers **19–22** containing the bis-2,2'-norbornylidene structure, which can also be used as an additive for fuels with high energy density. Thus, we can conclude that the currently available modified acid zeolite systems make it possible to maintain the norbornene structure during the heterogeneous catalytic dimerization of NBN.

Heterogeneous catalytic systems for the dimerization reactions of NBN and NBD derivatives, as well as their comparative characteristics, are presented in Table 3.

²⁰ ZSM-12 is a silica-rich zeolite with a one-dimensional 12-member system of annular channels and a pore opening of 5.7×6.1 Å, which is slightly larger than that of ZSM-5.

²¹ H β -25 is a hydrogen-type molecular zeolite catalyst H β with a frame ratio Si/Al = 25.

Analyzing the data in Tables 2 and 3, it can be seen from Fig. 3 that only a part of the structural dimers can be efficiently synthesized at present. Given the significant differences in the properties of various stereoisomers, the controlled synthesis of purer spatial dimers based on a combination of experimental and theoretical methods has broad research prospects. With a view to a more industrially oriented practical application, studies of catalytic systems for these processes have gradually moved from homogeneous metal complexes to heterogeneous catalysts. For NBD dimerization, the catalytic performance of heterogeneous catalysts is significantly lower than that of metal complex systems that have already become classical. On the other hand, the use of H β and HZSM-12 zeolites in NBN dimerization has already shown great success. Interestingly, the tiny difference in structure between NBD and NBN leads to a completely different course of the dimerization process. It is worth noting the progress in the field of creating heterogenized catalytic systems, which makes it possible to obtain dimers with a selectivity close to homogeneous systems. However, most works on the heterogeneous dimerization of NBN and NBD do not describe such important parameters as [67]: the real structure of the catalyst, its technological parameters, the possibility of its recycling, turnover frequency, as well as an important aspect in the immobilization of metal complexes—the problem of leaching of active particles, often changing the mechanism process, as well as contamination of products with metal particles [128–131]. In the future, the development of a new type of efficient heterogeneous catalyst or improvement of the recycling characteristics of metal complexes for dimerization of NBD is an urgent task, while it is important not to forget to investigate the exact mechanism of the catalyst.

CONCLUSIONS

In recent years, interest in compounds containing norbornene and norbornadiene fragments has grown significantly. The spheres of their use in the areas of obtaining both strained low molecular weight reactive substrates and new polymeric materials are constantly expanding. For the optimal and large-scale solution of the tasks set, accessible, reliable, and technological methods for the selective synthesis of norbornene monomers using heterogeneous catalysts are required, which allow the processes to be carried out with the maintenance of the strained norbornene structure.

Table 3. Heterogeneous catalysts of NBN and NBD dimerization


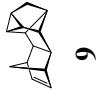
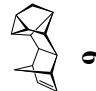
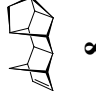
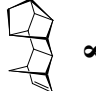
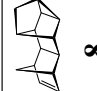
NBD dimerization							
Catalyst	Conversion, %	Main product	TON*	Selectivity, %	T, °C**	Reaction time, h	Link
5% Rh/C	90	 7	–	65	90	23	[108]
0.3% Rh/Na-pentasil (33.3)	16.8	 9	–	82	130	1	[110]
0.3% Rh/Na-TsVM	16.9	 9	–	82.5	130	1	[110]
Ni/(C ₈ H ₁₀ P) _n	99	–	1500	95/10	–	40–50	[113, 114]
Pd-0.5PEG2000/DMSNs	95–100	 8	–	90–93.6	110	3	[115]
HY	~68	 8	–	~42	250	12	[116, 117, 1205]
Hβ	~70	 8	–	~36	250	12	[116, 117, 120]

Table 3. Continued



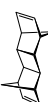




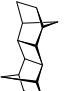
NBD dimerization							
Catalyst	Conversion, %	Main product	TON*	Selectivity, %	T, °C**	Reaction time, h	Link
HZSM-5	~63	 8	–	~33	250	12	[116, 117, 120]
Al-MCM-41	~69	 8	–	~30	250	12	[116, 117, 120]
HY	~38	 1	–	~58	250	8	[118]
Co/HY	~59	 1	–	~50	250	8	[118]
Al-KIT-6	44.7	 1	–	58	250	6	[119]
Co-Ni/Al-MCM-41	~92	 11	–	~90	200	9	[121]
Cr/SiO ₂	85	 1	2000	~76	60	3	[122]

Table 3. Continued

NBN dimerization							
Catalyst	Conversion, %	Main product	TON*	Selectivity, %	T, °C**	Reaction time, h	Link
CrO ₃ /SiO ₂	85	 23	100	90	95	14	[122]
ZSM, MCM-22, PSH-3, SSZ-25	81	19-25	–	7	75–250	19.1–25.9	[122]
Hβ HZSM-12	97–100	19-22	–	~57 89–93	80	1	[124, 125]
ASM-40	98	19-22	–	41	60	5	[126]
Hβ-25	99.5	19-22	–	72.9	140	8	[127]

* TON – Turnover number

** Temperature of the process

An analysis of the current state of this problem shows that only the first steps have been taken in this direction, and researchers will have to overcome many problems, both theoretical and experimental. However, some progress has already been made along this path. In a number of processes, it is possible not only to maintain the strained carbocyclic framework, but also to find ways to control the regio- and stereo-selectivity of the reaction. Sometimes the use of heterogeneous catalysts even gives a unique effect, allowing you to direct the process in a completely new direction.

The activity and selectivity of heterogeneous catalysts in reactions involving NBD are still significantly lower than in homogeneous systems. Catalyst performance improvement and recycling still require further study. The design and development of new types of heterogeneous catalysts, the immobilization of transition metal complexes, the use of new types of supports and surface modifiers for the qualitative fixation of active centers can become strategic directions. It will be necessary to study and use the phenomenon of synergy, which makes it possible to consistently predict and select optimal conditions for substrates and products of a given structure. This includes taking into account the possibility of leaching of active components from the surface of carriers during the reaction and other technologically unfavorable transformations of catalysts during their operation in order to optimize the reaction in continuous flow reactors.

Authors' contributions

Sergey A. Durakov – analysis of literary sources, conceptualization of the review idea, systematization of scientific publications, and writing the text of the review;

Alexey A. Kolobov – search for publications on the review topic, technical and bibliography editing, and design of illustrative materials;

Vitaly R. Flid – conceptualization of review materials, scientific editing, critical revision with the addition of valuable intellectual content.

The authors declare no conflicts of interest.

REFERENCES

1. Flid V.R., Gringolts M.L., Shamsiev R.S., Finkelshtein E.S. Norbornene, norbornadiene and their derivatives: promising semi-products for organic synthesis and production of polymeric materials. *Russ. Chem. Rev.* 2018;87(12):1169–1205. <https://doi.org/10.1070/RCR4834>
2. Gusevskaya E.V., Jiménez-Pinto J., Börner A. Hydroformylation in the Realm of Scents. *ChemCatChem.* 2014;6(2):382–411. <https://doi.org/10.1002/cctc.201300474>
3. González A.G., Barrera J.B. Chemistry and Sources of Mono- and Bicyclic Sesquiterpenes from *Ferula* Species. In: Herz W., Kirby G.W., Moore R.E., Steglich W., Tamm C. (Eds.). *Fortschritte der Chemie organischer Naturstoffe / Progress in the Chemistry of Organic Natural Products*. Vienna: Springer; 1995. V. 64. P. 1–92. https://doi.org/10.1007/978-3-7091-9337-2_1
4. Mane J., Clinet I., Muratore A., Clinet J.-C., Chanot J.-J. *New aldehydes with norbornane structures, their preparation and use in perfume making*: Pat. EP2112132A1. Publ. 28.10.2009.
5. Buchbauer G., Stappen I., Pretterklieber C., Wolschann P. Structure–activity relationships of sandalwood odorants: synthesis and odor of tricyclo β -santalol. *Eur. J. Med. Chem.* 2004;39(12):1039–1046. <https://doi.org/10.1016/j.ejmech.2004.09.014>
6. Monti H., Corriol C., Bertrand M. Synthese stereoselective DU (\pm)- β -santalol. *Tetrahedron Lett.* 1982;23(52):5539–5540. [https://doi.org/10.1016/S0040-4039\(00\)85888-8](https://doi.org/10.1016/S0040-4039(00)85888-8)
7. Corey E.J., Shibasaki M., Nicolaou K.C., Malmsten C.L., Samuelsson B. Simple, stereocontrolled total synthesis of a biologically active analog of the prostaglandin endoperoxides (PGH₂, PGG₂). *Tetrahedron Lett.* 1976;(10):737–740. [https://doi.org/10.1016/s0040-4039\(00\)77938-x](https://doi.org/10.1016/s0040-4039(00)77938-x)
8. Lee M., Ikeda I., Kawabe T., Mori S., Kanematsu K. Enantioselective Total Synthesis of *cis*-Triketrin B. *J. Org. Chem.* 1996;61(10):3406–3416. <https://doi.org/10.1021/jo951767q>
9. Hajiyeva G.E. Biologically Active Norbornene Derivatives: Synthesis of Bicyclo[2.2.1]heptene Mannich Bases. *Chemistry for Sustainable Development.* 2021;29(4):391–410. <https://doi.org/10.15372/CSD2021317>
10. Songstad D.D., Duncan D.R., Widholm J.M. Effect of α -aminocyclopropane- α -carboxylic acid, silver nitrate, and norbornadiene on plant regeneration from maize callus cultures. *Plant Cell Reports.* 1988;7(4):262–265. <https://doi.org/10.1007/bf00272538>
11. Brar M.S., Moore M.J., Al-Khayri J.M., Morelock T.E., Anderson E.J. Ethylene inhibitors promote *in vitro* regeneration of cowpea (*Vigna Unguiculata* L.). *In Vitro Cell. Dev. Biol.-Plant.* 1999;35(3):222–225. <https://doi.org/10.1007/s11627-999-0082-1>
12. Brooks G.T. Chlorinated Insecticides: Technology and Application. V. 1. CRC Press; 2017. 249 p. <https://doi.org/10.1201/9781315150390>
13. Tanaka R., Kamei I., Cai Z., Nakayama Y., Shiono T. Ethylene-Propylene Copolymerization Behavior of *ansa*-Dimethylsilylene(fluorenyl)(amido)dimethyltitanium Complex: Application to Ethylene-Propylene-Diene or Ethylene-Propylene-Norbornene Terpolymers. *J. Polym. Sci. Part A: Polym. Chem.* 2015;53(5):685–691. <https://doi.org/10.1002/pola.27494>
14. Kasyan L.I. Epoxidation of substituted norbornenes. Stereochemical aspects and accompanying intramolecular transformations. *Russ. Chem. Rev.* 1998;67(4):263–278. <https://doi.org/10.1070/RC1998v067n04ABEH000355>
15. Finkelshtein E.Sh., et al. Substituted polynorbornenes as promising materials for gas separation membranes. *Russ. Chem. Rev.* 2011;80(4):341–361. <https://doi.org/10.1070/RC2011v080n04ABEH004203>
16. Fonseca L.R., Silva Sa J.L., Carvalho V.P., Lima-Neto B.S. Cross-link in norbornadiene-based polymers from ring-opening metathesis polymerization with pyrrolidine-based Ru complex. *Polym. Bull.* 2018;75(8):3705–3721. <https://doi.org/10.1007/s00289-017-2236-3>
17. Ono Y., Kawashima N., Kudo H., Nishikubo T., Nagai T. Synthesis of new photoresponsive polyesters containing norbornadiene moieties by the ring-opening copolymerization of donor-acceptor norbornadiene dicarboxylic acid anhydride with donor-acceptor norbornadiene dicarboxylic acid monoglycidyl ester derivatives. *J. Polym. Sci. Part A: Polym. Chem.* 2005;43(19):4412–4421. <https://doi.org/10.1002/pola.20911>
18. Tsubata A., Uchiyama T., Kameyama A., Nishikubo T. Synthesis of Poly(ester-amide)s Containing Norbornadiene (NBD) Residues by the Polyaddition of NBD Dicarboxylic Acid Derivatives with Bis(epoxide)s and Their Photochemical Properties. *Macromolecules.* 1997;30(19):5649–5654. <https://doi.org/10.1021/ma970431a>
19. Yalcinkaya E.E., Balcan M., Güler C. Synthesis, characterization and dielectric properties of polynorbornadiene-clay nanocomposites by ROMP using intercalated Ruthenium catalyst. *Mater. Chem. Phys.* 2013;143(1):380–386. <https://doi.org/10.1016/j.matchemphys.2013.09.014>
20. Alentiev D.A., Bermeshev M.V. Design and Synthesis of Porous Organic Polymeric Materials from Norbornene Derivatives. *Polym. Rev.* 2022;62(2):400–437. <https://doi.org/10.1080/15583724.2021.1933026>
21. Alentiev D.A., Dzhaparidze D.M., Gavrilova N.N., Shantarovich V.P., Kiseleva E.V., Topchiy M.A., et al. Microporous Materials Based on Norbornadiene-Based Cross-Linked Polymers. *Polymers.* 2018;10(12):1382. <https://doi.org/10.3390/polym10121382>
22. Aladyshev A.M., Klyamkina A.N., Nedorezova P.M., Kiseleva E.V. Synthesis of Ethylene-Propylene-Diene Terpolymers and Their Heterophase Compositions with Polypropylene in the Presence of Metallocene Catalytic Systems. *Russ. J. Phys. Chem. B.* 2020;14(4):691–696. <https://doi.org/10.1134/S1990793120040028>
23. Sveinbjornsson B.R., Weitekamp R.A., Miyake G.M., Xia Y., Atwater H.A., Grubbs R.H. Rapid self-assembly of brush block copolymers to photonic crystals. *Proceedings of the National Academy of Sciences (PNAS).* 2012;109(36):14332–14336. <https://doi.org/10.1073/pnas.1213055109>
24. Grubbs R.H., Miyake G.M., Weitekamp R., Piunova V. *Chiral polymers for the self-assembly of photonic crystals*: Pat. US9575212-B2. Publ. 21.02.2017.
25. Wang Z., Chan C.L.C., Zhao T.H., Parker R.M., Vignolini S. Recent Advances in Block Copolymer Self-Assembly for the Fabrication of Photonic Films and Pigments. *Adv. Optical Mater.* 2021;9(21):2100519. <https://doi.org/10.1002/adom.202100519>

26. Kudo H., Yamamoto M., Nishikubo T., Moriya O. Novel Materials for Large Change in Refractive Index: Synthesis and Photochemical Reaction of the Ladderlike Poly(silsesquioxane) Containing Norbornadiene, Azobenzene, and Anthracene Groups in the Side Chains. *Macromolecules*. 2006;39(5):1759–1765. <https://doi.org/10.1021/ma052147m>
27. Kato Y., Muta H., Takahashi S., Horie K., Nagai T. Large Photoinduced Refractive Index Change of Polymer Films Containing and Bearing Norbornadiene Groups and Its Application to Submicron-Scale Refractive-Index Patterning. *Polym J.* 2001;33(11):868–873. <https://doi.org/10.1295/polymj.33.868>
28. Philippopoulos C., Economou D., Economou C., Marangozis J. Norbornadiene-quadracyclane system in the photochemical conversion and storage of solar energy. *Ind. Eng. Chem. Prod. Res. Dev.* 1983;22(4):627–633. <https://doi.org/10.1021/i300012a021>
29. Bren' V. A., et al. Norbornadiene-quadracyclane — an effective molecular system for the storage of solar energy. *Russ. Chem. Rev.* 1991;60(5):451–469. <https://doi.org/10.1070/RC1991v060n05ABEH001088>
30. Dubonosov A.D., et al. Norbornadiene-quadracyclane as an abiotic system for the storage of solar energy. *Russ. Chem. Rev.* 2002;71(11):917–927. <https://doi.org/10.1070/RC2002v071n11ABEH000745>
31. Jevric M., Petersen A.U., Manso M., Singh S.K., Wang Z., Dreos A., et al. Norbornadiene-Based Photoswitches with Exceptional Combination of Solar Spectrum Match and Long-Term Energy Storage. *Chem. Eur. J.* 2018;24(49):12767–12772. <https://doi.org/10.1002/chem.201802932>
32. Manso M., Petersen A.U., Wang Z., Erhart P., Nielsen M.B., Moth-Poulsen K. Molecular solar thermal energy storage in photoswitch oligomers increases energy densities and storage times. *Nat. Commun.* 2018;9(1):1945. <https://doi.org/10.1038/s41467-018-04230-8>
33. Wang Z., Roffey A., Losantos R., Lennartson A., Jevric M., Petersen A.U., et al. Macroscopic heat release in a molecular solar thermal energy storage system. *Energy Environ. Sci.* 2019;12(1):187–193. <https://doi.org/10.1039/C8EE01011K>
34. Dreos A., Wang Z., Udmark J., Ström A., Erhart P., Börjesson K., et al. Liquid Norbornadiene Photoswitches for Solar Energy Storage. *Adv. Energy Mater.* 2018;8(18):1703401. <https://doi.org/10.1002/aenm.201703401>
35. Bol'shakov G.F. *Khimiya i tekhnologiya komponentov zhidkogo raketnogo topliva (Chemistry and technology of liquid propellant components)*. Leningrad: Khimiya; 1983. 318 p. (in Russ.).
36. Norton R.V., Fisher D.H., Graham G.M., Frank P.J. *Method for preparing high density liquid hydrocarbon fuels*: pat. US-4355194-A. Publ. 19.10.1982.
37. Burns L.D. *Motor fuel*: Pat. US-4387257-A. Publ. 07.06.1983.
38. Lun P., Qiang D., Xiutianfeng E., Genkuo N., Xiangwen Z., Jijun Z. Synthesis Chemistry of High-Density Fuels for Aviation and Aerospace Propulsion. *Prog. Chem.* 2015;27(11):1531–1541. <https://doi.org/10.7536/PC150531>
39. Kim J., Shim B., Lee G., Han J., Jeon J.-K. Synthesis of High-energy-density Fuel through Dimerization of Bicyclo[2.2.1]hepta-2,5-diene over Co/HY Catalyst. *Appl. Chem. Eng.* 2018;29(2):185–190. <https://doi.org/10.14478/ace.2017.1116>
40. Norton R.V., Fisher D.H. *High density fuel compositions*: Pat. US-4286109-A. Publ. 25.08.1981.
41. Kim J., Shim B., Lee G., Han J., Kim J.M., Jeon J.-K. Synthesis of high-energy-density fuel over mesoporous aluminosilicate catalysts. *Catal. Today*. 2018;303:71–76. <https://doi.org/10.1016/j.cattod.2017.08.024>
42. Burdette G.W. *Liquid hydrocarbon air breather fuel*: Pat. US-441074-A. Publ. 18.10.1983.
43. Zou J.-J., Zhang X., Pan L. *High-Energy-Density Fuels for Advanced Propulsion: Design and Synthesis*. 1st ed. Wiley-VCH; 2020. 512 p.
44. Zhang C., Zhang X., Zou J., Li G. Catalytic dimerization of norbornadiene and norbornene into hydrocarbons with multiple bridge rings for potential high-density fuels. *Coord. Chem. Rev.* 2021;436:213779. <https://doi.org/10.1016/j.ccr.2021.213779>
45. Zarezin D.P., Rudakova M.A., Shorunov S.V., Sultanova M.U., Samoilov V.O., Maximov A.L., et al. Design and preparation of liquid polycyclic norbornanes as potential high performance fuels for aerospace propulsion. *Fuel Processing Technology*. 2022;225(3):107056. <https://doi.org/10.1016/j.fuproc.2021.107056>
46. Shi C., Xu J., Pan L., Zhang X., Zou J.-J. Perspective on synthesis of high-energy-density fuels: From petroleum to coal-based pathway. *Chin. J. Chem. Eng.* 2021;35(3):83–91. <https://doi.org/10.1016/j.cjche.2021.05.004>
47. Zhang X., Pan L., Wang L., Zou J.-J. Review on synthesis and properties of high-energy-density liquid fuels: Hydrocarbons, nanofluids and energetic ionic liquids. *Chem. Eng. Sci.* 2018;180:95–125. <https://doi.org/10.1016/j.ces.2017.11.044>
48. Smagin V.M., Ioffe A.E., Grigor'ev A.A., Strel'chik B.S., Ermolaeva E.M., Sirotina I.G. Preparation of norbornadiene, an important intermediate in organic synthesis. *Khimicheskaya promyshlennost' = Industry & Chemistry*. 1983;4:198–201 (in Russ.).
49. Strel'chik B.S., Smagin V.M., Chemykh S.P., Temkin O.N., Stychinskii G.F., Belen'kii V.M. *Norbornadiene preparation method*: RF Pat. RU2228324C1. Publ. 10.05.2004. (in Russ.).
50. Iaccino L.L., Lemoine R.O.V. *Processes and systems for converting hydrocarbons to cyclopentadiene*: Pat. WO2017078892A1. Publ. 11.05.2017.
51. Akhmed'yanova R.A., Miloslavskii D.G. Obtaining cyclopentadiene-1,3 from pyrolysis fractions containing dicyclopentadiene. *Vestnik tekhnologicheskogo universiteta = Bulletin of the Technological University*. 2016;19(23):33–34 (in Russ.).
52. Liakumovich A.G., Sedova S.N., Deev A.V., Magsumov I.A., Erkhov A.V., Cherezova E.N. Study of features of a stage of dicyclopentadiene rectification in a mix of industrial streams of petrochemical and coke-chemical raw materials at its excretion. *Neftepererabotka i neftekhimiya. Nauchno-tekhnicheskie dostizheniya i peredovoi opyt = Oil Processing and Petrochemistry*. 2010;12(3):30–33 (in Russ.).
53. Muldoon J.A., Harvey B.G. Bio-Based Cycloalkanes: The Missing Link to High-Performance Sustainable Jet Fuels. *ChemSusChem*. 2020;13(22):5777–5807. <https://doi.org/10.1002/cssc.202001641>
54. Harvey B.G. *Cyclopentadiene fuels*: Pat. US-11078139-B1. 2021.
55. Durakov S.A., Shamsiev R.S., Flid V.R., Gekhman A.E. Hydride transfer mechanism in the catalytic allylation of norbornadiene with allyl formate. *Russ. Chem. Bull.* 2018;67(12):2234–2240. <https://doi.org/10.1007/s11172-018-2361-7>

56. Durakov S.A., Shamsiev R.S., Flid V.R., Gekhman A.E. Isotope Effect in Catalytic Hydroallylation of Norbornadiene by Allyl Formate. *Kinet. Catal.* 2019;60(3):245–249. <https://doi.org/10.1134/S0023158419030042>
57. Durakov S.A., Melnikov P.V., Martsinkevich E.M., Smirnova A.A., Shamsiev R.S., Flid V.R. Solvent effect in palladium-catalyzed allylation of norbornadiene. *Russ. Chem. Bull.* 2021;70(1):113–121. <https://doi.org/10.1007/s11172-021-3064-z>
58. Efros I.E., Dmitriev D.V., Flid V.R. Catalytic Syntheses of Polycyclic Compounds Based on Norbornadiene in the Presence of Nickel Catalysts. *Kinet. Catal.* 2010;51(3):370–374. <https://doi.org/10.1134/S0023158410030079>
59. García-López J.A., Frutos-Pedreño R., Bautista D., Saura-Llamas I., Vicente J. Norbornadiene as a Building Block for the Synthesis of Linked Benzazocinones and Benzazocinium Salts through Tetranuclear Carbopalladated Intermediates. *Organometallics*. 2017;36(2):372–383. <https://doi.org/10.1021/acs.organomet.6b00795>
60. Egiazaryan K.T., Shamsiev R.S., Flid V.R. Quantum chemical investigation of the oxidative addition reaction of allyl carboxylates to Ni(0) and Pd(0) complexes. *Fine Chem. Technol.* 2019;14(6):56–65. <https://doi.org/10.32362/2410-6593-2019-14-6-56-65>
61. Shamsiev R.S., Flid V.R. Quantum chemical study of the mechanism of catalytic [2+2+2] cycloaddition of acrylic acid esters to norbornadiene in the presence of nickel(0) complexes. *Russ. Chem. Bull.* 2013;62(11):2301–2305. <https://doi.org/10.1007/s11172-013-0333-5>
62. Shamsiev R.S., Drobyshev A.V., Flid V.R. Quantum-chemical study on the mechanism of catalytic dimerization of norbornadiene in the presence of hydride nickel(I) complex. *Russ. J. Organ. Chem.* 2013;49(3):345–349. <https://doi.org/10.1134/S1070428013030056>
63. Siadati S.A., Nami N., Zardoost M.R. ADFT Study of Solvent Effects on the Cycloaddition of Norbornadiene and 3,4-Dihydroisoquinoline-N-Oxide. *Progress in Reaction Kinetics and Mechanism*. 2011;36(3):252–258. <https://doi.org/10.3184/146867811X13095326582455>
64. Kuisma M.J., Lundin A.M., Moth-Poulsen K., Hyldgaard P., Erhart P. Comparative Ab-Initio Study of Substituted Norbornadiene-Quadricyclane Compounds for Solar Thermal Storage. *J. Phys. Chem. C*. 2016;120(7):3635–3645. <https://doi.org/10.1021/acs.jpcc.5b11489>
65. Atta-Kumi J., Pipim G.B., Tia R., Adei E. Investigating the site-, regio-, and stereo-selectivities of the reactions between organic azide and 7-heteronorbornadiene: a DFT mechanistic study. *J. Mol. Model.* 2021;27(9):248. <https://doi.org/10.1007/s00894-021-04857-3>
66. Friend C.M., Xu B. Heterogeneous Catalysis: A Central Science for a Sustainable Future. *Acc. Chem. Res.* 2017;50(3):517–521. <https://doi.org/10.1021/acs.accounts.6b00510>
67. Hübner S., de Vries J.G., Farina V. Why Does Industry Not Use Immobilized Transition Metal Complexes as Catalysts? *Adv. Synth. Catal.* 2016;358(1):3–25. <https://doi.org/10.1002/adsc.201500846>
68. Hu X., Yip A.C.K. Heterogeneous Catalysis: Enabling a Sustainable Future. *Front. Catal.* 2021;1:667675. <https://doi.org/10.3389/ftcls.2021.667675>
69. Vogt C., Weckhuysen B.M. The concept of active site in heterogeneous catalysis. *Nat. Rev. Chem.* 2022;6(2):89–111. <https://doi.org/10.1038/s41570-021-00340-y>
70. Dzhemilev U.M., Popod'ko N.R., Kozlova E.V. *Metallokompleksnyi kataliz v organicheskom sinteze. Alitsiklicheskie soedineniya (Metal complex catalysis in organic synthesis. Alicyclic compounds)*. Moscow: Khimiya; 1999. 647 p. (in Russ.).
71. Fel'dblyum V.Sh. *Sintez i primeneni nepredel'nykh tsiklicheskiikh uglevodorodov (Synthesis and application of unsaturated cyclic hydrocarbons)*. Moscow: Khimiya; 1982. 208 p. (in Russ.).
72. Schrauzer G.N. On Transition Metal-Catalyzed Reactions of Norbornadiene and the Concept of π Complex Multicenter Processes. In: Eley D.D., Pines H., Weisz P.B. (Eds.). *Advances in Catalysis*. 1968. V. 18. P. 373–396. [https://doi.org/10.1016/S0360-0564\(08\)60431-9](https://doi.org/10.1016/S0360-0564(08)60431-9)
73. Khan R., Chen J., Fan B. Versatile Catalytic Reactions of Norbornadiene Derivatives with Alkynes. *Adv. Synth. Catal.* 2020;362(8):1564–1601. <https://doi.org/10.1002/adsc.201901494>
74. Dzhemilev U.M., Khusnutdinov R.I., Tolstikov G.A. Norbornadienes in the Synthesis of Polycyclic Strained Hydrocarbons with Participation of Metal Complex Catalysts. *Russ. Chem. Rev.* 1987;56(1):65–94. <https://doi.org/10.1070/RC1987v056n01ABEH003255>
75. Anikin O.V., Kornilov D.A., Nikitina T.V., Kiselev V.D. Variable Activity of Reagents with C=C and N=N Bonds in Cycloaddition Reactions. *Russ. J. Phys. Chem. B*. 2018;12(4):595–598. <https://doi.org/10.1134/S1990793118040176>
76. Chen Y., Kiattansakul R., Ma B., Snyder J.K. Transition Metal-Catalyzed [4+2+2] Cycloadditions of Bicyclo[2.2.1]hepta-2,5-dienes (Norbornadienes) and Bicyclo[2.2.2]octa-2,5-dienes. *J. Org. Chem.* 2001;66(21):6932–6942. <https://doi.org/10.1021/jo010268o>
77. Bermeshev M.V., Chapala P.P. Addition polymerization of functionalized norbornenes as a powerful tool for assembling molecular moieties of new polymers with versatile properties. *Prog. Polym. Sci.* 2018;84:1–46. <https://doi.org/10.1016/j.progpolymsci.2018.06.003>
78. Petrov V.A., Vasil'ev N.V. Synthetic Chemistry of Quadricyclane. *Curr. Org. Synthesis*. 2006;3(2):215–259. <http://doi.org/10.2174/157017906776819204>
79. Orrego-Hernández J., Drees A., Moth-Poulsen K. Engineering of Norbornadiene/Quadricyclane Photoswitches for Molecular Solar Thermal Energy Storage Applications. *Acc. Chem. Res.* 2020;53(8):1478–1487. <https://doi.org/10.1021/acs.accounts.0c00235>
80. Akioka T., Inoue Y., Yanagawa A., Hiyamizu M., Takagi Y., Sugimori A. A comparative study on photocatalytic hydrogen transfer and catalytic hydrogenation of norbornadiene and quadricyclane catalyzed by $[\text{Rh}_6(\text{CO})_{16}]$. *J. Mol. Catal. A: Chem.* 2003;202(1):31–39. [https://doi.org/10.1016/S1381-1169\(03\)00201-2](https://doi.org/10.1016/S1381-1169(03)00201-2)
81. Cuppoletti A., Dinnocenzo J.P., Goodman J.L., Gould I.R. Bond-Coupled Electron Transfer Reactions: Photoisomerization of Norbornadiene to Quadricyclane. *J. Phys. Chem. A*. 1999;103(51):11253–11256. <https://doi.org/10.1021/jp992884i>
82. Lahiry S., Halder C. Use of semiconductor materials as sensitizers in a photochemical energy storage reaction, norbornadiene to quadricyclane. *Solar Energy*. 1986;37(1):71–73. [https://doi.org/10.1016/0038-092X\(86\)90109-X](https://doi.org/10.1016/0038-092X(86)90109-X)

83. Ghandi M., Rahimi A., Mashayekhi G. Triplet photosensitization of myrcene and some dienes within zeolite Y through heavy atom effect. *J. Photochem. Photobiol. A*. 2006;181(1):56–59. <https://doi.org/10.1016/j.jphotochem.2005.10.033>
84. Gu L., Liu F. Photocatalytic isomerization of norbornadiene over Y zeolites. *React. Kinet. Catal. Lett.* 2008;95(1):143–151. <https://doi.org/10.1007/s11144-008-5326-2>
85. Zou J.-J., Zhang M.-Y., Zhu B., Wang L., Zhang X., Mi Z. Isomerization of Norbornadiene to Quadricyclane Using Ti-Containing MCM-41 as Photocatalysts. *Catal. Lett.* 2008;124(1–2):139–145. <https://doi.org/10.1007/s10562-008-9441-5>
86. Zou J.-J., Liu Y., Pan L., Wang L., Zhang X. Photocatalytic isomerization of norbornadiene to quadricyclane over metal (V, Fe and Cr)-incorporated Ti-MCM-41. *Appl. Catal. B*. 2010;95(3):439–445. <https://doi.org/10.1016/j.apcatb.2010.01.024>
87. Pan L., Zou J.-J., Zhang X., Wang L. Photoisomerization of Norbornadiene to Quadricyclane Using Transition Metal Doped TiO₂. *Ind. Eng. Chem. Res.* 2010;49(18):8526–8531. <https://doi.org/10.1021/ie100841w>
88. Zou J.-J., Pan L., Wang L., Zhang X. Photoisomerization of Norbornadiene to Quadricyclane Using Ti-Containing Photocatalysts. In: Saha S. (Ed.). *Molecular Photochemistry – Various Aspects*. 2012. P. 41–62. <https://doi.org/10.5772/26597>
89. Hirao K., Yamashita A., Yonemitsu O. Cycloreversion of acylquadricyclane to acylnorbornadiene promoted by metal oxides. *Tetrahedron Lett.* 1988;29(33):4109–4112. [https://doi.org/10.1016/S0040-4039\(00\)80429-3](https://doi.org/10.1016/S0040-4039(00)80429-3)
90. Koser G.F., Faircloth J.N. Silver(I)-promoted reactions of strained hydrocarbons. Oxidation vs. rearrangement. *J. Org. Chem.* 1976;41(3):583–585. <https://doi.org/10.1021/jo00865a048>
91. Ford J.F., Mann C.K., Vickers T.J. Monitoring the Heterogeneously Catalyzed Conversion of Quadricyclane to Norbornadiene by Raman Spectroscopy. *Appl. Spectrosc.* 1994;48(5):592–595. <https://doi.org/10.1366/0003702944924907>
92. Manassen J. Catalysis of a symmetry restricted reaction by transition metal complexes. The importance of the ligand. *J. Catal.* 1970;18(1):38–45. [https://doi.org/10.1016/0021-9517\(70\)90309-X](https://doi.org/10.1016/0021-9517(70)90309-X)
93. Miki S., Ohno T., Iwasaki H., Yoshida Z. Cobalt(II) tetraphenylporphyrin-catalyzed isomerization of electronegative substituted quadricyclanes. *Tetrahedron Lett.* 1985;26(29):3487–3490. [https://doi.org/10.1016/S0040-4039\(00\)98671-4](https://doi.org/10.1016/S0040-4039(00)98671-4)
94. Miki S., Maruyama T., Ohno T., Tohma T., Toyama S., Yoshida Z. Alumina-anchored Cobalt(II) Schiff Base Catalyst for the Isomerization of Trimethyldicyanoquadricyclane to the Norbornadiene. *Chem. Lett.* 1988;17(5):861–864. <https://doi.org/10.1246/cl.1988.861>
95. Wang Z., Roffey A., Losantos R., Lennartson A., Jevric M., Petersen A.U., et al. Macroscopic heat release in a molecular solar thermal energy storage system. *Energy Environ. Sci.* 2019;12(1):187–193. <https://doi.org/10.1039/C8EE01011K>
96. Kuznetsova N.A., Kaliya O.L., Leont'eva S.V., Manulik O.S., Negrimovskii V.M., Flid V.R., Shamsie R.S., Yuzhakova O.A., Yashtulov N.A. Catalyst and method for valence isomerisation of quadricyclane in norbornadiene: RF Pat. RU 2470030 C1. Publ. 20.11.1012. (in Russ.).
97. Flid V.R., Leont'eva S.V., Kaliya O.L., Durakov S.A. Method for carrying out the process of reversible isomerization of norbornadiene in a quadricyclane: RF Pat. RU 2618527 C1. Publ. 04.05.2017]. (in Russ.).
98. Roduner E. Size matters: why nanomaterials are different. *Chem. Soc. Rev.* 2006;35(7):583–592. <https://doi.org/10.1039/B502142C>
99. Pujari S.P., Scheres L., Marcelis A.T.M., Zuilhof H. Covalent surface modification of oxide surfaces. *Angew. Chem. Int. Ed. Engl.* 2014;53(25):6322–6356. <https://doi.org/10.1002/anie.201306709>
100. Luchs T., Lorenz P., Hirsch A. Efficient Cyclization of the Norbornadiene-Quadricyclane Interconversion Mediated by a Magnetic [Fe₃O₄-CoSalphen] Nanoparticle Catalyst. *ChemPhotoChem.* 2020;4(1):52–58. <https://doi.org/10.1002/cptc.201900194>
101. Lorenz P., Luchs T., Hirsch A. Molecular Solar Thermal Batteries through Combination of Magnetic Nanoparticle Catalysts and Tailored Norbornadiene Photoswitches. *Chem. Eur. J.* 2021;27(15):4993–5002. <https://doi.org/10.1002/chem.202005427>
102. Suld G., Schneider A., Myers Jr H.K.M. Catalytic dimerization of norbornadiene to Binor-S: Pat. US-4031150-A. Publ. 21.06.1977.
103. Warrenner R.N., Butler D.N., Golic M. The synthesis of geometric variants of rigidly-linked uracil-{spacer}-uracil and uracil-{spacer}-effector molecules using block assembly methods. *Nucleosides Nucleotides.* 1999;18(11–12):2631–2660. <https://doi.org/10.1080/07328319908044631>
104. Alentiev D.A., Dzhaparidze D.M., Bermeshev M.V., Starannikova L.E., Filatova M.P., Yampolskii Y.P., et al. Addition Copolymerization of Silicon-Containing Tricyclononene with 2,5-Norbornadiene Dimer. *Polym. Sci. Ser. B.* 2019;61(6):812–816. <https://doi.org/10.1134/S1560090419060022>
105. Rosenkoetter K.E., Garrison M.D., Quintana R.L., Harvey B.G. Synthesis and Characterization of a High-Temperature Thermoset Network Derived from a Multicyclic Cage Compound Functionalized with Exocyclic Allylidene Groups. *ACS Appl. Polym. Mater.* 2019;1(10):2627–2637. <https://doi.org/10.1021/acsapm.9b00542>
106. Solomatin D.V., Kuznetsova O.P., Zvereva U.G., Rochev V.Ya., Bekeshev V.G., Prut E.V. Mechanism of formation of fine rubber powder from ternary ethylene-propylene-diene vulcanizates. *Russ. J. Phys. Chem. B.* 2016;10(4):662–671. <https://doi.org/10.1134/S1990793116040102>
107. Kettles T., Tam W. Bicyclo[2.2.1]hepta-2,5-diene (Norbornadiene). In: *e-EROS Encyclopedia of Reagents for Organic Synthesis*. 2012. <https://doi.org/10.1002/047084289X.rm01411>
108. Mrowca J.J., Katz T.J. Catalysis of a Cycloaddition Reaction by Rhodium on Carbon. *J. Am. Chem. Soc.* 1966;88(17):4012–4015. <https://doi.org/10.1021/ja00969a021>
109. Chung H.S., Chen C.S.H., Kremer R.A., Boulton J.R., Burdette G.W. Recent Developments in High-Energy Density Liquid Hydrocarbon Fuels. *Energy Fuels.* 1999;13(3):641–649. <https://doi.org/10.1021/ef980195k>
110. Gol'dshleger N.F., Azbel' B.I., Isakov Ya.I., Shpiro E.S., Minachev Kh.M. Cyclodimerization of bicyclo[2.2.1]hepta-2,5-diene in the presence of rhodium-containing zeolite catalysts. *Russ. Chem. Bull.* 1994;43(11):1802–1808. <https://doi.org/10.1007/BF00696305>

111. Azbel' B.I., Gol'Dshleger N.F., Khidekel' M.L., Sokol V.I., Porai-Koshits M.A. Cyclodimerization of bicyclo [2.2.1]hepta-2,5-diene by rhodium carboxylates. *J. Molecul. Catal.* 1987;40(1):57–63. [https://doi.org/10.1016/0304-5102\(87\)80006-8](https://doi.org/10.1016/0304-5102(87)80006-8)
112. Yuffa A.Y., Lisichkin G.V. Heterogeneous Metal Complex Catalysts. *Russ. Chem. Rev.* 1978;47(8): 751–766. <https://doi.org/10.1070/RC1978v047n08ABEH002258>
113. Flid V.R., Ivanov A.V., Manulik O.S., Belov A.P. Heterogeneous catalytic dimerization of bicyclo[2.2.1]heptadiene. *Kinetika i kataliz = Kinetics and Catalysis.* 1994;35(5):774–775 (in Russ.).
114. Leont'eva S.V., Dmitriev D.V., Katsman E.A., Flid V.R. Catalytic syntheses of polycyclic compounds based on norbornadiene in the presence of nickel complexes. V. Codimerization of norbornadiene and methyl vinyl ketone on heterogenized nickel catalysts. *Kinet. Catal.* 2006;47(4):580–584. <https://doi.org/10.1134/S0023158406040148>
115. Li C., Zhang C., Liu R., Wang L., Zhang X., Li G. Heterogeneously supported active Pd(0) complex on silica mediated by PEG as efficient dimerization catalyst for the production of high energy density fuel. *Mol. Catal.* 2022;520:112170. <https://doi.org/10.1016/j.mcat.2022.112170>
116. Jeong B.H., Han J.S., Jeon J.K., Park E.S., Jeong K.H. *Method for Producing Norbornadiene Dimer Using Heterogeneous Catalyst*: Pat. KR101616071B1. Publ. 27.04.2016.
117. Jeong K., Kim J., Han J., Jeong B., Jeon J.K. Dimerization of Bicyclo[2.2.1]hepta-2,5-diene Over Various Zeolite Catalysts. *Top. Catal.* 2017;60(9–11):743–749. <https://doi.org/10.1007/s11244-017-0780-6>
118. Kim J., Shim B., Lee G., Han J., Jeon J.-K. Synthesis of High-energy-density Fuel through Dimerization of Bicyclo[2.2.1]hepta-2,5-diene over Co/HY Catalyst. *Appl. Chem. Eng.* 2018;29(2):185–190. <https://doi.org/10.14478/ACE.2017.1116>
119. Kim J., Shim B., Lee G., Han J., Kim J.M., Jeon J.-K. Synthesis of high-energy-density fuel over mesoporous aluminosilicate catalysts. *Catalysis Today.* 2018;303:71–76. <https://doi.org/10.1016/j.cattod.2017.08.024>
120. Jeong K., Kim J., Han J., Jeon J.-K. Synthesis of High-Energy-Density Fuel Through the Dimerization of Bicyclo[2.2.1]Hepta-2,5-Diene Over a Nanoporous Catalyst. *J. Nanosci. Nanotechnol.* 2017;17(11):8255–8259. <https://doi.org/10.1166/jnn.2017.15097>
121. Khan N., Abhyankar A.C., Nandi T. Cyclodimerization of norbornadiene (NBD) into high energy-density fuel pentacyclotetradecane (PCTD) over mesoporous silica supported Co–Ni nanocatalyst. *J. Chem. Sci.* 2021;133(1):29. <https://doi.org/10.1007/s12039-021-01890-w>
122. Wu M.M., Xiong Y. *Process for the catalytic cyclodimerization of cyclic olefins*: Pat. US5545790A. Publ. 13.08.1996.
123. Audeh C.A., Boulton J.R., Kremer R.A., Xiong Y. *Heterogeneous catalytic oligomerization of norbornene*: Pat. US5461181A. Publ. 24.10.1995.
124. Dzhemilev U.M., Kutepov B.I., Grigor'eva N.G., Bubennov S.V., Tselyutina M.I., Gizetdinova A.F. *Method of selective obtaining norbornene dimers*: RF Pat. RU2505514C1. Publ. 27.01. 2014. (in Russ.).
125. Grigor'eva N.G., Bubennov S.V., Khalilov L.M., Kutepov B.I. Dimerization of norbornene on zeolite catalysts. *Chinese J. Catal.* 2015;36(3):268–273. [https://doi.org/10.1016/S1872-2067\(14\)60251-5](https://doi.org/10.1016/S1872-2067(14)60251-5)
126. Bubennov S.V., Grigor'eva N.G., Serebrennikov D.V., Agliullin M.R., Kutepov B.I. Oligomerization of Unsaturated Compounds in the Presence of Amorphous Mesoporous Aluminosilicates. *Pet. Chem.* 2019;59(7):682–690. <https://doi.org/10.1134/S096554411907003X>
127. Chen Y., Shi C., Jia T., Cai Q., Pan L., Xie J., et al. Catalytic synthesis of high-energy-density jet-fuel-range polycyclic fuel by dimerization reaction. *Fuel.* 2022;308:122077. <https://doi.org/10.1016/j.fuel.2021.122077>
128. Ananikov V.P., Beletskaya I.P. Toward the Ideal Catalyst: From Atomic Centers to a “Cocktail” of Catalysts. *Organometallics.* 2012;31(5):1595–1604. <https://doi.org/10.1021/om201120n>
129. Eremin D.B., Ananikov V.P. Understanding active species in catalytic transformations: From molecular catalysis to nanoparticles, leaching, “Cocktails” of catalysts and dynamic systems. *Coord. Chem. Rev.* 2017;346:2–19. <https://doi.org/10.1016/j.ccr.2016.12.021>
130. Prima D.O., Kulikovskaya N.S., Galushko A.S., Mironenko R.M., Ananikov V.P. Transition metal ‘cocktail’-type catalysis. *Curr. Opin. Green Sustain. Chem.* 2021;31:100502. <https://doi.org/10.1016/j.cogsc.2021.100502>
131. Cantillo D., Kappe C.O. Immobilized Transition Metals as Catalysts for Cross-Couplings in Continuous Flow—A Critical Assessment of the Reaction Mechanism and Metal Leaching. *ChemCatChem.* 2014;6(12):3286–3305. <https://doi.org/10.1002/cctc.201402483>

About the authors:

Sergey A. Durakov, Cand. Sci. (Chem.), Associate Professor, Department of Physical Chemistry, M.V. Lomonosov Institute of Fine Chemical Technologies, MIREA – Russian Technological University (86, Vernadskogo pr., Moscow, 119571, Russia). E-mail: s.a.durakov@mail.ru. Scopus Author ID 57194217518, ResearcherID AAS-6578-2020, RSCI SPIN-code 9420-3916, <https://orcid.org/0000-0003-4842-3283>

Alexey A. Kolobov, Student, Department of Physical Chemistry, M.V. Lomonosov Institute of Fine Chemical Technologies, MIREA – Russian Technological University (86, Vernadskogo pr., Moscow, 119571, Russia). E-mail: a.a.kolobov@bk.ru. <https://orcid.org/0000-0003-2194-4935>

Vitaly R. Flid, Dr. Sci. (Chem.), Professor, Head of the Department of Physical Chemistry, M.V. Lomonosov Institute of Fine Chemical Technologies, MIREA – Russian Technological University (86, Vernadskogo pr., Moscow, 119571, Russia). E-mail: vitaly-flid@yandex.ru. Scopus Author ID 6602997346, ResearcherID H-1781-2017, RSCI SPIN-code 8790-3380, <https://orcid.org/0000-0001-6559-5648>

Об авторах:

Дураков Сергей Алексеевич, к.х.н., доцент кафедры физической химии им. Я.К. Сыркина Института тонких химических технологий им. М.В. Ломоносова, ФГБОУ ВО «МИРЭА – Российский технологический университет» (119571, Россия, Москва, пр-т Вернадского, д. 86). E-mail: s.a.durakov@mail.ru. Scopus Author ID 57194217518, ResearcherID AAS-6578-2020, SPIN-код РИНЦ 9420-3916, <https://orcid.org/0000-0003-4842-3283>

Колобов Алексей Андреевич, студент кафедры физической химии им. Я.К. Сыркина Института тонких химических технологий им. М.В. Ломоносова, ФГБОУ ВО «МИРЭА – Российский технологический университет» (119571, Россия, Москва, пр-т Вернадского, д. 86). E-mail: a.a.kolobov@bk.ru. <https://orcid.org/0000-0003-2194-4935>

Виталий Рафаилович Флид, д.х.н., профессор, заведующий кафедрой физической химии им. Я.К. Сыркина Института тонких химических технологий им. М.В. Ломоносова, ФГБОУ ВО «МИРЭА – Российский технологический университет» (119571, Россия, Москва, пр-т Вернадского, д. 86). E-mail: vitaly-flid@yandex.ru. Scopus Author ID 6602997346, ResearcherID H-1781-2017, SPIN-код РИНЦ 8790-3380, <https://orcid.org/0000-0001-6559-5648>

The article was submitted: May 11, 2022; approved after reviewing: May 23, 2022; accepted for publication: July 29, 2022.

Translated from Russian into English by H. Moshkov

ISSN 2686-7575 (Online)

<https://doi.org/10.32362/2410-6593-2022-17-4-298-310>



UDC 661.1 + 547.426

RESEARCH ARTICLE

Synthesis of stabilizers based on glycerides of monocarboxylic acids for industrial chloroparaffins

Yuriy L. Zotov[✉], Daria M. Zapravdina, Evgeniy V. Shishkin, Yuriy V. Popov

Volgograd State Technical University, Volgograd, 400005 Russia

[✉]Corresponding author, e-mail: ylzotov@mail.ru

Abstract

Objectives. The study aimed to develop new effective heat stabilizers based on glycerol esters of monocarboxylic acids for industrial chlorinated paraffins and to select of the optimal ratio of active ingredients in the stabilizing composition in order to provide the maximum thermostabilizing effect.

Methods. The thermostabilizing effect of the studied samples on chlorinated paraffins was evaluated according to the standard method for determining the thermal stability of liquid chlorinated paraffins in terms of the mass fraction of split off hydrogen chloride. Quantitative and qualitative analysis of the obtained mixtures of monocarboxylic acid glycerides was carried out using chromat-mass spectrometry.

Results. Glycerides of monocarboxylic acids (oleic, octanoic, hexanoic, and propionic acids) were obtained and identified, and the compositions of the resulting mixtures of mono-, di- and triesters were determined. The stabilizing effect of the obtained mixtures of glycerides of monocarboxylic acids in the amount of 0.5–2.0 wt parts per 100 wt parts of unstabilized industrial chlorinated paraffin CP-30 was determined. The combined use of glycerides of monocarboxylic acids with calcium-containing compounds as a complex stabilizer with a molar ratio of esters/Ca 0.93–0.86/0.07–0.14, respectively, was investigated. Chloroparaffin CP-470, stabilized by the developed complex stabilizer, was successfully used in a polyvinyl chloride composition for cable compound of the brand OM-40.

Conclusions. A proposed variant of a complex stabilizer for chlorinated paraffins based on Russian raw materials for import substitution will expand the range of effective stabilizers for organochlorine substances. Glycerides of monocarboxylic acids are shown to exhibit a thermostabilizing effect on industrial chlorinated paraffins. The relationship between the length of the hydrocarbon substituent of the carboxylic acid in the ester and the thermostabilizing effect is obtained. With an increase in the number of carbon atoms in the hydrocarbon substituent of the carboxylic acid, the heat-stabilizing ability decreases. The minimum sufficient concentration of glycerides of carboxylic acids was 0.05 ± 0.005 mol/kg, above which no increase in the thermostabilizing effect on chloroparaffin was observed. A synergistic ratio of the components of the stabilizing mixture in terms of thermal stability—glycerides of monocarboxylic acids/calcium-containing compounds—was found equal to 0.85–0.9/0.15–0.1.

Keywords: chloroparaffins, thermal stability, esterification, glycerol esters, calcium glyceroxide

For citation: Zotov Yu.L., Zapravdina D.M., Shishkin E.V., Popov Yu.V. Synthesis of stabilizers based on glycerides of monocarboxylic acids for industrial chloroparaffins. *Tonk. Khim. Tekhnol. = Fine Chem. Technol.* 2022;17(4):298–310 (Russ., Eng.). <https://doi.org/10.32362/2410-6593-2022-17-4-298-310>

НАУЧНАЯ СТАТЬЯ

Синтез стабилизаторов на основе глицеридов монокарбоновых кислот для промышленных хлорпарафинов

Ю.А. Зотов✉, Д.М. Заправдина, Е.В. Шишкин, Ю.В. Попов

Волгоградский государственный технический университет, Волгоград, 400005 Россия

✉ Автор для переписки, e-mail: ylzotov@mail.ru

Аннотация

Цели. Разработать новые эффективные термостабилизаторы на основе сложных эфиров глицерина монокарбоновых кислот для промышленных хлорпарафинов. Найти оптимальное соотношение действующих веществ стабилизирующей композиции обеспечивающее максимальное термостабилизирующее действие.

Методы. Оценку термостабилизирующего действия исследуемых образцов на хлорированные парафины проводили по стандартной методике определения термостабильности жидких хлорпарафинов в пересчете на массовую долю отцеplenного хлористого водорода. Количественный и качественный анализ полученных смесей глицеридов монокарбоновых кислот проводили с использованием хромато-масс-спектрометрического анализа.

Результаты. Получены и идентифицированы глицериды монокарбоновых кислот (олеиновой, октановой, гексановой и пропионовой кислот), определены составы образующихся смесей моно-, ди- и триэфиров. Определено стабилизирующее действие полученных смесей глицеридов монокарбоновых кислот в количестве 0.5–2.0 мас. ч. на 100 мас. ч. нестабилизированного промышленного хлорпарафина марки ХП-30. Исследовано совместное использование глицеридов монокарбоновых кислот с кальцийсодержащими соединениями в качестве комплексного стабилизатора с мольным соотношением эфиры/Са 0.93–0.86/0.07–0.14 соответственно. Хлорпарафин ХП-470, стабилизированный разработанным комплексным стабилизатором, успешно использован в поливинилхлоридной композиции для кабельного пластика марки ОМ-40.

Выводы. Предложен вариант комплексного стабилизатора для хлорпарафинов на основе российского сырья для импортозамещения, расширяющий ассортимент эффективных стабилизаторов хлорорганических веществ. Установлено, что глицериды монокарбоновых кислот проявляют термостабилизирующее действие на промышленные хлорпарафины. Обнаружена взаимосвязь длины углеводородного заместителя карбоновой кислоты в сложном эфире на термостабилизирующее действие. С увеличением числа атомов углерода в углеводородном заместителе карбоновой кислоты термостабилизирующая способность снижается. Установлена минимальная достаточная концентрация глицеридов карбоновых кислот 0.05 ± 0.005 моль/кг, выше которой не наблюдается увеличение термостабилизирующего действия на хлорпарафин. Найдено синергическое соотношение компонентов стабилизирующей смеси по термостабильности: глицериды монокарбоновых кислот/кальцийсодержащие соединения, равное $0.85-0.9/0.15-0.1$.

Ключевые слова: хлорпарафины, термостабильность, этерификация, сложные эфиры глицерина, глицерат кальция

Для цитирования: Зотов Ю.Л., Заправдина Д.М., Шишкин Е.В., Попов Ю.В. Синтез стабилизаторов на основе глицеридов монокарбоновых кислот для промышленных хлорпарафинов. *Тонкие химические технологии*. 2022;17(4):298–310. <https://doi.org/10.32362/2410-6593-2022-17-4-298-310>

INTRODUCTION

Representing multi-tonnage products of the organic synthesis industry, chlorinated paraffins are used as secondary plasticizers for polymer compositions based on polyvinyl chloride (PVC) to partially replace primary plasticizers such as phthalates and phosphate esters. The use of chlorinated paraffins makes it possible to increase the fire resistance and low-temperature strength of polymer products [1]. Chloroparaffins are widely used in the production of cable materials, wall panels, shoe plastic, and other products. However, chloroparaffins are subject to thermal decomposition. Technological temperatures of polyvinyl chloride processing exceed 200°C , leading to the decomposition of chloroparaffins, along with the release of gaseous hydrogen chloride, which is known [2] to initiate of the process of dehydrochlorination of organochlorine compounds.

To prevent the process of thermal degradation of chloroparaffins, which are part of the PVC

composition, the use of stabilizers is required to increase its own thermal stability. Chloroparaffins are traditionally stabilized with epoxy compounds, such as epoxidized soybean oil or epoxidized resins (ED-20) [3, 4]. For example, mixtures containing piperidine derivatives with phosphoric esters [5], aliphatic ketone with benzylamine, aliphatic amine, or amino alcohol [6], phosphoric acid esters with glycerol [7], adamantyl-containing imidic acid derivatives with epoxidized soybean oil [8] are used as stabilizers. Hydrogen chloride acceptors are also used as heat stabilizers, for example, salts of aliphatic carboxylic acids with the number of carbon atoms in the chain $\text{C}_{10}-\text{C}_{23}$ and alkaline earth metal of group II of the Periodic Table [9, 10]. Thus, a more pronounced thermostabilizing effect is achieved, both due to the well-known synergistic effect [11] and chemical processes occurring during thermal stabilization at different speeds and with different sequences of reaction of different salts.

The development of technologies for the production of biodiesel by transesterification of

vegetable oils with methanol (or other alcohols) has led to the appearance on the market of a significant quantity of glycerol, which is formed as a byproduct [12]. In this regard, the use of glycerol as a cheap Russian renewable and environmentally friendly raw material for the production of products with high added value has become relevant.

In order to improve the quality of industrial chlorinated paraffins, we are developing new complex stabilizers based on glycerol esters and calcium-containing compounds, which will not only increase the thermal stability of the initial chloroparaffin, but also favorably affect the physicomachanical properties of the polymer composition and finished products. Since there is no information in the scientific and technical literature about the stabilizing effect of carboxylic acid glycerides on chlorinated hydrocarbons, research in this direction is of practical and scientific interest.

MATERIALS AND METHODS

Glycerol (98.5 wt %, c.p.), oleic acid of the B-115 brand (97.4 wt %, tech.), octanoic acid (99.5 wt %, c.p.), hexanoic acid (99 wt %, c.p.), propionic acid (99 wt %, c.p.), calcium hydroxide (97 wt %, p.a., used after calcination at 300°C for 30 min), petroleum toluene (99 wt %, p.a.), chloroparaffin CP-30 grade A (STO 00203275-201-2006¹ with amendments 1, 2) (manufactured by *Chimmed* and *Kaustik*, Russia) were used in the work. To conduct studies of the thermostabilizing effect of monocarboxylic acid glycerides on organochlorine compounds, chloroparaffin CP-30 was specially synthesized in production conditions and sampled after the end of the hydrogen chloride blowing stage before the mixing operation with a prescription stabilizer.

Identification of the product obtained by esterification of glycerol with carboxylic acids was carried out using chromat-mass spectrometric analysis on a Saturn 2100T chromat-mass spectrometer (*Varian*, USA) with a quartz capillary column VF-1ms 30 M \times 0.25 mm \times 0.25 μ m and the following parameters: carrier gas—helium; flow rate—1.2 mL/min; injector with a 1:10 flow split; injector temperature—280°C. When programming the temperature of the capillary column, the following parameters were used: initial temperature—80°C; isotherm time—3 min; final temperature—300°C,

isotherm time—2 min; heating rate—10°C/min; total analysis time—30 min. The detector is mass selective with electron ionization energy of 70 eV. The spectra were recorded in full scan mode (SCAN) within the mass range from 40 to 650 Da at a data collection rate of 2000 Da/s.

Oleic acid monoglyceride: mass spectrum, m/z (I_{rel} , %): 356 (3.2) [M]⁺, 339 (23.7), 264 (99.9), 166 (15.7), 137 (24.9), 112 (23.3), 98 (45.9), 83 (31.8), 69 (32.4), 55 (60.3), 41 (55.7). **Oleic acid diglyceride:** mass spectrum, m/z (I_{rel} , %): 339 (11.8), 265 (8.6), 185 (51.2), 129 (99.9), 97 (14.3), 83 (21.4), 69 (28.2), 55 (59.1), 41 (42.4). **Oleic acid:** mass spectrum, m/z (I_{rel} , %): 282 (5.5) [M]⁺, 264 (41.9), 151 (18.9), 123 (24), 111 (30.3), 97 (65), 83 (67.8), 69 (66.4), 55 (99.9), 41 (80).

Octanoic acid monoglyceride: mass spectrum, m/z (I_{rel} , %): 218 (17.3) [M]⁺, 201 (100), 127 (62.5), 57 (74.9). **Octanoic acid diglyceride:** mass spectrum, m/z (I_{rel} , %): 327 (67.2), 242 (18.2), 201 (100), 127 (83.2), 57 (75.3). **Octanoic acid triglyceride:** mass spectrum, m/z (I_{rel} , %): 327 (100), 313 (12.2), 242 (17.5), 201 (25.4), 127 (71.5), 57 (57.8). **Octanoic acid:** mass spectrum, m/z (I_{rel} , %): 144 (13.6) [M]⁺, 126 (10.2), 114 (18.6), 100 (53.2), 73 (75), 60 (100), 55 (58.1), 43 (52.6).

Hexanoic acid monoglyceride: mass spectrum, m/z (I_{rel} , %): 190 (23.5) [M]⁺, 172 (99.9), 99 (87.3), 71 (49.8), 43 (100). **Hexanoic acid diglyceride:** mass spectrum, m/z (I_{rel} , %): 271 (99.9), 173 (29.9), 99 (10.3), 43 (13.8). **Hexanoic acid triglyceride:** mass spectrum, m/z (I_{rel} , %): 271 (7.4), 227 (7.5), 100 (6.7), 99 (99.9), 71 (20.6), 43 (22.8). **Hexanoic acid:** mass spectrum, m/z (I_{rel} , %): 116 (0.9) [M]⁺, 87 (13.4), 73 (44.5), 60 (100), 41 (19.6).

Propionic acid monoglyceride: mass spectrum, m/z (I_{rel} , %): 117 (12.7) [M]⁺, 88 (7.2), 61 (14.5), 57 (100). **Propionic acid diglyceride:** mass spectrum, m/z (I_{rel} , %): 187 (5.1), 148 (33.9), 131 (99.9), 117 (13.7), 57 (51.6). **Propionic acid triglyceride:** mass spectrum, m/z (I_{rel} , %): 187 (5.7), 173 (17.5), 121 (8.1), 117 (14.3), 57 (100). **Propionic acid:** mass spectrum, m/z (I_{rel} , %): 74 (100) [M]⁺, 57 (46.7), 45 (89.3).

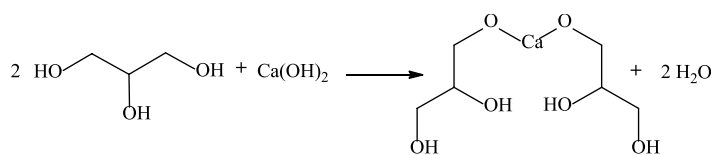
The infrared (IR) spectra of the obtained calcium glyceroxide were recorded in air at room temperature on a Nicolet-6700 IR Fourier spectrometer (*Thermo Scientific*, USA) in the region of 400–4000 cm^{−1} with a scanning step of 0.5 cm^{−1}.

The elemental analysis was performed using the Elementar Vario EL cube analyzer (*Abacus Analytical Systems GmbH*, Germany).

¹ <https://www.kaustik.ru/ru/index.php/produktsiya-i-uslugi/khlorparafiny/khlorparafin-khp-30>, accessed March 25, 2022.

Preparation of the catalyst

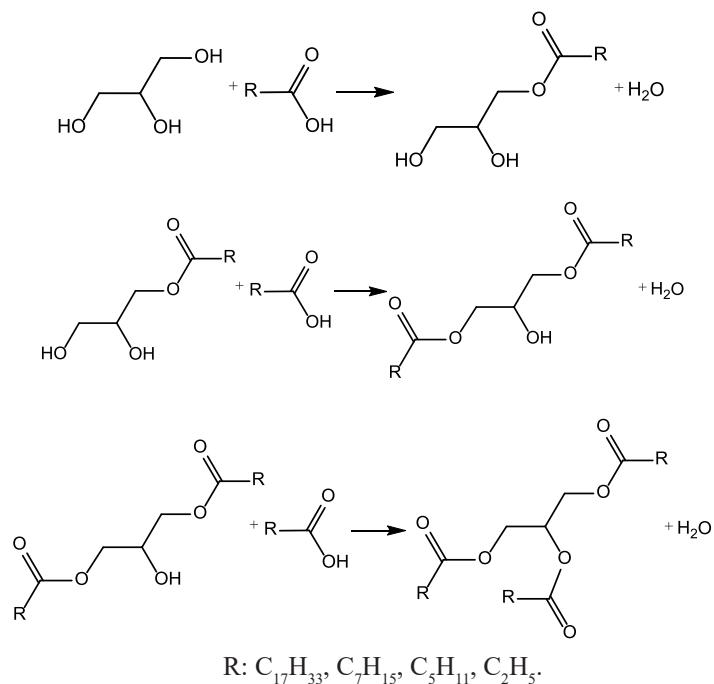
The synthesis of calcium glyceroxide [13] was carried out by the interaction of glycerol with calcium hydroxide (Scheme 1). For removing reaction water by azeotropic distillation using a reflux condenser and an upper-drive agitator, 1.36 mol of glycerol, 0.22 mol of calcium hydroxide, and 30 mL of toluene as an azeotropic forming agent were loaded into the reactor equipped with a Dean-Stark nozzle. The reaction mass was stirred at 450 ± 10 rpm and boiled with the withdrawal of reaction water in the Dean-Stark nozzle. After distilling the calculated amount of reaction water (duration about 7 h), the reaction mass was cooled. The resulting precipitate was separated by filtration under vacuum, washed with ethanol until the unreacted glycerol was completely removed, and dried for 1 h at a temperature of 105°C . The resulting calcium glyceroxide was stored in a desiccator under argon over solid NaOH. IR spectrum, ν , cm^{-1} : 3229 w (OH), 2874 m (C–H), 2836 w (C–H), 1128 w (C–O), 1091 m (C–O), 3641 (Ca–O), 1370 w [$\delta(\text{S–O–N})$], 1306 s [$\delta(\text{C–O–N})$]. Elemental analysis: found with ($29.9 \pm 3.0\%$), H ($6.0 \pm 0.6\%$) [$\text{Ca}(\text{C}_3\text{H}_7\text{O}_3)_2$]; calculated with (32.4%), H (6.3%).



Scheme 1. Synthesis of calcium glyceroxide.

Esterification of glycerol with monocarboxylic acids

The interaction of glycerol with carboxylic acids (Scheme 2) was carried out in a three-necked flask equipped with a reflux condenser, a Dean-Stark nozzle for removing reaction water by azeotropic distillation, a thermometer and an upper-drive agitator. Glycerol, calcium glyceroxide, monocarboxylic acid and toluene as an azeotroping agent were loaded into the reactor (Table 1). Then the temperature of the reaction mass was gradually increased until the azeotrope began to boil ($85\text{--}110^\circ\text{C}$) and kept at this temperature for 10 h. As the reaction progressed, the resulting reaction water was distilled with azeotrope and toluene. After distilling water in an amount of approximately 1 mol, toluene was distilled from the reaction mass in the vacuum of a water jet pump at a temperature of 110°C for 1 h. The unreacted glycerol was separated on the dividing funnel.



Scheme 2. Interaction of glycerol with carboxylic acids.

Method of isolation of glycerides of monocarboxylic acids

Following the esterification process, the reaction mass was mixed with acetone in a mass ratio of 1:1. The resulting mixture was loaded into the reactor and a few drops of phenolphthalein alcohol solution were added. Then, with stirring, a 0.1 mol/dm^3 sodium hydroxide solution was added dropwise to a stable weak pink color over more than 30 s. The resulting precipitate was separated by centrifugation. Then acetone was distilled from the centrifuge at atmospheric pressure.

Investigation of the thermal stability of chloroparaffins

The effectiveness of the obtained samples as complex stabilizers was evaluated according to the standard method for determining the thermal stability of liquid chloroparaffins in terms of the mass fraction of separated hydrogen chloride.

As model compositions, a mixture of the following composition was selected to test the stabilizing effect of additives: 100 wt parts of unstabilized chloroparaffin of the CP-30 brand and 0.5–2 wt parts of the tested additive.

The analyzed mixture in the amount of 9.5–10.5 g was loaded into a test tube equipped

² STO 00203275-201-2006 with amend. 1, 2.

Table 1. Loading of reagents for obtaining complex stabilizers

Sample No.	Starting reagents			
	Glycerol, mol	Carboxylic acid		Calcium glyceroxide, mol
		Name	Quantity, mol	
1*	1	Oleic	1	0.015
2*	1	Octane	1	0.015
3*	1	Hexane	1	0.015
4*	1	Propionic	1	0.015
6	1	Oleic	1.13	0.066
7	1	Oleic	1.21	0.104
8	1	Oleic	1.30	1.148
9	1	Octanoic acid	1.30	1.148
10	1	Hexane	1.30	1.148
11	1	Propionic	1.30	1.148

*Glycerides of monocarboxylic acids were isolated from the resulting reaction mixture according to the procedure.

with a nozzle for nitrogen injection. The test tube was connected to the nitrogen supply line. The exhaust pipe of the nozzle was connected to two sequentially connected Drexel flasks, into the second of which 100 mL of distilled water was pre-poured. The test tube with the analyzed mixture was placed in a bath filled with a thermostatic liquid, preheated to $175 \pm 2^\circ\text{C}$ and nitrogen was supplied through a rheometer at a speed of $30 \text{ cm}^3/\text{min}$. After holding the test tube for 4 h, the Drexel flask containing water was disconnected. The resulting aqueous solution was titrated with a solution of sodium hydroxide of molar concentration $C_{(\text{NaOH})} = 0.01 \text{ mol/dm}^3$ until the color change of the indicator.

Thermal stability was calculated in terms of the mass fraction of separated HCl (X) as a percentage using the formula

$$X = (V \times 0.0003646 \times 100 \times K)/m,$$

where V is the volume of sodium hydroxide solution of molar concentration $C_{(\text{NaOH})} = 0.01 \text{ mol/dm}^3$ spent on titration, cm^3 ; 0.0003646 g/cm^3 is HCl mass corresponding to 1 cm^3 of sodium hydroxide solution of molar concentration $C_{(\text{NaOH})} = 0.01 \text{ mol/dm}^3$; m is the mass of the analyzed sample, g; K is the coefficient of correction to the sodium hydroxide solution.

RESULTS AND DISCUSSION

Glycerol esters and monocarboxylic acids were selected as heat stabilizers for industrial chlorinated paraffins.

A method developed [14] for esterification of glycerol with monocarboxylic acids in the presence of calcium glyceroxide as a catalyst can be used to obtain glycerol esters without the formation of byproducts characteristic of acid catalysis. This process can be described by

successive reactions with the formation of the following products: monoglyceride, diglyceride, and triglyceride.

Glycerides of carboxylic acids synthesized according to the proposed method using monocarboxylic acids with different hydrocarbon substituent lengths were identified by chromatographic mass spectrometric analysis. The compositions of the obtained mixtures of glycerides are presented in Table 2.

The resulting mixtures of glycerides were tested as heat stabilizers of liquid chloroparaffins. The assessment of the thermostabilizing effect of the studied compounds was carried out by determining the thermal stability in terms of the mass fraction of separated hydrogen chloride. For unstabilized chloroparaffin CP-30 (control sample), the mass fraction of the separated hydrogen chloride of 0.714% was measured according to the above-described method.

The results of the study of the thermostabilizing effect of the studied mixtures of glycerides of monocarboxylic acids on chloroparaffin are presented in Figs. 1 and 2.

The results obtained indicate a high thermal stability value even with a small quantity of glycerides. Thus, with a content of 0.5 wt parts glycerides of oleic acid (sample 1) per 100 wt parts of unstabilized chloroparaffin, a mass fraction of separated hydrogen chloride of about 0.07% is achieved, which is 10 times lower than unstabilized chloroparaffin.

According to the graphs of the dependence of the mass fraction of separated hydrogen chloride on the content of carboxylic acid glycerides obtained after converting the weight parts to a molal

concentration (Fig. 2), an increase in the stabilizer concentration of more than 0.05 mol/kg does not lead to an increase in thermal stability.

The following conclusions can be drawn on the basis of the data analysis:

- the stabilizing effect of glycerides of carboxylic acids on industrial chloroparaffin was established. It was found that propionic acid glycerides have the most effective thermostabilizing effect;

- the relationship between the length of the hydrocarbon substituent of carboxylic acid in an ester and the thermostabilizing effect was obtained. It was shown that stabilizing ability decreases with an increase in the number of carbon atoms in the hydrocarbon substituent of carboxylic acid;

- the concentration of glycerides of carboxylic acids at which the maximum thermostabilizing ability is achieved was established. It is advisable to study additives consisting of mixtures of glycerides of various carboxylic acids at a concentration of 0.05 ± 0.005 mol/kg in order to study synergy.

Calcium compounds are standard stabilizers for organochlorine compounds [11]. According to the method developed by us [14], glycerides of carboxylic acids can be synthesized using calcium glyceroxide as a catalyst. During synthesis, calcium glyceroxide is converted into calcium carboxylate (Scheme 3) in the presence of an excess of carboxylic acid corresponding to the amount of catalyst to obtain a complex stabilizer containing glycerides of carboxylic acids and calcium-containing compounds as active substances.

Calcium salts are effective acceptors of hydrogen chloride; when used as part of a stabilizing additive, they neutralize hydrogen chloride to

Table 2. Compositions of the studied mixtures of glycerides of carboxylic acids

Sample No.	Carboxylic acid glycerides	Amount, wt %		
		MG	DG	TG
1	Oleic acid glycerides	81.8	18.2	–
2	Octanoic acid glycerides	68.4	30.4	1.2
3	Hexanoic acid glycerides	66.8	30.7	2.5
4	Propionic acid glycerides	67.5	29.4	3.1

Note: MG are monoglycerides; DG are diglycerides; TG are triglycerides.

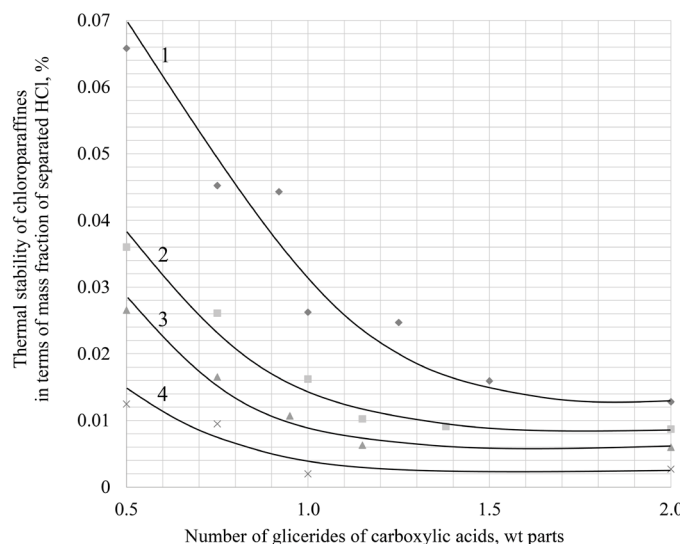


Fig. 1. Dependence of the mass fraction of cleaved hydrogen chloride for chlorpapafin CP-30 on the content of carboxylic acid glycerides (wt parts).

- ◆ Oleic acid glycerides;
- Octanoic acid glycerides;
- ▲ Hexanoic acid glycerides;
- × Propionic acid glycerides.

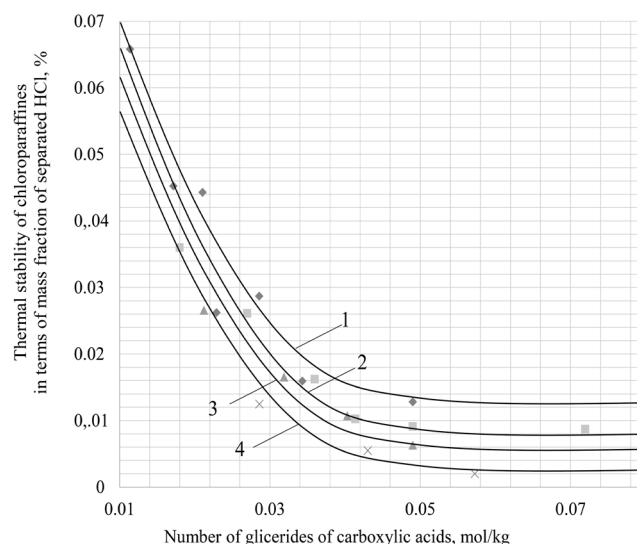


Fig. 2. Dependence of the mass fraction of cleaved hydrogen chloride for chlorpapafin CP-30 on the content of carboxylic acid glycerides (mol/kg).

- ◆ Oleic acid glycerides;
- Octanoic acid glycerides;
- ▲ Hexanoic acid glycerides;
- × Propionic acid glycerides.

prevent its catalytic effect on the reaction of dehydrochlorination of chlorparaffin. It has been assumed that the combined use of monocarboxylic acid glycerides with calcium-containing compounds could lead to a synergistic effect. To determine the ratio of the components of the synergetic composition, laboratory samples (6–8) with different molar ratios of active substances were prepared. Compositions obtained using oleic acid were selected as the object of research. The molar ratios of active substances and the results of thermal stability are presented in Table 3.

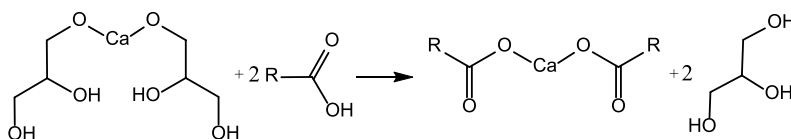
Model compositions for testing the stabilizing effect of the studied additives contain: 100 wt parts of unstabilized chlorparaffin of the CP-30 brand and 2 wt parts of the tested samples (1, 5–11).

The obtained results were compared with the thermostabilizing effect of individual components of the tested compositions: oleic

acid glycerides (sample 1) and calcium oleate (sample 5).

The analysis of the obtained results supports the conclusion that oleic acid glycerides exhibit a synergistic effect on thermal stability in combination with calcium-containing compounds (samples 7 and 8). This phenomenon is explained by the combined action of the used substances acting on various stabilization mechanisms. The resulting hydrogen chloride is chemically bound by calcium compounds. When chlorparaffins are stabilized, carboxylic acid glycerides stabilize labile chlorine atoms due to the dipole interaction between chlorine atoms in chlorparaffin and carbonyl groups of esters.

In accordance with the found synergistic ratio of the components of the stabilizing composition, laboratory samples (8–11) synthesized using monocarboxylic acids with different lengths of the hydrocarbon substituent were



Scheme 3. Conversion of calcium glyceroxide to calcium carboxylate.

Table 3. Influence of the molar ratio of the active substances of the stabilizing mixture on the thermal stability of chlorinated paraffin CP-30

Sample No.	Ratio of the components of the stabilizing compositions, mol		Thermal stability of chlorinated paraffin in terms of the mass fraction of split off HCl, %
	Oleic acid glycerides	Ca ²⁺	
1	1	—	0.0128
6	0.93	0.07	0.0093
7	0.90	0.10	0.0079
8	0.86	0.14	0.0042
5*	—	1	0.0085

*Calcium oleate was used to study the thermostabilizing effect of calcium-containing compounds.

prepared and tested. The obtained results of thermal stability of liquid chloroparaffin CP-30 are presented in Table 4 in terms of the mass fraction of separated hydrogen chloride.

Using the developed version of the complex stabilizer (sample 10), a stabilized sample of chloroparaffin of the CP-470 brand was subsequently used in the manufacture of OM-40 cable plastic

according to the production recipe. Table 5 presents the physical and mechanical parameters of the obtained PVC plastics.

The manufacture and testing of cable plastic was carried out in the *Kaustik* specialized laboratory (Volgograd, Russia) in accordance with the requirements of STO 22542799-04-2001, amend. 1, 2, to OM-40. The test results showed that

Table 4. Thermal stability of CP-30 chlorinated paraffin in terms of the mass fraction of cleaved hydrogen chloride for synergistic mixtures of active ingredients

Sample No.	Used carboxylic acid in the preparation of stabilizing compositions	Ratio of components of stabilizing compositions, mol		Thermal stability of chlorinated paraffin in terms of the mass fraction of split off HCl, %
		Oleic acid glycerides	Ca ²⁺	
8	Oleic acid	0.860	0.140	0.0042
9	Octanoic acid	0.864	0.136	0.0033
10	Hexanoic acid	0.866	0.134	<0.0027
11	Propionic acid	0.870	0.130	<0.0027

Table 5. Physicomechanical properties of cable plastic compound grade OM-40

Normalized indicators of cable compound	Requirements of STO 22542799-04-2001, amend. 1, 2, to OM-40	Actual indicators	
		Plastic compound is made using chlorinated paraffin CP-470A produced by <i>Kaustik</i> (control)	Plastic compound is made using chlorinated paraffin CP-470 stabilized by the proposed composition
Breaking strength, kgf/cm ² , not less	122.4	148	144
Elongation at break, %, not less	300	546	523
Specific volume electrical resistance, $\Omega \cdot \text{m cm}$, not less	$1 \cdot 10^{11}$	$8.3 \cdot 10^{12}$	$5.16 \cdot 10^{12}$
Shore hardness, scale units	70–85	74 ± 2	75 ± 2
Density, g/cm ³ , no more	1.45	1.41	1.41
Additional indicators			
Melt flow index of plastic compound granules at 185°C, 5 kgf, g/10 min ³	Non-standardized	17.53	19.52
Thermal stability of plastic compound granules at 200°C, Congo red, min ⁴	Non-standardized	100	110

the developed version of the stabilizer can be used to stabilize industrial chloroparaffins while maintaining the operational properties of the final products.

CONCLUSIONS

A variant of a complex stabilizer for chloroparaffins based on Russian raw materials for import substitution was proposed, expanding the range of effective stabilizers of organochlorine substances. It has been established that glycerides

of monocarboxylic acids exhibit a thermostabilizing effect on industrial chloroparaffins. The relationship of the length of the hydrocarbon substituent of carboxylic acid in the ester to the thermostabilizing effect was obtained. With an increase in the number of carbon atoms in the hydrocarbon substituent of carboxylic acid, the thermostabilizing ability decreases. The minimum sufficient concentration of glycerides of carboxylic acids 0.05 ± 0.005 mol/kg was established. Above this concentration, there is no increase in the thermal stabilizing effect on chloroparaffin. A synergistic ratio of the components of the stabilizing mixture in terms of thermal

³ GOST 11645-73. Plastics. Determination of flow index of thermoplastics melt by extrusion plastometer. Moscow: Izd. Standartov; 1994 (in Russ).

⁴ GOST 14041-91. Plastics. Determination of the tendency of compounds and products based on vinyl chloride homopolymers and copolymers to evolve hydrogen chloride and any other acidic products of elevated temperatures. Congo red method. Moscow: Izd. Standartov; 1992 (in Russ).

stability was obtained as follows: glycerides of monocarboxylic acids/calcium-containing compounds, equal to 0.85–0.9/0.15–0.1. The tests of the developed sample of the complex stabilizer carried out in the *Kaustik* specialized laboratory demonstrated the possibility of its use for the stabilization of commercial chloroparaffins.

Acknowledgments

The work was performed using the equipment of the Center for Collective Use "Physicochemical methods of Analysis" at the Volgograd State Technical University. The authors thank the specialists of *Kaustik*, Volgograd, for investigating a complex stabilizer for industrial chloroparaffins.

Authors' contributions

Yu.L. Zotov – research concept, development of the experiment, discussion and analysis of the results, and writing the text of the article;

D.M. Zapravdina – research concept, planning and conducting experimental studies, processing the data obtained, and preparation of the data obtained for publication;

E.V. Shishkin – consultation on conducting individual stages of the study, scientific editing;

Yu.V. Popov – consultation on conducting individual stages of the study, scientific editing.

The authors declare no conflicts of interest.

REFERENCES

1. Zotov Yu.L., Butakova N.A., Popov Yu.V. *Okislenie promyshlennykh khlorparafinov kislorodom vozdukh (Oxidation of industrial chlorinated paraffins with atmospheric oxygen)*. Volgograd: IUNL VolgGTU; 2014. 124 p. (in Russ.).
2. Oshin L.A., Treger Yu.A., Motsarev G.V., Sonin E.V., Sergeev E.V., Skibinskaya M.B., Gol'fand E.A. *Promyshlennye khlororganicheskie produkty: spravochnik (Industrial organochlorine products: handbook)*. Moscow: Khimiya; 1978. 656 p. (in Russ.).
3. Rysaev U.Sh., Nafikov A.B., Gil'mutdinov A.T., Nafikova R.F., Rysaev V.U. Synergistic stabilizing compositions for chlorine-containing hydrocarbons. *Bashkirskii khimicheskii zhurnal = Bashkir Chemical Journal*. 2007;14(4):32–36 (in Russ.).
4. Klichkov I.S., Krishtal' N.F., Nakhimovich M.L., Poselenov A.I., Levanovich V.S., Kharitonov V.I. *Method of stabilization of trichlorethylene and perchlorethylene*: USSR Pat. 680303. Publ. 27.12.1999 (in Russ.).
5. Tsuyoshi M., Takushi A., Hirota S. *Method for stabilizing chlorinated aliphatic hydrocarbon*: JP Pat. 2009046444. Prior publ. data 22.08.2007; date of patent 05.03.2009.
6. Krishtal' N.F., Klichkov I.S., Nakhimovich M.L., Poselenov A.I., Sankov B.G., Sveshnikov A.V., Velichko I.N., Gerasimov F.E. *Method for stabilizing methylene chloride*: USSR Pat. 1387349. Publ. 27.06.2000 (in Russ.).
7. Rasulev Z.G., Krishtal' N.F., Nakhimovich M.L., Abdrashitov Ya.M., Rakhimov R.R., Islamshin A.Z. *Method of stabilizing 1,2-dichloroethane or 1,2,3-trichloropropane*: USSR Pat. 1555321. Publ. 07.04.1990 (in Russ.).
8. No B.I., Zotov Yu.L., Klimov D.S., Shishkin E.V., Klimov S.A., Shatalin Yu.V., Knyazeva E.A. Multifunctional compositions "SINSTAD" for polymers. XVII. Adamantyl derivatives of imic acids as stabilizers of chlorinated paraffins. *Plasticheskie massy*. 2004;(2):40–41 (in Russ.).

СПИСОК ЛИТЕРАТУРЫ

1. Зотов Ю.Л., Бутакова Н.А., Попов Ю.В. *Окисление промышленных хлорпарафинов кислородом воздуха*. Волгоград: ИУНЛ ВолгГТУ; 2014. 124 с.
2. Ошин Л.А., Трегер Ю.А., Моцарев Г.В., Сонин Э.В., Сергеев Е.В., Скибинская М.Б., Гольфанд Е.А. *Промышленные хлорорганические продукты: справочник*. М.: Химия; 1978. 656 с.
3. Рысаев У.Ш., Нафиков А.Б., Гильмутдинов А.Т., Нафикова Р.Ф., Рысаев В.У. Синергические стабилизирующие композиции для хлорсодержащих углеводородов. *Башкирский химический журнал*. 2007;14(4):32–36.
4. Кличков И.С., Кришталь Н.Ф., Нахимович М.Л., Поселенов А.И., Леванович В.С., Харитонов В.И. *Способ стабилизации трихлорэтилена и перхлорэтилена*: пат. 680303 СССР. Заявка № 2607154/04, заявл. 18.04.1978; опубл. 27.12.1999.
5. Tsuyoshi M., Takushi A., Hirota S. *Method for stabilizing chlorinated aliphatic hydrocarbon*: JP Pat. 2009046444. Prior publ. data 22.08.2007; date of patent 05.03.2009.
6. Кришталь Н.Ф., Кличков И.С., Нахимович М.Л., Поселенов А.И., Санков Б.Г., Свешников А.В., Величко И.Н., Герасимов Ф.Е. *Способ стабилизации метилхлорида*: пат. 1387349 СССР. Заявка № 4098828/04, заявл. 28.07.1986; опубл. 27.06.2000.
7. Расулев З.Г., Кришталь Н.Ф., Нахимович М.Л., Абдрашитов Я.М., Рахимов Р.Р., Исламшин А.З. *Способ стабилизации 1,2-дихлорэтана или 1,2,3-трихлорпропана*: пат. 1555321 СССР. Заявка № 4207872/23-04, заявл. 06.03.1987; опубл. 07.04.1990, Бюл. № 13.
8. Но Б.И., Зотов Ю.Л., Климов Д.С., Шишкин Е.В., Климов С.А., Шаталин Ю.В., Князева Е.А. Многофункциональные композиции «СИНСТАД» для полимеров. XVII. Адамантилсодержащие производные имидовых кислот в качестве стабилизаторов хлорпарафинов. *Пластические массы*. 2004;(2):40–41.

9. Kutyanin L.I., Kuznetsov A.A., Poddubnyi I.S., Ivanova N.A., Sergeev S.A. *Method for stabilizing halogenated paraffins*: RF Pat. 2245318. Publ. 27.01.2005.

10. No B.I., Zotov Yu.L., Shipaeva T.A., Klimov D.S. Multifunctional compositions "SINSTAD" for polymers. II. Stabilization of chlorinated paraffins KhP-30 with metal stearates. *Plasticheskie massy*. 1997;(4):41–42 (in Russ.).

11. Minsker K.S., Fedoseeva G.T. *Destruktsiya i stabilizatsiya polivinilkhlorda (Destruction and stabilization of polyvinyl chloride)*. Moscow: Khimiya; 1979. 272 p. (in Russ.).

12. Quispe C.A.G., Coronado C.J.R., Carvalho J.A. Glycerol: Production, consumption, prices, characterization and new trends in combustion. *Renewable and Sustainable Energy Reviews*. 2013;27:475–493. <https://doi.org/10.1016/j.rser.2013.06.017>

13. León-Reina L., Cabeza Au., Rius J., Maireles-Torres P., Alba-Rubio A.C., Granados M.L. Structural and surface study of calcium glyceroxide, an active phase for biodiesel production under heterogeneous catalysis. *J. Catal.* 2013;300:30–36. <http://dx.doi.org/10.1016/j.jcat.2012.12.016>

14. Zotov Yu.L., Zapravdina D.M. *Method for obtaining plasticiser for polyvinyl chloride composition*: RF Pat. 2643996. Publ. 06.02.2018.

9. Кутянин Л.И., Кузнецов А.А., Поддубный И.С., Иванова Н.А., Сергеев С.А. *Способ стабилизации галогенированных парафинов*: пат. 2245318 РФ. Заявка № 2002122154/04, заявл. 14.08.2002; опубл. 27.01.2005, Бюл. № 3.

10. Но Б.И., Зотов Ю.Л., Шипаева Т.А., Климов Д.С. Многофункциональные композиции «СИНСТАД» для полимеров. II. Стабилизация хлорпарафинов ХП-30 стеаратами металлов. *Пластические массы*. 1997;(4):41–42.

11. Минскер К.С., Федосеева Г.Т. *Деструкция и стабилизация поливинилхлорида*. М.: Химия; 1979. 272 с.

12. Quispe C.A.G., Coronado C.J.R., Carvalho J.A. Glycerol: Production, consumption, prices, characterization and new trends in combustion. *Renewable and Sustainable Energy Reviews*. 2013;27:475–493. <https://doi.org/10.1016/j.rser.2013.06.017>

13. León-Reina L., Cabeza Au., Rius J., Maireles-Torres P., Alba-Rubio A.C., Granados M.L. Structural and surface study of calcium glyceroxide, an active phase for biodiesel production under heterogeneous catalysis. *J. Catal.* 2013;300:30–36. <http://dx.doi.org/10.1016/j.jcat.2012.12.016>

14. Зотов Ю.Л., Заправдина Д.М. *Способ получения пластификатора для поливинилхлоридной композиции*: пат. 2643996 РФ. Заявка №2017100414, заявл. 09.01.2017; опубл. 06.02.2018, Бюл. № 4. 6 с.

About the authors:

Yuriy L. Zotov, Dr. Sci. (Chem.), Professor, Department of Organic and Petrochemical Synthesis Technology, Volgograd State Technical University (28, pr. im. V.I. Lenina, Volgograd, 400005, Russia). E-mail: ylzotov@mail.ru. Scopus Author ID 7003371961, RSCI SPIN-code 7543-9740, <http://orcid.org/0000-0001-6301-0570>

Daria M. Zapravdina, Assistant, Department of Organic and Petrochemical Synthesis Technology, Volgograd State Technical University (28, pr. im. V.I. Lenina, Volgograd, 400005, Russia). E-mail: zapravdinadasha94@gmail.com. RSCI SPIN-code 2913-1891, <https://orcid.org/0000-0002-8654-2382>

Evgeniy V. Shishkin, Dr. Sci. (Chem.), Professor, Department of Organic and Petrochemical Synthesis Technology, Volgograd State Technical University (28, pr. im. V.I. Lenina, Volgograd, 400005, Russia). E-mail: shishkin@vstu.ru. Scopus Author ID 7004314557, RSCI SPIN-code 3280-1800, <https://orcid.org/0000-0002-2994-422X>

Yuriy V. Popov, Dr. Sci. (Chem.), Professor, Department of Organic and Petrochemical Synthesis Technology, Volgograd State Technical University (28, pr. im. V.I. Lenina, Volgograd, 400005, Russia). E-mail: iury.popov@yandex.ru. Scopus Author ID 26028090100, RSCI SPIN-code 4582-3342, <http://orcid.org/0000-0001-5659-028X>

Об авторах:

Зотов Юрий Львович, д.х.н., профессор кафедры технологии органического и нефтехимического синтеза ФГБОУ ВО «Волгоградский государственный технический университет» (400005, Россия, Волгоград, пр-т им. В.И. Ленина, д. 28). E-mail: ylzotov@mail.ru. Scopus Author ID 7003371961, SPIN-код РИНЦ 7543-9740, <http://orcid.org/0000-0001-6301-0570>

Заправдина Дарья Михайловна, ассистент кафедры технологии органического и нефтехимического синтеза ФГБОУ ВО «Волгоградский государственный технический университет» (400005, Россия, Волгоград, пр-т им. В.И. Ленина, д. 28). E-mail: zapravdinadasha94@gmail.com. SPIN-код РИНЦ 2913-1891, <https://orcid.org/0000-0002-8654-2382>

Шишкин Евгений Вениаминович, д.х.н., профессор кафедры технологии органического и нефтехимического синтеза ФГБОУ ВО «Волгоградский государственный технический университет» (400005, Россия, Волгоград, пр-т им. В.И. Ленина, д. 28). E-mail: shishkin@vstu.ru. Scopus Author ID 7004314557, SPIN-код РИНЦ 3280-1800, <https://orcid.org/0000-0002-2994-422X>

Попов Юрий Васильевич, д.х.н., профессор кафедры технологии органического и нефтехимического синтеза ФГБОУ ВО «Волгоградский государственный технический университет» (400005, Россия, Волгоград, пр-т им. В.И. Ленина, д. 28). E-mail: iury.popov@yandex.ru. Scopus Author ID 26028090100, SPIN-код РИНЦ 4582-3342, <http://orcid.org/0000-0001-5659-028X>

The article was submitted: May 23, 2022; approved after reviewing: June 08, 2022; accepted for publication: July 15, 2022.

Translated from Russian into English by N. Isaeva

Edited for English language and spelling by Thomas Beavitt

**CHEMISTRY AND TECHNOLOGY OF MEDICINAL COMPOUNDS
AND BIOLOGICALLY ACTIVE SUBSTANCES**

**ХИМИЯ И ТЕХНОЛОГИЯ ЛЕКАРСТВЕННЫХ ПРЕПАРАТОВ
И БИОЛОГИЧЕСКИ АКТИВНЫХ СОЕДИНЕНИЙ**

ISSN 2686-7575 (Online)

<https://doi.org/10.32362/2410-6593-2022-17-4-311-322>



UDC 547.792.6

RESEARCH ARTICLE

Synthesis of 5-oxymethyl-1,2,4-triazole-3-carboxamides

Lyubov E. Grebenkina[✉], **Alexander N. Prutkov**, **Andrey V. Matveev**,
Mikhail V. Chudinov

*MIREA – Russian Technological University (M.V. Lomonosov Institute of Fine Chemical Technologies),
Moscow, 119571 Russia*

[✉]Corresponding author, e-mail: LEGrebenkina@mail.ru

Abstract

Objectives. A key step in the synthesis of natural nucleoside analogs is the formation of a glycosidic bond between the carbohydrate fragment and the heterocyclic base. Glycosylation methods differ in terms of regio- and stereoselectivity. A promising method for the highly specific synthesis of new pharmacologically active compounds involves an enzymatic reaction catalyzed by genetically engineered nucleoside phosphorylases. This study is devoted to the synthesis of a library of analogs of nucleoside heterocyclic bases—5-oxymethyl-1,2,4-triazole-3-carboxamides—in order to investigate the substrate specificity of genetically engineered nucleoside phosphorylases.

Methods. A method of cyclization of acylamidrazones obtained from the single synthetic precursor β -N-tert-butyloxycarbonyl-oxalamidrazone was used to parallel-synthesize new 5-alkoxy/aryloxymethyl-1,2,4-triazole-3-carboxamides. Silica gel column chromatography was used to isolate and purify the synthesized compounds. A complex of physicochemical analysis methods (nuclear magnetic resonance spectroscopy, chromatography, and mass spectrometry) confirmed the structure of the compounds obtained in the work.

Results. 5-alkoxy/aryloxymethyl-1,2,4-triazole-3-carboxamides were obtained to study the substrate specificity of genetically engineered nucleoside phosphorylases. The possibility of obtaining new nucleoside analogs by the chemico-enzymatic method was demonstrated on the basis of preliminary assessment results.

Conclusions. The physicochemical characteristics of a series of novel 5-alkoxy/aryloxymethyl-1,2,4-triazole-3-carboxamides were studied along with their potential to act as substrates for the transglycosylation reaction catalyzed by nucleoside phosphorylases.

Keywords: nucleoside analogs, 5-oximethyl-1,2,4-triazole-3-carboxamides, parallel synthesis, nucleoside phosphorylase, substrate specificity

For citation: Grebenkina L.E., Prutkov A.N., Matveev A.V., Chudinov M.V. Synthesis of 5-oxymethyl-1,2,4-triazole-3-carboxamides. *Tonk. Khim. Tekhnol. = Fine Chem. Technol.* 2022;17(4):311–322 (Russ., Eng.). <https://doi.org/10.32362/2410-6593-2022-17-4-311-322>

НАУЧНАЯ СТАТЬЯ

Синтез 5-оксиметил-1,2,4-триазол-3-карбоксаминов

Л.Е. Гребенкина, А.Н. Прутков, А.В. Матвеев, М.В. Чудинов

МИРЭА – Российский технологический университет (Институт тонких химических технологий им. М.В. Ломоносова), Москва, 119571 Россия

✉ Corresponding author, e-mail: LEGrebenkina@mail.ru

Аннотация

Цели. Ключевая стадия синтеза аналогов природных нуклеозидов – образование гликозидной связи между углеводным фрагментом и гетероциклическим основанием. Методы гликозилирования различаются по регио- и стереоселективности. Ферментативная реакция, катализируемая генно-инженерными нуклеозидфосфорилазами – перспективный метод высокоспецифичного синтеза новых фармакологически активных соединений. Данное исследование посвящено синтезу библиотеки аналогов гетероциклических оснований нуклеозидов – 5-оксиметил-1,2,4-триазол-3-карбоксаминов для изучения субстратной специфичности генно-инженерных нуклеозидфосфорилаз.

Методы. Для параллельного синтеза новых 5-алкокси/арилоксиметил 1,2,4-триазол-3-карбоксаминов применен метод циклизации ациламидразонов, получаемых из единого синтетического предшественника – β -N-третбутилоксикарбонил-оксаламидразона. Для выделения и очистки синтезированных соединений использована колоночная хроматография на силикагеле. Структура полученных в работе соединений подтверждена комплексом методов физико-химического анализа: спектроскопией ядерного магнитного резонанса и хромато-масс-спектрометрией.

Результаты. Получены 5-алкокси/арилоксиметил-1,2,4-триазол-3-карбоксамины для изучения субстратной специфичности генно-инженерных нуклеозидфосфорилаз. По результатам предварительной оценки показана возможность получения из них новых аналогов нуклеозидов химико-ферментативным методом.

Выводы. Для серии новых 5-алкокси/арилоксиметил-1,2,4-триазол-3-карбоксаминов изучены физико-химические характеристики, а также их способность выступать в роли субстратов реакции трансгликозилирования, катализируемой нуклеозидфосфорилазами.

Ключевые слова: аналоги нуклеозидов, 5-оксиметил-1,2,4-триазол-3-карбоксамиды, параллельный синтез, нуклеозидфосфорилазы, субстратная специфичность.

Для цитирования: Гребенкина Л.Е., Прутков А.Н., Матвеев А.В., Чудинов М.В. Синтез 5-оксиметил-1,2,4-триазол-3-карбоксамидов. *Тонкие химические технологии*. 2022;17(4):311–322. <https://doi.org/10.32362/2410-6593-2022-17-4-311-322>

INTRODUCTION

The work of many research groups in the field of medical chemistry, molecular biology and biotechnology is focused on the study of the biological properties of nucleoside analogs (NA) [1–4]. These compounds are mainly used for antiviral [5–10], anticancer drug [2, 11–13] and antibiotic [3, 14–15] purposes. Various approaches and their combinations used in the design of biologically active nucleoside preparations include modification of both the carbohydrate fragment of the molecule and the aglycone [2, 16–19]. At the same time, most nucleoside analogs that exhibit biological activity retain the β -*N*-glycoside bond of natural nucleosides.

To date, the need for drugs based on modified nucleoside analogs is mainly being met using effective chemical synthesis protocols. However, the chemico-enzymatic method of glycosylation of heterocyclic bases using recombinant enzymes is also a promising alternative approach to implementing the creation of a β -*N*-glycoside bond, comprising one of the key stages of nucleoside production [20]. The variety of nucleoside analogs obtained via classical chemical synthesis is limited by the stereo- and regioselectivity of glycosylation strategies, as well as the stability of intermediates during chemical transformations. The chemico-enzymatic method, conversely, is strictly stereo- and regiospecific, but the variety of target compounds obtained by this pathway is limited by the substrate specificity of the enzyme used.

Genetically engineered bacterial nucleoside phosphorylases (NP) of the pentosyltransferase group (CF 2.4.2) are often used for the chemico-enzymatic production of nucleoside analogs [21–23]. These enzymes catalyze several reactions: the synthesis of nucleotides and their phosphorolysis, as well as the transfer of a carbohydrate fragment

of nucleosides to heterocyclic bases (transglycosylation reaction). Due to their rather low substrate specificity, they are suitable for use in the synthesis of a number of drugs [24–28]. Chemico-enzymatic transglycosylation becomes a convenient tool for obtaining new nucleoside analogs with modified heterocyclic bases and different carbohydrate fragments on account of the low selectivity of bacterial nucleoside phosphorylases [28–31]. In order to study the potential of nucleoside phosphorylases as a research and technological tool, an important task is the synthesis of heterocyclic bases of nucleoside analogs—potential substrates of these enzymes. In particular, derivatives of 1,2,4-triazole-3-carboxamide can form substrates for the biotechnological production of analogs of the antiviral drug ribavirin (1- β -D-ribofuranosyl-1,2,4-triazole-3-carboxamide, virazole). In the present study, we developed a synthetic approach and obtained a series of 5-alkoxy/aryloxymethyl-1,2,4-triazole-3-carboxamides, substrates for the chemico-enzymatic synthesis of new ribavirin analogs.

RESULTS AND DISCUSSION

Although isosteric to purine bases 1,2,4-triazole-3-carboxamide is an excellent substrate of genetically engineered purine nucleoside phosphorylases (PNP) and uridine phosphorylases (UrP), the introduction of substituents in the 5 position of the 1,2,4-triazole ring significantly affects the ability of such derivatives to react with enzymatic transglycosylation. Studies of the substrate properties of heterocyclic bases synthesized in our laboratory, which were carried out in the Laboratory of Biotechnology of the Shemyakin and Ovchinnikov Institute of Bioorganic Chemistry, Russian Academy of Sciences (IBCh RAS), initially led us to believe that steric difficulties in

the active center of NP limit substrate properties with an increase in the size of the substituent. With the exception of 5-methyl-1,2,4-triazole-3-carboxamide, 1,2,4-triazole-3-carboxamides containing a halogen, a nitro group, a hydroxyl, or simple alkyl substituents at position 5 were not found to be suitable for use as substrates for NP [32]. However, recently obtained results have contradicted this point of view. Some of the compounds synthesized by us, which contained an oxymethyl fragment at the 5 position of the 1,2,4-triazole ring, unexpectedly entered into an enzymatic transglycosylation reaction. In order to establish the limits of the substrate specificity of NP with respect to homologs of 5-oxymethyl-1,2,4-triazole-3-carboxamide, we synthesized a library of derivatives of 1,2,4-triazole-3-carboxamide **6a-i** with alkoxyethyl substituents increasing along the length of the carbon backbone, up to *n*-decyloxyethyl, as well as bulk 5-isopropoxy-, 5-phenoxy-, and 5-benzyloxyethyl substituents.

The main methods of synthesis of 1,2,4-triazole-3-carboxylic acid derivatives are based on the cyclization of amidrazones [17–20]. In order to obtain a homologous library of derivatives of 5-substituted 1,2,4-triazole-3-carboxamide, we considered two previously developed methods (Scheme 1). Although the first [33] can be used to synthesize a number of compounds in parallel from a single precursor of β -*N*-Boc-oxalamidrazone (**a**), (where Boc is the *tert*-butyloxycarbonyl protective group), it has the disadvantage of relatively low yields of target compounds. Conversely, while the second method [34] produces high yields of 5-substituted 1,2,4-triazole-3-carboxylic acids, it requires the production of individual synthetic precursors for each target compound, thus increasing the time of the experiment [35]. Therefore, in order to solve the problem of combinatorial

synthesis, we chose a parallel method for obtaining derivatives of 1,2,4-triazole-3-carboxylic acids **c** (method I in Scheme 1).

A single synthetic precursor of β -*N*-Boc-oxalamidrazone (**3**) was obtained by the interaction of thiooxamic acid ethyl ester (**2**) with Boc-hydrazine (**1**) (Scheme 2).

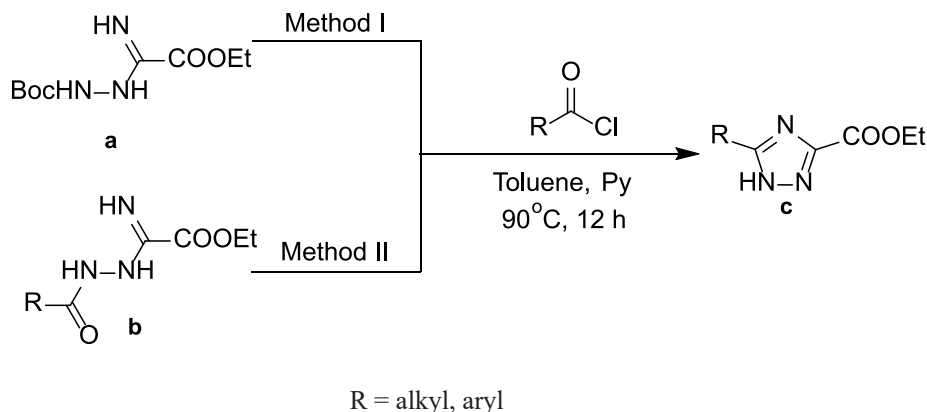
Ethyl esters of 5-alkoxy/aryloxyethyl-1,2,4-triazole-3-carboxylic acids **5a-h** were obtained by acylation of amidrazones **3** with **4a-h** hydroxyacetic acids chlorides followed by cyclization in pyridine at a boiling point (115°C). Further, the **5a-h** esters were converted into the corresponding **6a-h** amides by treatment with an aqueous-methanolic solution of ammonia (Scheme 3).

Compound **6j** was also prepared according to the above procedure. However, it was difficult to isolate the ethyl ether of 5-acetoxymethyl-1,2,4-triazole-3-carboxylic acid **5i** following cyclization in this case since the labile acetyl group was partially hydrolyzed during the treatment of the reaction mixture. A mixture of ethyl esters of 5-acetoxymethyl-**5i** and 5-hydroxymethyl-1,2,4-triazole-3-carboxylic acid **5j** was received. This mixture was treated with an ammonia solution, resulting in the complete removal of the acetyl group to obtain amide **6j** (Scheme 4).

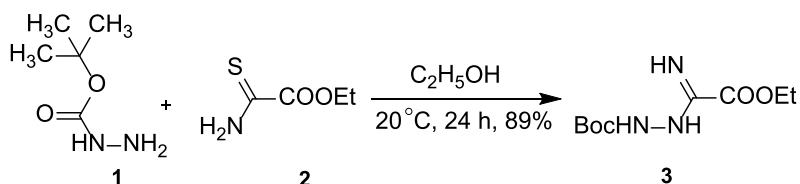
The structure and purity of all final and intermediate compounds are proved by methods ^1H and ^{13}C nuclear magnetic resonance (NMR) spectroscopy and high-performance liquid chromatography (HPLC) with a mass spectrometric (MS) detector, the outputs are shown in Table 1.

The primary results of a preliminary study of the substrate specificity of NP in relation to synthesized amides **6a-h**, **6j** carried out in the Laboratory of Biotechnology of the IBCh RAS by the previously described method [32] are given in Table 2.

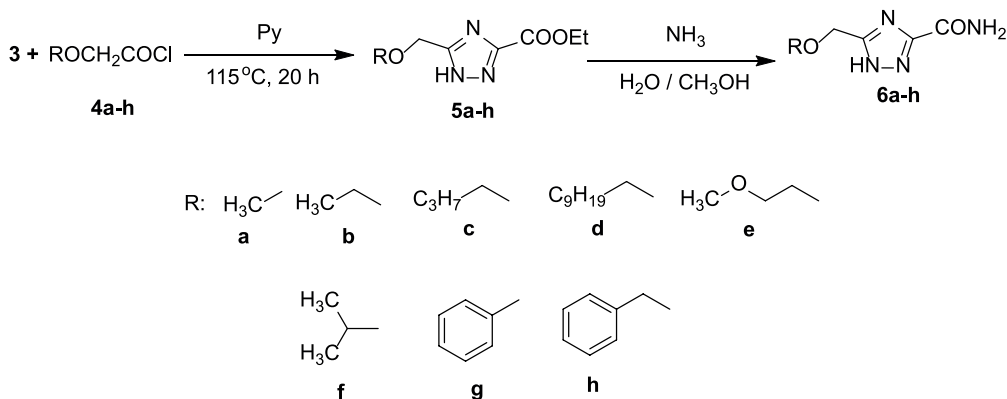
As can be seen from the data, the chemico-enzymatic method can be used to obtain



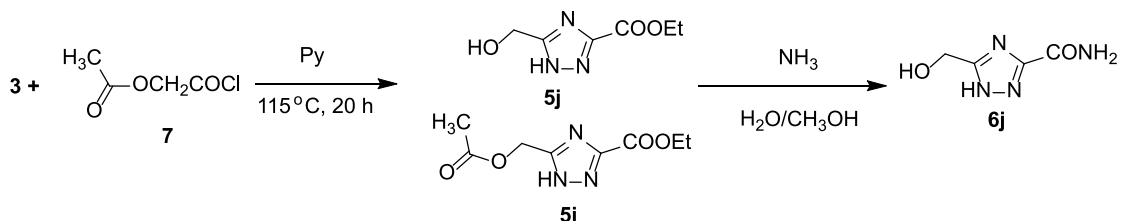
Scheme 1. 5-Substituted 1,2,4-triazole-3-carboxamide derivatives main synthesis methods (Boc is *tert*-butyloxycarbonyl; Et is ethyl; Py is pyridine).



Scheme 2. Synthesis of ethyl β -*N*-Boc-oxalamidrazone (Boc is *tert*-butyloxycarbonyl; Et is ethyl).



Scheme 3. Synthesis of 5-alkoxy/aryloxymethyl-1,2,4-triazole-3-carboxamides **6a-h** (Et is ethyl; Py is pyridine).



Scheme 4. Synthesis of 5-hydroxymethyl-1,2,4-triazole-3-carboxamide **6j** (Et is ethyl; Py is pyridine).

deoxyribosides from almost the entire range of synthesized compounds **6a-h**, **6j** (Schemes 3 and 4). Conversely, it seems to be impossible to obtain ribosides of 5-hydroxymethyl-1,2,4-triazole-3-carboxamides using this method.

EXPERIMENTAL

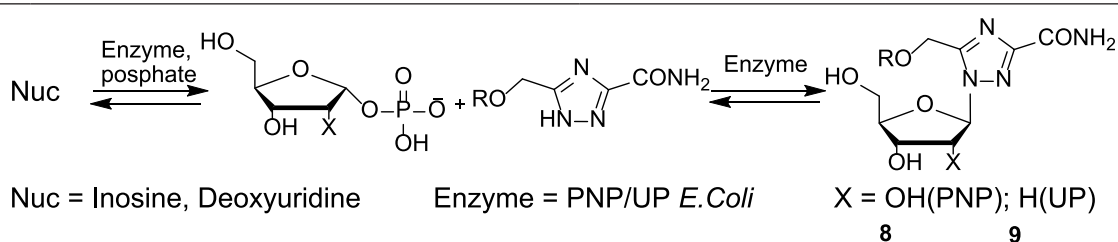
The solvents used in the work were purified by standard methods, with absorption being carried out in the usual way [32]. The reactions were monitored using thin-layer chromatography (TLC) on PTSH-AF-A-ultra violet (UV) plates (aluminum base; fractionated silica gel particle size is 5–17 μ m; sorbent layer thickness is 90–120 μ m; phosphor is 254 nm) (*Sorbfil*, Russia). The substances were visualized in UV light at 254 nm; phosphoric-molybdenum acid, ninhydrin, and iodine were

additionally used. Kieselgel 60 Å (0.040–0.063 mm) silica gel (*Merck*, Germany) was used for column chromatography.

^1H and ^{13}C NMR spectra were recorded on a DPX-300 instrument (*Bruker*, Germany) with a resonant frequency for protons of ^1H = 300 MHz, ^{13}C = 75 MHz. Notation in ^1H NMR spectra as follows: s is a singlet, d is a doublet, dd is a doublet of doublets, t is a triplet, q is a quartet, m is a multiplet, w is a widened signal. Chromatography-mass spectrometry studies were performed on the LCMS-2020 device (*Shimadzu*, Japan) on the Luna C18 column (*Phenomenex*, USA) in gradient mode with electrospray ionization (150 \times 4.6 mm, particle size is 3 μ m, pore size is 100 Å. Mobile phases: A is 0.1% formic acid solution in water, B is acetonitrile. Gradient: up to 0.5 min—5% V, from 0.5 to 10.5 min—from 5 to 100% V, from 10.5 to 12 min—100% V, from 12 to 14 min—from 100% to

Table 1. Yields of synthesized compounds

Compound	5a	5b	5c	5d	5e	5f	5g	5h	5i+5j
Yield, %	57	22	45	36	31	14	63	59	–
Compound	6a	6b	6c	6d	6e	6f	6g	6h	6j
Yield, %	64	84	21	50	60	33	89	77	79

 Table 2. Specificity of uridine phosphorylase towards 5-alkoxy/aryloxymethyl-1,2,4-triazole-3-carboxamides **6a-h**, **6j**


No.	R	PNP	UP
6a	Me	–	+
6b	<i>n</i> -Pr	–	+
6c	<i>n</i> -Bu	–	+
6d	<i>n</i> -C ₁₀ H ₂₁	–	–
6e	–CH ₂ CH ₂ OMe	–	+
6f	<i>i</i> -Pr	–	+
6g	Ph	–	–
6h	Bn	–	+
6j	H	+	+

Note: Minus sign indicates, that products of the enzymatic reaction **8** and **9** were not detected in the reaction mass by the HPLC–MS method. Plus sign indicates, that the products of the enzymatic reaction **8** and **9** were found in the reaction mass by the HPLC–MS method. PNP is purine nucleoside phosphorylase; UP is uridine phosphorylase; Me is methyl; *n*-Pr is *n*-propyl; *n*-Bu is *n*-butyl; *i*-Pr is isopropyl; Ph is phenyl; Bn is benzyl; H is hydrogen; Nuc is inosine, deoxyuridine; *E. coli* is *Escherichia coli*.

5% V. The volume of the injected sample is 2–10 μL . Mass spectra were recorded in the positive ion mode (range from 160 to 2000 Da). Parameters of the ionization source: heater temperature is 40°C, capillary temperature is 25°C, desiccant gas flow is 15 L/min, spray gas is 1.5 L/min, ionization voltage is 4.5 kV).

Ethyl- β -*N*-Boc-oxalamidrazone (3)

A mixture of 18.23 g (137 mmol) of thiooxamic acid ethyl ether **2** and 18.10 g (137 mmol) of Boc-hydrazine **1** was dissolved in 80 mL of ethyl alcohol. The reaction mixture was stirred for 24 h. The resulting precipitate was filtered, washed with 10 mL of ethyl alcohol and dried in air. Product yield: 28.25 g (89%), $T_{\text{m.p.}}$ = 178–180°C.

^1H NMR spectrum (dimethyl sulfoxide ($\text{DMSO}-d_6$), δ , ppm: 1.23 (3H, t, J = 7.14 Hz, CH_2CH_3); 1.43 (9H, s, $\text{C}(\text{CH}_3)_3$); 4.19 (2H, q, J = 7.14 Hz, CH_2CH_3); 6.21 (2H, s, NHNH); 9.22 (1H, s, NH). ^{13}C NMR spectrum ($\text{DMSO}-d_6$), δ , ppm: 13.90; 28.01; 61.31; 79.12; 136.70; 152.51; 162.09. For $\text{C}_9\text{H}_{18}\text{N}_3\text{O}_4$, m/z $[\text{M}+\text{H}]^+$ calculated: 232.13; found: 232.12.

General procedure for synthesis of ethyl esters of 5-alkoxy/aryloxyethyl-1,2,4-triazole-3-carboxylic acids 5a-j

Carboxylic acid chlorohydrate (2.15 eq.) was added drop-by-drop to a suspension of **1** eq. of ethyl- β -*N*-Boc-oxalamidrazone **3** in absolute pyridine when cooled to 0°C. The reaction mass was heated to boiling point and stirred for 20 h. After the end of the reaction (reaction controlled by TLC; chloroform-methanol 5% system), the solvent was removed on a vacuum rotary evaporator. A 1 M aqueous HCl solution was added to the residue and extracted 3 times with ethyl acetate in equal portions. The organic phases were combined and dried Na_2SO_4 , the solvent was removed on a vacuum rotary evaporator. The product was isolated using column chromatography on silica gel, the chloroform eluent was methanol (with a methanol gradient from 0 to 7%).

Ethyl ether of 5-(methoxymethyl)-1,2,4-triazole-3-carboxylic acid (5a)

1.00 g (4.32 mmol) of ethyl- β -*N*-Boc-oxalamidrazone **3**, 10 mL of absolute pyridine, 0.85 mL (9.31 mmol) of methoxyacetic acid chlorangidride. R_f = 0.58. Product yield: 0.46 g (57%).

^1H NMR spectrum (CDCl_3), δ , ppm: 1.40 (3H, t, J = 7.14 Hz, CH_2CH_3); 3.47 (3H, s, CH_3OCH_2); 4.46 (2H, q, J = 7.14 Hz, CH_2CH_3); 4.72 (2H, s, CH_3OCH_2). ^{13}C NMR spectrum (CDCl_3), δ , ppm: 13.91; 58.86;

61.96; 65.69; 153.24; 156.19; 159.52. For $\text{C}_7\text{H}_{11}\text{N}_3\text{O}_3$, m/z $[\text{M}+\text{H}]^+$ calculated: 186.19; found: 186.17.

Ethyl ether of 5-(ethoxymethyl)-1,2,4-triazole-3-carboxylic acid (5b)

1.00 g (4.3 mmol) ethyl- β -*N*-Boc-oxalamidrazone **3**, 10 mL of absolute pyridine, 1.11 g (9.3 mmol) ethoxyacetic acid chlorangidride. R_f = 0.55. Product yield: 0.19 g (22%).

^1H NMR spectrum (CDCl_3), δ , ppm: 1.16 (3H, t, J = 7.00 Hz, $\text{CH}_2\text{O}-\text{CH}_2\text{CH}_3$); 1.35 (3H, t, J = 7.14 Hz, $\text{COO}-\text{CH}_2\text{CH}_3$); 3.59 (2H, q, J = 7.01 Hz, $\text{CH}_2\text{O}-\text{CH}_2\text{CH}_3$); 4.42 (2H, q, J = 7.14 Hz, CH_2CH_3); 4.73 (2H, s, $\text{CH}_2\text{O}-\text{CH}_2\text{CH}_3$). ^{13}C NMR spectrum (CDCl_3), δ , ppm: 14.09; 14.84; 62.08; 64.13; 67.08; 153.92; 156.57; 159.65. For $\text{C}_8\text{H}_{13}\text{N}_3\text{O}_3$, m/z $[\text{M}+\text{H}]^+$ calculated: 200.22; found: 200.20.

Ethyl ether of 5-(*n*-butoxymethyl)-1,2,4-triazole-3-carboxylic acid (5c)

1.16 g (5 mmol) of ethyl- β -*N*-Boc-oxalamidrazone **3**, 10 mL of absolute pyridine, 1.61 g (13 mmol) of *n*-butoxyacetic acid chlorangidride. R_f = 0.45. Product yield: 0.51 g (45%).

^1H NMR spectrum (CDCl_3), δ , ppm: 0.90 (3H, t, J = 7.32 Hz, $\text{O}(\text{CH}_2)_3-\text{CH}_3$); 1.30–1.43 (2H, m, $\text{O}(\text{CH}_2)_2-\text{CH}_2\text{CH}_3$); 1.41 (3H, t, J = 7.14 Hz, $\text{CO}-\text{CH}_2\text{CH}_3$); 1.54–1.64 (2H, m, $\text{OCN}_2\text{CH}_2\text{CH}_2\text{CH}_3$); 3.58 (2H, t, J = 6.63 Hz, $\text{O}-\text{CH}_2(\text{CH}_2)_2\text{CH}_3$); 4.46 (2H, q, J = 7.14 Hz, $\text{CO}-\text{CH}_2\text{CH}_3$); 4.73 (2H, s, $\text{CH}_3(\text{CH}_2)_3\text{OCH}_2-$). ^{13}C NMR spectrum (CDCl_3), δ , ppm: 13.80; 14.20; 19.11; 29.66; 31.44; 62.13; 64.71; 71.74; 154.10; 156.77; 159.60. For $\text{C}_{10}\text{H}_{17}\text{N}_3\text{O}_3$, m/z $[\text{M}+\text{H}]^+$ calculated: 228.27; found: 228.26.

Ethyl ether of 5-(*n*-decyloxymethyl)-1,2,4-triazole-3-carboxylic acid (5d)

0.40 g (1.7 mmol) ethyl- β -*N*-Boc-oxalamidrazone **3**, 10 mL of absolute pyridine, 0.84 g (3.6 mmol) decyloxyacetic acid chlorangidride. R_f = 0.62. Product yield: 0.19 g (36%).

^1H NMR spectrum (CDCl_3), δ , ppm: 0.83–0.87 (3H, m, $\text{CH}_2\text{CH}_2-\text{CH}_3$); 1.23 (14H, s, $\text{OCH}_2\text{CH}_2-(\text{CH}_2)_7\text{CH}_3$); 1.40 (3H, t, J = 7.14 Hz, $\text{COOCH}_2-\text{CH}_3$); 1.54–1.63 (2H, m, $\text{OCH}_2-\text{CH}_2(\text{CH}_2)_7\text{CH}_3$); 3.56 (2H, t, J = 6.72 Hz, $\text{O}-\text{CH}_2(\text{CH}_2)_8\text{CH}_3$); 4.46 (2H, q, J = 7.14 Hz, $\text{COO}-\text{CH}_2\text{CH}_3$); 4.73 (2H, s, $\text{CH}_3(\text{CH}_2)_9\text{OCH}_2-$). ^{13}C NMR spectrum, (CDCl_3), δ , ppm: 29.27; 29.37; 29.40; 29.52; 29.51; 14.08; 14.18; 22.63; 25.91; 31.84; 62.14; 64.62; 65.33; 67.78; 72.05; 126.98; 127.65; 128.53; 153.96; 156.71; 159.58. For $\text{C}_{16}\text{H}_{29}\text{N}_3\text{O}_3$, m/z $[\text{M}+\text{H}]^+$ calculated: 312.43; found: 312.41.

Ethyl ether 5-[1-(2-methoxy)ethoxymethyl]-1,2,4-triazole-3-carboxylic acid (5e)

1.00 g (4.3 mmol) of ethyl- β -N-Boc-oxalamidrazone **3**, 10 mL of absolute pyridine, 1.40 g (9.3 mmol) of 1-(2-methoxy) ethoxyacetic acid chlorohydride. $R_f = 0.47$. Product yield: 0.30 g (31%).

^1H NMR spectrum (CDCl_3), δ , ppm: 1.39 (3H, t, $J = 7.11$ Hz, $\text{COO}-\text{CH}_2\text{CH}_3$); 3.45 (3H, s, $\text{CH}_2\text{O}-\text{CH}_3$); 3.60–3.63 (2H, m, $\text{CH}_2-\text{CH}_2\text{OCH}_3$); 3.76–3.79 (2H, m, $\text{O}-\text{CH}_2\text{CH}_2\text{OCH}_3$); 4.45 (2H, q, $J = 7.14$ Hz, $\text{COO}-\text{CH}_2\text{CH}_3$); 4.82 (2H, s, $-\text{CH}_2\text{OCH}_2\text{CH}_2\text{OCH}_3$). ^{13}C NMR spectrum (CDCl_3), δ , ppm: 14.19; 59.01; 61.91; 65.42; 70.74; 71.82; 154.86; 156.51; 159.83. For $\text{C}_9\text{H}_{16}\text{N}_3\text{O}_4$, m/z $[\text{M}+\text{H}]^+$ calculated: 230.24; found: 230.22.

Ethyl ether of 5-(isopropoxyethyl)-1,2,4-triazole-3-carboxylic acid (5f)

6.74 g (27 mmol) ethyl- β -N-Boc-oxalamidrazone **3**, 15 mL of absolute pyridine, 7.74 g (57 mmol) isopropoxyacetic acid chlorangidride. $R_f = 0.45$. Product yield: 0.78 g (14%).

^1H NMR spectrum (CDCl_3), δ , ppm: 1.22 (6H, d, $J = 6.17$ Hz ($(\text{CH}_3)_2\text{CHO}-$); 1.42 (3H, t, $J = 7.14$ Hz, $\text{COO}-\text{CH}_2\text{CH}_3$); 3.73–3.81 (1H, m, $(\text{CH}_3)_2-\text{CHOCH}_2$); 4.47 (2H, q, $J = 7.12$ Hz, $\text{COO}-\text{CH}_2\text{CH}_3$); 4.74 (2H, s, $(\text{CH}_3)_2\text{CHO}-\text{CH}_2$). ^{13}C NMR spectrum (CDCl_3), δ , ppm: 14.19; 21.84; 62.09; 62.23; 73.03; 154.26; 156.95; 159.69. For $\text{C}_9\text{H}_{16}\text{N}_3\text{O}_3$, m/z $[\text{M}+\text{H}]^+$ calculated: 214.24; found: 214.21.

Ethyl ether of 5-(phenoxymethyl)-1,2,4-triazole-3-carboxylic acid (5g)

1.19 g (5.15 mmol) ethyl- β -N-Boc-oxalamidrazone **3**, 10 mL of absolute pyridine, 1.88 g (11.02 mmol) phenoxyacetic acid chlorangidride. $R_f = 0.46$. Product yield: 0.80 g (63%).

^1H NMR spectrum (CDCl_3), δ , ppm: 1.34 (3H, t, $J = 7.14$ Hz, CH_3Et); 4.38 (2H, q, $J = 7.14$ Hz, CH_2Et); 5.29 (2H, s, 5- CH_2); 6.88 (2H, d, $J = 8.19$ Hz, 2-CH, and 6-CH Ph); 6.97 (1H, t, $J = 7.39$ Hz, 4-CH Ph); 7.25 (2H, t, $J = 7.98$ Hz, 3-CH, and 5-CH Ph). ^{13}C NMR spectrum (CDCl_3), δ , ppm: 14.03; 61.98; 62.31; 114.46; 121.90; 129.62; 153.42; 155.78; 157.41; 159.47. For $\text{C}_{12}\text{H}_{14}\text{N}_3\text{O}_3$, m/z $[\text{M}+\text{H}]^+$ calculated: 248.26; found: 248.24.

Ethyl ether 5-[(benzyloxy)methyl]-1,2,4-triazole-3-carboxylic acid (5h)

16.00 g (69 mmol) of ethyl- β -N-Boc-oxalamidrazone **3**, 30 mL of absolute pyridine, 23.50 mL (149 mmol) of benzyloxyacetic acid chlorangidride. $R_f = 0.63$. Product yield: 10.71 g (59%).

^1H NMR spectrum (CDCl_3), δ , ppm: 1.40 (3H, t, $J = 7.14$ Hz, CH_3Et); 4.45 (2H, q, $J = 7.1$ Hz, CH_2Et); 4.61 (2H, s, 5- CH_2); 4.77 (2H, s, CH_2Bn); 7.28–7.36 (5H, m, CHBn). ^{13}C NMR spectrum (CDCl_3), δ , ppm: 14.15; 62.13; 62.35; 72.35; 128.00; 128.25; 128.56; 136.57; 153.79; 156.45; 159.54. For $\text{C}_{13}\text{H}_{16}\text{N}_3\text{O}_3$, m/z $[\text{M}+\text{H}]^+$ calculated: 262.29; found: 262.27.

Ethyl ether of 5-(acetoxymethyl)-1,2,4-triazole-3-carboxylic acid (5i) and ethyl ether of 5-(hydroxymethyl)-1,2,4-triazole-3-carboxylic acid (5j)

1.00 g (4.32 mmol) of ethyl- β -N-Boc-oxalamidrazone **3**, 10 mL of absolute pyridine, 1.00 mL (9.29 mmol) of acetoxyacetic acid chlorangidride. $R_f = 0.65$ (main product); $R_f = 0.55$ (byproduct). 0.52 g of a mixture of esters of 5-acetoxymethyl- (main product) and 5-hydroxymethyl-1,2,4-triazole-3-carboxylic acid (byproduct) was isolated, which was used at the next stage without additional separation.

^1H NMR spectrum (CDCl_3), δ , ppm: 1.37 (3H, t, $J = 7.13$ Hz, CH_3Et , impurity); 1.38 (3H, t, $J = 7.13$ Hz, CH_3Et , main product); 2.09 (3H, s, CH_3 acetyl group, main product); 4.44 (2H, q, $J = 7.16$ Hz, CH_2Et , main product); 4.45 (2H, q, $J = 7.16$ Hz, CH_2Et , impurity); 4.65 (2H, s, 5- CH_2 , impurity); 5.32 (2H, s, 5- CH_2 , main product).

^{13}C NMR spectrum (CDCl_3), δ , ppm: 13.98 (CH_3Et , impurity); 14.03 (CH_3Et , main product); 20.48 (CH_3 acetyl group, main product); 57.54 (5- CH_2 , main product); 60.54 (5- CH_2 , impurity); 62.41 (CH_2Et , main product); 62.70 (CH_2Et , impurity); 151.61 (C^3 , impurity); 152.36 (C^3 , main product); 155.44 (C^5 , impurity); 155.44 (C^5 , main product); 158.16 (3- COO , impurity); 158.94 (3- COO , main product); 170.88 (COO of the acetyl group, main product).

General procedure for obtaining amides of 5-alkoxy/aryloxymethyl-1,2,4-triazole-3-carboxylic acids 6a-h, 6j

Ethyl ether of 5-hydroxymethyl-1,2,4-triazole-3-carboxylic acid **5a-i** was dissolved in 1.50 mL of 10 M methanol ammonia solution and heated to boiling point in a reflux flask with 0.50 mL of 14 M aqueous ammonia solution being added every 12 h. At the end of the reaction (complete conversion of ether, TLC control, eluent of 5% methanol in chloroform), the solvent was removed on a vacuum rotary evaporator. The product was suspended in anhydrous acetone, filtered and dried in a desiccator at reduced pressure above NaOH for 12 h.

Amide of 5-(methoxymethyl)-1,2,4-triazole-3-carboxylic acid (6a)

0.52 g (2.81 mmol) of 5-(methoxymethyl)-1,2,4-triazole-3-carboxylic acid ethyl ether, reaction time 72 h. Product yield: 280 mg (64%).

^1H NMR spectrum (DMSO- d_6), δ , ppm: 3.30 (3H, s, CH_3MeO); 4.49 (2H, s, 5-CH_2); 7.71 and 8.01 (2H, 2s, NH_2). ^{13}C NMR spectrum (DMSO- d_6), δ , ppm: 57.96; 65.82; 153.38; 157.41; 159.60. For $\text{C}_5\text{H}_9\text{N}_4\text{O}_2$, m/z $[\text{M}+\text{H}]^+$ calculated: 157.15; found: 157.13.

Amide of 5-ethoxymethyl-1,2,4-triazole-3-carboxylic acid (6b)

70 mg (3.5 mmol) ethyl ether of 5-(ethoxymethyl)-1,2,4-triazole-3-carboxylic acid, reaction time 48 h. Product yield: 50 mg (84%). $T_{\text{m.p.}} = 161\text{--}163^\circ\text{C}$.

^1H NMR spectrum (DMSO- d_6), δ , ppm: 1.12 (3H, t, $J = 6.98$ Hz, $-\text{CH}_2\text{CH}_3$); 3.51 (2H, q, $J = 6.98$ Hz, CH_2CH_3); 4.5 (2H, s, $-\text{O}-\text{CH}_2$); 7.69 and 7.99 (2H, 2s, CONH_2). ^{13}C NMR spectrum (DMSO- d_6), δ , ppm: 14.94; 63.89; 65.52; 153.40; 157.58; 159.61. For $\text{C}_6\text{H}_{11}\text{N}_4\text{O}_2$, m/z $[\text{M}+\text{H}]^+$ calculated: 171.18; found: 171.15.

Amide of 5-(butoxymethyl)-1,2,4-triazole-3-carboxylic acid (6c)

215 mg (0.8 mmol) ethyl ether of 5-(butoxymethyl)-1,2,4-triazole-3-carboxylic acid, reaction time 48 h. Product yield: 40 mg (21%). $T_{\text{m.p.}} = 125^\circ\text{C}$ (partially), $135\text{--}136^\circ\text{C}$ (completely).

^1H NMR spectrum (DMSO- d_6), δ , ppm: 0.84 (3H, t, $J = 6.47$ Hz, CH_2-CH_3); 1.25–1.50 (4H, m, $\text{CH}_2-\text{CN}_2\text{CH}_2\text{CH}_3$); 3.44 (2H, t, $J = 5.99$ Hz, $-\text{CH}_2\text{O}$); 4.34 and 4.5 (2H, s, OCH_2); 7.68 and 7.99 (2H, 2s, CONH_2). ^{13}C NMR spectrum (DMSO- d_6), δ , ppm: 13.74; 18.74; 31.10; 31.25; 64.08; 65.30; 69.25; 69.81; 153.40; 155.12; 157.54; 159.62; 160.04. For $\text{C}_8\text{H}_{15}\text{N}_4\text{O}_2$, m/z $[\text{M}+\text{H}]^+$ calculated: 199.23; found: 199.20.

Amide of 5-(decyloxymethyl)-1,2,4-triazole-3-carboxylic acid (6d)

110 mg (0.4 mmol) ethyl ether of 5-(decyloxymethyl)-1,2,4-triazole-3-carboxylic acid, 48 h. Product yield: 50 mg (50%). $T_{\text{m.p.}} = 140^\circ\text{C}$ (partially), $153\text{--}155^\circ\text{C}$ (completely).

^1H NMR spectrum (DMSO- d_6), δ , ppm: 0.84 (3H, t, $J = 6.24$ Hz, $(\text{CH}_2)_9-\text{CH}_3$); 1.22 (14H, s, $\text{CH}_2-(\text{CH}_2)_7\text{CH}_3$); 1.49 (2H, m, $-\text{CH}_2\text{CH}_2\text{O}$); 3.43 (2H, t, $J = 6.52$ Hz, $-\text{CH}_2\text{O}$); 4.49 (2H, s, $\text{O}-\text{CH}_2$); 7.69 and 7.99 (2H, 2s, CONH_2). ^{13}C NMR spectrum (DMSO- d_6), δ , ppm: 13.97; 22.11; 25.55; 28.71; 28.84; 29.02; 31.30; 64.10; 70.13; 153.32; 157.61;

159.57. For $\text{C}_{14}\text{H}_{27}\text{N}_4\text{O}_2$, m/z $[\text{M}+\text{H}]^+$ calculated: 283.39; found: 283.37.

Amide of 5-(1-(2-methoxy) ethoxymethyl)-1,2,4-triazole-3-carboxylic acid (6e)

250 mg (0.8 mmol) of 5-(1-(2-methoxy) ethyl etherethoxymethyl)-1,2,4-triazole-3-carboxylic acid, reaction time 48 h. Product yield: 150 mg (60%). $T_{\text{m.p.}} = 109\text{--}112^\circ\text{C}$.

^1H NMR spectrum (DMSO- d_6), δ , ppm: 3.22 (3H, d, $\text{O}-\text{CH}_2$); 3.43–3.46 (2H, m, $\text{O}-\text{CH}_2\text{CH}_2$); 3.57–3.60 (2H, m, OCH_2-CH_2); 4.54 (2H, d, OCH_2); 7.70 and 8.01 (2H, 2d, CONH_2). ^{13}C NMR spectrum (DMSO- d_6), δ , ppm: 58.07; 64.38; 69.35; 71.09; 153.25; 157.55; 159.53. For $\text{C}_7\text{H}_{13}\text{N}_4\text{O}_3$, m/z $[\text{M}+\text{H}]^+$ calculated: 201.20; found: 201.17.

Amide of 5-isopropoxyxymethyl-1,2,4-triazole-3-carboxylic acid (6f)

310 mg (1.5 mmol) of 5-(isopropoxyxymethyl)-1,2,4-triazole-3-carboxylic acid ethyl ether, reaction time 48 h. Product yield: 90 mg (33%). $T_{\text{m.p.}} = 160\text{--}161^\circ\text{C}$, $T_{\text{subl}} = 144^\circ\text{C}$.

^1H NMR spectrum (DMSO- d_6), δ , ppm: 1.11 (6H, d, $J = 6.08$ Hz, $(\text{CH}_3)_2-\text{CH}_2$); 3.63–3.73 (1H, m, $(\text{CH}_3)_2-\text{CH}_2-\text{O}$); 4.50 (2H, s, $-\text{O}-\text{CH}_2$); 7.66 and 7.96 (2H, s, CONH_2). ^{13}C NMR spectrum (DMSO- d_6), δ , ppm: 21.85; 61.52; 70.96; 153.50; 157.80; 159.67. For $\text{C}_7\text{H}_{13}\text{N}_4\text{O}_2$, m/z $[\text{M}+\text{H}]^+$ calculated: 185.20; found: 185.19.

Amide of 5-(phenoxymethyl)-1,2,4-triazole-3-carboxylic acid (6g)

400 mg (1.62 mmol) ethyl ether of 5-(phenoxymethyl)-1,2,4-triazole-3-carboxylic acid, reaction time 96 h. Product yield: 310 mg (89%).

^1H NMR spectrum (DMSO- d_6), δ , ppm: 5.16 (2H, s, 5-CH_2); 6.96 (1H, t, $J = 7.30$ Hz, 4CH, Ph); 7.04 (2H, d, $J = 8.00$ Hz, 2CH and 6CH, Ph); 7.30 (2H, t, $J = 7.91$ Hz, 3CH, and 5CH, Ph); 7.79 and 8.10 (2H, 2s, NH_2). ^{13}C NMR spectrum (DMSO- d_6), δ , ppm: 62.17; 114.68; 121.16; 129.57; 152.69; 157.34; 157.89; 159.08. For $\text{C}_{10}\text{H}_{11}\text{N}_4\text{O}_2$, m/z $[\text{M}+\text{H}]^+$ calculated: 219.22; found: 219.20.

Amide 5-[(benzyloxy)methyl]-1,2,4-triazole-3-carboxylic acid (6h)

350 mg (2.45 mmol) of 5-[(benzyloxy)-ethyl ethermethyl]-1,2,4-triazole-3-carboxylic acid, reaction time 72 h. Product yield: 240 mg (77%).

^1H NMR spectrum (DMSO- d_6), δ , ppm: 4.57 (2H, s, 5-CH_2); 4.60 (2H, s, CH_2Bn); 7.28–7.37 (5H,

m, CHBn); 7.72 and 8.02 (2H, 2s, NH₂). ¹³C NMR spectrum (DMSO-*d*₆), δ, ppm: 63.68; 71.75; 127.63; 127.77; 128.28; 137.74; 153.21; 157.50; 159.48. For C₁₁H₁₃N₄O₂, *m/z* [M+H]⁺ calculated: 233.25; found: 233.22.

Amide of 5-hydroxymethyl-1,2,4-triazole-3-carboxylic acid (6j)

0.52 g (2.44 mmol) mixtures of ethyl esters of 5-acetoxymethyl- and 5-hydroxymethyl-1,2,4-triazole-3-carboxylic acid, reaction time 72 h. Product yield: 270 mg (77%).

¹H NMR spectrum (DMSO-*d*₆), δ, ppm: 4.55 (2H, s, 5-CH₂); 7.49 and 7.76 (2H, 2s, NH₂). ¹³C NMR spectrum (DMSO-*d*₆), δ, ppm: 55.98; 154.83; 159.70; 160.69. For C₄H₇N₄O₂, *m/z* [M+H]⁺ calculated: 143.12; found: 143.09.

CONCLUSIONS

By applying the method of parallel synthesis to the solution of the problem of obtaining 5-substituted 1,2,4-triazole-3-carboxamides, it was possible to expand the range of their synthetic availability. The physicochemical characteristics of the obtained series of new 5-alkoxy/aryloxymethyl-1,2,4-triazole-3-carboxamides were studied. In addition, the demonstrated possibility for these compounds to be used as substrates of a transglycosylation reaction catalyzed by genetically engineered nucleoside phosphorylases allowing the synthesis new potentially pharmacologically

active analogs of deoxynucleosides by a chemico-enzymatic method. The esters of 5-alkoxy/aryloxymethyl-1,2,4-triazole-3-carboxylic acids obtained in the course of this work can also be used for the synthesis of ribonucleosides by chemical glycosylation methods. As a result of the conducted research, a method for obtaining 5-alkoxy/aryloxymethyl-1,2,4-triazole-3-carboxamides, comprising heterocyclic bases of nucleoside analogs and esters of 5-alkoxy/aryloxymethyl-1,2,4-triazole-3-carboxylic acids as convenient precursors of chemical ribosylation, was introduced into the synthesis procedure. Thus, a necessary synthetic base has been created for the study of ribavirin analogs with 5-alkoxy/aryloxymethyl substituents.

Acknowledgments

We are grateful to I.D. Konstantinova, O.S. Smirnova, I.V. Fateev, and other employees of the Laboratory of Biotechnology of the IBCh RAS for conducting primary tests of the NP substrate properties in relation to synthesized compounds. NMR spectra were registered using the equipment of the RTU MIREA Collective Use Center (Agreement No. 075-15-2021-689 dated 01.09.2021, unique identification number 2296.61321X0010).

Authors' contributions

L.E. Grebenkina – conducting experiments;
A.N. Prutkov – conducting experiments;
A.V. Matveev – creating a research concept, processing experimental data, adjustment of experimental studies;
M.V. Chudinov – creating a research concept.

The authors declare no conflicts of interest.

REFERENCES

- Jordheim L.P., Durantel D., Zoulim F., Dumontet C. Advances in the development of nucleoside and nucleotide analogues for cancer and viral diseases. *Nat. Rev. Drug Discov.* 2013;12(6):447–464. <https://doi.org/10.1038/nrd4010>
- Shelton J., Lu X., Hollenbaugh J.A., Cho J.H., Amblard F., Schinazi R.F. Metabolism, Biochemical Actions, and Chemical Synthesis of Anticancer Nucleosides, Nucleotides, and Base Analogs. *Chem. Rev.* 2016;116(23):14379–14455. <https://doi.org/10.1021/acs.chemrev.6b00209>

- Thomson J.M., Lamont I.L. Nucleoside analogues as antibacterial agents. *Front. Microbiol.* 2019;10:952. <https://doi.org/10.3389/fmicb.2019.00952>
- Geraghty R.J., Aliota M.T., Bonnac L.F. Broad-spectrum antiviral strategies and nucleoside analogues. *Viruses.* 2021;13(4):667. <https://doi.org/10.3390/v13040667>
- De Clercq E., Li G. Approved antiviral drugs over the past 50 years. *Clin. Microbiol. Rev.* 2016;29(3):695–747. <https://doi.org/10.1128/CMR.00102-15>
- De Clercq E. New Nucleoside Analogues for the Treatment of Hemorrhagic Fever Virus Infections. *Chem. Asian J.* 2019;14(22):3962–3968. <https://doi.org/10.1002/asia.201900841>

7. Kasianenko K.V., Lvov N.I., Maltsev O.V., Zhdanov K.V. Nucleoside analogues for the treatment of influenza: History and experience. *Journal Infektology*. 2019;11(3):20–26 (in Russ.). <https://doi.org/10.22625/2072-6732-2019-11-3-20-26>
8. Pruijssers A.J., Denison M.R. Nucleoside analogues for the treatment of coronavirus infections. *Curr. Opin. Virol.* 2019;35:57–62. <https://doi.org/10.1016/j.coviro.2019.04.002>
9. Borbone N., Piccialli G., Roviello G.N., Oliviero G. Nucleoside analogs and nucleoside precursors as drugs in the fight against SARS-CoV-2 and other coronaviruses. *Molecules*. 2021;26(4):986. <https://doi.org/10.3390/molecules26040986>
10. Yoshida Y., Honma M., Kimura Y., Abe H. Structure, Synthesis and Inhibition Mechanism of Nucleoside Analogues as HIV-1 Reverse Transcriptase Inhibitors (NRTIs). *ChemMedChem*. 2021;16(5):743–766. <https://doi.org/10.1002/cmdc.202000695>
11. Zhang Y., Liu X., Lin Y., Lian B., Lan W., Iovanna J.L., et al. Novel triazole nucleoside analogues promote anticancer activity: Via both apoptosis and autophagy. *Chem. Commun.* 2020;56(69):10014–10017. <https://doi.org/10.1039/D0CC04660D>
12. Wang D., Yu C., Xu L., Shi L., Tong G., Wu J., et al. Nucleoside Analogue-Based Supramolecular Nanodrugs Driven by Molecular Recognition for Synergistic Cancer Therapy. *J. Am. Chem. Soc.* 2018;140(28):8797–8806. <https://doi.org/10.1021/jacs.8b04556>
13. Zeng X., Hernandez-Sanchez W., Xu M., Whited T.L., Baus D., Zhang J., et al. Administration of a Nucleoside Analog Promotes Cancer Cell Death in a Telomerase-Dependent Manner. *Cell Reports*. 2018;23(10):3031–3041. <https://doi.org/10.1016/j.celrep.2018.05.020>
14. Sun R., Wang L. Inhibition of Mycoplasma pneumoniae growth by FDA-approved anticancer and antiviral nucleoside and nucleobase analogs. *BMC Microbiol.* 2013;13:184. <https://doi.org/10.1186/1471-2180-13-184>
15. Pastuch-Gawolek G., Gillner D., Krol E., Walczak K., Wandzik I. Selected nucleos(t)ide-based prescribed drugs and their multi-target activity. *Eur. J. Pharmacol.* 2019;865:172747. <https://doi.org/10.1016/j.ejphar.2019.172747>
16. Seley-Radtke K.L., Yates M.K. The evolution of nucleoside analogue antivirals: A review for chemists and non-chemists. Part 1: Early structural modifications to the nucleoside scaffold. *Antiviral Res.* 2018;154:66–86. <https://doi.org/10.1016/j.antiviral.2018.04.004>
17. Yates M.K., Seley-Radtke K.L. The evolution of antiviral nucleoside analogues: A review for chemists and non-chemists. Part II: Complex modifications to the nucleoside scaffold. *Antiviral Res.* 2019;162:5–21. <https://doi.org/10.1016/j.antiviral.2018.11.016>
18. Zeidler J., Baraniak D., Ostrowski T. Bioactive nucleoside analogues possessing selected five-membered azaheterocyclic bases. *Eur. J. Med. Chem.* 2015;97:409–418. <https://doi.org/10.1016/j.ejmech.2014.11.057>
19. Merino P. (Ed.). *Chemical Synthesis of Nucleoside Analogues*. NY: John Wiley & Sons, Inc.; 2013. 912 p. ISBN: 978-1-118-49808-8
20. Mikhailopulo I.A., Miroshnikov A.I. Biologically important nucleosides: modern trends in biotechnology and application. *Mendelev Comm.* 2011;21(2):57–68. <https://doi.org/10.1016/j.mencom.2011.03.001>
21. Yehia H., Kamel S., Paulick K., Wagner A., Neubauer P. Substrate spectra of nucleoside phosphorylases and their potential in the production of pharmaceutically active compounds. *Curr. Pharm. Des.* 2017;23(45):6913–6935. <http://dx.doi.org/10.2174/1381612823666171024155811>
22. Kamel S., Yehia H., Neubauer P., Wagner A. Enzymatic Synthesis of Nucleoside Analogues by Nucleoside Phosphorylases. In: Lucas F.J., Rius M.-J.C. (Eds.). *Enzymatic and Chemical Synthesis of Nucleic Acid Derivatives*. Wiley-VCH Verlag GmbH & Co; 2018. P. 1–28. <https://doi.org/10.1002/9783527812103.ch1>
23. Barai V.N., Zinchenko A.I., Eroshevskaya L.A., Kalinichenko E.N., Kulak T.I., Mikhailopulo I.A. A Universal Biocatalyst for the Preparation of Base- and Sugar-Modified Nucleosides via an Enzymatic Transglycosylation. *Heb. Chim. Acta*. 2002;85(7):1901–1908. [https://doi.org/10.1002/1522-2675\(200207\)85:<1901::AID-HLCA1901>3.0.CO;2-C](https://doi.org/10.1002/1522-2675(200207)85:<1901::AID-HLCA1901>3.0.CO;2-C)
24. Konstantinova I.D., Leont'eva N.A., Galegov G.A., Ryzhova O.I., Chuvikovskii D.V., Antonov K.V., et al. Ribavirin: Biotechnological synthesis and effect on the reproduction of Vaccinia virus. *Russ. J. Bioorg. Chem.* 2004;30(6):553–560. <https://doi.org/10.1023/B:RUBI.0000049772.18675.34>
25. Konstantinova I.D., Esipov R.S., Muravieva T.I., Taran S.A., Verevkin K.N., Gurevich A.I., et al. Method for preparing 1-β-D-ribofuranosyl-1,2,4-triazole-3-carboxamide (ribavirin): RF Pat. 2230118. Publ. 10.03.2004 (in Russ.).
26. Sakharov V., Baykov S., Konstantinova I., Esipov R., Dorogov M. An Efficient Chemoenzymatic Process for Preparation of Ribavirin. *International Journal of Chemical Engineering*. 2015;2015:734851. <https://doi.org/10.1155/2015/734851>
27. Rabuffetti M., Bavaro T., Semplici R., Cattaneo G., Massone M., Morelli C.F., et al. Synthesis of Ribavirin, Tecadenoson, and Cladribine by Enzymatic Transglycosylation. *Catalysts*. 2019;9(4):355. <https://doi.org/10.3390/catal9040355>
28. Fateev I.V., Antonov K.V., Konstantinova I.D., Muravyova T.I., Seela F., Esipov R.S., et al. The chemoenzymatic synthesis of clofarabine and related 2'-deoxyfluoroarabinosyl nucleosides: the electronic and stereochemical factors determining substrate recognition by E. coli nucleoside phosphorylases. *Beilstein J. Org. Chem.* 2014;10:1657–1669. <https://doi.org/10.3762/bjoc.10.173>
29. Zhou X., Szeker K., Jiao L.-Y., Oestreich M., Mikhailopulo I.A., Neubauer P. Synthesis of 2,6-Dihalogenated Purine Nucleosides by Thermally Stable Nucleoside Phosphorylases. *Adv. Synth. Catal.* 2015;357(6):1237–1244. <https://doi.org/10.1002/adsc.201400966>
30. Vichier-Guerre S., Dugue L., Bonhomme F., Pochet S. Expedient and generic synthesis of imidazole nucleosides by enzymatic transglycosylation. *Org. Biomol. Chem.* 2016;14(14):3638–3653. <https://doi.org/10.1039/C6OB00405A>
31. Hatano A., Wakana H., Terado N., Kojima A., Nishioka C., Iizuka Y., et al. Bio-catalytic synthesis of unnatural nucleosides possessing a large functional group such as a fluorescent molecule by purine nucleoside phosphorylase. *Catal. Sci. Technol.* 2019;9(18):5122–5129. <https://doi.org/10.1039/C9CY01063G>

32. Konstantinova I.D., Chudinov M.V., Fateev I.V., Matveev A.V., Zhurilo N.I., Shvets V.I., Miroshnikov A.I. Nucleosides of 1,2,4-triazole: Possibilities and limitations of the chemical enzymatic method of preparation. *Bioorganicheskaya Khimiya*. 2013;39(1):61–80 (in Russ.). <https://doi.org/10.7868/S0132342313010053>

[Konstantinova I.D., Chudinov M.V., Fateev I.V., et al. Chemoenzymatic method of 1,2,4-triazole nucleoside synthesis: Possibilities and limitations. *Russ. J. Bioorg. Chem.* 2013;39(1):53–71. <https://doi.org/10.1134/S1068162013010056>]

33. Matveev A.V., Prutkov A.N., Chudinov M.V. *Method of producing 5-substituted 1,2,4-triazole-3-carboxylic acids and derivatives thereof from universal precursor*: RF pat. 2605414. Publ. 20.12.2015 (in Russ.).

34. Chudinov M.V., Matveev A.V., Zhurilo N.I., Prutkov A.N., Shvets V.I. An Efficient Route to Ethyl 5-Alkyl-(Aryl)-1H-1,2,4-triazole-3-carboxylates. *J. Heterocycl. Chem.* 2015;52(5):1273–1277. <https://doi.org/10.1002/jhet.1934>

35. Matveev A.V., Grebenkina L.E., Prutkov A.N., Chudinov M.V. 5-Substituted 1,2,4-Triazole-3-Carboxylates and 5-Substituted Ribavirin Analogs Synthesis. *Curr. Protoc.* 2021;1(11):e281 <https://doi.org/10.1002/cpz1.281>

About the authors:

Lyubov E. Grebenkina, Assistant, Department of Biotechnology and Industrial Pharmacy, M.V. Lomonosov Institute of Fine Chemical Technologies, MIREA – Russian Technological University (86, Vernadskogo pr., Moscow, 119571, Russia). E-mail: LEGrebenkina@mail.ru. Scopus Author ID 57189663430, RSCI SPIN-code 6518-1280, <https://orcid.org/0000-0002-5995-5608>

Alexander N. Prutkov, Postgraduate Student, Department of Biotechnology and Industrial Pharmacy, M.V. Lomonosov Institute of Fine Chemical Technologies, MIREA – Russian Technological University (86, Vernadskogo pr., Moscow, 119571, Russia). E-mail: alex_prutkov@mail.ru. ResearcherID G-4025-2016, Scopus Author ID 56228508300, RSCI SPIN-code 2965-1335, <https://orcid.org/0000-0001-9522-7387>

Andrey V. Matveev, Cand. Sci. (Chem.), Associate Professor, Department of Biotechnology and Industrial Pharmacy, M.V. Lomonosov Institute of Fine Chemical Technologies, MIREA – Russian Technological University (86, Vernadskogo pr., Moscow 119571, Russia). E-mail: 4motya@gmail.com. Scopus Author ID 7102723461, RSCI SPIN-code 7420-3188, <https://orcid.org/0000-0002-0830-3036>

Mikhail V. Chudinov, Cand. Sci. (Chem.), Associate Professor, Department of Biotechnology and Industrial Pharmacy, M.V. Lomonosov Institute of Fine Chemical Technologies, MIREA – Russian Technological University (86, Vernadskogo pr., Moscow 119571, Russia). E-mail: chudinov@mirea.ru. ResearcherID L-5728-2016, Scopus Author ID 6602589900, RSCI SPIN-code 3920-8067, <https://orcid.org/0000-0001-9735-9690>

Об авторах:

Гребенкина Любовь Евгеньевна, ассистент кафедры биотехнологии и промышленной фармации Института тонких химических технологий им. М.В. Ломоносова ФГБОУ ВО «МИРЭА – Российский технологический университет» (119571, Россия, Москва, пр-т Вернадского, д. 86). E-mail: LEGrebenkina@mail.ru. Scopus Author ID 57189663430, SPIN-код РИНЦ 6518-1280, <https://orcid.org/0000-0002-5995-5608>

Прутков Александр Николаевич, аспирант кафедры биотехнологии и промышленной фармации Института тонких химических технологий им. М.В. Ломоносова ФГБОУ ВО «МИРЭА – Российский технологический университет» (119571, Россия, Москва, пр-т Вернадского, д. 86). E-mail: alex_prutkov@mail.ru. ResearcherID G-4025-2016, Scopus Author ID 56228508300, SPIN-код РИНЦ 2965-1335, <https://orcid.org/0000-0001-9522-7387>

Матвеев Андрей Валерьевич, к.х.н., доцент кафедры биотехнологии и промышленной фармации Института тонких химических технологий им. М.В. Ломоносова ФГБОУ ВО «МИРЭА – Российский технологический университет» (119571, Россия, Москва, пр-т Вернадского, д. 86). E-mail: 4motya@gmail.com. Scopus Author ID 7102723461, SPIN-код РИНЦ 7420-3188, <https://orcid.org/0000-0002-0830-3036>

Чудинов Михаил Васильевич, к.х.н., доцент кафедры биотехнологии и промышленной фармации Института тонких химических технологий им. М.В. Ломоносова ФГБОУ ВО «МИРЭА – Российский технологический университет» (119571, Россия, Москва, пр-т Вернадского, д. 86). E-mail: chudinov@mirea.ru. ResearcherID L-5728-2016, Scopus Author ID 6602589900, SPIN-код РИНЦ 3920-8067, <https://orcid.org/0000-0001-9735-9690>

The article was submitted: February 17, 2022; approved after reviewing: March 11, 2022; accepted for publication: July 25, 2022.

Translated from Russian into English by N. Isaeva

Edited for English language and spelling by Thomas Beavitt

CHEMISTRY AND TECHNOLOGY OF MEDICINAL COMPOUNDS
AND BIOLOGICALLY ACTIVE SUBSTANCES

ХИМИЯ И ТЕХНОЛОГИЯ ЛЕКАРСТВЕННЫХ ПРЕПАРАТОВ
И БИОЛОГИЧЕСКИ АКТИВНЫХ СОЕДИНЕНИЙ

ISSN 2686-7575 (Online)

<https://doi.org/10.32362/2410-6593-2022-17-4-323-334>



UDC 547.415.5: 547.426.253

RESEARCH ARTICLE

Amination of epoxides as a convenient approach for the synthesis of lipophilic polyamines

Elizaveta A. Eshtukova-Shcheglova¹, Ksenia A. Perevoshchikova¹,
Artur V. Eshtukov-Shcheglov², Dmitriy A. Cheshkov², Mikhail A. Maslov^{1,✉}

¹MIREA – Russian Technological University (M.V. Lomonosov Institute of Fine Chemical Technologies),
Moscow, 119571 Russia

²State Scientific Research Institute of Chemistry and Technology of Organoelement Compounds,
Moscow, 105118 Russia

✉ Corresponding author, e-mail: mamaslov@mail.ru

Abstract

Objectives. Alkylated derivatives of polyamines are able to block the growth of cancer cells due to their embedding into the polyamine biosynthesis mechanisms. The study aimed to synthesize lipophilic derivatives of norspermine or triethylenetetramine based on the formation of a C–N bond during the opening of the oxirane ring by primary amines to expand a number of synthetic polyamine derivatives with antitumor activity.

Methods. The starting compounds—glycidol alcoholate or epichlorohydrin—were reacted with hexadecyl bromide or sodium hexadecanolate to give glycidyl hexadecyl ether. The key reaction for the preparation of lipophilic polyamines was the amination of lipophilic epoxides with polyamines in the presence of calcium triflate. Acylation of the hydroxyl group formed during the opening of oxirane was carried out by the action of 4-dimethylaminopyridine and acetic anhydride. The introduction of an alkyl substituent in the presence of sodium hydride led to intramolecular cyclization with the formation of an oxazolidine cycle. The regioselectivity of the oxirane ring opening reaction at the C(1) position of glycerol was confirmed by two-dimensional heteronuclear $\{^1\text{H}, ^{13}\text{C}\}$ nuclear magnetic resonance spectroscopy.

Results. An approach to the synthesis of novel lipophilic polyamines based on the catalytic amination of epoxides was developed and tested. Compounds based on norspermine and triethylenetetramine containing a hydroxyl group at the C(2) atom of the glycerin backbone were obtained. For norspermine derivatives, the hydroxyl group was modified: an acetyl substituent was introduced and a derivative containing an oxoazolidine cycle was obtained.

Conclusions. The obtained lipophilic polyamines can be considered as potential antitumor agents, for which cytotoxicity against various cancer cells will be evaluated in the future.

Keywords: lipophilic polyamines, lipids, alkyl glycerolipids, oxiranes

For citation: Eshtukova-Shcheglova E.A., Perevoshchikova K.A., Eshtukov-Shcheglov A.V., Cheshkov D.A., Maslov M.A. Amination of epoxides as a convenient approach for lipophilic polyamines synthesis. *Tonk. Khim. Tekhnol. = Fine Chem. Technol.* 2022;17(4):323–334 (Russ., Eng.). <https://doi.org/10.32362/2410-6593-2022-17-4-323-334>

НАУЧНАЯ СТАТЬЯ

Аминирование эпоксидов как удобный способ синтеза липофильных полиаминов

Е.А. Ештукова-Щеглова¹, К.А. Перевощикова¹, А.В. Ештуков-Щеглов², Д.А. Чешков², М.А. Маслов^{1,✉}

¹МИРЭА – Российский технологический университет (Институт тонких химических технологий им. М.В. Ломоносова), Москва, 119571 Россия

²Государственный научно-исследовательский институт химии и технологии элементо-органических соединений, Москва, 105118 Россия

✉ Автор для переписки, e-mail: tamaslov@mail.ru

Аннотация

Цели. Алкилированные производные полиаминов способны блокировать рост раковых клеток за счет встраивания в механизмы биосинтеза полиаминов. Цель исследования – синтезировать новые липофильные производные норспермина или триэтилентетрамина, основанные на формировании связи C–N при раскрытии оксиранового кольца первичными аминами, для расширения ряда синтетических производных полиаминов, обладающих противоопухолевой активностью.

Методы. Исходные соединения – алкохолат глицидола или эпихлоргидрин – вводили во взаимодействие с гексадецилбромидом или гексадецилатом натрия, получая гексадецилглицидиловый эфир. Ключевой реакцией получения липофильных полиаминов являлось аминирование липофильных эпоксидов полиаминами в присутствии трифлата кальция. Ацилирование гидроксильной группы, образовавшейся в ходе раскрытия оксирана, проводили действием 4-диметиламинопиридина и уксусного ангидрида. Введение алкильного заместителя в присутствии гидрида натрия приводило к внутримолекулярной циклизации с образованием оксоазолидинового цикла. Региоселективность реакции раскрытия оксиранового цикла по C(1) положению глицерина подтверждали двумерной гетероядерной $\{^1\text{H}, ^{13}\text{C}\}$ спектроскопией ядерного магнитного резонанса.

Результаты. Разработан и апробирован подход к синтезу новых липофильных полиаминов, основанный на каталитическом аминировании эпоксидов. Получены соединения на основе норспермина и триэтилентетрамина, содержащие гидроксильную группу при C(2) атоме глицеринового остова. Для производных норспермина проведена модификация гидроксильной группы: введен ацетильный заместитель и получено производное, содержащее оксоазолидиновый цикл.

Выводы. Полученные липофильные полиамины можно рассматривать как потенциальные противоопухолевые агенты, для которых в дальнейшем будет проведена оценка цитотоксичности против различных раковых клеток.

Ключевые слова: липофильные полиамины, липиды, алкильные глицеролипиды, оксираны

Для цитирования: Ештукова-Щеглова Е.А., Перевощикова К.А., Ештуков-Щеглов А.В., Чешков Д.А., Маслов М.А. Аминирование эпоксидов как удобный способ синтеза липофильных полиаминов. *Тонкие химические технологии*. 2022;17(4):323–334. <https://doi.org/10.32362/2410-6593-2022-17-4-323-334>

INTRODUCTION

Natural polyamines (NPs) such as spermine, spermidine, and putrescine play an important role in homeostasis and proliferation of eukaryotic cells; moreover, their level in tumor cells is higher than in normal cells [1]. Alkylated derivatives of natural and synthetic NPs can reduce the intracellular content of natural NPs and block the growth of cancer cells due to incorporation into the mechanisms of NP biosynthesis [1–4]. Conjugation of NPs with antitumor agents leads to an increase in both the therapeutic effect and the selectivity of the latter; this is due to the activation of the NP transport system in cancer cells, which require NP for rapid proliferation [5–9].

Positively charged derivatives of alkyl glycerolipids are promising antitumor agents, which are capable to inhibit the growth of cancer cells depending on the structure of the cationic domain [10, 11]. Earlier in order to find potential antitumor agents, we carried out the synthesis of unsymmetrical conjugates of NPs and alkyl glycerolipids (Fig. 1) based on the interaction of bromo derivatives of diglycerides with regioselectively protected 2-nitrobenzenesulfonylamide derivatives of NPs, followed by ethylation and removal of protective groups [12]. Dialkylated lipophilic NPs based on norspermine and triethylenetetramine had the highest antitumor activity, while the length of the alkyl substituent at the C(1) atom of glycerol was found to have no significant effect on the ability of the compounds to induce cancer cell death.

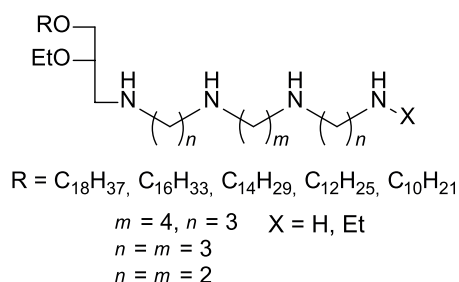


Fig. 1. Structure of asymmetric lipophilic polyamines.

In order to expand the range of synthetic NP derivatives offering antitumor activity, we developed the synthesis of new conjugates of norspermine or triethylenetetramine with glycerolipids, based on the opening of oxiranes by primary amines. The resulting hydroxy-containing NP derivatives can additionally be subjected to acylation or intramolecular cyclization, which leads to new lipophilic NP derivatives.

MATERIALS AND METHODS

We used commercial solvents and reagents (*Chimmed*, Russia; *Component-Reaktiv*, Russia; *Sigma-Aldrich*, USA; *Acros-Organics*, USA). Prior to the reaction, dichloromethane (DCM) was boiled over CaH_2 ; methanol was boiled over magnesium shavings; tetrahydrofuran (THF) was kept over KOH, boiled over Na in the presence of benzophenone and distilled; dimethylformamide (DMF) was kept over calcined 4 Å molecular sieves.

The reaction progress was monitored by thin layer chromatography on Silica gel 60 F₂₅₄ plates (*Merck*, Germany). Spots were visualized under ultraviolet light (254 nm) or phosphomolybdic acid-Ce(SO₄)₂ reagent followed by heating. Column chromatography was performed on silica gel 0.040–0.063 mm Kieselgel 60 (*Merck*, Germany).

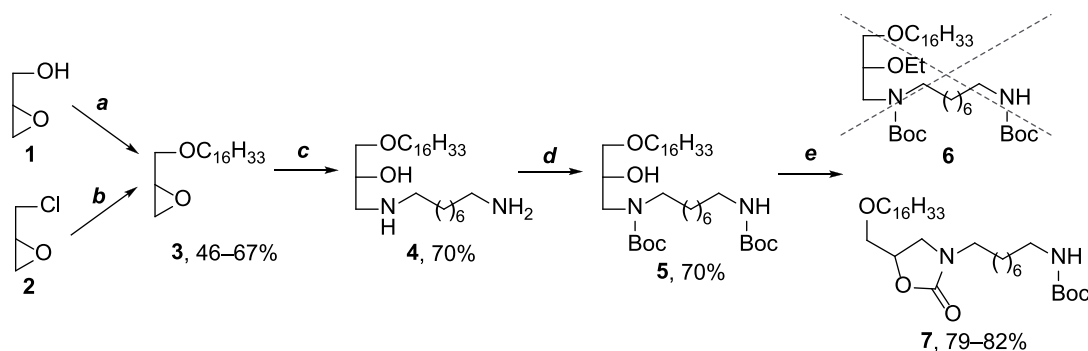
¹H, ¹³C nuclear magnetic resonance (NMR), ¹H,¹H correlation spectroscopy (COSY), ¹H,¹³C heteronuclear single quantum coherence (HSQC), and ¹H,¹³C heteronuclear multiple bond correlation (HMBC) spectra were recorded on DPX-300 and Avance II 600 pulsed Fourier transform spectrometers (*Bruker*, Germany) in CDCl₃, CD₃OD, or D₂O. Chemical shifts (δ) are given in parts per million with respect to the peak of the residual proton of the solvent, spin-spin coupling constants (*J*) are given in Hz. Mass spectra were recorded on an Apex Ultra 7T Fourier-transform ion cyclotron resonance (FT-ICR) mass spectrometer (*Bruker*, Germany).

RESULTS AND DISCUSSION

The synthetic approach to the preparation of lipophilic NPs includes several key steps: synthesis of an alkyl glycidyl ether, opening of the oxirane ring with amines, and modification of the hydroxyl group at the C(2) atom of glycerol. In order to evaluate this approach, its stepwise optimization was initially carried out using *N,N'*-diaminooctane, a structural analogue of the synthetic NP triethylenetetramine (Scheme 1).

The synthesis of glycidyl hexadecyl ether (**3**) was carried out in several ways, starting from *rac*-glycidol (**1**) or *rac*-epichlorohydrin (**2**). Thus, *rac*-glycidol (**1**) was treated with sodium hydride and then reacted with hexadecyl bromide to give compound **3** in 46% yield (Table 1).

In order to increase the yield of compound **3**, its synthesis was optimized using *rac*-epichlorohydrin (**2**) as the starting compound (see Table). Hexadecanol was converted to



Scheme 1. Synthetic approach to obtaining lipophilic polyamines.

Reagents and conditions: *a* – NaH, C₁₆H₃₃Br, DMF, 24°C; *b* – C₁₆H₃₃OH, NaOH or NaH, hexane, 60°C; *c* – NH₂(CH₂)₆NH₂, Ca(OTf)₂, MeCN, 24°C, *d* – Boc₂O, Et₃N, CH₂Cl₂, 24°C or Boc₂O, K₂CO₃, MeOH, 24°C; *e* – EtBr, Na/dimethyl sulfoxide (DMSO), benzene, 24°C or EtBr, NaH, THF, 65°C.

Table. Synthesis parameters of hexadecylglycidyl ether

Terms	Reagents	Conditions	Yield, %
<i>a</i>	<i>rac</i> -glycidol (1), C ₁₆ H ₃₃ Br	NaH, DMF, 24°C	46
<i>b</i>	<i>rac</i> -epichlorohydrin (2), C ₁₆ H ₃₃ OH	NaH, hexane, 60°C	52
		NaOH, hexane, 60°C	67
		NaOH, DMF, 60°C	7
		NaOH, 60°C	59

alcoholate by the action of sodium hydroxide or hydride, which was then treated with *rac*-epichlorohydrin (**2**). The highest yield of compound **3** (67%) was achieved when the reaction was carried out in hexane using sodium hydroxide; the replacement of the solvent with DMF led to a decrease in the yield to 7%. The condensation of *rac*-epichlorohydrin (**2**) and hexadecanol in the absence of a solvent yielded 59%. Replacing sodium hydroxide with hydride in hexane gave compound **3** in 52% yield.

The noncatalytic opening of oxiranes by amines with the formation of β -amino alcohols is characterized by a low reaction rate and modest regioselectivity [13]. An universal approach to the aminolysis of epoxides is the use of metal salts as catalysts, which increase the electrophilicity of epoxides due to coordination

with metal atoms [13]. The use of cheap and easy-to-prepare calcium trifluoromethanesulfonate (triflate) allows regioselective opening of epoxides [14]. The oxirane ring of compound **3** was opened by the action of *N,N'*-diaminooctane in the presence of calcium triflate (0.5 equiv.) in acetonitrile, which led to the formation of amino alcohol **4** in 70% yield. The regioselectivity of the reaction (opening of the oxirane ring at the C(1) position of glycerol) was confirmed by the data of two-dimensional heteronuclear $\{^1\text{H}, ^{13}\text{C}\}$ NMR spectroscopy (Fig. 2a) by the presence of cross peaks corresponding to the simultaneous interaction of protons of the CH_2O and CH groups of glycerol (A and B) and methylene protons (C) of the NHCH_2 -group of the diamine with the carbon of the CH_2NH -group of the glycerol skeleton.

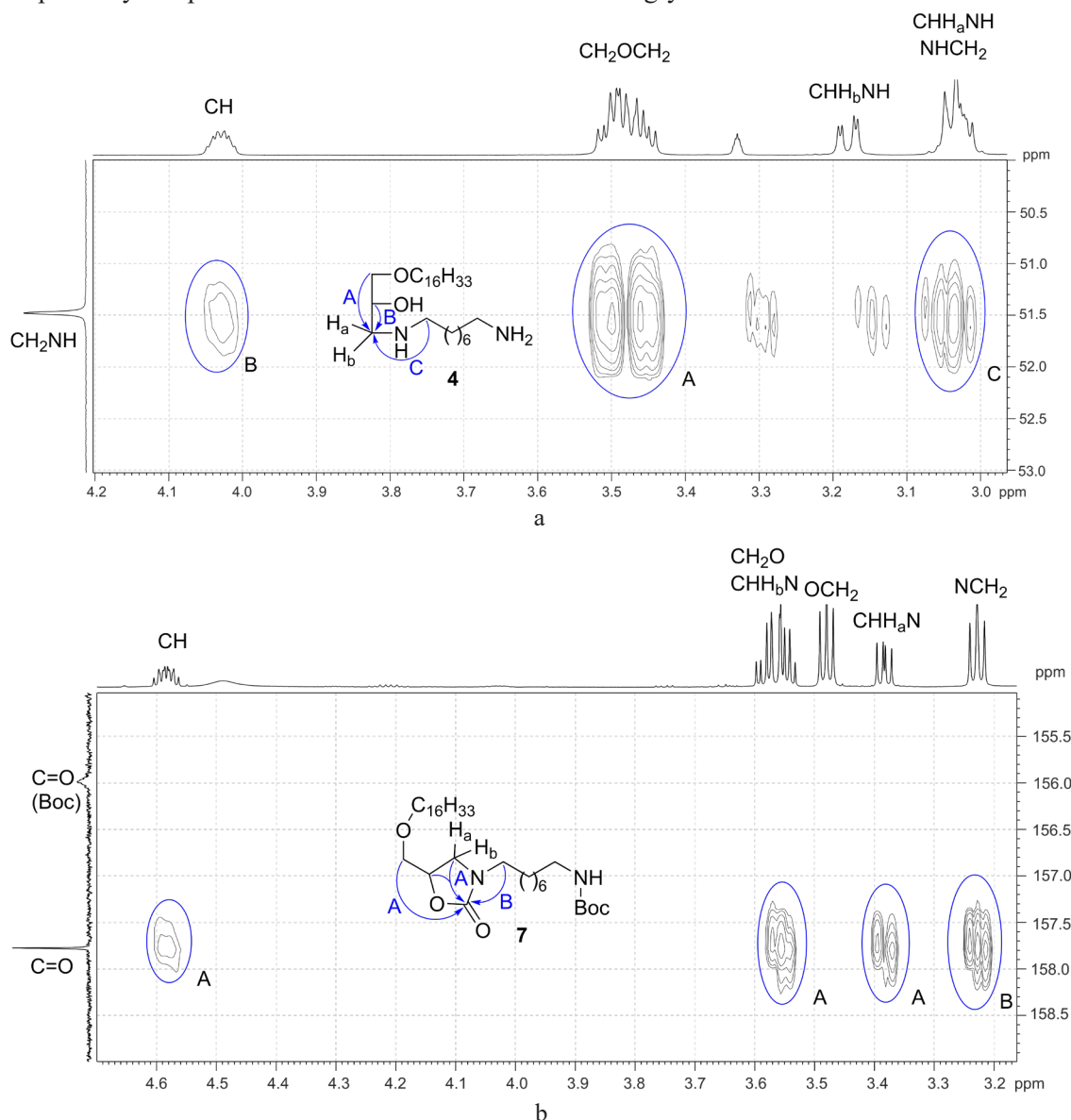


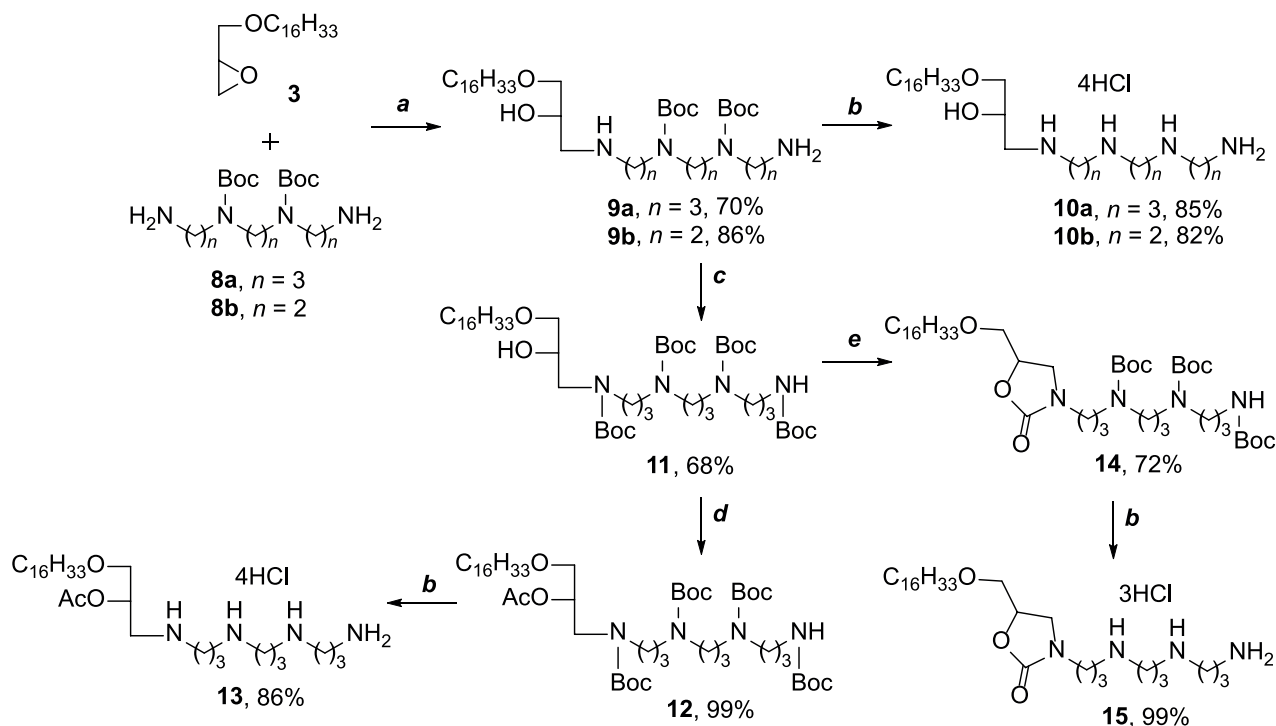
Fig. 2. (a) Fragment of the ^1H , ^{13}C HMBC spectrum of compound **4**, (b) fragment of the ^1H , ^{13}C HMBC spectrum of compound **7**.

For the further introduction of an alkyl substituent at the OH group at the C(2) atom of the glycerol backbone, the amino groups were protected. To this end, compound **4** was treated with di-*tert*-butyl dicarbonate in the presence of triethylamine or calcium carbonate to give compound **5** in 78% yield. To ethylate the hydroxyl group at the C(2) atom of glycerol, compound **5** was converted into an alcoholate by the action of sodium hydride and treated with ethyl bromide, with the expectation of obtaining compound **6**. However, following isolation of the reaction product, no signals of the ethyl group protons were detected in the ^1H NMR spectrum; the proton signal at C(2) glycerol atom shifted downfield (δ 4.55–4.62 ppm). In addition to the signal of the carbonyl carbon of the Boc group, an additional signal appeared in the ^{13}C NMR spectrum in the low field with a chemical shift of 157.67 ppm. Analysis of the heteronuclear correlation spectra $\{^1\text{H}, ^{13}\text{C}\}$ -HMBC (Fig. 2b) indicated the presence of cross peaks characterizing the interaction of this carbonyl carbon atom both with all protons of the glycerol backbone (A) and with protons of the CH_2N group of the diamine (B); however, no correlations with the Boc protection carbonyl carbon were detected.

Based on NMR spectroscopy data collection, we hypothesized that compound **5** in the presence of the strong base undergoes intramolecular cyclization via the transesterification mechanism to form compound **7** containing an oxazolidine ring, which was subsequently confirmed by literature data [15] and high-resolution mass spectrometry data.

Based on model synthesis, we implemented an approach to the synthesis of lipophilic NPs containing free hydroxyl groups (**10a** and **10b**) or an acyl substituent (**13**) at the C(2) atom of glycerol, as well as a derivative (**15**) with an oxazoline ring (Scheme 2). Epoxide **3** was opened using a 3-fold excess of previously obtained Boc-protected derivatives of norspermine **8a** and triethylenetetramine **8b** [16]. The reaction was carried out in the presence of calcium triflate in acetonitrile at 85°C. Compounds **9a** and **9b** were isolated by column chromatography in 70% and 86% yields, respectively. Removal of the Boc-protected groups of compound **9a** and **9b** by the action of a 4N HCl solution in dioxane led to the formation of lipophilic NPs **10a** and **10b** with a free hydroxyl group at the C(2) atom of the glycerol backbone.

To modify the hydrophobic domain of the lipophilic norspermine **9a**, the primary and secondary amino groups of NPs were blocked with



Scheme 2. Synthetic approach to obtaining lipophilic polyamines.

Reagents and conditions: **a** – $\text{Ca}(\text{OTf})_2$, MeCN, 85°C; **b** – HCl-dioxane, CH_2Cl_2 , 24°C;

c – Boc_2O , K_2CO_3 , MeOH, 24°C; **d** – Ac_2O , 4-dimethylaminopyridine (DMAP), CH_2Cl_2 , 24°C; **e** – NaH, THF, 65°C.

Boc-protection group under basic conditions to obtain compound **11** in 68% yield. Further introduction of the acetyl group was achieved by treating compound **11** with a mixture of 4-dimethylaminopyridine and acetic anhydride in quantitative yield, and subsequent deprotection of the amino groups of compound **12** led to lipophilic NPs **13**. Treatment of norspermine derivative **11** with sodium hydride in tetrahydrofuran gave compound **14** in 72% yield; removing of Boc groups allowed NPs **15** with an oxazolidine ring to be obtained.

CONCLUSIONS

The developed approach to the synthesis of new lipophilic derivatives of norspermine and triethylenetetramine based on the opening of oxiranes by polyamines is presented. In the course of a model interaction with *N,N'*-diaminooctane, it was shown that the opening of the oxirane ring occurs regioselectively at the C(1) atom of the glycerol backbone. Lipophilic NPs containing a hydroxyl or acetyl group at the C(2) atom of glycerol, as well as a derivative with an oxazolidine ring, were obtained, for which antitumor activity will be studied in the future.

EXPERIMENTAL

Obtaining the compounds

rac-Hexadecylglycidyl ether (**3**)

A) 73 mg (1.843 mmol) of NaH (60% dispersion in mineral oil) was added in portions to a solution of *rac*-glycidol (**1**) (0.112 mL, 1.675 mmol) cooled to 4°C in 10 mL of anhydrous DMF and stirred for 20 min. Then $C_{16}H_{33}Br$ (0.665 mL, 2.178 mmol) and a catalytic amount of TBAI were added and stirred for 20 h. The reaction mixture was diluted with water (20 mL), extracted with Et_2O (4 × 15 mL), the organic layer was washed with saturated aqueous NaCl solution (4 × 10 mL), dried with Na_2SO_4 , filtered, and evaporated. The residue was chromatographed on a silica gel column eluting with a petroleum ether–EtOAc (25:1) system. The yield of compound **3** was 160 mg (46%).

B) Anhydrous NaOH (174 mg, 4.355 mmol) and TBAI (112 mg, 0.350 mmol) were added to a solution of $C_{16}H_{33}OH$ (849 mg, 3.500 mmol) in 15 mL of hexane with vigorous stirring, and the mixture was stirred for 15 min at 4°C. Then a solution of *rac*-epichlorohydrin (**2**) (0.341 mL, 4.355 mmol) in 5 mL of hexane was added dropwise.

The reaction mixture was stirred for 16 h at 60°C. The precipitate was filtered off; the organic solvent was removed in vacuo. The residue was chromatographed on a silica gel column eluting with a petroleum ether–EtOAc (25:1) system. The yield of compound **3** was 673 mg (67%).

C) To a solution of $C_{16}H_{33}OH$ (0.406 g, 1.675 mmol) cooled to 4°C in 10 mL of hexane, 80 mg (2.010 mmol) of NaH (60% dispersion in mineral oil) was added in portions with active stirring and stirred for 15 min. Then, with vigorous stirring, a catalytic amount of TBAI and a solution of *rac*-epichlorohydrin (**2**) (0.196 mL, 2.513 mmol) in 5 mL of hexane were added. The reaction mixture was stirred for 16 h at 60°C, cooled, diluted with water (25 mL), extracted with DCM (4 × 20 mL), the organic layer was washed with water (4 × 20 mL), dried with Na_2SO_4 , filtered, and evaporated. The residue was chromatographed on a silica gel column eluting with a petroleum ether–EtOAc (25:1) system. The yield of compound **3** was 260 mg (52%).

D) A catalytic amount of TBABr was added to $C_{16}H_{33}OH$ (3.0 g, 12.37 mmol) melted at 55°C, the reaction mixture was heated to 70°C, NaOH (742 mg, 18.56 mmol) was added, and the mixture was stirred for 20 min. Then, *rac*-epichlorohydrin (**2**) (1.9 mL, 24.75 mmol) was added to the reaction mixture and stirred for 12 h at 70°C. The reaction mixture was cooled, diluted with water (25 mL), extracted with DCM (4 × 30 mL), the organic layer was washed with water (4 × 25 mL), dried with Na_2SO_4 , filtered, and evaporated. The residue was chromatographed on a silica gel column eluting with a petroleum ether–EtOAc (25:1) system. The yield of compound **3** was 2.17 g (59%).

1H NMR (300 MHz, $CDCl_3$) δ 0.86 (t, J = 6.7 Hz, 3 H, CH_3), 1.24 (br. s., 26 H, $(CH_2)_{13}CH_3$), 1.27–1.65 (m, 2 H, OCH_2CH_2), 2.54–2.80 (m, 2 H, CH_2OCH), 3.04–3.17 (m, 1 H, CH), 3.29–3.70 (m, 4 H, CH_2OCH_2). ^{13}C NMR (75 MHz, $CDCl_3$) δ 14.26, 22.83, 29.50, 29.61, 29.73, 29.74, 29.80, 29.83, 32.06, 44.47, 51.04, 71.58, 71.86.

N-(*rac*-3-hexadecyloxy-2-hydroxyprop-1-yl)-1,8-diaminooctane (**4**)

N,N'-diaminooctane (218 mg, 1.520 mmol) and $Ca(OTf)_2$ (142 mg, 0.2529 mmol) were added to a solution of compound **3** (150 mg, 0.5059 mmol) in 5 mL of MeCN and stirred for 2 h at 24°C. The solvents were removed in vacuo, the residue was chromatographed on a silica gel column, eluting with a DCM–MeOH–25% aq. NH_3 (3:1:0.1) system. The yield of compound **4** was 156 mg (70%).

^1H NMR (600 MHz, CD_3OD) δ 0.90 (t, $J = 7.0$ Hz, 3 H, CH_3), 1.28 (br. s, 26 H, $(\text{CH}_2)_{13}\text{CH}_3$), 1.39 (br. s, 8 H, $(\text{CH}_2)_4$), 1.53–1.61 (m, 2 H, NHCH_2CH_2), 1.62–1.73 (m, 4 H, OCH_2CH_2 , NHCH_2CH_2), 2.89–2.93 (m, 2 H, NH_2CH_2), 2.98–3.20 (m, 4 H, CH_2NHCH_2), 3.41–3.51 (m, 4 H, CH_2OCH_2), 3.98–4.04 (m, 1 H, CH). ^{13}C NMR (151 MHz, $\text{MeOH}-d_4$) δ 14.61, 23.80, 26.87, 27.14, 27.18, 27.29, 28.34, 29.81, 30.59, 30.64, 30.69, 30.86, 30.90, 33.13, 40.63, 48.97, 51.48, 66.87, 72.64, 73.74. FT-ICR mass spectrum, m/z : 443.457 $[\text{M}+\text{H}]^+$, calculated for $\text{C}_{27}\text{H}_{58}\text{N}_2\text{O}_2$ 442.458.

***N*¹-(*rac*-3-hexadecyloxy-2-hydroxyprop-1-yl)-*N*^{1,8}-bis(*tert*-butyloxycarbonyl)-1,8-diaminooctane (5)**

A solution of Boc_2O (53 mg, 0.244 mmol) in 1 mL of MeOH was added in drops to a solution of compound 4 (36 mg, 0.0813 mmol) and K_2CO_3 (45 mg, 0.325 mmol) cooled to 4°C in 4 mL of MeOH and stirred for 10 h at 20°C . The precipitate was filtered off; the organic solvent was removed in vacuo. The residue was chromatographed on a silica gel column, eluting with a toluene–methyl ethyl ketone (MEK) (7:1) system. The yield of compound 5 was 36 mg (70%).

^1H NMR (600 MHz, CDCl_3) δ 0.88 (t, $J = 7.0$ Hz, 3 H, CH_3), 1.26 (br. s, 26 H, $(\text{CH}_2)_{13}\text{CH}_3$), 1.30 (br. s, 8 H, $(\text{CH}_2)_4$), 1.44–1.47 (m, 20 H, $2\text{C}(\text{CH}_3)_3$, NHCH_2CH_2), 1.49–1.54 (m, 2 H, NCH_2CH_2), 1.54–1.59 (m, 2 H, OCH_2CH_2), 3.06–3.13 (m, 2 H, NHCH_2), 3.17–3.33 (m, 4 H, CH_2NCH_2), 3.33–3.47 (m, 4 H, CH_2OCH_2), 3.88–3.93 (m, 1 H, CH). ^{13}C NMR (151 MHz, CDCl_3) δ 14.18, 22.81, 26.32, 26.90, 26.91, 28.61, 29.40, 29.44, 29.76, 29.77, 29.79, 29.81, 29.82, 29.83, 29.84, 30.26, 70.78, 71.82, 72.81, 79.15, 80.01, 156.15.

***rac*-*N*-[(8-*tert*-butyloxycarbonylamino)octyl]-5-(hexadecyloxymethyl)-oxoazolidin-2-one (7)**

NaH (3 mg, 0.0762 mmol, 60% dispersion in mineral oil) was added to a solution of compound 5 (25 mg, 0.0381 mmol) cooled to 4°C in 10 mL of anhydrous THF and stirred for 7 h, gradually heating the mixture to 65°C . After 5 h the organic solvent was removed in vacuo. The residue was chromatographed on a silica gel column, eluting with a toluene–MEK (7:1) system. The yield of compound 7 was 18 mg (82%).

^1H NMR (600 MHz, CDCl_3) δ 0.88 (t, $J = 7.1$ Hz, 3 H, CH_3), 1.22–1.33 (m, 34 H, $(\text{CH}_2)_{13}\text{CH}_3$,

$(\text{CH}_2)_4$), 1.40–1.48 (m, 11 H, $\text{C}(\text{CH}_3)_3$, NHCH_2CH_2), 1.50–1.58 (m, 4 H, OCH_2CH_2 , NCH_2CH_2), 3.06–3.12 (m, 2 H, NHCH_2), 3.21–3.40 (m, 4 H, CH_2NCH_2), 3.46–3.60 (m, 4 H, CH_2OCH_2), 4.55–4.62 (m, 1 H, CH). ^{13}C NMR (151 MHz, CDCl_3) δ 14.07, 22.65, 26.01, 26.45, 26.67, 27.22, 28.41, 29.09, 29.13, 29.33, 29.43, 29.59, 29.67, 31.89, 40.55, 44.00, 46.61, 71.09, 71.68, 72.12, 78.97, 155.86, 157.67. FT-ICR mass spectrum, m/z : 569.488 $[\text{M}+\text{H}]^+$, calculated for $\text{C}_{33}\text{H}_{64}\text{N}_2\text{O}_5$ 569.489.

General procedure for obtaining compounds 9a and 9b

Compound 8a or 8b (0.5019 mmol) and $\text{Ca}(\text{OTf})_2$ (0.0836 mmol) were added to a solution of compound 3 (0.1673 mmol) in 5 mL of MeCN, and the mixture was stirred for 7 h at 85°C . The precipitate was filtered off; the organic solvent was removed in vacuo. The residue was chromatographed on a silica gel column, eluting with a DCM–MeOH–25% aq. NH_3 (5:1:0.1) system.

***N*⁴,*N*⁸-bis(*tert*-butyloxycarbonyl)-1-[*N*-(*rac*-3-hexadecyloxy-2-hydroxyprop-1-yl)amino]-11-amino-4,8-diazoundecane (9a)**

The yield was 80 mg (70%). ^1H NMR (300 MHz, CDCl_3 – CD_3OD (3:1)) δ 0.84 (t, $J = 6.6$ Hz, 3 H, CH_3), 1.22 (br. s, 26 H, $(\text{CH}_2)_{13}\text{CH}_3$), 1.41 (br. s, 18 H, $2\text{C}(\text{CH}_3)_3$), 1.47–1.57 (m, 2 H, OCH_2CH_2), 1.58–1.79 (m, 6 H, $3\text{NCH}_2\text{CH}_2\text{CH}_2\text{N}$), 2.58–2.75 (m, 6 H, CH_2NHCH_2 , CH_2NH_2), 3.15 (m, 8 H, $2\text{CH}_2\text{NBocCH}_2$), 3.19–3.30 (m, 4 H, CH_2OCH_2), 3.77–3.91 (m, 1 H, CH). ^{13}C NMR (75 MHz, CDCl_3 – CD_3OD (3:1)) δ 14.06, 22.63, 26.06, 28.42, 28.97–30.22, 31.87, 39.15, 44.81, 46.77, 52.21, 68.64, 71.66, 73.43, 79.43, 155.59. FT-ICR mass spectrum, m/z : 687.606 $[\text{M}+\text{H}]^+$, 721.599 $[\text{M}+\text{Cl}]^+$, calculated for $\text{C}_{38}\text{H}_{79}\text{N}_4\text{O}_6$ 687.6060, calculated for $\text{C}_{38}\text{H}_{79}\text{ClN}_4\text{O}_6$ 721.561.

***N*³,*N*⁶-bis(*tert*-butyloxycarbonyl)-1-[*N*-(*rac*-3-hexadecyloxy-2-hydroxyprop-1-yl)amino]-8-amino-3,6-diazaoctane (9b)**

The yield was 93 mg (86%). ^1H NMR (300 MHz, CDCl_3 – CD_3OD (3:1)) δ 0.86 (t, $J = 6.6$ Hz, 3 H, CH_3), 1.23 (br. s, 26 H, $(\text{CH}_2)_{13}\text{CH}_3$), 1.44 (br. s, 18 H, $2\text{C}(\text{CH}_3)_3$), 1.43–1.49 (m, 2 H, OCH_2CH_2), 2.56–2.89 (m, 6 H, CH_2NHCH_2 , CH_2NH_2), 3.18–3.36 (m, 8 H, $2\text{CH}_2\text{NBocCH}_2$), 3.36–3.48 (m, 4 H, CH_2OCH_2), 3.76–3.89 (m, 1 H, CH). ^{13}C NMR (75 MHz, CDCl_3 – CD_3OD (3:1)) δ 14.13, 22.69, 26.10, 28.47, 29.23–29.96, 31.93, 40.72,

45.81, 48.09, 51.96, 68.83, 71.72, 73.32, 79.86, 155.70. FT-ICR mass spectrum, m/z : 645.560 $[M+H]^+$, calculated for $C_{35}H_{73}N_4O_6$ 645.553.

***N*⁴,*N*⁸-bis(*tert*-butyloxycarbonyl)-1-[*N*-(*rac*-3-hexadecyloxy-2-hydroxyprop-1-yl)-*N*-(*tert*-butoxycarbonyl)amino]-11-(*tert*-butoxycarbonyl)-amino-4,8-diazaundecane (11)**

A solution of Boc_2O (42 mg, 0.1908 mmol) in 1 mL of MeOH was added in drops to a solution of compound **7a** (44 mg, 0.0636 mmol) and K_2CO_3 (35 mg, 0.254 mmol) cooled to 4°C in 4 mL of MeOH and stirred for 10 h at 20°C. The organic solvent was removed in vacuo, the residue was chromatographed on a silica gel column, eluting with a toluene–MEK (5:1) system. The yield of compound **11** was 24 mg (68%).

1H NMR (300 MHz, $CDCl_3$) δ 0.85 (t, J = 6.9 Hz, 3 H, CH_3), 1.23 (br. s., 26 H, $(CH_2)_{13}CH_3$), 1.36–1.48 (m, 36 H, 4 $C(CH_3)_3$), 1.48–1.49 (m, 2 H, OCH_2CH_2), 1.58–1.69 (m, 2 H, $NHCH_2CH_2$), 1.69–1.82 (m, 4 H, NCH_2CH_2), 3.00–3.19 (m, 8 H, 3 NCH_2 , CH_2NH), 3.19–3.38 (m, 10 H, 3 NCH_2 , CH_2OCH_2), 3.83–3.97 (m, 1 H, CH). ^{13}C NMR (75 MHz, $CDCl_3$) δ 14.13, 22.69, 26.11, 28.44, 28.97–30.32, 31.91, 37.34, 44.78, 46.91, 51.02, 70.46, 71.64, 72.60, 79.69, 155.36, 156.03.

***N*⁴,*N*⁸-di(*tert*-butyloxycarbonyl)-1-[*N*-(*rac*-3-hexadecyloxy-2-acetoxyp-1-yl)-*N*-(*tert*-butoxycarbonyl)amino]-11-(*tert*-butoxycarbonyl)-amino-4,8-diazaundecane (12)**

Ac_2O (7.3 μ L, 0.0777 mmol) was added to a solution of DMAP (6.3 mg, 0.0518 mmol) in 1 mL of DCM and stirred for 5 min. The resulting mixture was added to a solution of compound **9** (23 mg, 0.0259 mmol) in 2 mL of DCM and stirred for 20 h. The organic solvent was removed in vacuo, the residue was chromatographed on a silica gel column, eluting with a toluene–EtOAc (5:1) system. The yield of compound **12** was 24 mg (99%).

1H NMR (600 MHz, $CDCl_3$) δ 0.87 (t, J = 6.9 Hz, 3 H, CH_3), 1.25 (br. s., 26 H, $(CH_2)_{13}CH_3$), 1.40–1.48 (m, 36 H, 4 $C(CH_3)_3$), 1.50–1.57 (m, 2 H, OCH_2CH_2), 1.61–1.77 (m, 4 H, NCH_2CH_2), 2.05 (s, 3 H, $C(O)CH_3$), 3.05–3.11 (m, 2 H, CH_2NH), 3.11–3.54 (m, 18 H, 7 CH_2N , CH_2OCH_2), 5.15–5.19 (m, 1 H, CH). ^{13}C NMR (151 MHz, $CDCl_3$) δ 14.25, 21.30, 22.82, 26.18, 28.56, 28.60, 29.49, 29.61, 29.69, 29.79, 29.83, 32.06, 44.99, 45.93, 70.15, 71.60, 71.85, 79.73, 155.49, 156.19, 170.56.

***rac*-*N*-[(*N*⁴,*N*⁸-bis(*tert*-butyloxycarbonyl)-11-(*tert*-butoxycarbonyl)amino]-4,8-diazaundecanyl)-5-(hexadecyloxymethyl)-oxoazolidin-2-one (14)**

NaH (1.2 mg, 0.0311 mmol, 60% dispersion in mineral oil) was added to a solution of compound **11** (15 mg, 0.0169 mmol) cooled to 4°C in 5 mL of anhydrous THF and stirred for 20 h, gradually heating to 65°C. The organic solvent was removed in vacuo, the residue was chromatographed on a silica gel column, eluting with a toluene–MEK (5:1) system. The yield of compound **14** was 10 mg (72%).

1H NMR (600 MHz, $CDCl_3$) δ 0.88 (t, J = 6.9 Hz, 3 H, CH_3), 1.26 (br. s., 26 H, $(CH_2)_{13}CH_3$), 1.40–1.50 (m, 27 H, 3 $C(CH_3)_3$), 1.50–1.60 (m, 2 H, OCH_2CH_2), 1.60–1.70 (m, 2 H, $NHCH_2CH_2$), 1.70–1.85 (m, 4 H, NCH_2CH_2), 3.04–3.66 (m, 18 H, 6 NCH_2 , CH_2OCH_2), 4.51–4.57 (m, 1 H, CH). ^{13}C NMR (151 MHz, $CDCl_3$) δ 14.25, 22.82, 26.15, 28.58, 28.60, 28.62, 29.49, 29.60, 29.72, 29.73, 29.77, 29.79, 29.81, 29.82, 29.83, 32.06, 42.12, 44.87, 46.86, 71.19, 72.00, 72.27, 79.78, 79.85, 155.47, 157.91.

General procedure for removing *tert*-butoxycarbonyl protecting groups

4N HCl in dioxane (1 mL) was added to a solution of compounds **9a**, **9b**, **12**, **14** (0.0291 mmol) in 2 mL DCM and stirred for 1 h at 24°C. The organic solvent was removed in vacuo.

1-[*N*-(*rac*-3-hexadecyloxy-2-hydroxyprop-1-yl)amino]-11-amino-4,8-diazaundecane tetrahydrochloride (10a)

The yield was 16 mg (85%). 1H NMR (300 MHz, D_2O-CD_3OD (1:1)) δ 0.97 (t, J = 6.9 Hz, 3 H, CH_3), 1.36 (br. s., 26 H, $(CH_2)_{13}CH_3$), 1.59–1.75 (m, 2 H, OCH_2CH_2), 2.12–2.38 (m, 6 H, $NHCH_2CH_2$), 3.11–3.38 (m, 14 H, 6 CH_2NH , CH_2NH_2), 3.51–3.68 (m, 4 H, CH_2OCH_2), 4.11–4.29 (m, 1 H, CH). ^{13}C NMR (75 MHz, D_2O-CD_3OD (1:1)) δ 14.11, 22.70, 26.00, 28.47, 29.37, 29.46, 29.54–29.90, 31.94, 37.51, 41.97, 44.74, 46.74, 71.07, 71.86, 72.14, 79.70. FT-ICR mass spectrum, m/z : 487.495 $[M+H]^+$, calculated for $C_{28}H_{63}N_4O_2$ 487.492.

1-[*N*-(*rac*-3-hexadecyloxy-2-hydroxyprop-1-yl)amino]-8-amino-3,6-diazaoctane tetrahydrochloride (10b)

The yield was 23 mg (82%). 1H NMR (300 MHz, D_2O-CD_3OD (1:1)) δ 0.88 (t, J = 6.9 Hz, 3 H, CH_3),

1.23 (br. s., 26 H, $(\text{CH}_2)_{13}\text{CH}_3$), 1.52–1.67 (m, 2 H, OCH_2CH_2), 3.10–3.73 (m, 14 H, 6 CH_2NH , CH_2NH_2), 3.36–3.48 (m, 4 H, CH_2OCH_2), 3.76–3.89 (m, 1 H, CH). ^{13}C (75 MHz, $\text{D}_2\text{O}-\text{CD}_3\text{OD}$ (1:1)). ^{13}C NMR (75 MHz, $\text{D}_2\text{O}-\text{CD}_3\text{OD}$ (1:1)) δ 14.11, 22.70, 26.00, 28.47, 29.37, 29.46, 29.54–29.90, 31.94, 37.51, 41.97, 44.74, 46.74, 71.07, 71.86, 72.14, 79.70. FT-ICR mass spectrum, m/z : 445.448 $[\text{M}+\text{H}]^+$, calculated for $\text{C}_{25}\text{H}_{57}\text{N}_4\text{O}_2$ 445.447.

1-[N-(*rac*-3-hexadecyloxy-2-acetoxyprop-1-yl)amino]-11-amino-4,8-diazaundecane tetrahydrochloride (13).

The yield was 15 mg (86%). ^1H NMR (600 MHz, $\text{D}_2\text{O}-\text{CD}_3\text{OD}$ (1:1)) δ 0.88 (t, $J = 6.9$ Hz, 3 H, CH_3), 1.26 (br. s., 26 H, $(\text{CH}_2)_{13}\text{CH}_3$), 1.53–1.59 (m, 2H, OCH_2CH_2), 2.10–2.22 (m, 9 H, $\text{C}(\text{O})\text{CH}_3$, NHCH_2CH_2 , NCH_2CH_2), 3.09–3.42 (m, 14 H, 6 CH_2NH , CH_2NH_2), 3.46–3.67 (m, 4 H, CH_2OCH_2), 5.25–5.29 (m, 1 H, CH). ^{13}C NMR (151 MHz, $\text{D}_2\text{O}-\text{CD}_3\text{OD}$ (1:1)) δ 14.58, 23.49, 23.82, 24.81, 24.89, 26.74, 30.21, 30.30, 30.38, 30.52, 30.77, 32.78, 37.63, 41.97, 45.70, 45.72, 45.80, 46.29, 47.18, 72.03, 72.82, 74.58, 160.59. FT-ICR mass spectrum, m/z : 529.506 $[\text{M}+\text{H}]^+$, calculated for $\text{C}_{30}\text{H}_{65}\text{N}_4\text{O}_3$ 529.505.

***rac*-N-[11-(11-amino-4,8-diazaundecanyl)]-5-(hexadecyloxymethyl)oxoazolidin-2-one trihydrochloride (15)**

The yield was 8 mg (99%). ^1H NMR (600 MHz, $\text{D}_2\text{O}-\text{CD}_3\text{OD}$ (1:1)) δ 0.88 (t, $J = 6.7$ Hz,

3 H, CH_3), 1.27 (br. s., 26 H, $(\text{CH}_2)_{13}\text{CH}_3$), 1.53–1.60 (m, 2 H, OCH_2CH_2), 1.97–2.03 (m, 2 H, $\text{NH}_2\text{CH}_2\text{CH}_2$), 2.09–2.21 (m, 4 H, NCH_2CH_2), 3.07–3.72 (m, 18 H, 6 CH_2NH , CH_2NH_2 , CH_2OCH_2), 3.78–3.85 (m, 1 H, CH). ^{13}C NMR (151 MHz, $\text{D}_2\text{O}-\text{CD}_3\text{OD}$ (1:1)) δ 14.58, 23.49, 23.82, 24.81, 24.89, 26.74, 30.21, 30.30, 30.38, 30.52, 30.77, 32.78, 37.63, 41.97, 45.70, 45.72, 45.80, 46.29, 47.18, 72.03, 72.82, 74.58, 160.59. FT-ICR mass spectrum, m/z : 529.515 $[\text{M}-\text{H}+\text{H}_2\text{O}]^-$, calculated for $\text{C}_{29}\text{H}_{61}\text{N}_4\text{O}_4$ 529.469.

Acknowledgments

This study was supported by the Ministry of Science and Higher Education of the Russian Federation (project No. 0706-2020-0019), and performed using the equipment of the Shared Science and Training Center for Collective Use of RTU MIREA (agreement No. 075-15-2021-689 dated 01.09.2021 (unique identification number 2296.61321X0010).

Authors' contributions

E.A. Eshtukova-Shcheglova – carrying out the synthesis, writing the text of the article;

K.A. Perevoshchikova – design of experiments, writing the text of the article, carrying out the synthesis;

A.V. Eshtukov-Shcheglov – NMR spectroscopy studies and data processing;

D.A. Cheshkov – NMR spectroscopy studies and data processing, scientific advice;

M.A. Maslov – supervising of works, design of experiments, editing the article.

The authors declare no potential or actual conflicts of interest.

REFERENCES

1. Casero R.A., Murray Stewart T., Pegg A.E. Polyamine metabolism and cancer: treatments, challenges and opportunities. *Nat. Rev. Cancer*. 2018;18(11):681–695. <https://doi.org/10.1038/s41568-018-0050-3>
2. Khomutov M.A., Mikhura I.V., Kochetkov S.N., et al. C-Methylated Analogs of Spermine and Spermidine: Synthesis and Biological Activity. *Russ. J. Bioorg. Chem.* 2019;45(6):463–487. <https://doi.org/10.1134/S1068162019060207>
3. Goyal L., et al. Phase 1 study of N(1),N(11)-diethylnorspermine (DENSPM) in patients with advanced hepatocellular carcinoma. *Cancer Chemother. Pharmacol.* 2013;72(6):1305–1314. <https://doi.org/10.1007/s00280-013-2293-8>

4. Murray-Stewart T.R., Woster P.M., Casero R.A. Targeting polyamine metabolism for cancer therapy and prevention. *Biochem. J.* 2016;473(19):2937–2953. <https://doi.org/10.1042/bcj20160383>

5. Ma J., et al. A Polyamine-Based Dinitro-Naphthalimide Conjugate as Substrates for Polyamine Transporters Preferentially Accumulates in Cancer Cells and Minimizes Side Effects *in vitro* and *in vivo*. *Front. Chem.* 2020;8:106. <https://doi.org/10.3389/fchem.2020.00166>

6. Thibault B., et al. F14512, a polyamine-vectorized inhibitor of topoisomerase II, exhibits a marked anti-tumor activity in ovarian cancer. *Cancer Lett.* 2016;370(1):10–18. <https://doi.org/10.1016/j.canlet.2015.09.006>

7. Kazakova O.B., et al. Evaluation of Cytotoxicity and α -Glucosidase Inhibitory Activity of Amide and Polyamino-Derivatives of Lupane Triterpenoids. *Molecules*. 2020;25(20):4833. <https://doi.org/10.3390/molecules25204833>
8. Hodon J., et al. Design and synthesis of pentacyclic triterpene conjugates and their use in medicinal research. *Eur. J. Med. Chem.* 2019;182:111653. <https://doi.org/10.1016/j.ejmech.2019.111653>
9. Mohamad Reza Nazifi S., et al. Structure–activity relationship of polyamine conjugates for uptake via polyamine transport system. *Struct. Chem.* 2019;30(10):175–184. <https://doi.org/10.1007/s11224-018-1175-4>
10. Markova A.A., Plyavnik N.V., Morozova N.G., et al. Antitumor phosphate-containing lipids and non-phosphorus alkyl cationic glycerolipids: Chemical structures and perspectives of drug development. *Russ. Chem. Bull.* 2014;63(5):1081–1087. <https://doi.org/10.1007/s11172-014-0552-4>
11. Varlamova E.A., Isagulieva A.K., Morozova N.G., et al. Non-Phosphorus Lipids As New Antitumor Drug Prototypes. *Russ. J. Bioorg. Chem.* 2021;47(5):965–979. <https://doi.org/10.1134/S1068162021050356>
12. Perevoshchikova K.A., Nichugovskiy A.I., Isagulieva A.K., et al. Synthesis of novel lipophilic tetraamines with cytotoxic activity. *Mendeleev Commun.* 2019;29(6):616–618. <https://doi.org/10.1016/j.mencom.2019.11.003>
13. Saddique F.A., Zahoor A.F., Faiz S., et al. Recent trends in ring opening of epoxides by amines as nucleophiles. *Synth. Commun.* 2016;46(10):831–868. <https://doi.org/10.1080/00397911.2016.1170148>
14. Cepanec I., Litvic M., Mikuldas H., et al. Calcium trifluoromethanesulfonate catalysed aminolysis of epoxides. *Tetrahedron*. 2003;59(14):2435–2439. [https://doi.org/10.1016/S0040-4020\(03\)00292-8](https://doi.org/10.1016/S0040-4020(03)00292-8)
15. Ishigami K., Katsuta R., Shibata C., et al. Synthesis and structure revision of tyroscherin, and bioactivities of its stereoisomers against IGF-1-dependent tumor cells. *Tetrahedron*. 2009;65(18):3629–3638. <https://doi.org/10.1016/j.tet.2009.03.003>
16. Petukhov I.A., Maslov M.A., Morozova N.G., et al. Synthesis of polycationic lipids based on cholesterol and spermine. *Russ. Chem. Bull.* 2010;59(1):260–268. <https://doi.org/10.1007/s11172-010-0071-x>

About the authors:

Elizaveta A. Eshtukova-Shcheglova, Postgraduate Student, N.A. Preobrazhensky Department of Chemistry and Technology of Biologically Active Compounds, Medicinal and Organic Chemistry, M.V. Lomonosov Institute of Fine Chemical Technologies, MIREA – Russian Technological University (86, Vernadskogo pr., Moscow, 119571, Russia). E-mail: shchegs.ea@gmail.com. <https://orcid.org/0000-0002-3729-4466>

Ksenia A. Perevoshchikova, Trainee Researcher, N.A. Preobrazhensky Department of Chemistry and Technology of Biologically Active Compounds, Medicinal and Organic Chemistry, M.V. Lomonosov Institute of Fine Chemical Technologies, MIREA – Russian Technological University (86, Vernadskogo pr., Moscow, 119571, Russia). E-mail: perevoshchikova@mirea.ru. Scopus Author ID 57189095507, <https://orcid.org/0000-0001-9478-2960>

Artur V. Eshtukov-Shcheglov, Junior Researcher, State Scientific Research Institute of Chemistry and Technology of Organoelement Compounds (38, Entuziastov sh., Moscow, 105118, Russia). E-mail: nemtcev.94.nmr@gmail.com. <https://orcid.org/0000-0002-8975-9958>

Dmitriy A. Cheshkov, Cand. Sci. (Phys.-Math.), Leading Researcher, State Scientific Research Institute of Chemistry and Technology of Organoelement Compounds (38, Entuziastov sh., Moscow, 105118, Russia). E-mail: cheshkov_d@mail.ru. Scopus Author ID 23481189200, RSCI SPIN-code 5722-6745, <https://orcid.org/0000-0002-9024-4353>

Mikhail A. Maslov, Dr. Sci. (Chem.), Director of the Institute of Fine Chemical Technologies, Professor, N.A. Preobrazhensky Department of Chemistry and Technology of Biologically Active Compounds, Medicinal and Organic Chemistry, M.V. Lomonosov Institute of Fine Chemical Technologies, MIREA – Russian Technological University (86, Vernadskogo pr., Moscow, 119571, Russia). E-mail: maslov@mail.ru. ResearcherID A-3011-2012, Scopus Author ID 7003427092, RSCI SPIN-code 6451-6580, <https://orcid.org/0000-0002-5372-1325>

Об авторах:

Ештуркова-Щеглова Елизавета Александровна, аспирант кафедры химии и технологии биологически активных соединений, медицинской и органической химии им. Н.А. Преображенского Института тонких химических технологий им. М.В. Ломоносова ФГБОУ ВО «МИРЭА – Российский технологический университет» (119571, Россия, Москва, пр-т Вернадского, д. 86). E-mail: shchegs.ea@gmail.com. <https://orcid.org/0000-0002-3729-4466>

ПЕРЕВОЩИКОВА Ксения Андреевна, стажер-исследователь кафедры химии и технологии биологически активных соединений, медицинской и органической химии им. Н.А. Преображенского Института тонких химических технологий им. М.В. Ломоносова ФГБОУ ВО «МИРЭА – Российский технологический университет» (119571, Россия, Москва, пр-т Вернадского, д. 86). E-mail: perevoshchikova@mirea.ru. Scopus Author ID 57189095507, <https://orcid.org/0000-0001-9478-2960>

Ешутков-Щеглов Артур Владимирович, младший научный сотрудник, Государственный научный центр РФ, Акционерное общество «Научно-исследовательского институт химии и технологии элементоорганических соединений» (105118, Россия, Москва, ш. Энтузиастов, д. 38). E-mail: nemtcev.94.nmr@gmail.com. <https://orcid.org/0000-0002-8975-9958>

Чешков Дмитрий Александрович, к.ф.-м.н., ведущий научный сотрудник, Государственный научный центр РФ, Акционерное общество «Научно-исследовательского институт химии и технологии элементоорганических соединений» (105118, Россия, Москва, ш. Энтузиастов, д. 38). E-mail: cheshkov_d@mail.ru. Scopus Author ID 23481189200, SPIN-код РИНЦ 5722-6745, <https://orcid.org/0000-0002-9024-4353>

Маслов Михаил Александрович, д.х.н., директор Института тонких химических технологий, профессор кафедры химии и технологии биологически активных соединений, медицинской и органической химии им. Н.А. Преображенского Института тонких химических технологий им. М.В. Ломоносова ФГБОУ ВО «МИРЭА – Российский технологический университет» (119571, Россия, Москва, пр-т Вернадского, д. 86). E-mail: mamaslov@mail.ru. ResearcherID A-3011-2012, Scopus Author ID 7003427092, SPIN-код РИНЦ 6451-6580, <https://orcid.org/0000-0002-5372-1325>

The article was submitted: February 17, 2022; approved after reviewing: April 15, 2022; accepted for publication: July 07, 2022.

Translated from Russian into English by H. Moshkov

Edited for English language and spelling by Thomas Beavitt

**CHEMISTRY AND TECHNOLOGY OF MEDICINAL COMPOUNDS
AND BIOLOGICALLY ACTIVE SUBSTANCES**

**ХИМИЯ И ТЕХНОЛОГИЯ ЛЕКАРСТВЕННЫХ ПРЕПАРАТОВ
И БИОЛОГИЧЕСКИ АКТИВНЫХ СОЕДИНЕНИЙ**

ISSN 2686-7575 (Online)

<https://doi.org/10.32362/2410-6593-2022-17-4-335-345>



UDC 615.28

RESEARCH ARTICLE

Antibacterial activity of green fabricated silver-doped titanates

Anh C. Ha^{1,2,✉}, Tri Nguyen^{3,4}, Phung A. Nguyen³, Van M. Nguyen⁴

¹Vietnam National University Ho Chi Minh City, Linh Trung Ward, Thu Duc District, Ho Chi Minh City, Vietnam

²Faculty of Chemical Engineering, Ho Chi Minh City University of Technology (HCMUT), 268 Ly Thuong Kiet Street, Ho Chi Minh City, Vietnam

³Institute of Chemical Technology, Vietnam Academy of Science and Technology, 01A TL29 Street, Thanh Loc Ward, District 12, Ho Chi Minh City, Vietnam

⁴Ho Chi Minh City Open University, 97 Vo Van Tan Street, District 3, Ho Chi Minh City, Vietnam

✉Corresponding author, e-mail: hcanh@hcmut.edu.vn

Abstract

Objectives. The study aimed to synthesize the multifunctional materials silver-added titanates via reduction of sol-gel fabricating titanates (Fe_2TiO_5 and NiTiO_3) with Jasminium subtriplinerve Blume leaf extract.

Methods. The physicochemical characteristics of the obtained materials were determined by X-ray diffraction, energy dispersive X-Ray spectroscopy, Raman spectroscopy, Brunauer–Emmett–Teller specific surface area, scanning electron microscopy, and UV–Vis absorption spectroscopy.

Results. The results demonstrated good dispersion of silver on the surface of Fe_2TiO_5 and NiTiO_3 to create photocatalysts with two light-absorbing regions. The obtained materials were applied as antibacterial agents in polluted water. The Ag– Fe_2TiO_5 (Ag–FTO) samples showed better properties and antibacterial activity than Ag– NiTiO_3 (Ag–NTO) due to the better dispersion of silver nanoparticles on the FTO surface. Besides, the antibacterial results exhibit increased inhibiting activity against gram-negative (–) bacteria as compared with gram-positive (+) bacteria.

Conclusions. Nanomaterials Fe_2TiO_5 and NiTiO_3 added Ag were successfully synthesized. These materials showed excellent inhibition against *Bacillus cereus*, *Escherichia coli*, *Pseudomonas aeruginosa*, *Salmonella typhi*, and *Staphylococcus aureus*. Additionally, the Ag- Fe_2TiO_5 samples showed much better antibacterial activity than the Ag- NiTiO_3 sample.

Keywords: Iron(III) titanate, nickel titanate, *Jasminum subtriplinerne* Blume leaf, antibacterial activity

For citation: Ha C.A., Nguyen T., Nguyen P.A., Nguyen V.M. Antibacterial activity of green fabricated silver-doped titanates. *Tonk. Khim. Tekhnol. = Fine Chem. Technol.* 2022;17(4):335–345. <https://doi.org/10.32362/2410-6593-2022-17-4-335-345>

НАУЧНАЯ СТАТЬЯ

Антибактериальная активность биосинтетических титанатов, допированных серебром

А.К. Ха^{1,2,✉}, Т. Нгуен^{3,4}, П.А. Нгуен³, В.М. Нгуен⁴

¹Вьетнамский национальный университет Хошимина, Линь Чунг Уорд, Район Тхёк, г. Хошимин, Вьетнам

²Химико-технологический факультет, Технологический университет Хошимина, 268 Ли Тхыонг Кьет ул., г. Хошимин, Вьетнам

³Химико-технологический институт, Академия наук Вьетнама, 01A TL29 ул., Тха Лог Вард, Район 12, г. Хошимин, Вьетнам

⁴Открытый Университет Хошимина, 97, Во Ван Тан ул., Район 3, г. Хошимин, Вьетнам

✉ Автор для переписки, e-mail: hcanh@hcmut.edu.vn

Аннотация

Цели. Синтезировать многофункциональные материалы титанаты с добавлением серебра путем восстановления золь-гелевых производных титанатов (Fe_2TiO_5 и NiTiO_3) экстрактом листьев *subtriplinerne* Blume жасмина.

Методы. Физико-химические характеристики полученных материалов определяли методами рентгеновской дифракции, энергодисперсионной рентгеновской спектроскопии, спектроскопии комбинационного рассеяния, удельной поверхности Брунауэра – Эммета – Теллера, сканирующей электронной микроскопии и абсорбционная спектроскопия в УФ-видимой области.

Результаты. Результаты показывают, что серебро имеет хорошую дисперсию на поверхности Fe_2TiO_5 и NiTiO_3 и создает фотокатализаторы с двумя светопоглощающими областями. Полученные материалы применялись в качестве антибактериальных средств в загрязненных водах. Образцы Ag- Fe_2TiO_5 (Ag-FTO) показали лучшие свойства и антибактериальную активность, чем Ag- NiTiO_3 (Ag-NTO) за счет лучшего диспергирования наночастиц серебра на поверхности FTO. Кроме того, антибактериальные результаты демонстрируют большую ингибирующую активность в отношении грамотрицательных (–) бактерий, чем в отношении грамположительных (+) бактерий.

Выводы. Успешно синтезированы наноматериалы Fe_2TiO_5 и NiTiO_3 с добавлением Ag. Полученные составы показали отличное ингибирование в отношении восковой бациллы (*Bacillus cereus*), кишечной палочки (*Escherichia coli*), синегнойной палочки (*Pseudomonas aeruginosa*), сальмонеллы тифи (*Salmonella typhi*) и золотистого стафилококка (*Staphylococcus aureus*). Кроме того, образцы $\text{Ag-Fe}_2\text{TiO}_5$ показали гораздо лучшую антибактериальную активность, чем образец Ag-NiTiO_3 .

Ключевые слова: титанат железа(III), титанат никеля, листья *subtripplinerve Blume* жасмина, антибактериальный

Для цитирования: Ha C.A., Nguyen T., Nguyen P.A., Nguyen V.M. Antibacterial activity of green fabricated silver-doped titanates. *Tonk. Khim. Tekhnol. = Fine Chem. Technol.* 2022;17(4):335–345. <https://doi.org/10.32362/2410-6593-2022-17-4-335-345>

INTRODUCTION

The increasing number of industrial production and complex human life activities has seriously affected water quality creating safety concerns. Wastewater contains not only a large number of persistent pollutants but also many dangerous bacteria affecting human health [1, 2]. Therefore, there is an urgent need to overcome these problems, especially in developing countries.

Contemporary treatment methods such as chemical oxidizing agents, chlorination, ultraviolet (UV) radiation, membrane, ozonation, etc., have been considered for water treatment and disinfection purposes [3–5]. Although these methods have demonstrated effectiveness, they also have various disadvantages, such as the creation of toxic byproducts after treatment, high operating costs, and the inability to treat bacteria [3]. The main limitation of catalytic oxidation is the inability to kill bacteria present in wastewater. Semiconductor photocatalytic oxidation is one of the advanced oxidation processes being researched and applied in the wastewater treatment industry.

Although silver (Ag) is well known as a disinfectant against a wide range of bacteria having been widely used in sterilization and bactericidal applications, its practical application is limited due to the ease of oxidation, which can cause aggregation and loss of antimicrobial activity over time. Therefore, Ag requires a supporting substrate to enhance stability of

morphological features and maintain antimicrobial efficacy. Therefore, the research aimed at enhancing the antibacterial ability of photocatalyst materials by modifying them or adding another material with antibacterial properties is required.

The widely used TiO_2 semiconductor catalyst has been commercialized as $\text{TiO}_2\text{-P25}$. However, its practical application is limited by the large bandgap energy (3.2 eV) and high recombination of electron and hole pairs [6, 7]. Therefore, the modification of TiO_2 structure to improve its catalytic efficiency and stability has been receiving much interest from researchers along with the study of new potential semiconductor materials.

Perovskite-like materials possessing suitable properties, such as chemically inert, high mechanical strength, high absorption coefficient, low activation energy, and significant transparency, are being researched and developed for photocatalytic applications [6, 7]. Among them, titanate-based materials have shown their potential with high activity and stability. Fe_2TiO_5 pseudobrookite has received much attention due to its low band gap energy (1.9–2.2 eV), higher energy level minimum conduction band, superior photochemical stability, and low cost, representing a promising photocatalyst product [8–10]. Another titanate, NiTiO_3 perovskite, comprising an n-type semiconductor with an ilmenite-type crystal structure, has attracted considerable attention due to its superior photocatalytic and electro-optical properties and low dielectric constant [11, 12]. NiTiO_3 also exhibits an optical absorption

spectrum with band gap energy around 3.0 eV, offering excellent potential for visible light photocatalytic applications [13]. Thus, the Ag-added titanates can be used to create multifunctional composites with excellent photocatalytic antibacterial activity in wastewater. However, there are almost no studies on the addition of Ag to Fe_2TiO_5 and NiTiO_3 to enhance their antibacterial ability.

In our research, multifunctional Ag-added titanates (Fe_2TiO_5 and NiTiO_3) were synthesized by biosynthesis using *Jasminium subtripplinerve* Blume (JS) leaf extract as a reducing agent of AgNO_3 solution to Ag^0 , in which Fe_2TiO_5 and NiTiO_3 are prepared by the sol-gel method. JS is a member of the Oleaceae genera. Compounds such as triterpenoids, oleanolic acid, flavonoids, glucosides, etc. [14–16], which have been identified and reported in its phytochemicals, can be employed as reducing reagents in the process of biosynthesizing silver nanoparticles. The physicochemical properties of the prepared nanoparticles have been investigated. The antibacterial action of prepared nanoparticles was evaluated with the help of bacteria such as gram-negative *Escherichia coli* (*E. coli*), *Pseudomonas aeruginosa* (*P. aeruginosa*), and *Salmonella typhi* (*Salmonella*), and gram-positive *Bacillus cereus* (*B. cereus*) and *Staphylococcus aureus* (*S. aureus*), which are typically present in wastewater.

MATERIALS AND METHODS

Pseudobrookite Fe_2TiO_5 and perovskite NiTiO_3 were prepared by sol-gel method according to the procedure described in detail in the works [17, 18], respectively. First, 4.04 g of $\text{Fe}(\text{NO}_3)_3 \cdot 9\text{H}_2\text{O}$ (99.9%, Merck, Germany) or $\text{Ni}(\text{NO}_3)_2 \cdot 6\text{H}_2\text{O}$ (99.9%, Merck, Germany) and 2.1 g of $\text{C}_6\text{H}_8\text{O}_7 \cdot \text{H}_2\text{O}$ (99.9%, Merck, Germany) were dissolved with 5 mL of $\text{C}_2\text{H}_5\text{OH}$ (99%, Merck, Germany). Next, 3 mL of $\text{Ti}(\text{OC}_3\text{H}_7)_4$ (99.7%, Merck, Germany) was added drop by drop. The synthetic gel was dried at 60°C for 24 h and follows by heating at 700°C for 2 h to obtain a Fe_2TiO_5 and NiTiO_3 samples.

Ag-doped Fe_2TiO_5 (Ag-FTO) and Ag-doped NiTiO_3 (Ag-NTO) catalysts were synthesized using JS leaf extract as a reducing agent of AgNO_3 solution to Ag^0 . JS leaf was collected from Ho Chi Minh City in Vietnam. After washing and shredding, JS leaf is dried at a temperature of 60°C for 4 h. Next, 50 g of the JS leaf were mixed with 1000 mL of deionized water and heated to 80°C for 2 h under stirring. Finally, the JS leaf extract

was filtered and preserved at 4°C for further experiments. Silver nitrate (AgNO_3 , >99.8%, Merck, Germany) was purchased. The optimized conditions for the Ag nanoparticles (AgNPs) synthesis using JS extract as a reducing agent were determined based on our previous publication [16], involving the presence of the light illumination, a synthesis time of 150 min, a volume ratio of AgNO_3 solution/JS extract of 18:2, a AgNO_3 concentration of 1.0 mM and a stirring rate of 300 rpm at temperature of 20°C. To synthesize Ag-FTO and Ag-NTO, Fe_2TiO_5 and NiTiO_3 powders were initially added together in a determined proportion with 1 mM AgNO_3 precursor. The samples are denoted as $x\text{Ag-FTO}$ and $x\text{Ag-NTO}$, where x represents the silver content added to titanates.

The physicochemical characteristics were studied including X-ray diffraction (XRD), Raman spectroscopy, scanning electron microscopy (SEM), Brunauer–Emmett–Teller adsorption (BET), energy dispersive X-ray spectroscopy (EDS), and UV–Vis absorption spectra techniques. The method of implementation is as detailed in our previous study [19].

The obtained samples have been tested for antibacterial activity against gram-negative *E. coli*, *P. aeruginosa*, and *Salmonella*, and gram-positive *B. cereus* and *S. aureus* by the minimum inhibitory concentration (MIC). These methods have been presented in our previous studies [20].

RESULTS AND DISCUSSION

The XRD pattern (Fig. 1) of the Ag-FTO samples shows mainly diffraction peaks of the pseudobrookite Fe_2TiO_5 at $2\theta = 18.2^\circ$, 25.7° , 27.6° , 32.7° , 37.5° , 40.6° , 46.3° , 49.0° , 52.5° , and 60.1° (JCPDS¹ card No. 41-1432). In addition, a few other characteristic peaks of rutile with low intensity at $2\theta = 27.3^\circ$, 36.1° , and 41.5° (JCPDS card No. 21-1276) were observed. There was practically no appearance of characteristic peaks of anatase (JCPDS card No. 21-1272). Some silver peaks with low intensity were also observed for Ag-FTO samples at $2\theta = 37.4^\circ$, 39.0° , and 41.1° (JCPDS card No. 04-0783). Diffraction peaks of Ag^0 species were observed more clearly in the 1.0Ag-NTO sample, where Ag concentration was loaded up to 1.0 wt %. The phase composition of the Ag-FTO sample completely coincides with that of the pure Fe_2TiO_5 sample [17], indicating that Ag does not change the phase structure of

¹ JCPDS (Joint Committee on Powder Diffraction Standards)—International Center for Diffraction Data.

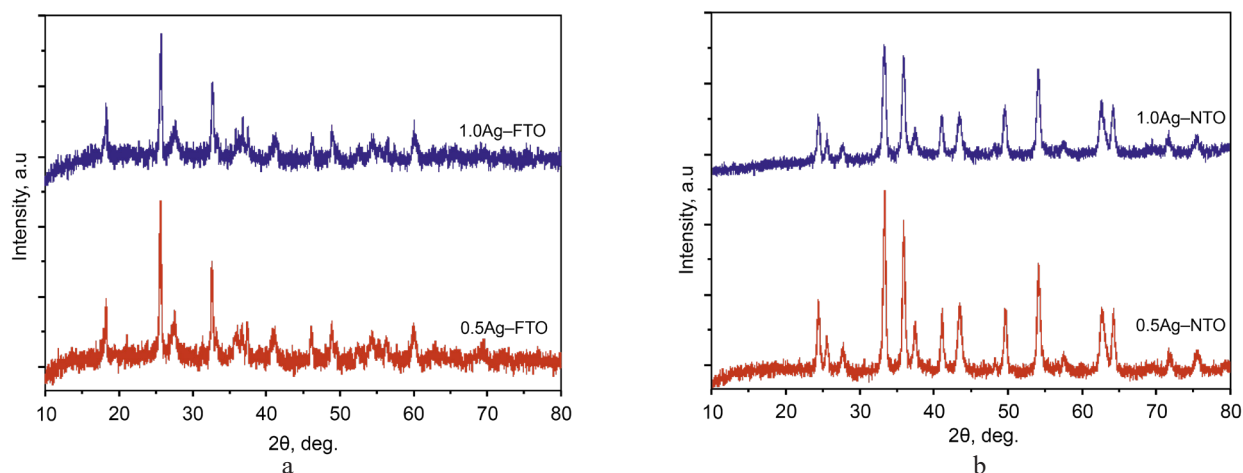


Fig. 1. XRD patterns of Ag-FTO (a) and Ag-NTO (b) catalysts.

pseudobrookite. However, the presence of Ag reduced the crystal size of Fe_2TiO_5 from 31.6 nm to 18.6 nm as calculated based on the Scherrer equation. For the Ag-NTO samples, the peaks of NiTiO_3 were observed at $2\theta = 23.9^\circ$; 32.8° ; 35.4° ; 53.4° ; 61.9° ; and 63.5° (JCPDS 75-3757). The XRD spectra of these samples also demonstrated the presence of anatase crystalline phase at $2\theta = 25.4^\circ$ and rutile crystalline phase at $2\theta = 27.6^\circ$, as well as some characteristic peaks of Ag at $2\theta = 37.4$,

39.0 , and 41.1° . The average crystal size of NiTiO_3 is 17–18 nm, which were approximately the same for the Ag-FTO samples. From the XRD diagram, the crystal size of Ag^0 is estimated to be a few nm.

The elemental compositions of the 0.5Ag-FTO and 0.5Ag-NTO samples were determined by EDS analysis. EDS images show that both silver-modified samples have a uniform distribution of Ag crystals on the Fe_2TiO_5 and NiTiO_3 surfaces (Fig. 2). In which, the Ag distribution is more

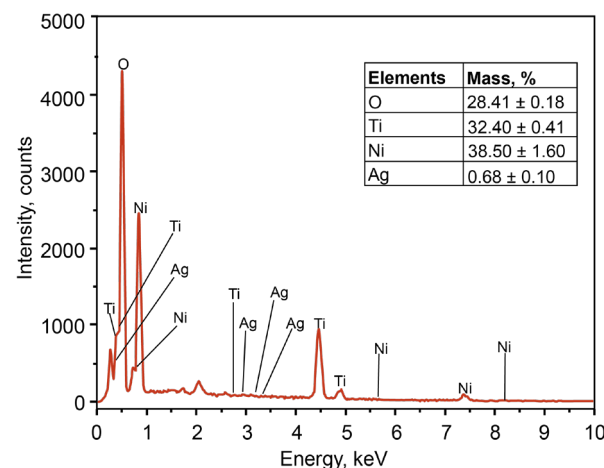
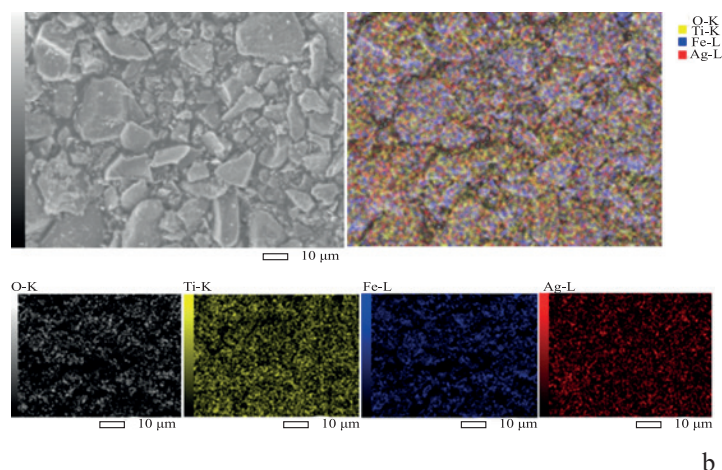
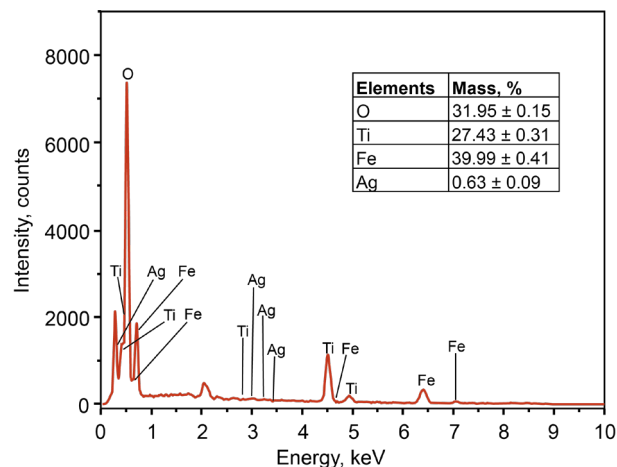
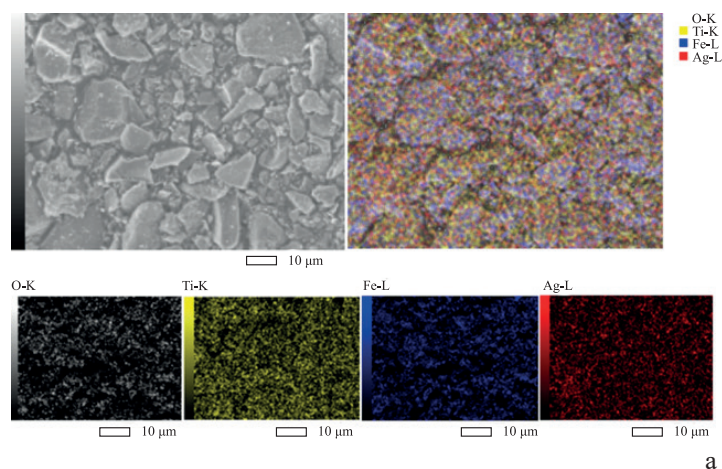


Fig. 2. EDS analysis of 0.5Ag-FTO (a) and 0.5Ag-NTO (b) samples.

dominant for 0.1Ag–FTO sample than that of 0.1Ag–NTO sample. Meanwhile, the EDS spectrum of the 0.1Ag–FTO sample shows the characteristic peaks of Fe, Ti, O, and Ag. The mass ratio of these elements corresponds to 39.99:27.43:31.95:0.63, which is nearly equivalent to the theoretical mass ratio of 0.1Ag–FTO (46.43:19.09:33.17:0.50). The EDS spectrum of sample 0.1Ag–NTO also shows characteristic peaks of Ni, Ti, O, and Ag with mass ratios 38.50:32.40:28.41:0.68, respectively. This ratio is also quite close to the theoretical mass ratio of 0.1Ag–NTO (37.78:30.82:30.90:0.50). Comparing 0.1Ag–FTO and 0.1Ag–NTO samples, the 0.1Ag–FTO sample seems to have a more similar experimental mass ratio of elements and theoretical mass ratio than that of 0.1Ag–NTO, demonstrating the higher purity of this sample. In addition, some unassigned peaks on the EDS spectra of both samples were characteristic peaks of the carbon tape material covering the samples. From the EDS and XRD results, it can be concluded that the silver was formed and uniformly dispersed on the surface as well as inside the structure of Fe_2TiO_5 and NiTiO_3 .

The Raman spectrum of Ag–FTO samples (Fig. 3) shows the appearance of absorption peaks characteristic for Fe_2TiO_5 structure at 144 cm^{-1} , 199 cm^{-1} , 222 cm^{-1} , 292 cm^{-1} , 327 cm^{-1} , 394 cm^{-1} , 661 cm^{-1} , 787 cm^{-1} , and 1294 cm^{-1} [21]. Here, the characteristic Ag oscillations at 199 , 327 , and 787 cm^{-1} correspond to the strain vibration in the inner plane of the O–Ti bond, the symmetric stretching vibration of the O–Fe bond, and the symmetrical bending vibrations of the O–Ti bond. Meanwhile, the B_{1g} oscillations at 144 cm^{-1} , 222 cm^{-1} , and 661 cm^{-1} are formed by the out-of-plane rotation of the O–Ti bond, bending vibrations in the plane of the O–Fe bond, and external

bending vibrations of the Ti–O bond, respectively. Moreover, the characteristic peaks of Fe_2O_3 are not significantly present in the Raman spectrum. Therefore, this result proves that the obtained Fe_2TiO_5 has high crystallinity with a stable phase structure. Meanwhile, for Ag–NTO samples, the Raman vibrational modes for NiTiO_3 are located at 192 cm^{-1} (A_g), 229 cm^{-1} (B_g), 246 cm^{-1} (A_g), 291 cm^{-1} (B_g), 345 cm^{-1} (B_g), 394 cm^{-1} (A_g), 465 cm^{-1} (B_g), 484 cm^{-1} (A_g), 613 cm^{-1} (B_g), and 709 cm^{-1} (B_g). The characteristic A_g and B_g oscillations correspond to the strain vibration in the inner plane of the O–Ti bond, symmetrical bending vibrations of the O–Ti bond, and the symmetric stretching vibration of the O–Ni bond. Since the Raman spectrum shows almost no characteristic oscillations of Ag for both Ag–FTO and Ag–NTO samples, it can be concluded that silver is present in low concentrations and well dispersed on the surface of Fe_2TiO_5 and NiTiO_3 .

SEM images (Fig. 4) show that the Ag–FTO and Ag–NTO materials exist in the form of small quasi-spherical particles and large bulk. For both Ag–FTO and Ag–NTO samples, samples containing 0.5% Ag exhibited less agglomeration, smaller clumps, and better dispersion of brightly colored spherical Ag particles. This means that there will be better porosity for bacteria location and conversion.

Figure 5a shows the N_2 adsorption-desorption isotherms of 0.5Ag–FTO and 0.5Ag–NTO samples. According to the IUPAC nomenclature [22], the shape of the nitrogen isotherm of two samples could be considered to be a type IV isotherm, which is typical for mesoporous materials. Here, the width of the hysteresis loop of the Ag–FTO sample is much higher than that of the Ag–NTO sample, demonstrating the better adsorption capacity of this material for bacteria. The curve of

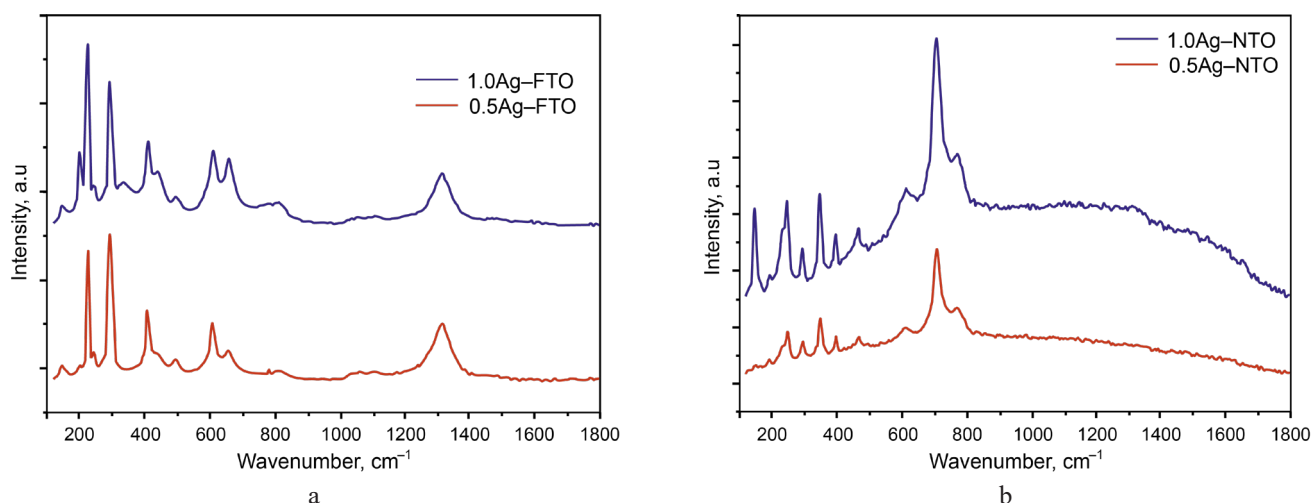


Fig. 3. Raman spectra of Ag–FTO (a) and Ag–NTO (b) catalysts.

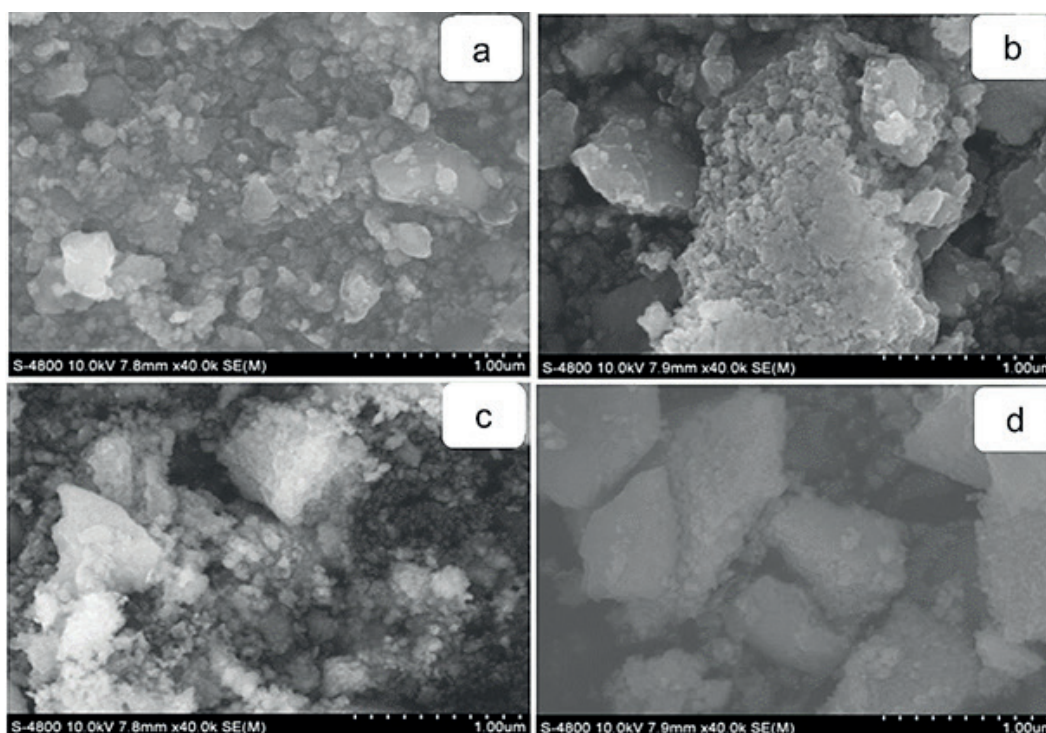


Fig. 4. SEM images of samples: 0.5Ag-FTO (a), 1.0Ag-FTO (b), 0.5Ag-NTO (c), 1.0Ag-NTO (d).

the pore size distribution of the 0.5Ag-FTO and 0.5Ag-NTO samples according to their diameters additionally allowed the maximum diameter densities of 24.0 Å and 23.4 Å, respectively, to be determined (Fig. 5b). These were used to calculate the BET data for 0.5Ag-FTO and 0.5Ag-NTO samples. For the 0.5Ag-FTO sample, the specific surface area of the examined sample was 20.2 m²/g, while the total pore volume was found to be 0.025 cm³/g. Meanwhile, these values reach 13.8 m²/g and 0.017 cm³/g for the 0.1Ag-NTO sample, respectively. These results demonstrate that Ag-FTO has better adsorption capacity than the Ag-NTO.

The absorbed wavelength and the band gap energy of the catalysts were determined by UV-Vis spectroscopy and the Tauc plot. The obtained results show that there is almost no difference in absorption wavelength and band gap between Ag-added samples. Specifically, for the Ag-FTO samples (Fig. 6a), it can be seen that the absorbed light band and band gap energy form two different regions: the first region has an absorption wavelength range in the range of 630–633 nm corresponding to a band gap energy of 1.96–1.97 eV. The second region has an absorption wavelength range of 493–496 nm corresponding to a band gap energy of 2.50–2.52 eV.

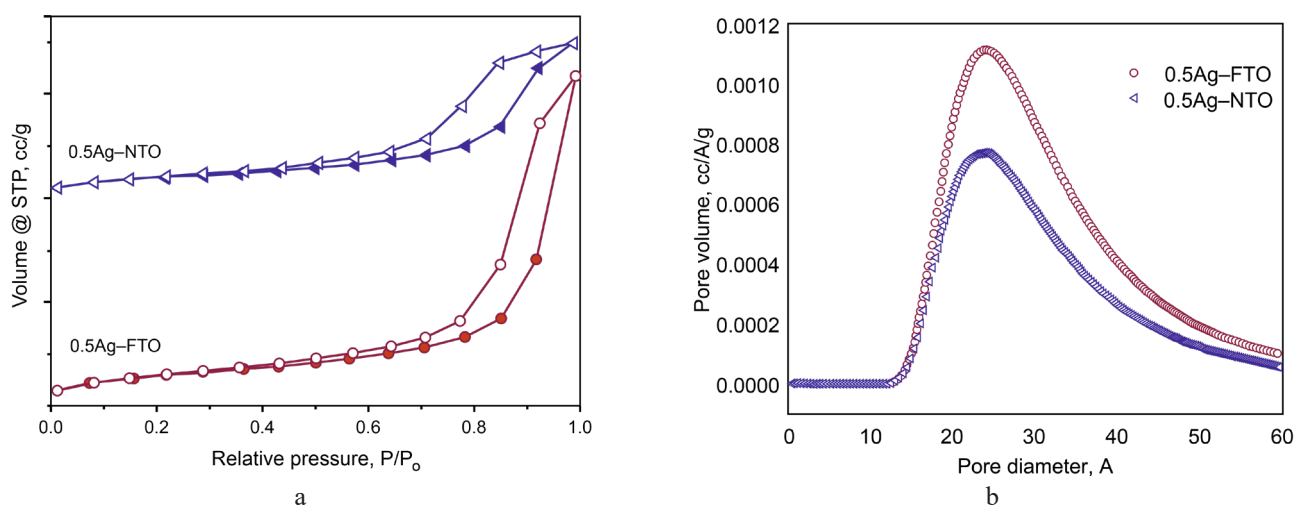


Fig. 5. N₂ adsorption-desorption isotherms (a) and pore size distribution (b) of 0.5Ag-FTO and 0.5Ag-NTO samples.

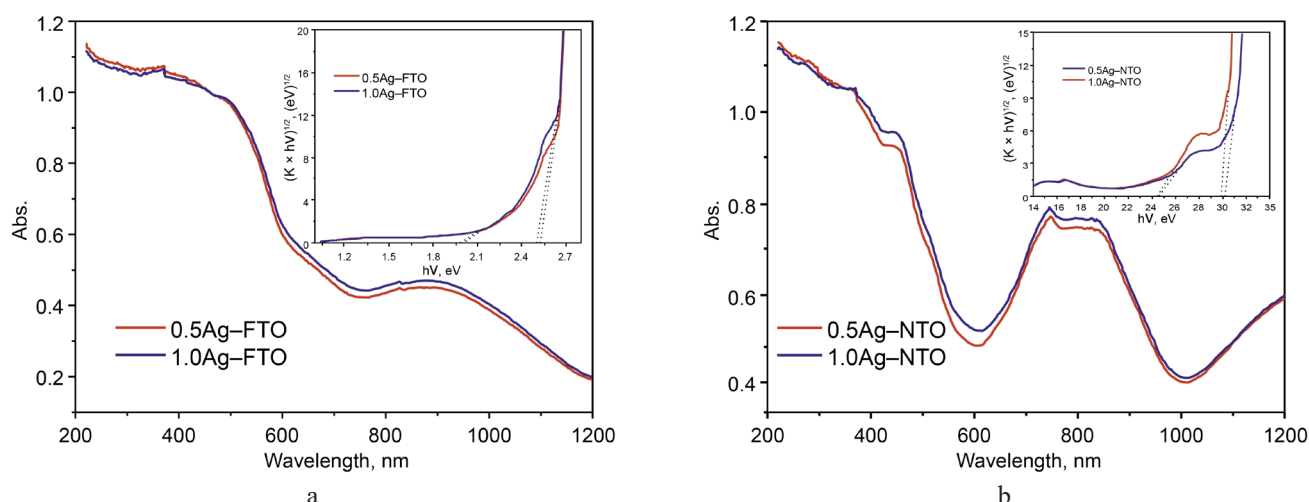


Fig. 6. UV-Vis diffuse reflectance spectra and Tauc plot of the Ag-FTO (a) and Ag-NTO (b) samples.

According to previous studies [8–10], Fe_2TiO_5 has a band gap energy of 1.9–2.1 eV (corresponding to an absorption wavelength of about 590–650 nm), which is consistent with the first band data; meanwhile, silver has an absorption wavelength in the range of 400–500 nm (band gap energy in the range of 2.4–3.1 eV) [23], which is consistent with the second band parameters. The appearance of two absorption wavelength regions and band gap energies is similar for Ag-NTO samples (Fig. 6b). In which, the first region corresponds to 411–414 nm and 3.0–3.02 eV; and the second region is 504–406 nm and 2.45–2.46 eV, respectively. According to author [13], NiTiO_3 has a band gap energy of about 3.0 eV, which is consistent with the first band results of the catalysts, while the second is also compatible with the absorption region of silver. It can be concluded that the combination of silver with Fe_2TiO_5 and NiTiO_3 leads to the appearance of a smaller frequency band, which increases flexibility in the light absorption of the material. It can be found that the Ag-FTO materials with bandgap absorb light and bandgap better than the Ag-NTO samples. This is an essential property of photocatalyst materials, which can lead to their improved activity.

The antibacterial properties of the samples were determined by their minimum inhibitory concentration (MIC). Five types of bacterial including *E. coli*, *P. aeruginosa*, *Salmonella*, and *S. aureus* were used in this study. The exponential phase of bacteria was observed to be delayed in the presence of samples; this phenomenon was more obvious with the rise of Ag-FTO and Ag-NTO concentrations (Fig. 7). The samples were able to inhibit the exponential stage of both gram-negative and gram-positive bacteria. The MIC against *B. cereus*, *E. coli*, *P. aeruginosa*, *Salmonella*, and *S. aureus* of Ag-FTO and Ag-NTO samples are described

in Table. Here it can be seen that the 0.5Ag-FTO were able to completely inhibit the growth of *B. cereus*, *E. coli*, *P. aeruginosa*, *Salmonella*, and *S. aureus* at a similar MIC of 1.25, 0.31, 1.25, 1.25, and 2.50 $\mu\text{g/mL}$, respectively. The almost doubled MIC value when increasing the silver content up to 1.0% for the Fe_2TiO_5 samples (1.0Ag-FTO) demonstrates their enhanced antimicrobial activity with the addition of silver. Meanwhile, the antibacterial ability of 0.5Ag-NTO proved to be lower than that of 0.5Ag-FTO with MIC values of 5.00, 2.50, 2.50, 2.50, and 5.00 $\mu\text{g/mL}$ respectively. A similar phenomenon was observed for the 1.0Ag-FTO sample with an improvement in antibacterial activity with increasing Ag concentration. It is clear that the Ag-FTO samples exhibit much higher antibacterial activity than Ag-NTO due to the better dispersion of silver nanoparticles on the Fe_2TiO_5 surface (shown by their physicochemical properties). The synthesized samples in this study were shown to be more effective against the negative bacterial (*E. coli*, *Salmonella*, and *P. aeruginosa*) as compared to the positive bacterial (*B. cereus* and *S. aureus*). These results were the agreement with previous reports [24, 25] when assuming that the gram-negative bacteria had thinner cell walls than the gram-positive bacteria; thus, the antibacterial materials can more easily penetrate and inhibit gram-negative bacteria.

As compared to some similar earlier reported materials, the obtained materials exhibit superior antibacterial ability. Specifically, silver nanoparticles (AgNPs) synthesized using *Acalypha indica* leaf extract had an MIC of 10 $\mu\text{g/mL}$ against *E. coli* and *Vibrio cholera* (*V. cholera*) [26], while LaAlO_3 perovskite nanoparticles had an MIC of 63 $\mu\text{g/mL}$ against gram-negative bacteria *P. aeruginosa* [27] and

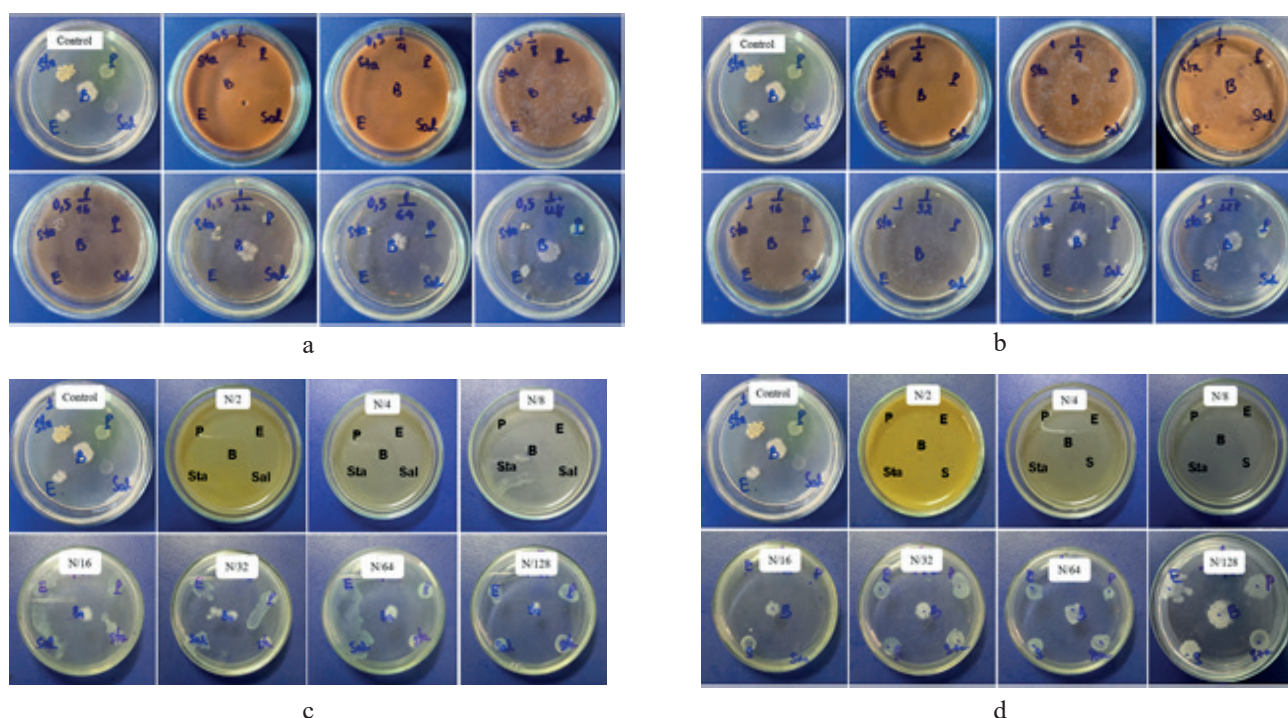


Fig. 7. Minimum inhibitory concentrations of 0.5Ag-FTO (a), 1.0Ag-FTO (b), 0.5Ag-NTO (c), 1.0Ag-NTO (d) samples against five bacteria.

Table. Minimum inhibitory concentrations (MIC) on samples against five bacteria

Bacteria	MIC ($\mu\text{g/mL}$)			
	0.5Ag-FTO	1.0Ag-FTO	0.5Ag-NTO	1.0Ag-NTO
<i>Bacillus cereus</i>	1.25	0.63	5.00	2.50
<i>Escherichia coli</i>	0.31	0.31	2.50	1.25
<i>Pseudomonas aeruginosa</i>	1.25	0.63	2.50	1.25
<i>Salmonella topi</i>	1.25	0.63	2.50	1.25
<i>Staphylococcus aureus</i>	2.50	1.25	5.00	2.50

the modified perovskite material $\text{LaCo}_{0.4}\text{Fe}_{0.6}\text{O}_3$ showed an MIC of 63 $\mu\text{g/mL}$ against two bacteria *S. aureus* and *P. aeruginosa* [28]. Studies on perovskite materials and silver nanoparticles have shown effective bactericidal ability against both gram-negative and gram-positive bacteria. Perovskite-like materials combined with silver not only release metal ions Fe^{3+} , Ni^{2+} , Ti^{+4} but also Ag^+ ions having a positive charge, causing electrostatic attraction with negative charge of bacterial cell membrane. As a consequence, ionic particles easily adhere to cell walls and membranes, changing the membrane structure to destroy the bacterial cell [29, 30].

CONCLUSIONS

In summary, Ag-added Fe_2TiO_5 and NiTiO_3 nanomaterials were successfully synthesized by

biosynthesis combined with the sol-gel method. Well-distributed silver nanoparticles on Fe_2TiO_5 and NiTiO_3 surfaces on a nanoscale and with a low band gap were observed for the samples. The antibacterial efficacy of Ag-FTO and Ag-NTO samples has been demonstrated through excellent inhibition against *B. cereus*, *E. coli*, *P. aeruginosa*, *Salmonella*, and *S. aureus* with the low MIC minimum inhibitory concentration due to the excellent dispersion of Ag on the surface of the perovskite. At the same time, the Ag-FTO samples also showed much better antibacterial activity than the Ag-NTO samples as a result of the excellent dispersion of Ag on the Fe_2TiO_5 surface. Hence, according to the findings of this research, the use of Ag-FTO nanomaterials may suggest potential applications in disinfection and sterilization applications in future wastewater treatment approaches.

Acknowledgments

We acknowledge the support of time and facilities from Ho Chi Minh University of Technology (HCMUT), VNU-HCM for this study.

Благодарности

Авторы благодарят Технологический университет Хо Ши Мина за поддержку в этом исследовании.

Authors' contribution

All authors equally contributed to the research work.

Вклад авторов

Все авторы в равной степени внесли свой вклад в исследование.

The authors declare no conflicts of interest.

Авторы заявляют об отсутствии конфликта интересов.

REFERENCES

1. Xiang W., *et al.* Biochar technology in wastewater treatment: A critical review. *Chemosphere*. 2020;252:126539. <https://doi.org/10.1016/j.chemosphere.2020.126539>
2. Yaqoob A.A., Parveen T., Umar K., Mohamad Ibrahim M.N. Role of nanomaterials in the treatment of wastewater: A review. *Water*. 2020;12(2):495. <https://doi.org/10.3390/w12020495>
3. Crini G., Lichtfouse E. Advantages and disadvantages of techniques used for wastewater treatment. *Environ. Chem. Lett.* 2019;17(1):145–155. <https://doi.org/10.1007/s10311-018-0785-9>
4. Salgot M., Folch M. Wastewater treatment and water reuse. *Curr. Opin. Environ. Sci. Health*. 2018;2:64–74. <https://doi.org/10.1016/j.coesh.2018.03.005>
5. Rizzo L., *et al.* Best available technologies and treatment trains to address current challenges in urban wastewater reuse for irrigation of crops in EU countries. *Sci. Total Environ.* 2020;710:36312. <https://doi.org/10.1016/j.scitotenv.2019.136312>
6. Dai Y., Poidevin C., Ochoa-Hernández C., Auer A.A., Tüysüz H. A supported bismuth halide perovskite photocatalyst for selective aliphatic and aromatic C–H bond activation. *Angew. Chemie Int. Ed.* 2020;59(14):5788–5796. <https://doi.org/10.1002/anie.201915034>
7. Kanhere P., Chen Z. A review on visible light active perovskite-based photocatalysts. *Molecules*. 2014;19(12):19995–20022. <https://doi.org/10.3390/molecules191219995>
8. Nikolic M., Lukovic M., Vasiljevic Z., Labus N., Aleksic O. Humidity sensing potential of Fe₂TiO₅-pseudobrookite. *J. Mater. Sci.: Mater. Electron.* 2018;29(11):9227–9238. <https://doi.org/10.1007/s10854-018-8951-1>
9. Thambiliyagodage C., Mirihana S., Wijesekera R., Dinu S.M., Kandanapitiye M., Bakker M. Fabrication of Fe₂TiO₅/TiO₂ binary nanocomposite from natural ilmenite and their photocatalytic activity under solar energy. *Curr. Res. Green Sustain. Chem.* 2021;4:100156. <https://doi.org/10.1016/j.crgsc.2021.100156>
10. Lou Z., Li Y., Song H., Ye Z., Zhu L. Fabrication of Fe₂TiO₅/TiO₂ nanoheterostructures with enhanced visible-light photocatalytic activity. *RSC Advances*. 2016;6(51):45343–45348. <https://doi.org/10.1039/C6RA06763H>
11. Lakhera S.K., *et al.* Enhanced photocatalytic degradation and hydrogen production activity of *in situ* grown TiO₂ coupled NiTiO₃ nanocomposites. *Appl. Surf. Sci.* 2018;449:790–798. <https://doi.org/10.1016/j.apsusc.2018.02.136>
12. Li H., Huang W., Wang G.-L., Wang W.-L., Cui X., Zhuang J. Transcriptomic analysis of the biosynthesis, recycling, and distribution of ascorbic acid during leaf development in tea plant (*Camellia sinensis* (L.) O. Kuntze). *Sci. Rep.* 2017;7(1):46212. <https://doi.org/10.1038/srep46212>
13. Xing C., *et al.* Porous NiTiO₃/TiO₂ nanostructures for photocatalytic hydrogen evolution. *J. Mater. Chem. A*. 2019;7(28):17053–17059. <https://doi.org/10.1039/C9TA04763H>
14. Ngan D.H., Hoai H.T.C., Huong L.M., Hansen P.E., Vang O. Bioactivities and chemical constituents of a Vietnamese medicinal plant Che Vang, *Jasminum subtriplinerne Blume* (Oleaceae). *Nat. Prod. Res.* 2008;22(11):942–949. <https://doi.org/10.1080/14786410701647119>
15. Nguyen T.M.-T., *et al.* Novel biogenic silver nanoparticles used for antibacterial effect and catalytic degradation of contaminants. *Res. Chem. Intermed.* 2020;46(3):1975–1990. <https://doi.org/10.1007/s11164-019-04075-w>
16. Nguyen P.A., *et al.* Sunlight irradiation-assisted green synthesis, characteristics and antibacterial activity of silver nanoparticles using the leaf extract of *Jasminum subtriplinerne Blume*. *J. Plant Biochem. Biotechnol.* 2022;31:202–205. <https://doi.org/10.1007/s13562-021-00667-z>
17. Nguyen P.A., *et al.* Environmentally friendly fabrication of Fe₂TiO₅-TiO₂ nanocomposite for enhanced photodegradation of cinnamic acid solution. *Adv. Natural Sci.: Nanosci. Nanotechnol.* 2022;12(4):045015. <https://doi.org/10.1088/2043-6262/ac498d>
18. Nguyen P.A., *et al.* Exceptional photodecomposition activity of heterostructure NiTiO₃-TiO₂ catalyst. *J. Sci.: Adv. Mater. Dev.* 2022;7(1):100407. <https://doi.org/10.1016/j.jsamd.2021.100407>
19. Nguyen D.T., Ha C.A., Nguyen T., Phuong P.H., Hoang T.C. A low temperature fabrication and photoactivity of Al₂TiO₅ in cinnamic acid degradation. *Mater. Trans.* 2019;60(9):2022–2027. <https://doi.org/10.2320/matertrans.M2019076>

20. Nguyen P.A., Duong N.L., Nguyen V.M., Nguyen T. Positive effects of the ultrasound on biosynthesis, characteristics and antibacterial activity of silver nanoparticles using *Fortunella Japonica*. *Mater. Trans.* 2019;60(9):2053–2058. <https://doi.org/10.2320/matertrans.M2019065>
21. Rodrigues J.E., *et al.* Spin-phonon coupling in uniaxial anisotropic spin-glass based on Fe_2TiO_5 pseudobrookite. *J. Alloys Comp.* 2019;799:563–572. <https://doi.org/10.1016/j.jallcom.2019.05.343>
22. Burhan M., Shahzad M.W., Ng K.C. Energy distribution function based universal adsorption isotherm model for all types of isotherm. *Int. J. Low-Carbon Technol.* 2018;13(3):292–297. <https://doi.org/10.1093/ijlct/cty031>
23. Barone P., Stranges F., Barberio M., Renzelli D., Bonanno A., Xu F. Study of Band Gap of Silver Nanoparticles–Titanium Dioxide Nanocomposites. *J. Chem.* 2014;2014:589707. <http://dx.doi.org/10.1155/2014/589707>
24. Ankanna S., Prasad T.N.V.K.V., Elumalai E., Savithamma N. Production of biogenic silver nanoparticles using *Boswellia ovalifoliolata* stem bark. *Dig. J. Nanomater. Biostruct.* 2010;5(2):369–372.
25. Morones J.R., *et al.* The bactericidal effect of silver nanoparticles. *Nanotechnology.* 2005;16(10):2346–2353. <https://doi.org/10.1088/0957-4484/16/10/059>
26. Krishnaraj C., *et al.* Synthesis of silver nanoparticles using *Acalypha indica* leaf extracts and its antibacterial activity against water borne pathogens. *Colloids Surf. B: Biointerfaces.* 2010;76(1):50–56. <https://doi.org/10.1016/j.colsurfb.2009.10.008>
27. Manjunatha C. *et al.* Perovskite lanthanum aluminate nanoparticles applications in antimicrobial activity, adsorptive removal of Direct Blue 53 dye and fluoride. *Mater. Sci. Eng.: C Mater. Biol. Appl.* 2019;101:674–685. <https://doi.org/10.1016/j.msec.2019.04.013>
28. Singh C., Wagle A., Rakesh J.V. Doped LaCoO_3 perovskite with Fe: A catalyst with potential antibacterial activity. *Vacuum.* 2017;146:468–473. <https://doi.org/10.1016/j.vacuum.2017.06.039>
29. Dakal T.C., Kumar A., Majumdar R.S., Yadav V. Mechanistic basis of antimicrobial actions of silver nanoparticles. *Front. Microbiol.* 2016;7:1831. <https://doi.org/10.3389/fmicb.2016.01831>
30. Yin I.X., Zhang J., Zhao I.S., Mei M.L., Li Q., Chu C.H. The antibacterial mechanism of silver nanoparticles and its application in dentistry. *Int. J. Nanomedicine.* 2020;15:2555–2562. <https://doi.org/10.2147/IJN.S246764>

About the Authors:

Anh C. Ha, PhD, Doctor of Medicinal Chemistry, Faculty of Chemical Engineering, Ho Chi Minh City University of Technology (268 Ly Thuong Kiet Street, District 10, Ho Chi Minh City, Vietnam); Vietnam National University Ho Chi Minh City (Linh Trung Ward, Thu Duc District, Ho Chi Minh City, Vietnam). E-mail: hcanh@hcmut.edu.vn. <https://orcid.org/0000-0001-7919-4028>

Tri Nguyen, PhD, Doctor of Chemical Engineering, Institute of Chemical Technology, Vietnam Academy of Science and Technology (01A TL29 Street, Thanh Loc Ward, District 12, Ho Chi Minh City, Vietnam); Ho Chi Minh City Open University (97 Vo Van Tan Street, District 3, Ho Chi Minh City, Vietnam). E-mail: ntri@ict.vast.vn. <https://orcid.org/0000-0001-9486-5096>

Anh Ph. Nguyen, Master of Chemical Engineering, Institute of Chemical Technology, Vietnam Academy of Science and Technology (01A TL29 Street, Thanh Loc Ward, District 12, Ho Chi Minh City, Vietnam). Email: npanh@ict.vast.vn. <https://orcid.org/0000-0002-5816-9832>

Minh V. Nguyen, Master of Biotechnology, Ho Chi Minh City Open University (97 Vo Van Tan Street, District 3, Ho Chi Minh City, Vietnam). E-mail: minh.nv@ou.edu.vn. <https://orcid.org/0000-0002-1615-4966>

Об авторах:

Ань К. Ха, PhD, к.фарм.н., Химико-технологический факультет, Технологический университет Хошимина (268 Ли Тхыонг Кьет ул., Район 10, г. Хошимин, Вьетнам); Вьетнамский национальный университет Хошимина (Линь Чунг Уорд, Район Тхёк, г. Хошимин, Вьетнам). E-mail: hcanh@hcmut.edu.vn. <https://orcid.org/0000-0001-7919-4028>

Три Нгуен, PhD, к.т.н., Химико-технологический институт, Академия наук Вьетнама, (01A TL29 ул., Тха Лог Вард, Район 12, г. Хошимин, Вьетнам); Открытый Университет Хошимина (97, Во Ван Тан ул., Район 3, г. Хошимин, Вьетнам). E-mail: ntri@ict.vast.vn. <https://orcid.org/0000-0001-9486-5096>

Ань Ф. Нгуен, магистр химической технологии, Химико-технологический институт, Академия наук Вьетнама, (01A TL29 ул., Тха Лог Вард, Район 12, г. Хошимин, Вьетнам). E-mail: npanh@ict.vast.vn. <https://orcid.org/0000-0002-5816-9832>

Минх В. Нгуен, магистр биотехнологии, Открытый Университет Хошимина (97, Во Ван Тан ул., Район 3, г. Хошимин, Вьетнам). E-mail: minh.nv@ou.edu.vn. <https://orcid.org/0000-0002-1615-4966>

The article was submitted: April 18, 2022; approved after reviewing: May 31, 2022; accepted for publication: August 03, 2022.

The text was submitted by the authors in English

Edited for English language and spelling by Thomas Beavitt

**SYNTHESIS AND PROCESSING OF POLYMERS
AND POLYMERIC COMPOSITES**

**СИНТЕЗ И ПЕРЕРАБОТКА ПОЛИМЕРОВ
И КОМПОЗИТОВ НА ИХ ОСНОВЕ**

ISSN 2686-7575 (Online)

<https://doi.org/10.32362/2410-6593-2022-17-4-346-356>



UDC 655.028

RESEARCH ARTICLE

Method for hidden marking of transparent polypropylene film

Alexander A. Nikolaev[✉], Alexander P. Kondratov

Moscow Polytechnic University, Moscow, 127008 Russia

[✉]Corresponding author, e-mail: nikolaevaleksandr1992@gmail.com

Abstract

Objectives. To quantitatively describe the thermochromic properties of films of isotactic polypropylene, a large-tonnage polymer widely used in the production of flexible packaging for goods and foodstuffs, as well as substantiate the possibility of covert labeling of transparent packaging.

Methods. Differential scanning calorimetry, polarization photometry, infrared Fourier spectrometry, gravimetry, temperature control, physical and mechanical strength testing.

Results. The identified thermochromic effect of dichroism in polarized light on industrial samples of transparent biaxially oriented film of isotactic polypropylene was studied. A change in the phase composition of the film-forming composition during short-term heating during marking was established. The absence of heat shrinkage and change in transparency in non-polarized light was shown, which provides the possibility of hidden recording of information and its contrast manifestation in a passing light stream at a certain arrangement of light filters.

Conclusions. The causes and optimal conditions of the thermochromic effect are established. It is proposed to use local contact heat treatment of a polypropylene film for covert recording of information and marking of product packaging in order to protect against counterfeiting.

Keywords: oriented film, polarized light, heat treatment, isotactic polypropylene, differential calorimetry, dichroism, color difference, hidden marking

For citation: Nikolaev A.A., Kondratov A.P. Method for hidden marking of transparent polypropylene film. *Tonk. Khim. Tekhnol. = Fine Chem. Technol.* 2022;17(4):346–356 (Russ., Eng.). <https://doi.org/10.32362/2410-6593-2022-17-4-346-356>

НАУЧНАЯ СТАТЬЯ

Скрытая маркировка прозрачной пленки полипропилена

А.А. Николаев✉, А.П. Кондратов

Московский политехнический университет, Москва, 107023 Россия

✉ Автор для переписки, e-mail: nikolaevaleksandr1992@gmail.com

Аннотация

Цели. Количественно описать термохромные свойства пленок изотактического полипропилена – крупнотоннажного полимера, широко используемого в производстве гибкой упаковки товаров и продуктов питания, и обосновать возможности скрытой маркировки прозрачной упаковки.

Методы. Дифференциальная сканирующая калориметрия, поляризационная фотометрия, ИК Фурье-спектрометрия, гравиметрия, термостатирование, физико-механические испытания, в том числе прочности.

Результаты. Обнаружен и исследован термохромный эффект дихроизма в поляризованном свете на промышленных образцах прозрачной двуслоноориентированной пленки изотактического полипропилена. Установлено изменение фазового состава пленкообразующей композиции в процессе кратковременного нагревания при маркировке. Показано отсутствие термоусадки и изменения прозрачности в неполяризованном свете, обеспечивающее возможность скрытой записи информации и ее контрастного проявления в проходящем потоке света при определенном расположении светофильтров.

Выводы. Установлены причины и оптимальные условия термохромного эффекта. Предложено использовать локальную контактную термообработку пленки полипропилена для скрытой записи информации и маркировки упаковки товаров и продуктов с целью защиты от подделок.

Ключевые слова: ориентированная пленка, поляризованный свет, термообработка, изотактический полипропилен, дифференциальная калориметрия, дихроизм, цветовое различие, скрытая маркировка

Для цитирования: Николаев А.А., Кондратов А.П. Скрытая маркировка прозрачной пленки полипропилена. *Тонкие химические технологии*. 2022;17(4):346–356. <https://doi.org/10.32362/2410-6593-2022-17-4-346-356>

INTRODUCTION

The central problem of innovative materials science for mass-demand products is the optimization of the ratio of the price of the material and the product result of its use in industrial production. The pleochroism effect in anisotropic polymer films can become the basis of new technologically sophisticated methods of protecting marketable products and packaging of

unique products from counterfeiting that do not require the use of expensive materials [1]. The pleochroism effect of polyolefins has previously been studied in multilayer polyethylene films used for food packaging, as well as in direct contact with rapidly perishable products. Several layers of a film of the same polymer, layered and glued together, and the resulting color effects in polarized light make it possible to apply such a technology to create coding according to the Microsoft Tag system [2–4].

In the works presented earlier, it was proposed to use multilayer polymer films to obtain identification and protective elements on goods of value. These elements are used both in the visible light range of 400–700 nm, but at different viewing angles, and in the infrared and ultraviolet ranges using special devices and auxiliary elements (polarizers, light sources in the wavelength range of 360–400 nm, etc.) [5–8]. Patent sources describe high-cost and material-intensive, but similar in technology, methods for marking multilayer birefringent films [9].

In this paper, an experimental substantiation of the possibility of labeling polypropylene film packaging by short-term local heat treatment under pressure using industrial equipment for thermal welding of thermoplastic polymers and thermogravimetry is proposed [10]. With a local thermal effect on the film with a certain periodicity and frequency of repetition of heat treatment along the length or width, its properties change, and the homogeneous film material becomes interval. To clarify and further use the term “interval material,” it should be indicated that this term refers to a special case or one of the variants of the implementation of the so-called “gradient” polymers. This term was first introduced by A.A. Askadsky in reports at conferences on the results of theoretical and experimental work on the technology of inhomogeneously crosslinked elastomers, after which he received international recognition [11]. Periodicity or frequency, size and amplitude, differences in the properties of intervals can act as a key in recording and reading information and be used in labeling packaging. If the difference in the properties of the intervals is not visually determined, but requires a special light source, a method of illumination, or the use of polarizers [12], then such interval

materials are promising in lighting engineering [8], technology of hidden optical and relief marking [13], and the fight against counterfeiting of packaged products or goods [9].

MATERIALS AND METHODS

The objects of research were commercial samples of a biaxially oriented “sleeve” film of isotactic polypropylene (*Bureaucrat*, Russia and *Business Center*, Russia) with a thickness of $22 \pm 1.5 \mu\text{m}$ (hereinafter BOPP-22) and a thickness of $105 \pm 2 \mu\text{m}$ (hereinafter BOPP-105), respectively.

To assess the mechanical properties and calculate the possible anisotropy of the films, the tensile strength was measured at a constant speed of 50 mm/min in accordance with GOST 11262-2017 (ISO 527-2:2012¹).

In order to assess the internal stresses and control the shrinkage of films at a temperature corresponding to the temperature of thermomechanical processing, in the process of marking and obtaining samples of interval materials, a laboratory technique and specialized equipment have been developed to prevent warping and sticking of the film when heated to the melting point of polypropylene. The technique involves the production of an envelope with an anti-adhesive Teflon coating, inside which film samples of $50 \times 50 \text{ mm}$ are placed. An envelope with a sample of polypropylene film is heated on the surface of the molten Wood alloy to a temperature of 150°C for 5–50 s.

To evaluate the optical properties of the film in transmitted polarized light, a viewing table [14] modified to produce polarized light was used (Fig. 1). The light source was a light-emitting diode strip with a luminous intensity of 300 lm and a color temperature of 6500 K. In order to

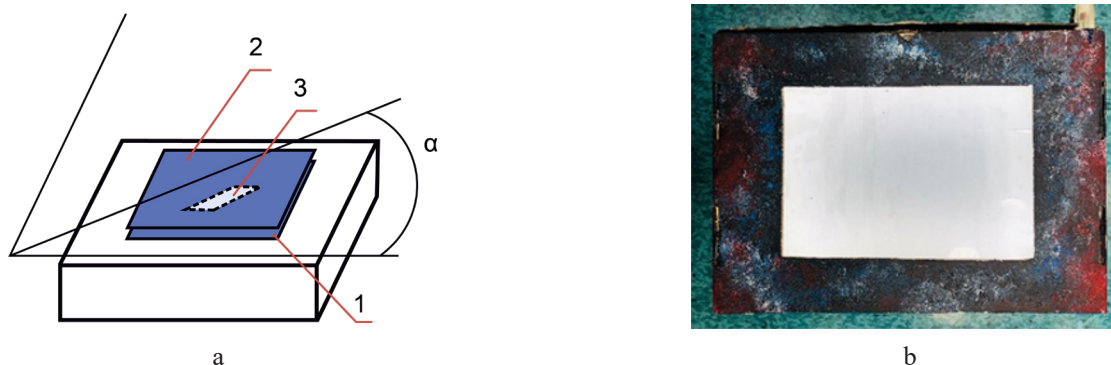


Fig. 1. Viewing table: (a) schematic representation; (b) top view (photo).

1 – polarizer; 2 – analyzer; 3 – polypropylene film; α is the angel of rotation of the polypropylene film.

¹ ISO 527-2:2012. Plastics – Determination of tensile properties. Part 2: Test conditions for mouldings and extrusions plastics. Publication date: 2012.02.

polarize the light, a general-purpose polarizer with a single permeability of 44.5%, a polarization effect of 95.8% (Nitto, Japan) was used. Shade *a* is *N*-bromosuccinimide (NBS) 25 – (–1.6), shade *b* is NBS 25 – (–0.9).

The description of optical effects following heat treatment and measurement of film color parameters in transmitted light were carried out from photographs obtained in room (laboratory) conditions under different lighting conditions using a 12 MP camera and a Display P3 color profile.

The color effect was evaluated by the color coordinates of the equal-contrast color evaluation system $L^*a^*b^*$, as well as by the magnitude of the color difference ΔE_{ab}^* :

$$\Delta E_{ab}^* = \sqrt{(L_2^* - L_1^*)^2 + (a_2^* - a_1^*)^2 + (b_2^* - b_1^*)^2},$$

where L^* is lightness, a^* are coordinates of the red-green shade, b^* are the coordinates of the yellow-blue hue, according to the CIELab color space (more precisely, CIE 1976 $L^*a^*b^*$ or CIE-76).

The color coordinates L , a , b were measured from photographs in Adobe Photoshop software (Adobe Systems, USA) at 10 points of the field with the calculation of the average value. The photo was opened in the program using the built-in DisplayP3 color profile. Without changing the color profile in the photo, the Eyedropper tool selected 10 arbitrary points, which correspond to the color coordinates of the $L^*a^*b^*$ system.

To measure thermochromic effects, several series of 5 samples of two types were prepared. Rectangular samples of 30×50 mm in size were cut from polypropylene films with a thickness of 22 ± 1.5 μm and 105 ± 2 μm in mutually perpendicular directions both along the direction of the predominant orientation of macromolecules (maximum strength) (Arrow 1) and perpendicular to the direction of the predominant orientation of macromolecules (Arrow 2) (Fig. 2).

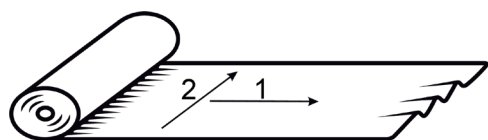


Fig. 2. Preparation of a biaxially oriented polypropylene film (=),

Arrow 1 is the direction of preferential orientation macromolecules, Arrow 2 is the perpendicular direction (\perp).

To determine the optimal mode of observation and optical measurements, the dependence of the color difference of adjacent film intervals on the location of the sample between the polarizers in a crossed (closed) position with a step of 15° was investigated (Fig. 1a). The condition for photofixation of the maximum thermochromic effect was established based on the results of optical measurements and calculation of the color difference of adjacent film intervals (Fig. 3).

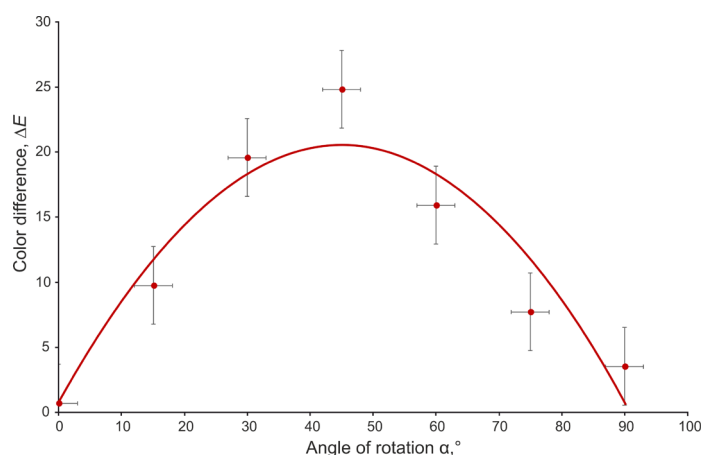


Fig. 3. Dependence of the color difference intervals in a polypropylene film 105 ± 5 μm thick on the angle of their arrangement between polarizers.

The greatest color difference is observed when the film sample is rotated by 45° relative to the polarizers, and the smallest when rotated by 0° and 90° . Based on this effect, then the position of 45° of the film in relation to the polarizers will be called **active**, and when located at 0° or 90° —**inert**.

Short-term (≤ 1 s) thermomechanical treatment was performed on a laboratory heat-welding stand of the HSE-3 brand (RDM Test Equipment, Great Britain) under a pressure of 0.2 MPa (30 psi). Cooling took place spontaneously on the surface of the table at the temperature of the laboratory room under the same conditions for all samples. The stand for welding films in automatic mode uniformly and uniformly compresses the flat surfaces of the heater.

Thus, objects for the study of optical properties and thermochromic effects were obtained: two types of samples of interval films with a thermomodified structure of intervals periodically repeating along their length and located in mutually perpendicular directions along or across the direction of the predominant orientation of polypropylene macromolecules.

A differential scanning calorimeter (DSC) was used to evaluate the crystal structure of interval polypropylene films with a thermomodified structure DSC 204 F1 Phoenix (NETZSCH, Germany). Diagrams in the DSC sensor signal–temperature coordinates were obtained at a heating rate of 10°C/min.

The chemical composition of the film was studied by the method of multiple disturbed total internal reflection on the FSM 2201/2202 IR Fourier spectrometer (*Infraspec*, Russia) using spectrum libraries: HR Spectra Polymers and Plasticizers by ATR, HR Hummel Polymer and Additives, Hummel Polymer Sample Library, Synthetic Fibers by Microscope and HR Nicolt Sampler Library.

RESULTS AND DISCUSSION

Earlier [15, 16], it was shown that when natural sunlight and light obtained using modern indoor lighting systems pass through a “polarizer–multilayer polymer film (Stoletov’s foot)–polarizer” system, the pleochroism effect is observed, providing a significant color difference between films having different number of layers. The color and quantitative parameters of the polarized light passing through the multilayer package depend on the chemical composition of the film-forming polymer, the structure and the presence of internal stresses in the films. The brightest colors were found on shrink films made of glassy polymers—polystyrene and polyvinyl chloride obtained by uniaxial orientation extraction, which is characterized by a high level of internal stresses and thermostimulated shrinkage of up to 60%. The macromolecular disorientation and reduction

of internal stresses by heat treatment affects the intensity of the pleochroism effect, which is proposed for use to record information and hidden labeling of film packaging made of these polymers [3, 4].

Since most industrially produced films of isotactic polypropylene widely used in the production of flexible packaging of goods and food do not demonstrate the pleochroism effect when assembled multilayer materials, they cannot be used in hidden labeling. The absence of optical activity of polypropylene films may have been associated with a low level of internal stresses, insufficient anisotropy or orthotropy of the films. However, it is reasonable to assume that when polypropylene films are heated to a temperature close to the melting temperature range, recrystallization and/or disorientation of macromolecules will occur. This would allow optical marking of films in the form of “watermarks” that are visually distinguishable in polarized light.

Before searching for technological ways of optical marking of transparent polypropylene packaging, the presence of internal stresses in the studied samples was evaluated by the magnitude of shrinkage and anisotropy of mechanical properties, which are known factors determining the effects of dichroism or pleochroism [17].

The results of the strength tests of the films and the assessment of shrinkage at a temperature of 150°C are presented in Table 1.

While the samples of isotactic polypropylene film differ in thickness by 5 times, both samples are anisotropic. The fact that the tensile strength of the thin film in the direction of the predominant orientation of macromolecules exceeds the strength of the film having a thickness of 105 µm by almost 2 times is a consequence of the extrusion effect and a greater multiplicity of

Table 1. Mechanical properties of polypropylene films in mutually perpendicular directions

Film (thickness, µm)	BOPP-22		BOPP-105	
	1 (=)	2 (⊥)	1 (=)	2 (⊥)
Die cutting direction	1 (=)	2 (⊥)	1 (=)	2 (⊥)
Tensile strength, MPa	67 ± 2	41 ± 2	45 ± 2	25 ± 2
Strength anisotropy	1.63		1.8	
Thermal shrinkage of the film, %	2 ± 0.5	2 ± 0.5	2 ± 0.5	2 ± 0.5
Degree of crystallinity, %	44.4		37.6	

extraction during its manufacture. The anisotropy of the mechanical properties of the films as determined by the ultimate strength is 60–80%; however, this does not significantly manifest itself during heat shrinkage.

Since industrial grade polypropylene macromolecules have deviations from isotacticity and different average lengths, as well as forming defective crystals that correspond to different melting temperatures [17], it is reasonable to expect a change in the structure and optical characteristics of films and the intensity of the dichroism effect when they are heated in the temperature range below the average melting temperature of isotactic polypropylene. Local heat treatment in the temperature range below the average melting point of isotactic polypropylene is considered in this study as a method for hidden optical marking of the film since it is unlikely to affect the shape and overall dimensions of a package or label of a thermally fixed film or cause their noticeable warping.

For testing, the temperature interval of the metal heat transmitter was selected by contact heat exchange from the maximum temperature of the product packaged in the film to the melting temperature of the polymer; here, the time intervals of their contact were comparable to the time of the packaging in high-performance packaging equipment that seals the packaging with thermal welding and/or labeling.

Thermomechanical processing of samples of polypropylene film with a thickness of $105 \pm 2 \mu\text{m}$ at a temperature of 120°C and under a pressure of 0.207 MPa (30 psi) for 0.5 s led to a noticeable change in the lightness of the sample in polarized light. Since the heat-treated area of the film sample (hereinafter referred to as the modified interval) scatters the passing stream of polarized light, it has a lighter shade in the photo (Fig. 4). When varying the angle at which the interval film sample is positioned between two polarizers in a crossed (closed) position, a visually noticeable lightening

of the modified film interval is observed while preserving the color of the unmodified part (Fig. 4).

The dichroism in the sample of the polypropylene interval film may be explained in terms of a change in the supramolecular and/or crystal structure of the orthotropically oriented film extract at different temperatures or the chemical composition of the film-forming polymer due to heating in contact with the metal electrode of the welding unit under pressure.

To separate the influence and quantification of thermal, mechanical and chemical (prescription) factors on the optical properties of the film, interval film samples were studied by IR spectroscopy, gravimetry and differential scanning calorimetry (DSC).

It was found on the IR spectrometer that in both samples of the polymer film there may be an impurity of the low molecular weight olefin fraction (Fig. 5a), which after heating from the film to $130\text{--}150^\circ\text{C}$ is removed and not identified on the surface of the film (Fig. 5b).

The sublimation of the component from the polypropylene film can be confirmed by comparing the masses of the films before and after heating on high-precision scales. Pre-prepared samples (20 pieces with a total weight of about 5 g) are weighed on analytical scales of various designs with an accuracy of up to 4 digits and placed in a preheated thermostat. After thermostating, the total mass of the film samples decreased by an average of 0.003 g, which is an order of magnitude higher than the mass measurement error.

Based on the gravimetry of the film samples before and after thermostating, it can be assumed that this component of the thermoplastic composition of isotactic polypropylene is sublimated during heating (with hidden labeling), which affects its optical (color) characteristics. This assumption is confirmed by the DSC result (Fig. 6). On the endothermic DSC curves of samples following thermomodification in the

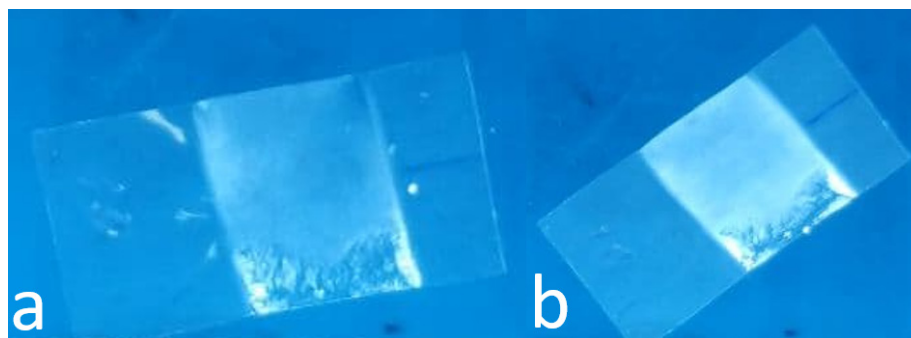
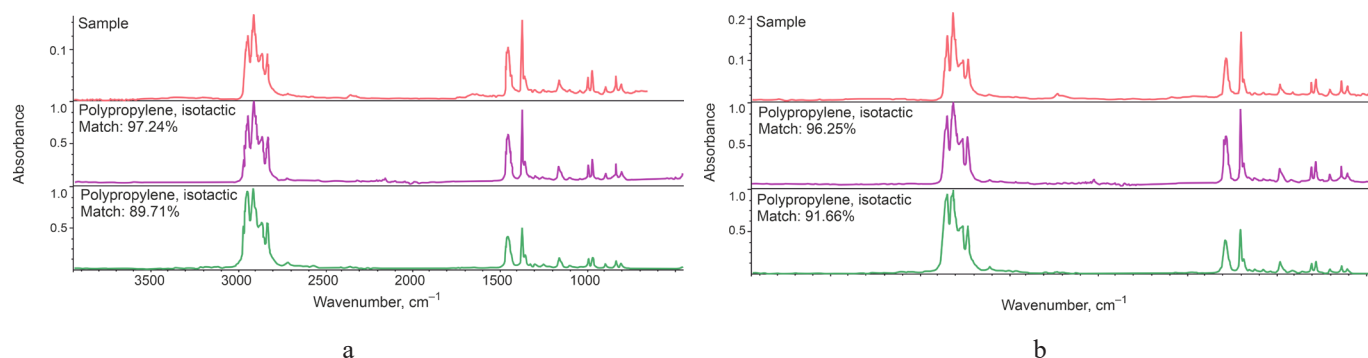


Fig. 4. Dichroism effect in a sample interval polypropylene film in transmitted polarized light when film sample is located relative to polarizers at angles 15° (a) and 45° (b).



Index	Match, %	Compound	Index	Match, %	Compound
67	97.24	Polypropylene, isotactic	67	96.25	Polypropylene, isotactic
942	89.71	Polypropylene, isotactic	942	91.66	Polypropylene, isotactic
41	88.46	Polypropylene, atactic	566	90.29	Polypropylene, atactic
67	88.12	Polypropylene, isotactic	324	89.86	Polypropylene+poly(ethylene:propylene)
943	87.31	Polypropylene, atactic	67	89.85	Polypropylene, isotactic
129	86.24	Olefin	1061	86.94	Poly(propylene:butanone), 2:1
566	86.22	Polypropylene, atactic	41	86.52	Polypropylene, atactic

Fig. 5. Identification of the IR-spectra BOPP-105 film: (a) before heat treatment; (b) after heat treatment.

low temperature range (60–80°C), the endopic “disappears.” The “disappearance” of the endopic on the DSC diagrams at 60–80°C reflects the sublimation, pre-polymerization and crystallization of olefin. The degree of crystallinity increases one and a half times from 37% to 57%. The added crystallinity appears to be defective and represents small supramolecular structures scattering the polarized light flux passing through the modified sections of the film.

According to the DSC diagrams (Fig. 6), the temperature interval at which the heat treatment of the polypropylene film can cause maximum color change and provide contrast of adjacent intervals in polarized light

is selected. For isotactic polypropylene, this film temperature range is 60–100°C. However, taking into account the high thermal resistance of the contacting surfaces and the need to minimize the contact time of the marked film and the heating tool to increase the productivity of the process, the temperature range of 60–170°C was investigated.

The marking result is presented in the form of photographs of fragments of transition zones and modified intervals obtained in transmitted polarized light on film samples with a thickness of $22 \pm 1.5 \mu\text{m}$, cut in direction 1 (Tables 2 and 3). Similar results were obtained on a film with a thickness of $105 \pm 2 \mu\text{m}$.

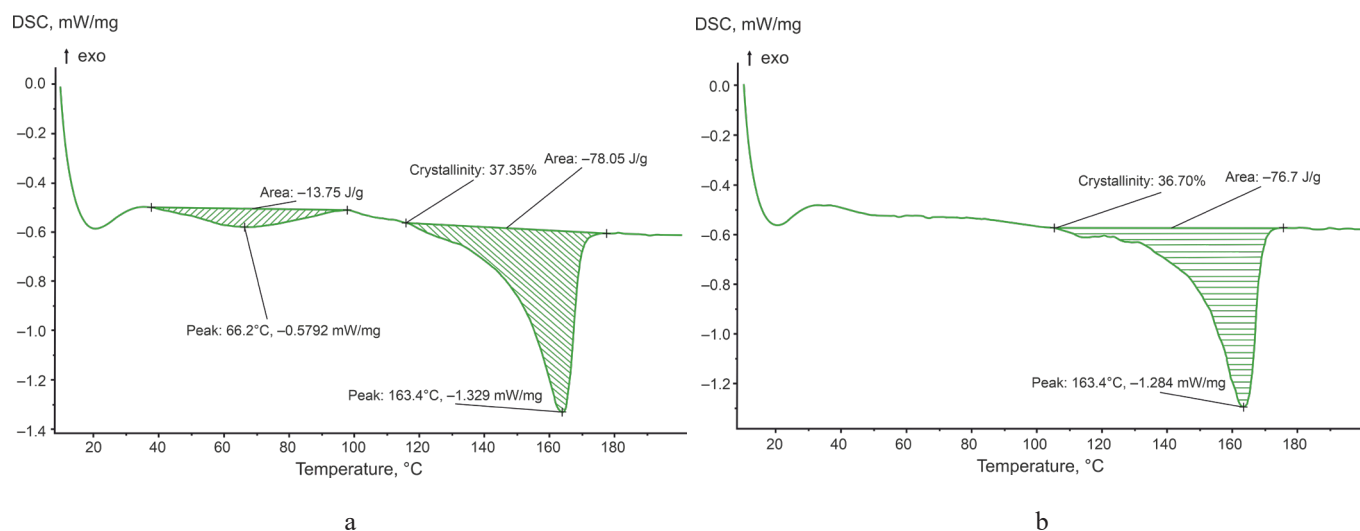


Fig. 6. Differential scanning calorimetry diagrams of polypropylene films:
(a) before heat treatment; (b) after heat treatment.






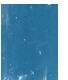





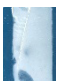
Table 2. Color difference of intervals in a BOPP-22 polypropylene film with active $\alpha = 45^\circ$ arrangement of samples (Fig. 3)

Temperature, °C	60	70	80	90	100	110
Visual evaluation of the effect						
Color difference, ΔE	0	1.86	15.73	24.81	32.51	33.80
Temperature, °C	120	130	140	150	160	170
Visual evaluation of the effect						
Color difference, ΔE	47.51	48.80	53.80	39.14	32.39	30.90

From the fragments of photographs and the values of the color difference of adjacent intervals, a color change in the transmitted polarized light is already observed following heat treatment with the active arrangement of the film starting from 70°C; however, the value of the color difference is lower than necessary for the sensitivity of the human eye [3, 4]. The maximum color difference of the adjacent intervals of the polypropylene

film with a thickness of 22 μm observed at a temperature of 140°C is 53.8. A similar change in the optical properties of the film after heat treatment is also observed at the inert position of the interval film samples between polarizers, but at higher temperatures. The maximum color difference as a result of short-term contact (0.25 s) reaches 59 at a temperature of 170°C, i.e., in the middle of the melting interval of polypropylene

Table 3. Color difference of intervals in a BOPP-22 polypropylene film with an inert $\alpha = 90^\circ$ arrangement of samples (Fig. 3)

Temperature, °C	60	70	80	90	100	110
Visual evaluation of the effect						
Color difference, ΔE	0	0	0	2.11	1.94	3.15
Temperature, °C	120	130	140	150	160	170
Visual evaluation of the effect						
Color difference, ΔE	0.94	12.03	9.78	57.68	57.53	59.00

crystallites [17]. At the same time, the maximum color difference of adjacent intervals of the polypropylene film with a thickness of 105 μm significantly depends on the location of the samples between the polarizers (Fig. 7).

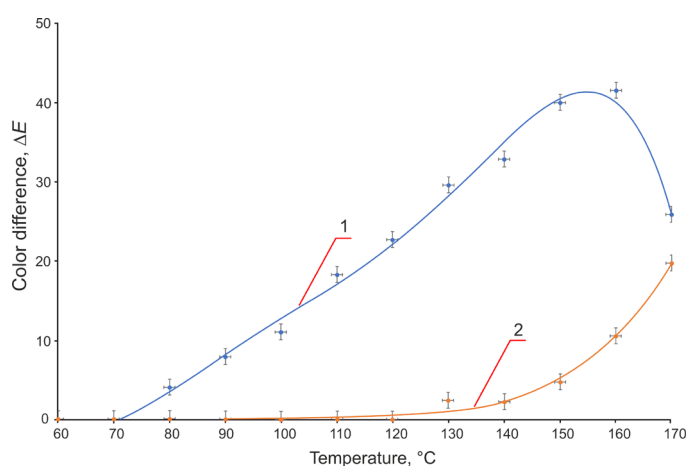


Fig. 7. Color difference between adjacent intervals of a polypropylene film (BOPP-105) after thermal marking with active $\alpha = 45^\circ$ (1) and inert $\alpha = 90^\circ$ (2) arrangement of samples polarizers.

Since a further increase in temperature or an increase in processing time does not increase the color change, the most effective treatment mode for polypropylene film with a thickness of 22 μm is 130°C for 0.1 s. However, at 130°C, the film softens and can stick to the processing equipment; therefore, it is recommended to either reduce the exposure time to 0.05 s or process the film at 125°C for 0.1 s.

CONCLUSIONS

The possibility of changing the color of a transparent biaxially oriented “sleeve” film of isotactic polypropylene in passing polarized light using the thermochromic effect for hidden labeling of transparent packaging by short-term local heat treatment is demonstrated. Heat treatment of a biaxially oriented isotactic polypropylene film stimulates partial removal and prolonged amorphization of the low molecular weight olefin fraction without heat shrinkage, changes in the degree of crystallinity and average melting point of the crystal structure.

The optimal temperature-time conditions for the contact treatment of the film with a tool heated to a temperature below the melting point of isotactic

polypropylene have been established to obtain the maximum color difference between adjacent sections of the treated and untreated film.

The demonstrated significant dependence of the color difference of adjacent polypropylene film intervals on the location of the heat-treated film section between crossed polarizers can be used in the instrumental design of a new method for identifying thermochromic labeling of transparent polymer packaging.

Authors' contributions

A.A. Nikolaev – planning the experiment, carrying out the study, collection and provision of the material, writing the text of the article;

A.P. Kondratov – writing the text of the article, scientific editing.

The authors declare no conflicts of interest.

REFERENCES

1. Jonza J.M., Ouderkirk A.J., Weber M.F. *Clear to colored security film*: US Pat. US6045894. Publ. 04.04.2000.
2. Hebrink T.J., Gilbert L.R., Jonza J.M., Ruff A.T. *Optical polarizing films with designed color shifts*: European patent application EP3067721 A1. Publ. 14.09.2016. Bull. 2016/37.
3. Kondratov A.P., Yakubov V., Volinsky A.A. Recording digital color information on transparent polyethylene films by thermal treatment. *Appl. Opt.* 2019;58(1):172–176. <https://doi.org/10.1364/ao.58.000172>
4. Kondratov A.P., Volinsky A.A., Chen J. Scaling Effects on Color and Transparency of Multilayer Polyethylene Films in Polarized Light. *Adv. Polym. Technol.* 2018;37(3):668–673. <https://doi.org/10.1002/adv.21708>
5. Lehtonen J. *Marking method*: European patent application EP1111409 A3. Publ. 27.06.2001. Bull. 2001/26.
6. Lui Y.J., Jonza J.M. *Color shifting film with a plurality of fluorescent colorants*: Pat. US6506480B2. Publ. US20020114929A1. Publ. 22.08.2002.
7. Smithson R. L.W., Biernath R.W. *Optically active materials and articles and systems in which they may be used*: Pat. WO 2010074875A1. Publ. 01.07.2010
8. Kondratov A.P. New materials for light strain-optical panels. *Light & Engineering.* 2014;22(3):74–77.
9. Free M.B., Wolk M.B., Biernath R.W., Johnson S.A., Merrill W.W., Edmonds W.F., Jalbert C.A. *Patterned marking of multilayer optical film by thermal conduction*: Pat. WO 2015034910 A1. Publ. 12.03.2015
10. Svatikov A.Yu., Simonov-Emelyanov I.D. The thermal stability of polymer cable compounds with a flame-retarding filler. *Fine Chem. Technol.* 2018;13(6):35–41 (in Russ.). <https://doi.org/10.32362/2410-6593-2018-13-6-35-41>
11. Askadskii A.A. *Physical Properties of Polymers. Prediction and Control*. Amsterdam: Gordon and Breach Publishers; 1996. 336 p.
12. Krakhalev M.N., Prishchepa O.O., Sutormin V.S., Zyryanov V.Y. Polymer dispersed nematic liquid crystal films with conical boundary conditions for electrically controllable polarizers. *Opt. Mater.* 2019;89:1–4. <https://doi.org/10.1016/j.optmat.2019.01.004>
13. Cherkasov E.P., Kondratov A.P., Nazarov V.G. The process of tactile (relief) marking of thermo shrinkable membranes and labels. *J. Phys.: Conf. Ser.* 2019;1399:044036 <https://doi.org/10.1088/1742-6596/1399/4/044036>
14. Ihara H., Takafuji M., Kuwahara Y. Transparent polymer films functionally-webbed with glutamide-based supramolecular gels and their optical applications. *Kobunshi Ronbunshu.* 2016;73(1):30–41. <https://doi.org/10.1295/koron.2015-0056>
15. Kozawa Y., Sato S. Generation of a radially polarized laser beam by use of a conical Brewster prism. *Opt. Lett.* 2005;30(22):3063–3065. <https://doi.org/10.1364/OL.30.003063>
16. Nikolaev A.A., Nagornova I.V., Kondratov A.P. Contactless monitoring method both carbon-chain thermoplastics inhomogeneity as applicable to the blown type extruders. *J. Phys.: Conf. Ser.* 2019;1260(3):032029. <https://doi.org/10.1088/1742-6596/1260/3/032029>
17. Hanna L.A., Cudby M.E.A., Hendra P.J., Maddams W., Willis H.A., Zichy V. Vibrational spectroscopic study of structural changes in isotactic polypropylene below the melting point. *Polymer.* 1988;29(10):1843–1847. [https://doi.org/10.1016/0032-3861\(88\)90401-6](https://doi.org/10.1016/0032-3861(88)90401-6)

About the authors:

Alexander A. Nikolaev, Lecturer, Department of Innovative Materials of the Print Media Industry, Moscow Polytechnic University (38, Bolshaya Semenovskaya ul., Moscow, 127008, Russia). E-mail: nikolaevaleksandr1992@gmail.com. RSCI SPIN-code 8146-7143.

Alexander P. Kondratov, Dr. Sci. (Eng.), Professor, Department of Innovative Materials of the Print Media Industry, Moscow Polytechnic University (38, Bolshaya Semenovskaya ul., Moscow, 127008, Russia). E-mail: apkrezerv@mail.ru. Scopus Author ID 6603924314, RSCI SPIN-code 8689-3888, <https://orcid.org/0000-0001-6118-0808>

Об авторах:

Николаев Александр Африканович, преподаватель кафедры «Инновационные материалы принтмедиаиндустрии», Полиграфический институт, ФГАОУ ВО «Московский политехнический университет» (127008, Россия, Москва, ул. Большая Семеновская, д. 38). E-mail: nikolaevaleksandr1992@gmail.com. SPIN-код РИНЦ 8146-7143.

Кондратов Александр Петрович, д.т.н., профессор кафедры «Инновационные материалы принтмедиаиндустрии», Полиграфический институт, ФГАОУ «Московский политехнический университет» (127008, Россия, Москва, ул. Большая Семеновская, д. 38). E-mail: apkrezerv@mail.ru. Scopus Author ID 6603924314, SPIN-код РИНЦ 8689-3888, <https://orcid.org/0000-0001-6118-0808>

The article was submitted: February 04, 2022; approved after reviewing: March 30, 2022; accepted for publication: July 18, 2022.

Translated from Russian into English by N. Isaeva

Edited for English language and spelling by Thomas Beavitt

CHEMISTRY AND TECHNOLOGY OF INORGANIC MATERIALS
ХИМИЯ И ТЕХНОЛОГИЯ НЕОРГАНИЧЕСКИХ МАТЕРИАЛОВ

ISSN 2686-7575 (Online)

<https://doi.org/10.32362/2410-6593-2022-17-4-357-368>



UDC 661.842.532

RESEARCH ARTICLE

Technology for processing phosphogypsum into a fluorescent dye based on calcium sulfide

Oleg A. Medennikov[✉], Nina P. Shabelskaya

Platov South-Russian State Polytechnic University (NPI), Novocherkassk, 346428 Russia

[✉]Corresponding author, e-mail: monomors@yandex.ru

Abstract

Objectives. There is considerable economic demand for products obtained by processing phosphogypsum. In particular, calcium sulfide-based materials having luminescent properties are the object of intensive study due to the wide range of possibilities for their use. The alloying of the structure of calcium sulfide with cations of rare earth elements leads to the appearance of a glow having various colors. However, the high cost of such phosphorescent materials is due to the high chemical purity of the reagents required for their synthesis. The development of efficient methods for obtaining calcium sulfide-based luminescent materials from phosphogypsum is part of an integrated approach to solving the problem of synthesizing economically demanded materials from production waste.

Methods. The synthesized materials were studied using X-ray phase analysis and scanning electron microscopy. Photos of the samples were taken under illumination with an incandescent lamp or a fluorescent ultraviolet lamp.

Results. According to X-ray phase analysis, phosphogypsum is mainly comprised of calcium sulfate dihydrate and calcium sulfate hemihydrate. Heat treatment of a phosphogypsum sample at a temperature of 1073 K is accompanied by the formation of anhydrous calcium sulfate. In the presence of a reducing agent, a composite material is formed containing a phase of anhydrous calcium sulfate and calcium sulfide. Due to the calcium sulfide content, phosphogypsum has luminescent properties when heat-treated in the presence of various reducing agents, including activated carbon, wood charcoal, vegetable oil, citric acid, starch, and sucrose.

Conclusions. Optimal technological conditions for obtaining a composite material exhibiting luminescent properties are revealed. The successful synthesis of phosphor from without non-pretreated phosphogypsum is demonstrated. Optimal technological conditions for obtaining a composite material exhibiting luminescent properties are as follows: heat treatment temperature is 1073–1173 K; isothermal holding time is 60 min; reducing agent quantity is 37–50% (mol). The study results are widely applicable to processing wastes obtained from large-scale chemical production involving the production of a highly demanded inorganic product.

Keywords: phosphogypsum, thermal reduction, luminescent materials, calcium sulfide

For citation: Medennikov O.A., Shabelskaya N.P. Technology for processing phosphogypsum into a fluorescent dye based on calcium sulfide. *Tonk. Khim. Tekhnol. = Fine Chem. Technol.* 2022;17(4):357–368 (Russ., Eng.). <https://doi.org/10.32362/2410-6593-2022-17-4-357-368>

НАУЧНАЯ СТАТЬЯ

Технология переработки фосфогипса в люминесцентный краситель на основе сульфида кальция

О.А. Меденников[✉], Н.П. Шабельская

Южно-Российский государственный политехнический университет (НПИ) имени М.И. Платова,
Новочеркасск, 346428 Россия

[✉] Автор для переписки, e-mail: monomors@yandex.ru

Аннотация

Цели. Материалы с люминесцентными свойствами на основе сульфида кальция являются объектом интенсивного изучения ввиду широкого круга возможностей их использования. Легирование структуры сульфида кальция катионами редкоземельных элементов приводит к появлению свечения различной окраски. Синтез подобных материалов осуществляют из химически чистых реактивов, что приводит к высокой стоимости люминофоров. Разработка способа получения люминесцентного материала на основе сульфида кальция из фосфогипса является актуальной задачей химической технологии, позволяющей осуществить комплексный подход к решению проблемы получения экономичных востребованных материалов из отходов производства.

Методы. Синтезированные материалы были изучены с помощью рентгенофазового анализа, растровой электронной микроскопии. Фотографии образцов выполняли при освещении лампой накаливания или люминесцентной ультрафиолетовой лампой.

Результаты. Согласно данным рентгенофазового анализа, фосфогипс представляет собой двухводный сульфат кальция и полуводный сульфат кальция. Термообработка при температуре 1073 К образца фосфогипса сопровождается образованием безводного сульфата кальция, в присутствии восстановителя происходит образование композиционного материала, содержащего фазу безводного сульфата кальция и сульфида кальция. Термообработанный в присутствии ряда восстановителей — активированного угля,

березового угля, растительного масла, лимонной кислоты, крахмала, сахарозы — фосфогипс обладает способностью к люминесценции, обусловленной наличием сульфида кальция.

Выводы. Выявлены оптимальные технологические условия получения композиционного материала, проявляющего люминесцентные свойства. Показано, что для синтеза люминофора наиболее удачным является использование фосфогипса без предварительной обработки. Оптимальные технологические условия получения композиционного материала, проявляющего люминесцентные свойства: температура термообработки 1073–1173 К, продолжительность изотермической выдержки 60 мин, количество восстановителя – 37–50 мол. %. Проведенное исследование открывает широкие возможности переработки отхода многотоннажного химического производства с получением востребованного неорганического продукта.

Ключевые слова: фосфогипс, термическое восстановление, люминесцентные материалы, сульфид кальция

Для цитирования: Меденников О.А., Шабельская Н.П. Технология переработки фосфогипса в люминесцентный краситель на основе сульфида кальция. *Тонкие химические технологии*. 2022;17(4):357–368. <https://doi.org/10.32362/2410-6593-2022-17-4-357-368>

INTRODUCTION

Modern technologies for extracting inorganic materials exert increasing environmental pressures. One of the most actively developing industries involves the production of mineral fertilizers. In particular, phosphogypsum is formed from apatite raw materials during the production of phosphoric acid for further processing into phosphorus-containing fertilizers. However, large-scale phosphogypsum dumps occupying significant areas involve a serious burden on the ecosystem [1, 2]. Thus, developing the foundations of methods for processing such inorganic production wastes is an urgent chemico-technological task. Currently, phosphogypsum byproducts are mainly reused for building materials—wall panels, dry mixes, etc. [3–5]—and in the production of fertilizers [6, 7]. The accumulated reserves of phosphogypsum can be equated to natural resources with zero extraction costs. In this regard, it is relevant to study the possibility of processing phosphogypsum to obtain demanded inorganic products.

Calcium sulfide serves as a matrix for the production of inorganic phosphors [8–10]. In the contemporary world, materials with luminescent properties are the object of intensive study due to a wide range of possibilities for their use [11–13]. One widely used material is calcium sulfide-based phosphor [14–17]. Doping of the calcium sulfide structure with europium cations leads to the appearance of a red

[14–16] or orange [14] glow; the presence of cerium in the composition produces a green and yellow-green glow [16]; cations of some d-elements can be used in the production of materials having a purple, blue [9], or yellow [17] glow. As a rule, the synthesis of such materials is carried out from chemically pure reagents, which leads to a high cost of phosphors (EUR 50–70 per kg).

In this regard, the purpose of this study is to develop a method for obtaining calcium sulfide from phosphogypsum as part of an integrated approach to synthesizing valuable materials from production wastes.

MATERIALS AND METHODS

In order to study the possibility of obtaining an inorganic luminescent material, phosphogypsum containing $\text{CaSO}_4 \cdot 2\text{H}_2\text{O}$ of at least 99 wt % was used. Sucrose (PTO OSNOVA, Russia), A grade birch activated carbon (SBV GRUPP, Russia), wood charcoal (PKF SISTEMA, Russia), vegetable oil (GK YUG ROSSII, Russia), citric acid (Standart, Russia), and starch (KF Bogorodskaya, Russia) were used as reducing agents.

The following phosphogypsum samples were used to assess the ability to recover to the target product:

- 1) pre-heat-treated at 1073 K for 60 min;
- 2) dried in a drying cabinet at a temperature of 473 K for 5 h to a constant weight;

3) without preliminary heat treatment, with the addition of water in an amount of 10 wt % by weight of phosphogypsum;

4) without pretreatment.

The study of the possibility of recovery was carried out as follows. A reducing agent was added to phosphogypsum according to the formulation. The samples were homogenized in a 0.45 kW mixer with a speed of 1500 rpm, after which they were placed in alund crucibles in the working space of a muffle furnace and heat-treated according to the following regime: heating rate is 13 K/min; treatment temperature is 1073 K; time at this temperature is 60 min. Following heat treatment, the samples were cooled to a furnace temperature of 293 K, weighed and crushed in a mortar.

For each sample, the relative luminous flux emitted by the surface of the sample of a fixed area was measured using an original installation (Fig. 1) comprising an ultraviolet (UV) radiation source, light filters, and a recording sensor. A sample and reference sample used as a phosphor yellow YAG:Ce were placed in the installation and illuminated with a radiation having a wavelength of 380 nm. The luminous flux from the surface of the sample and the reference sample was recorded through a light filter that excludes ultraviolet rays. The relative luminous flux was obtained as the ratio of the luminous flux from the surface of the test sample to the luminous flux from the surface of the reference sample.

In order to determine the optimal heat treatment time, the phosphogypsum samples and reducing agent were homogenized in a manner similar that described above. Next, the samples were heat-treated according to the following regime: heating rate is 13 K/min;

heat-treatment temperature is 1173 K. After reaching the heat-treatment temperature, the sample batches were moved every 10 min to a cooling chamber made of thermal insulation material and cooled slowly to a temperature of 293 K. After weighing the samples and crushing them in a mortar, the relative luminous flux emitted by the surface of the sample of a fixed area was measured.

In order to select the reducing agent and the heat treatment temperature, phosphogypsum weighing 17.20 g and the reducing agent were weighed with an accuracy of 0.01 g on technical electronic scales according to the ratios indicated in Table 1, homogenized in a 0.45 kW mixer with a speed of 1500 rpm, after which they were placed in alund crucibles in the working space of a muffle furnace, where they were produced heat treatment according to the following modes: samples were heated at a rate of 13 K/min to the calcination temperature, which was 1073 K, 1173 K, and 1273 K. Upon reaching the calcination temperature, the samples were kept at this temperature for 60 min. At the end of the heat treatment, the samples were cooled together with the furnace to a temperature of 293 K. After that, the samples were crushed in a mortar to a powdery state. The relative luminous flux emitted by the sample surface of a fixed area was measured.

Phase composition was studied on an ARL X'TRA X-ray diffractometer (ARL, Switzerland) using monochromatized Cu-K α radiation by point-by-point scanning (step 0.01°, accumulation time at point 2 s) in the range of values 2θ from 15° to 80°. The qualitative phase composition was determined using PDF-2 in the Crystallographica software¹.

Micrographs of the samples were obtained using a Quanta 200 scanning electron microscope (FEI, USA). The images were taken at an accelerating voltage of up to 30 kV.

Photos of the samples were taken under illumination with an incandescent lamp or a fluorescent ultraviolet lamp FT5 BLACK LIGHT (Camelion, Russia).

RESULTS AND DISCUSSION

According to X-ray phase analysis, phosphogypsum is a dihydrous calcium sulfate (Calcium Sulfate Hydrate gypsum low, PDF Number: 010-70-7008) and semi-aqueous calcium sulfate (Calcium Sulfate Hydrate, PDF Number: 010-80-1235) (Fig. 2a). Heat treatment at a temperature of

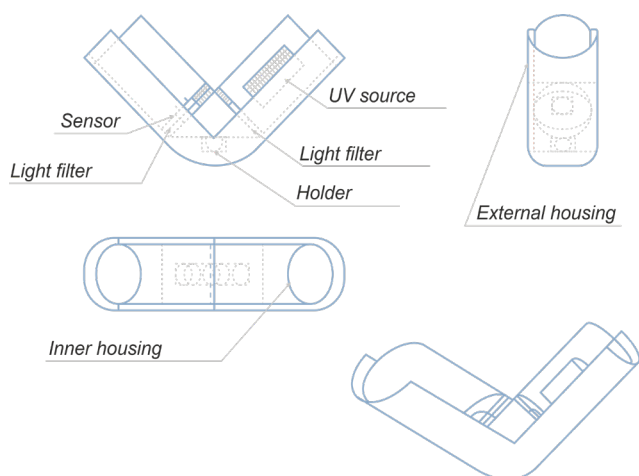


Fig. 1. Diagram of the installation for measuring the luminous flux from the surface of the irradiated UV sample.

¹ PDF-2. The Powder Diffraction File™. International Center for Diffraction Data (ICDD), PDF-2 Release 2012, www.icdd.com (2014).

Table 1. Ratio of phosphogypsum and reducing agents

Reducing agent	Reducing agent mass, g	Molar fraction of the reducing agent, %
A grade birch activated carbon	0.30	12.5
	0.60	25
	1.20	50
	1.80	75
	2.40	100
	3.00	125
	3.60	150
	4.80	200
Sugar	0.70	12.28
	1.40	24.56
	2.90	50.88
	4.30	75.44
	5.70	100.00
	7.10	124.56
	8.60	150.88
	11.40	200.00
Vegetable oil	0.30	13.64
	0.60	27.27
	1.10	50.00
	1.70	77.27
	2.20	100.00
	2.80	127.27
	3.40	154.55
	4.40	200.00
Citric acid	1.10	6.40
	2.10	12.21
	4.30	25.00
	6.40	37.21
	8.50	49.42
	10.70	62.21
	12.80	74.42
	17.10	99.42
Starch	0.70	12.96
	1.40	25.93
	2.70	50.00
	4.10	75.93
	5.40	100.00
	6.80	125.93
	8.10	150.00
	10.80	200.00

1073 K of a phosphogypsum sample is accompanied by the formation of anhydrous calcium sulfate (PDF Number: 010-74-2421) (Fig. 2b). Heat treatment at a temperature of 1073 K of a phosphogypsum sample in the presence of a reducing agent leads to the formation of a composite material containing a phase of anhydrous calcium sulfate (Calcium Sulfate, PDF Number: 010-70-0909) and calcium sulfide (Calcium Sulfide, PDF Number: 000-08-0464) (Fig. 2c) (data for phosphogypsum reduced in the presence of sucrose are given as an example).

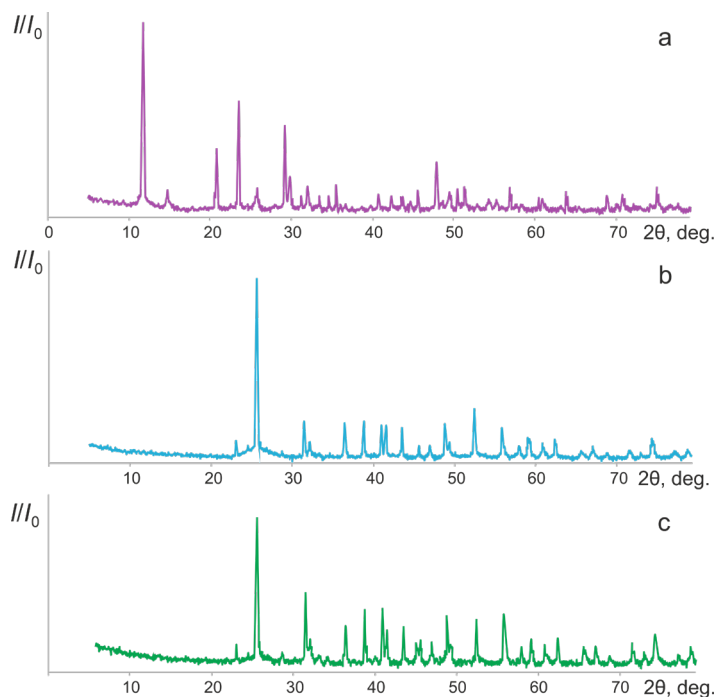


Fig. 2. X-ray diffraction patterns of the phosphogypsum samples: (a) dried at a temperature of 473 K, (b) heat-treated at a temperature of 1073 K, (c) heat-treated in the presence of a reducing agent at a temperature of 1073 K.

Various micrographs of phosphogypsum were also obtained: dried at a temperature of 473 K (Fig. 3a); heat-treated at a temperature of 1073 K (Fig. 3b); heat-treated in the presence of a reducing agent at a temperature of 1073 K (Fig. 3c), where data for phosphogypsum reduced in the presence of sucrose are given as an example.

Figure 3 represents samples of phosphogypsum, heat-treated at temperatures of 473 K and 1073 K as lamellar crystals. Cracks appearing on the crystals at increased heat treatment temperatures may be due to the processes of removing crystallization water. Heat treatment in the presence of a reducing agent is accompanied by partial destruction of the structure: plate crystals lose boundary clarity, while clusters of the reduced material form on their surface. Figure 4

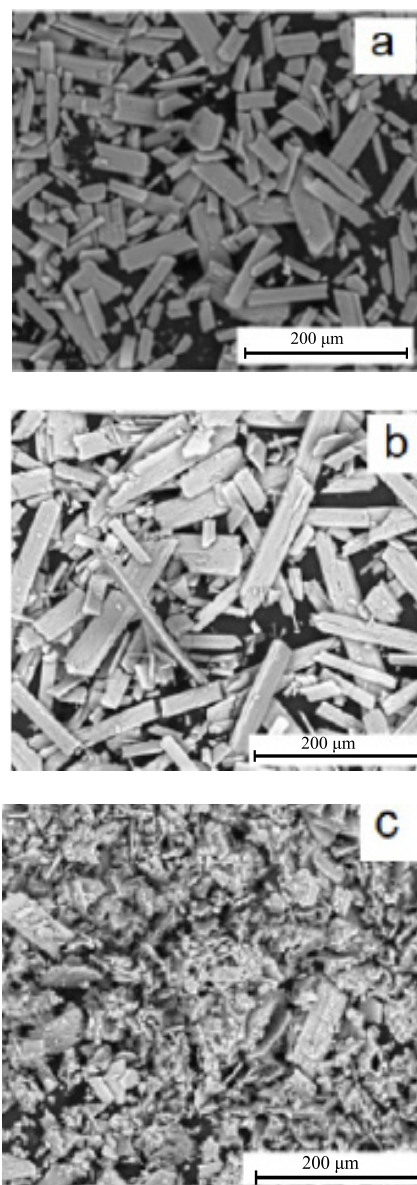


Fig. 3. Micrographs of phosphogypsum: (a) dried at a temperature of 473 K, (b) heat-treated at a temperature of 1073 K, (c) heat-treated in the presence of a reducing agent at a temperature of 1073 K.

schematically represents the process of transition of the original structure to the restored one.

The luminescent properties of phosphogypsum heat-treated in the presence of a reducing agent (Fig. 5) are due to the presence of calcium sulfide. Figure 5 shows photos of samples under visible illumination (Fig. 5a) and ultraviolet illumination (Fig. 5b and 5c); a light filter is used to remove the UV part of the radiation (Fig. 5b).

Results of studying the effect of pretreatment

The results of measuring the relative luminous flux from the surface of the studied phosphogypsum

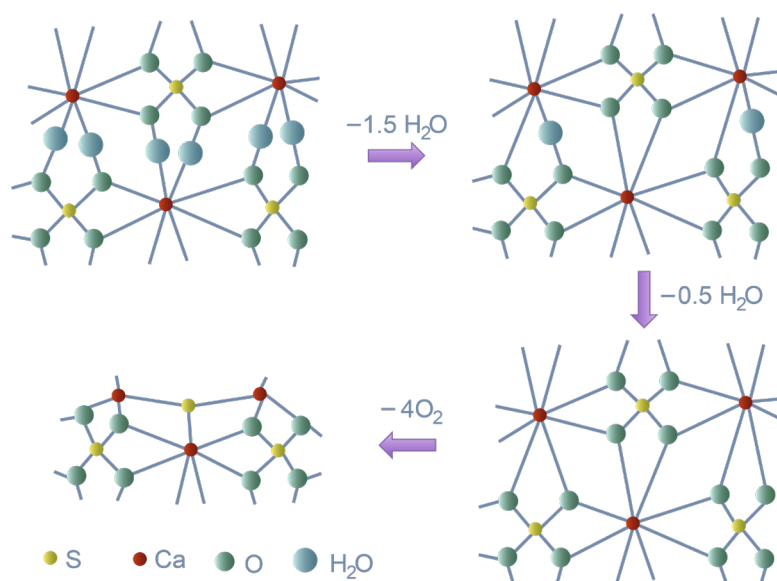


Fig. 4. Schematic representation of the formation of the composite material CaSO_4/CaS .

sample obtained with various preliminary preparations are shown in Table 2.

From the results shown in Table 2, it follows that phosphogypsum without pretreatment is more suitable for the synthesis of phosphor.

Determination of the optimal heat treatment time

When calculating the change in the mass of the sample, the final mass of the sample, the mass of the reducing agent and the mass of water were subtracted from the initial mass of the sample. The results of these calculations and measurements are shown in Table 3.

The data obtained indicate that at a given temperature, the exposure time of 60 min was optimal for obtaining a luminescent material. It can be assumed that a shorter holding time is not enough for the recovery process to proceed,

which is also evidenced by the insufficient loss of mass, compared with the calculated one, and traces of unreacted coal in the calcined samples. A longer calcination time leads to the reverse oxidation reaction of the compounds obtained during the reduction process.

Selection of reducing agent

The following reducing agents were selected for the recovery process: A grade birch activated carbon, sugar, vegetable oil, citric acid, and starch.

The following reduction reactions of phosphogypsum to calcium sulfide (1)–(5) have been proposed for these reducing agents.

For coal (1):

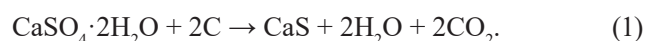


Fig. 5. Samples of reduced phosphogypsum under illumination: ordinary light (a), ultraviolet light (b, c), and ultraviolet light with a light filter (b).

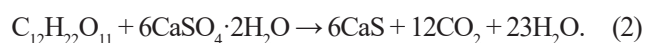
Table 2. Results of the recovery of phosphogypsum that has undergone various pretreatment

Phosphogypsum samples	Average mass loss, g	Relative luminous flux
Pre-heat treated at 1073 K for 60 min	0.24	0.36
Dried in an oven at 473 K for 5 h	0.27	0.51
Without pre-heat treatment with the addition of water	0.23	0.52
Without pretreatment	0.21	0.88

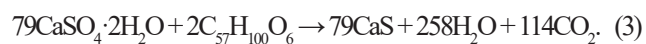
Table 3. Determination of the optimal heat treatment time

Time, min	Mass change, g	Relative luminous flux
0	−0.48	0.10
10	−0.02	0.15
20	0.03	0.24
30	0.12	0.34
40	0.14	0.68
50	0.18	0.71
60	0.21	0.88
70	0.21	0.85
80	0.18	0.81
90	0.12	0.80
100	0.11	0.75
110	0.05	0.69

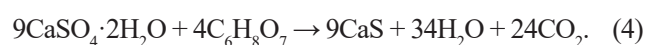
For sucrose (2):



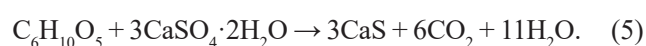
For vegetable oil, it was assumed that sunflower oil is glycerin oleodilinoleate (3):



For citric acid (4):



For starch (5):



Based on the proposed reactions, 2.40 g of coal, 5.70 g of sucrose, 2.20 g of vegetable oil, 8.50 g of citric acid and 5.40 g of starch were taken as 100%.

In order to check the effect of heat treatment conditions on pure reducing agents, samples of reducing agents were placed in crucibles in a muffle furnace and calcined for 60 min at a temperature of 1073 K. At the end of the heat treatment, the crucibles were empty, the reducing agents were completely burned.

Table 4 shows data on the study of the effect of various reducing agents on the process of obtaining the target material. In all experiments, the mass of the phosphogypsum sample was 17.20 g.

To test the possibility of using wood charcoal instead of A birch activated carbon, the cost of which is lower, phosphogypsum samples weighing

17.20 g and a reducing agent, which is A grade birch activated carbon and wood charcoal of various weights, were heat treated at a temperature of 1173 K, the same as described above. The results of the study are shown in Table 5.

Table 5 data indicates that birch activated carbon and wood charcoal are equally well suited for use as phosphogypsum reducing agents; however, the price of wood charcoal makes it more economically attractive.

According to Tables 4 and 5, the best values of the relative luminous flux were noted for phosphogypsum samples with sucrose and starch as a reducing agent at a molar fraction of the reducing agent of 50% and a heat treatment temperature of 1173 K. For samples with reducing agents—vegetable oil and citric acid—the optimal

Table 4. Results of heat treatment of phosphogypsum with various reducing agents at different temperatures

Reducing agent	Reducing agent mass, g	Mole fraction of the reducing agent, %	Relative luminous flux at heat treatment temperature, K		
			1073	1173	1273
A grade birch activated carbon	0.30	12.5	0.12	0.12	0.10
	0.60	25	0.15	0.14	0.25
	1.20	50	0.20	0.88	0.61
	1.80	75	0.11	0.73	0.55
	2.40	100	0.10	0.68	0.48
	3.00	125	0.09	0.59	0.30
	3.60	150	0.06	0.25	0.16
	4.80	200	0.05	0.05	0.06
Sugar	0.70	12.28	0.17	0.14	0.10
	1.40	24.56	0.49	0.38	0.14
	2.90	50.88	0.38	1.13	0.86
	4.30	75.44	0.33	1.00	0.88
	5.70	100.00	0.24	0.85	0.81
	7.10	124.56	0.19	0.82	0.92
	8.60	150.88	0.14	0.77	0.83
	11.40	200.00	0.10	0.72	0.38
Vegetable oil	0.30	13.64	0.20	0.12	0.10
	0.60	27.27	0.29	0.14	0.10
	1.10	50.00	0.80	0.22	0.10
	1.70	77.27	0.79	0.40	0.10
	2.20	100.00	0.78	0.65	0.10
	2.80	127.27	0.73	0.59	0.20
	3.40	154.55	0.70	0.42	0.10
	4.40	200.00	0.74	0.42	0.20

Table 4. Continued

Reducing agent	Reducing agent mass, g	Mole fraction of the reducing agent, %	Relative luminous flux at heat treatment temperature, K		
			1073	1173	1273
Citric acid	1.10	6.40	0.24	0.10	0.10
	2.10	12.21	0.39	0.12	0.10
	4.30	25.00	0.86	0.35	0.15
	6.40	37.21	0.93	0.75	0.15
	8.50	49.42	0.91	0.90	0.15
	10.70	62.21	0.90	0.88	0.10
	12.80	74.42	0.84	0.80	0.26
	17.10	99.42	0.63	0.60	0.21
Starch	0.70	12.96	0.20	0.14	0.14
	1.40	25.93	0.37	0.33	0.19
	2.70	50.00	0.52	1.00	0.62
	4.10	75.93	0.52	0.97	0.81
	5.40	100.00	0.36	0.92	0.92
	6.80	125.93	0.27	0.82	0.83
	8.10	150.00	0.27	0.69	0.79
	10.80	200.00	0.27	0.41	0.60

Table 5. Comparison of A grade birch activated carbon and wood charcoal

Reducing agent	Reducing agent mass, g	Mole fraction of the reducing agent, %	Relative luminous flux
A grade birch activated carbon	1.2	50	0.88
	1.8	75	0.73
	2.4	100	0.68
	4.8	200	0.05
Wood charcoal	1.2	50	0.86
	1.8	75	0.77
	2.4	100	0.70
	4.8	200	0.10

temperature was 1073 K, at which the maximum value of the relative luminous flux was reached with a reducing agent molar fraction of 37–50%.

CONCLUSIONS

A comprehensive study of the possibility of obtaining the demanded inorganic luminescent

material from the multi-tonnage waste of orthophosphoric acid production was carried out. The following main results were obtained:

1) The study of the effect of preliminary preparation of phosphogypsum in the form of heat treatment at different temperatures, humidification of samples, allowed us to establish that for the synthesis of phosphor the most successful is the use of phosphogypsum without pretreatment.

2) Heat treatment at a temperature of 1073 K of a phosphogypsum sample is accompanied by the formation of an anhydrous compound – calcium sulfate. Heat treatment in the presence of a reducing agent leads to the formation of a composite material containing a phase of anhydrous calcium sulfate and calcium sulfide.

3) When the temperature of the heat treatment increases, cracks appear on the crystals, which may be due to the processes of removing crystallization water. Heat treatment in the presence of a reducing agent is accompanied by partial destruction of the structure, plate crystals lose the clarity of the boundaries, clusters of the reduced material form on their surface.

4) Heat-treated phosphogypsum in the presence of a number of reducing agents – A grade birch activated carbon, wood charcoal, vegetable oil, citric acid, starch, and sucrose – has the ability to luminescence due to the presence of calcium sulfide.

5) The optimal technological conditions for obtaining a composite material exhibiting luminescent properties were revealed: the heat treatment temperature is 1073–1173 K, the duration

of isothermal exposure is 60 min, the amount of reducing agent is 37–50 mol %.

6) The conducted research opens up wide possibilities for processing waste from multi-tonnage chemical production to obtain a sought-after inorganic product.

Acknowledgments

The work was supported by the RTU MIREA grant of “Innovations in the implementation of priority areas of science and technology development,” the Research Institute Project No. 28/29/948-YuU. The authors thank A.N. Yatsenko, Candidate of Sciences (Engineering), the employee of the Center for Collective Use of Platov South-Russian State Polytechnic University (NPI), for his help in shooting and decoding X-ray data and performing microscopic studies.

Authors' contributions

O.A. Medennikov – synthesis and experimental study of sample properties, interpretation of experimental results, writing the text of the article;

N.P. Shabelskaya – interpretation of experimental results, writing the text of the article.

The authors declare no conflicts of interest.

REFERENCES

1. Xu J.P., Fan L.R., Xie Y.C., Wu G. Recycling-equilibrium strategy for phosphogypsum pollution control in phosphate fertilizer plants. *J. Clean. Prod.* 2019;215:175–197. <https://doi.org/10.1016/j.jclepro.2018.12.236>
2. El Zrelli R., Rabaoui L., Abda H., Daghbouj N., Perez-Lopez R., Castet S., Aigouy T., Bejaoui N., Courjault-Rade P. Characterization of the role of phosphogypsum foam in the transport of metals and radionuclides in the Southern Mediterranean Sea. *J. Hazard. Mater.* 2019;63:258–267. <https://doi.org/10.1016/j.jhazmat.2018.09.083>
3. Szajerski P., Celinska J., Bern H., Gasiorowski A., Anyszk A., Dziugan P. Radium content and radon exhalation rate from sulfur polymer composites (SPC) based on mineral fillers. *Constr. Build. Mater.* 2019;198:390–398. <https://doi.org/10.1016/j.conbuildmat.2018.11.262>
4. Miękoś E., Zieliński M., Kolodziejczyk K., Jaksender M. Application of industrial and biopolymers waste to stabilise the subsoil of road surfaces. *Road Mater. Pavement Des.* 2017;20(2):440–453. <https://doi.org/10.1080/14680629.2017.1389766>
5. James J. Strength benefit of sawdust/wood ash amendment in cement stabilization of an expansive soil. *Revista Facultad de Ingenieria, Universidad Pedagogica y Tecnologica de Colombia.* 2019;28(50):44–61. <https://doi.org/10.19053/01211129.v28.n50.2019.8790>

6. Michalovicz L., Muller M.M.L., Tormena C.A., Dick W.A., Vicensi M., Meert L. Soil chemical attributes, nutrient uptake and yield of no-till crops as affected by phosphogypsum doses and parceling in southern Brazil. *Archives of Agronomy and Soil Science.* 2019;65(3):385–399. <https://doi.org/10.1080/03650340.2018.1505041>
7. Fedotov P.S., Petropavlovsk I.A., Norov A.M., Malyavin A.S., Ovchinnikova K.N. Production of PKS-fertilizers grade 0-20-20-5S using different phosphate raw materials. *Khimicheskaya promyshlennost' segodnya = Chemical industry today.* 2016;(2):6–11 (in Russ.).
8. Zhuang Y.F., Li T.Y., Yuan P., Li Y.Q., Yang Y.M., Yang Z.P. The novel red persistent phosphor CaS: Yb²⁺, Cl⁻ potentially applicable in AC LED. *Appl. Phys. A.* 2019;125(2):141. <https://doi.org/10.1007/s00339-019-2447-6>
9. Tong X.B., Yang J.X., Wu P.P., Zhang X.M., Seo Y.J. Color tunable emission from CaS: Cu⁺, Mn²⁺ rare-earth-free phosphors prepared by a simple carbon-thermal reduction method. *J. Alloys Compd.* 2018;779:399–403. <https://doi.org/10.1016/j.jallcom.2018.11.325>
10. Medennikov O.A., Shabelskaya N.P., Gaidukova Y.A., Astakhova M.N., Chernysheva G.M. The use of phosphoric acid waste product for calcium sulfide production. *IOP Conf. Ser.: Earth Environ. Sci.* 2021;677(5):052049. <https://doi.org/10.1088/1755-1315/677/5/052049>

11. Yankova T.V., Melnikov P.V., Yashtulov N.A., Zaitsev N.K. Chemiluminescent reactions of luminol and *N*-octylluminol with a hypochlorite in non-ionic surfactants. *Tonk. Khim. Tekhnol. = Fine Chem. Technol.* 2019;14(3) 90–97 (in Russ.). <https://doi.org/10.32362/2410-6593-2019-14-3-90-97>
12. Get'man E.I., Oleksii Yu.A., Radio S.V., Ardanova L.I. Determining the phase stability of luminescent materials based on the solid solutions of oxyorthosilicates $(\text{Lu}_{1-x}\text{Ln}_x)[(\text{SiO}_4)_{0.5}\text{O}_{0.5}]$, where $\text{Ln} = \text{La}–\text{Yb}$. *Tonk. Khim. Tekhnol. = Fine Chem. Technol.* 2020;15(5):54–62. <https://doi.org/10.32362/2410-6593-2020-15-5-54-62>
13. Tomina E.V., Lastochkin D.A., Maltsev S.A. The synthesis of nanophosphors $\text{YP}_x\text{V}_{1-x}\text{O}_4$ by spray pyrolysis and microwave methods. *Kondensirovannye sredy i mezhfaznye granitsy = Condensed Matter and Interphases.* 2020;22(4):496–503. <https://doi.org/10.17308/kcmf.2020.22/3120>
14. Rosa J., Lahtinen J., Julin J., Sun Z., Lipsanen H. Tuning of emission wavelength of CaS:Eu by addition of oxygen using atomic layer deposition. *Materials.* 2021;14(20):5966. <https://doi.org/10.3390/ma14205966>
15. Wang X., Ke J., Wang Y., Liang Y., He J., Song Z., Lian S., Qiu Z. One-Step Design of a Water-Resistant Green-to-Red Phosphor for Horticultural Sunlight Conversion. *ACS Agric. Sci. Technol.* 2021;1(2):55–63. <https://doi.org/10.1021/acsagritech.0c00062>
16. Arai M., Fujimoto Y., Koshimizu M., Kawamura I., Nakauchi D., Yanagida T., Asai K. Development of rare earth doped CaS phosphors for radiation detection. *Journal of the Ceramic Society of Japan.* 2020;128(8):523–531. <https://doi.org/10.2109/jcersj2.20036>
17. Sharma R., Bhatti H.S., Kyhm K. Enhanced transition probabilities and trapping state emission of quencher impurities doped CaS:Mn phosphors. *J. Optoelektron. Adv. Mater.* 2009;11(1):62–69.

About the authors:

Oleg A. Medennikov, Postgraduate Student, Department of Ecology and Industrial Safety, Platov South-Russian State Polytechnic University (NPI) (132, ul. Prosveshcheniya, Novocherkassk, Rostov oblast, 346428, Russia). E-mail: monomors@yandex.ru. Scopus Author ID 57222569316, Researcher ID AGR-5187-2022, <https://orcid.org/0000-0002-4269-8684>

Nina P. Shabelskaya, Dr. Sci. (Eng.), Associate Professor, Head of the Department Ecology and Industrial Safety, Platov South-Russian State Polytechnic University (NPI) (132, ul. Prosveshcheniya, Rostov oblast, Novocherkassk, 346428, Russia). E-mail: nina_shabelskaya@mail.ru. Scopus Author ID 57222569316, ResearcherID P-9749-2019, RSCI SPIN-code 8696-7146, <https://orcid.org/0000-0001-8266-2128>

Об авторах:

Меденников Олег Александрович, аспирант кафедры «Экология и промышленная безопасность», ФГБОУ ВО Южно-Российский государственный политехнический университет (НПИ) имени М.И. Платова (346428, Россия, Ростовская обл., г. Новочеркасск, ул. Просвещения, 132). E-mail: monmors@yandex.ru. Scopus Author ID 57222569316, ResearcherID AGR-5187-2022, <https://orcid.org/0000-0002-4269-8684>

Шабельская Нина Петровна, д.т.н., доцент, заведующая кафедрой «Экология и промышленная безопасность», ФГБОУ ВО Южно-Российский государственный политехнический университет (НПИ) имени М.И. Платова (346428, Россия, Ростовская обл., г. Новочеркасск, ул. Просвещения, 132). E-mail: nina_shabelskaya@mail.ru. Scopus Author ID 57222569316, ResearcherID P-9749-2019, SPIN-код РИНЦ 8696-7146, <https://orcid.org/0000-0001-8266-2128>

The article was submitted: February 24, 2022; approved after reviewing: April 19, 2022; accepted for publication: July 11, 2022.

Translated from Russian into English by N. Isaeva

Edited for English language and spelling by Thomas Beavitt

MIREA – Russian Technological University
78, Vernadskogo pr., Moscow, 119454, Russian Federation.
Signed to print on *August 31, 2022*.
Not for sale

МИРЭА – Российский технологический университет
119454, РФ, Москва, пр-т Вернадского, д. 78.
Дата опубликования *31.08.2022*.
Не для продажи

<http://www.finechem-mirea.ru>

